

Mekong River Basin Water Resources Assessment: Impacts of Climate Change



Judy Eastham, Freddie Mpelasoka, Mohammed Mainuddin, Catherine Ticehurst, Peter Dyce, Geoff Hodgson, Riasat Ali and Mac Kirby.

August 2008

Australia is founding its future on science and innovation. Its national science agency, CSIRO, is a powerhouse of ideas, technologies and skills.

CSIRO initiated the National Research Flagships to address Australia's major research challenges and opportunities. They apply large scale, long term, multidisciplinary science and aim for widespread adoption of solutions. The Flagship Collaboration Fund supports the best and brightest researchers to address these complex challenges through partnerships between CSIRO, universities, research agencies and industry.

The Water for a Healthy Country Flagship aims to achieve a tenfold increase in the economic, social and environmental benefits from water by 2025.

For more information about Water for a Healthy Country Flagship or the National Research Flagship Initiative visit www.csiro.au/org/HealthyCountry.html

Citation: Eastham, J., F. Mpelasoka, M. Mainuddin, C. Ticehurst, P. Dyce, G. Hodgson, R. Ali and M. Kirby, 2008. Mekong River Basin Water Resources Assessment: Impacts of Climate Change. CSIRO: Water for a Healthy Country National Research Flagship

Copyright and Disclaimer

© 2008 CSIRO To the extent permitted by law, all rights are reserved and no part of this publication covered by copyright may be reproduced or copied in any form or by any means except with the written permission of CSIRO.

Important Disclaimer:

CSIRO advises that the information contained in this publication comprises general statements based on scientific research. The reader is advised and needs to be aware that such information may be incomplete or unable to be used in any specific situation. No reliance or actions must therefore be made on that information without seeking prior expert professional, scientific and technical advice. To the extent permitted by law, CSIRO (including its employees and consultants) excludes all liability to any person for any consequences, including but not limited to all losses, damages, costs, expenses and any other compensation, arising directly or indirectly from using this publication (in part or in whole) and any information or material contained in it.

ACKNOWLEDGEMENTS

Funding from AusAID to undertake this work is gratefully acknowledged. Thanks are due to Francis Chiew for helpful discussions on climate change and hydrological analyses, and to Albert Van Dijk and Munir Hanjra for their review of the draft report.

EXECUTIVE SUMMARY

This study investigates how the climate is likely to change in the Mekong Basin by 2030, and quantifies the uncertainty around future climate projections. It provides a preliminary assessment of the potential impact of these changes on water resources and productivity.

Our results indicate a likely increase in basin mean temperature of 0.79 °C, with greater increases for the colder catchments in the north of the basin. Annual precipitation is also projected to increase by ~ 0.2 m (13.5%), resulting mainly from an increase in wet season (May to October) precipitation in all catchments. Dry season rainfall is projected to increase in northern catchments, and to decrease in catchments in the south of the basin (including central and southern Laos, eastern Thailand, Cambodia and Vietnam).

Our study suggests that the melting of glaciers in the Upper Mekong is likely to increase under 2030 climate projections. However, since the area and volume of glaciers in the basin is small, the impact on flow and water availability in the Lower Mekong basin is likely to be insignificant both during the period of enhanced melting, and after the glaciers have ceased to exist.

Under the projected climate in 2030, total annual runoff from the basin is likely to increase by 21%, an increase of ~107,000 mcm. Runoff increases are projected for all catchments, primarily resulting from increased runoff during the wet season. Dry season runoff is projected to remain the same or to increase in 14 catchments of the basin, with small decreases in dry season runoff likely in the 4 remaining catchments. Despite likely increases in water withdrawals for irrigation, domestic and industrial purposes under future (2030) compared with historic climate conditions, the increase in projected runoff across the basin will maintain or improve annual water availability in all catchments. However, catchments in north-east Thailand will still experience moderate or medium-high levels of water stress, and high stress levels in the dry season. The Tonle Sap catchment of Cambodia is also projected to suffer high levels of stress during the dry season.

It is likely that increased flooding will affect all parts of the basin under the projected climate for 2030. We may expect the impact to be greatest in downstream catchments on the mainstream of the Mekong River, because of the cumulative impact of runoff increases from catchments upstream. We have quantified the impact at Kratie, where the frequency of 'extreme wet' flood events is likely to increase from an annual probability of 5% under historic conditions to a 76% probability under the future climate.

The productivity of capture fisheries, a key source of food for the population, is likely to be affected by the changing hydrology of the basin. Fisheries from the Tonle Sap Lake provide a critical source of food for Cambodia. Under the most likely projections for 2030, storages in the lake will increase causing both the maximum and minimum area and maximum and minimum levels of the lake to increase each year. The timing of the onset of flood is also likely to be impacted, with water levels rising earlier in the year, and the duration of flooding likely to increase. The effect of the changing hydrology on the productivity of fisheries from the Tonle Sap and the broader impact on the basin requires further investigation.

Indicative results on agricultural productivity suggest a 3.6% increase in productivity of the basin under the most likely projected climate for 2030. We did not assess any adverse effects of increased flooding or waterlogging on productivity, so this is likely to be an overestimate. However, we conclude that food scarcity is likely to increase in parts of the basin as a result of population growth. Food production in excess of demand is likely to be reduced across the basin. Thus separate to the negative impact of population growth on food scarcity, there will likely be further negative economic impacts on the population.

In summary, key impacts under future projections for climate and population in 2030 include increasing flood risk, increases in food scarcity and likely changes in the productivity of fisheries through hydrological impacts on the ecology of rivers, waterbodies and floodplains.

EXTENDED SUMMARY

Climate change analyses

In the study, we used simulations from the 4th Intergovernmental Panel on Climate Change (IPCC) assessment to investigate how the climate is likely to change in the Mekong basin, and the impact of change on basin water resources. We applied a rigorous statistical approach to selecting the Global Climate Models (GCMs) which best simulated the historic climate conditions of the Mekong Basin. We evaluated the capacity of the models to simulate both the magnitude and spatial and temporal pattern of monthly temperature and seasonal precipitation for catchments of the basin. On this basis, we selected 11 GCMs to construct scenarios of future (2030) temperature and precipitation for the IPCC A1B scenario. In analysing the climate projections we took the median for the 11 climate models to represent our best estimate of the projected future (2030) climate. We excluded the highest and lowest model projections for each parameter and used the difference between the 2nd lowest and 2nd highest values (~ 10th and 90th percentiles) to represent the range in future temperature and precipitation. Thus our study describes our best estimate of future climatic conditions, but also indicates the uncertainty around these estimates, based on the variation amongst projections from different GCMs.

Climate projections indicate an increase in mean temperatures across the basin of 0.79 °C. The uncertainty around this estimate is relatively small, and ranges from 0.68 to 0.81°C. Projected temperature increases tend to be greater towards the northern parts of the basin with the greatest increase in temperature projected for the coldest catchment of the basin (Upper Mekong). The uncertainty in future temperature projections is low for all months and for all catchments of the basin. Consistent with the trend in projected temperature, potential evaporation is projected to increase by 2030 in all months and all catchments. The increase in annual potential evaporation averaged across the basin is ~ 0.03 m, a change of 2%, and uncertainty around this estimate is low.

There is greater uncertainty around future (2030) precipitation projections. The most likely projected response in annual precipitation averaged across the basin is an increase of ~ 0.2 m (13.5%), but the projections from different GCMs indicate increases ranging from ~0.03 to ~0.36 m. The projected increase in precipitation varies considerably for different catchments of the basin, with increases ranging from < 0.05 m to > 0.3 m for different catchments. Projected increases in annual precipitation result chiefly from an increase in wet season (May to October) precipitation for all catchments of the basin. The projected response in dry season rainfall varies across catchments, with dry season rainfall increasing by up to 0.013 m in northern catchments. For catchments in the south of the basin (including central and southern Laos, eastern Thailand, Cambodia and Vietnam) dry season rainfall is projected to decrease by amounts less than 0.13 m. Thus the disparity between wet and dry season precipitation will be accentuated for all catchments, but particularly for catchments in the south where both decreases in dry season and increases in wet season precipitation are greatest.

Surface water availability

We analysed the impact of projected future (2030) climate on runoff, flows, water uses and water availability in the basin. In order to obtain a best estimate and likely range for future projections for each of these parameters, we adopted a similar approach to our climate analyses. We used monthly precipitation, temperature and potential evaporation projections constructed from simulations from the 11 GCMs in the water account model. For all the

modelled output parameters, we took the median for the 11 climate models to represent our best estimate of projected future (2030) value for that parameter. We excluded the highest and lowest model outputs for each parameter and used the difference between the 2nd lowest and 2nd highest values (~ 10th and 90th percentiles) to represent the range in each parameter. Thus our study describes our best estimate of each parameter for future climate conditions, but also indicates the uncertainty around these estimates, based on the variation amongst projections from different GCMs.

Under historical climate conditions, there is strong seasonality in runoff from the basin as a whole, with the greatest runoff observed in the wet months from May to October when precipitation is greatest (Figure 1). Under the projected climate in 2030, total annual runoff from the basin is likely to increase by 21%, an increase of ~107,000 mcm (Figure 1). There is uncertainty around this estimate associated with climate projections from different GCMs, ranging from a decrease of ~41,000 mcm (8%) to an increase of ~460,000 mcm (90%). The median runoff projections for 2030 suggest that total basin runoff will increase in all months of the year, with the largest projected increases occurring in the months of May to September. Thus the seasonality of rainfall conditions is likely to be enhanced under the most likely climate projections.

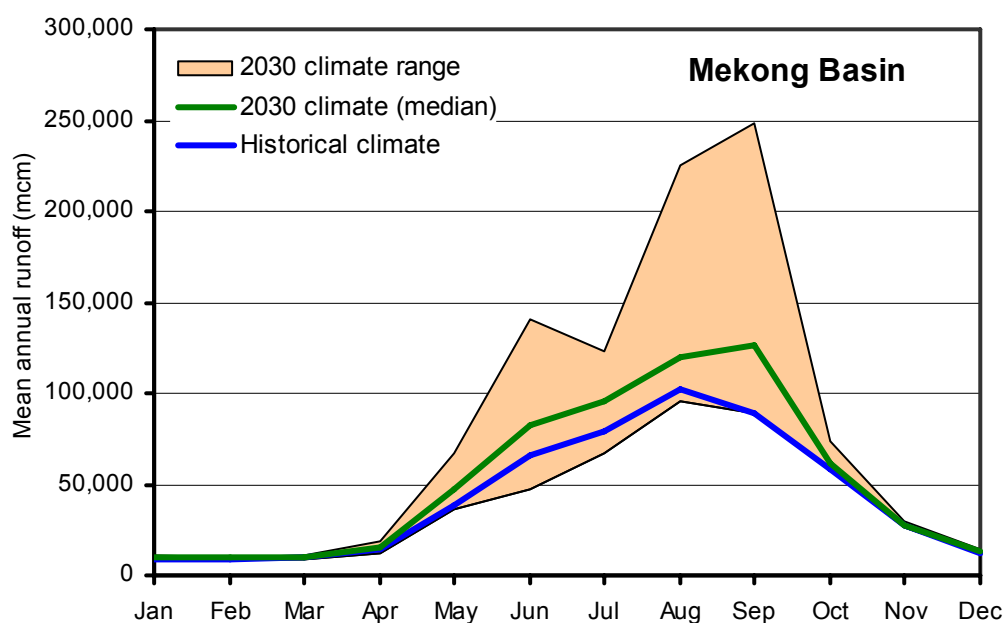


Figure 1. Historical (1951-2000) and future (2030) monthly runoff

The response in runoff to projected climate change varies across the catchments of the basin. Under the most likely projections, annual runoff will increase in all catchments, with most of this increase resulting from increased runoff during the wet season. Projected increases in annual runoff range from 0.055 m in the Delta catchment to 0.251 at Pakse. Under the most likely future climate, dry season runoff is projected to remain the same or to increase by up to 0.04 m in 14 catchments of the basin. In contrast, small decreases in dry season runoff (up to 0.006 m) are projected for the Ban Keng Done, Se San, Border and Delta catchments.

Compared to water used by rain fed land uses and net runoff, water applied as irrigation, domestic and industrial water uses are small components of the total water used in the basin, both under historic and projected (2030) climate conditions. There is variability across the catchments of the Mekong basin in the amounts of water used for irrigation, domestic and industrial uses. In the majority of catchments, the amount of water applied as irrigation is

larger than domestic and industrial consumption, both under historic and projected 2030 climate conditions. Domestic and industrial water use in all catchments is projected to increase by 2030, because of the increasing population. Under the most likely 2030 climate projections, irrigation applications are also likely to increase in all catchments except Yasothon and Ubon Ratchathani.

Under historic climate conditions, annual water availability per capita is high and levels of water stress low for most catchments of the basin. Exceptions are the Yasothon and Ubon Ratchathani catchments, which have medium-high levels of water stress. Water availability/capita is also low for the Yasothon catchment under the historic climate. Despite likely increases in water withdrawals for irrigation, domestic and industrial purposes under future (2030) compared with historic climate conditions, the increase in projected runoff across the basin will maintain or improve annual water availability in all catchments. Annual water availability/capita will be improved in the Yasothon catchment to a level such that annual water availability will no longer be limiting. Annual water stress levels are likely to decline by 2030 in both the Yasothon and Ubon Ratchathani catchments, and water stress in Yasothon is likely to be reduced to moderate. However, it is likely that Ubon Ratchathani will still experience medium-high levels of stress.

Under the historic climate and population, ~15 million people experience medium-high annual water stress in the Yasothon and Ubon Ratchathani catchments, with the remainder of the basin under low stress levels. Under the most likely climate (median) projections for 2030, the impact of annual water stress will be somewhat reduced, but ~10 million people will still experience medium-high stress in Ubon Ratchathani, with ~7 million people in Yasothon experiencing moderate stress.

Although levels of water stress, expressed on an annual basis, are likely to be reduced across the basin under the future climate and population, seasonal variation in water availability and water withdrawals causes water stress conditions to occur during the dry season in the Yasothon, Ubon Ratchathani and Tonle Sap catchments both under the historic climate, and the most likely projected (2030) climate. Even under the wettest climate projections for 2030 the ratio indicates high levels of stress in these catchments. These high levels of stress relate to generally greater water withdrawals for dry season irrigation in these catchments compared with other catchments.

It is important to note that these analyses, carried out at a catchment scale, may mask water stress conditions occurring at a finer scale due to local variations in water availability, water uses and population distribution within a catchment. Thus scrutiny of water availability and withdrawals at a finer scale is recommended for catchments where water availability or levels of water stress are close to threshold levels.

Melting of glaciers and flow from the Upper Mekong Basin

Following the release of IPCC reports on climate change and its impacts, there has been general concern about potential negative impacts on water availability in river basins across the world where water from glacial melt contributes to flow. Our study suggests that under the historic climate, annual glacial melt contributes only a small proportion (0.1 %) to discharge into the Lower Mekong Basin at Chiang Saen. The small contribution to flows results from the fact that the area and volume of glaciers in the Upper Mekong is small (316.3 km² and 17.3 km³, respectively). The most likely response in future (2030) mean annual discharge at Chiang Saen is an increase of ~19,000 mcm. Glacial melt is also projected to increase, but its contribution to discharge at Chiang Saen is likely to remain similar to historical conditions at 0.1% of mean annual discharge. Under the most likely response to future climate, the volume of glaciers is projected to diminish at a faster rate than under historic conditions. However, the impact on flow and water availability is likely to be

insignificant both during the period of enhanced melting, and after the glaciers have ceased to exist.

Groundwater availability

Generally the groundwater resources of the Mekong Basin have not been investigated in detail. Very limited information about the groundwater resource size, use, sustainability and quality is available from the literature. Only a few studies exist, focusing on some local areas within the Mekong Basin exist where they have made an assessment of the resource, use and/or quality. Due to increasing population, the pressures on the groundwater resources of the Mekong Basin are increasing. The impact of climate change on use of this resource is likely to be complex, and the response may vary across catchments of the basin. The projected increase in annual runoff in all catchments may reduce the reliance on groundwater for irrigation for areas where this increased surface water is accessible. Small decreases in dry season runoff are likely in the Ban Keng Done, Se San, Border and Delta catchments, so available groundwater resources of appropriate quality may be used to supplement surface water in these catchments. Since the irrigation requirement of dry season crops is projected to increase under the most likely future climate for 2030, the demand on groundwater resources is likely to increase where surface water resources are inaccessible or unavailable. Intensification of irrigated cropping to meet the food demand of the growing population may also increase groundwater use. In some areas such as southern Cambodia, arsenic contamination may be exacerbated by increased groundwater use in a changed climate. The impact on climate change on groundwater availability is likely to be complex and requires further investigation.

Flooding and Saline Intrusion

The Mekong delta is the most highly productive and densely populated part of the Basin. The area is prone to flooding in the wet season and to intrusion of seawater during dry months when discharge is low. Given the potential vulnerability of the population and economic activities in the delta to projected hydrological impacts of climate change, we assessed the response in flooding and indicators of saline intrusion to climate change.

Under the most likely future (2030) climate, annual discharge at Kratie will increase by 22%. Discharge is projected to increase in all months, with larger increases in the wet season. Minimum monthly flow each year is likely to increase by an average of 580 mcm under the most likely (median) projection. Since low flows at Kratie influence intrusion of salt water into the Delta, increases in minimum monthly flow may have a positive impact on reducing saline intrusion into the delta. The impact on saline intrusion needs to be assessed using a hydraulic model which also considers the impact of climate change on sea level rise. Assessing the potential impact is important, since the productivity of both agriculture and aquaculture in the highly productive and populous delta area depend on salinity levels, their areal extent and their duration.

Annual flood volumes are likely to increase at Kratie, with greater peak flows and longer duration of flooding compared with historic conditions. The frequency of 'extreme wet' flood events is likely to increase from an annual probability of 5% under historic conditions to a 76% probability under the future climate. Using a relationship between modelled annual flood volume at Kratie and the area of flooding downstream of Kratie determined from satellite images, we estimated the area affected by flooding each year from modelled flood volumes for the historic and future climate. Using this method of estimation, the indicative area of flooding in the delta is likely to increase by an annual average of ~3800 km². The analysis did not include an assessment of any impact of climate change on sea level rise, which may also contribute to increasing the flooded area.

Given the projected increase in runoff for all catchments of the basin, it is likely that other parts of the basin will also be adversely affected to varying degrees by increased flooding

under the projected climate for 2030. We may expect the impact may be greatest on the mainstream of the Mekong River, particularly in downstream catchments, because of the cumulative impact of the projected increase in runoff from catchments upstream. It is recommended that the impact of climate change on the frequency of flood events of different magnitude are investigated for other flood prone areas of the basin, so that the impact of greater rainfall and runoff can be better quantified across the basin.

Of all the likely impacts of climate change in the Mekong basin, it is likely that the impact of flooding in the delta and other areas will have the most significant negative consequences on the Mekong basin. The Delta catchment has the highest current and projected population of all catchments of the basin, followed closely by the Phnom Penh and Border catchments. Furthermore, it is the most productive part of the basin with high levels of agricultural productivity and aquaculture also contributing to food production.

Responses of the Tonle Sap Lake

Since the fisheries of the Tonle Sap Lake play a key role in the livelihoods of the people of Cambodia, we investigated the impact of projected changes in rainfall and runoff on the area and water level of the Tonle Sap Lake. The hydrology of the lake is closely linked to the productivity of capture fisheries, so any potential changes under climate change could have significant impacts on the Cambodian population. Under the most likely projections for 2030, storages in the lake will increase causing both the maximum and minimum area and maximum and minimum levels of the lake to increase each year. The timing of the onset of flood is also likely to be impacted, with water levels rising earlier in the year, and the duration of the flood each year likely to increase. These factors combine to influence a suite of conditions which will impact the local population either directly through changing their physical environment (by flood damage to housing and infrastructure), or indirectly through influencing their livelihoods. Both fisheries and agricultural activities around the lake are likely to be affected. The net impact of these changes in hydrology on fisheries production should be estimated using an existing model for the Tonle Sap, which links fish stocks in the lake to water levels and flows into the lake. The impacts of climate change on the complex ecology of the floodplain are diverse and inter-related, and require further investigation to elucidate them and determine the flow on effects on the population and livelihoods in the region.

Agricultural productivity

Our study investigated the likely impacts of climate change on agricultural productivity across the basin. The study was intended to give indicative responses only, since the large spatial scale and short timeframe for the project precluded a more detailed analysis. We found that under the most likely climate conditions for 2030, growing season rainfall increased across the basin for crops grown in the wet season. However, increases in seasonal rainfall did not translate to increases in yield for all crops and in all catchments, and the yield response was variable. In general, yield responses to projected changes in climate were small and ranged from -2.0% to + 3.3% for different crops and catchments. The irrigation requirement for crops grown in the dry season was greater for all catchments under the likely future climate than the requirement under the historical climate. If irrigation applications were maintained at historic levels, yields of crops irrigated in the dry season would decrease across the basin by approximately 2%. However, since runoff is projected to increase in all catchments under the most likely future (2030) climate, the increased irrigation requirement could generally be met from this increased water availability. Yields from crops irrigated during the dry season will thus be maintained under the likely future climate.

Basin-wide productivity is expected to increase by 3.6% under the most likely projected climate for 2030. All climate projections for different GCMs indicate productivity increases in the basin. We assumed a food requirement per capita of 300 kg/year of paddy or equivalent

to estimate food demand under both historic and projected future (2030) conditions. Based on this requirement, demand would increase from ~17 million tonnes for 2000 to ~ 33 million tonnes for the 2030 projected population. Productivity under both historic and projected climate will be more than adequate to meet this demand at a basin scale. However, at a catchment scale, demand will exceed supply in 8 catchments of the basin under the most likely projected climate for 2030 (compared with only 5 catchments under the historic climate). Thus because of population growth, a greater area of the basin is likely to be affected by food scarcity in the future, compared with the situation under the historic climate. Under historic conditions, excess production above food demand is estimated to be ~25 million tonnes. Under likely projections for climate and population for 2030, this will be reduced to ~11 million tonnes. Thus separate to the negative impact of population growth on food scarcity, there will likely be further negative economic impacts on the population.

Wider impacts of climate change

There are a range of proposed basin development scenarios under evaluation for the Mekong Basin. These scenarios include population growth, development initiatives such as irrigation, hydropower development and inter-basin diversions, as well as impacts of dams that are planned in China. Clearly the impacts of projected changes in climate need to be considered in evaluating the likely impact of these scenarios. Irrigation systems will need to be designed to deliver increased amounts. Dam storages may need to be increased to meet increased irrigation withdrawals. The capacity for hydropower generation is likely to be increased across the basin, so systems should be designed to capture the likely capacity for power generation. Dam design will have to take into account changing probabilities of rainfall and runoff events of different magnitudes.

There are a suite of other important conditions in the Mekong basin that are likely to be influenced by the changing climate, though these are beyond the scope of this study. Soil erosion is likely to increase because of increased runoff in all catchments, and erosion of river banks and channels may also occur. Land use and soil management practices need to be developed and adopted to minimise the erosion risk. Water quality is likely to be affected, and there are likely to be increased sediment loads in tributaries and in the mainstream of the Mekong River. There may be increased sedimentation in dams. Navigation on the river is likely to be affected, with potentially greater navigability in the dry season in some catchments because of increasing runoff and flows. Temperature increases will affect the physical, chemical and biological properties of freshwater lakes and rivers, with predominantly adverse effects on individual freshwater species, community composition, and water quality. Sea level rise may exacerbate water resource constraints of the delta area due to increased salinisation of groundwater supplies.

Summary of potential impacts of climate change

Table 1 summarises the potential impacts of climate change of the basin catchments. The table shows the impacts under the likely projected climate for 2030 for the A1B scenario. Impacts on agricultural productivity shown in the table are indicative only, as our analysis doesn't include impacts of other important factors (discussed in the text) such as flood damage. Food scarcity in this table refers to a deficit between availability and demand for agricultural production within a catchment, and doesn't include other potential food sources (e.g. fish, livestock and imported produce).

Table 1. Summary of potential impacts of climate change on catchments of the Mekong Basin

Potential Impacts of Climate Change (2030)
<p>Upper Mekong: China, Yunnan Province Temperature and annual precipitation increased; Dry season precipitation increased; Annual runoff increased; Dry season runoff increased; Melting of glaciers increased; Potential for increased flooding (not quantified).</p>
<p>Chiang Saen: China, Myanmar, Northern Laos Temperature and annual precipitation increased; Dry season precipitation increased; Annual runoff increased; Dry season runoff increased; Annual flows into Lower Mekong Basin increased by 30%; No reduction in dry season flow; Potential for increased flooding (not quantified).</p>
<p>Moung Nouy: Northern Laos Agricultural productivity decreased; Existing food scarcity increased; Temperature and annual precipitation increased; Dry season precipitation increased; Annual runoff increased; Dry season runoff increased; Potential for increased flooding (not quantified).</p>
<p>Luang Prabang: Northern Thailand and Northern Laos Agricultural productivity decreased; Existing food scarcity increased; Temperature and annual precipitation increased; Dry season precipitation increased; Annual runoff increased; Dry season runoff increased; Potential for increased flooding (not quantified)</p>
<p>Vientiane: Northern Laos and of North-east Thailand Agricultural productivity increased; Food availability in excess of demand decreased; Temperature and annual precipitation increased; Dry season precipitation increased; Annual runoff increased; Dry season runoff increased; Potential for increased flooding (not quantified)</p>
<p>Tha Ngon: Central Laos Agricultural productivity decreased; Existing food scarcity increased; Temperature and annual precipitation increased; Dry season precipitation decreased; Annual runoff increased; Dry season runoff increased; Potential for increased flooding (not quantified)</p>
<p>Nakhon Phanom: Central Laos and North-east Thailand Agricultural productivity increased; Existing food scarcity increased through population growth; Temperature and annual precipitation increased; Dry season precipitation decreased; Annual runoff increased; Dry season runoff decreased; Potential for increased flooding (not quantified).</p>
<p>Mukdahan: Southern Laos and North-east Thailand Agricultural productivity unaffected; Existing food scarcity increased through population growth; Temperature and annual precipitation increased; Dry season precipitation decreased; Annual runoff increased; Dry season runoff increased; Potential for increased flooding (not quantified).</p>
<p>Ban Keng Done: Central Laos Agricultural productivity increased; Food availability in excess of demand decreased; Temperature and annual precipitation increased; Dry season precipitation decreased; Annual runoff increased; Dry season runoff decreased; Potential for increased flooding (not quantified).</p>

<p>Yasothon: Northeast Thailand Agricultural productivity increased; Food availability in excess of demand decreased; Temperature and annual precipitation increased; Dry season precipitation decreased; Annual runoff increased; Dry season runoff increased; Annual water stress (ratio withdrawals: availability) reduced to moderate; Dry season water stress decreased but remains high; Potential for increased flooding (not quantified).</p>
<p>Ubon Ratchathani: Northeast Thailand Agricultural productivity increased; Food availability in excess of demand increased; Temperature and annual precipitation increased; Dry season precipitation decreased; Annual runoff increased; Dry season runoff increased; Annual water stress (ratio withdrawals: availability) reduced to medium-high; Dry season water stress decreased but remains high; Potential for increased flooding (not quantified).</p>
<p>Pakse: Southern Laos and Northeast Thailand Agricultural productivity increased; Food availability in excess of demand decreased; Temperature and annual precipitation increased; Dry season precipitation decreased Annual runoff increased; Dry season runoff increased; Potential for increased flooding (not quantified).</p>
<p>Se San: Southern Laos, North-east Cambodia and Central Highlands of Vietnam Agricultural productivity increased; Food availability in excess of demand decreased; Temperature and annual precipitation increased; Dry season precipitation decreased; Annual runoff increased; Dry season runoff decreased; Potential for increased flooding (not quantified).</p>
<p>Kratie: Southern Laos and Central Cambodia Agricultural productivity increased; Food availability in excess of demand decreased; Temperature and annual precipitation increased; Dry season precipitation decreased; Annual runoff increased; Dry season runoff decreased; Frequency of extreme floods increased from 5% to 76% annual probability; Peak flows, flood duration and flooded area increased; Dry season minimum flows increased.</p>
<p>Tonle Sap: Central Cambodia Agricultural productivity increased; Food availability in excess of demand decreased; Temperature and annual precipitation increased; Dry season precipitation decreased; Annual runoff increased; Dry season runoff decreased; Dry season water stress increased and remains high; High probability of increased flooding (not quantified); Seasonal fluctuation in Tonle Sap Lake area and levels increased; Minimum area of Tonle Sap Lake increased, areas of flooded forest permanently submerged and possibly destroyed reducing fish habitat; Net impact on capture fisheries uncertain; Maximum area of Tonle Sap lake increased with possible negative impacts on agricultural areas, housing and infrastructure.</p>
<p>Phnom Penh: South-eastern Cambodia Food scarcity due to population increase; Temperature and annual precipitation increased; Dry season precipitation decreased; Annual runoff increased; Dry season runoff increased; High probability of increased flooding; Flooded area increased.</p>
<p>Border: Southern Cambodia and South Vietnam Agricultural productivity decreased; Food scarcity due to population increase; Temperature and annual precipitation increased; Dry season precipitation decreased; Annual runoff increased; Dry season runoff decreased; High probability of increased flooding; Flooded area increased.</p>

Delta: South Vietnam

Food scarcity due to population increase; Temperature and annual precipitation increased; Dry season precipitation decreased; Annual runoff increased; Dry season runoff decreased; High probability of increased flooding; Flooded area increased; Dry season minimum flows increased and possible reduction in saline intrusion.

We selected the A1B scenario for in-depth investigation for this study, as it represents a mid-range scenario in terms of development impacts on GHG emissions. In order to give perspective on the results presented for responses to changing climate for the A1B scenario projections in this study, we used pattern-scaling to calculate projected temperature and annual precipitation for the A1F1, A2, B2, A1T, and B1 scenarios, and for 2050 and 2070 for the A1B scenario. The projected precipitation and temperature responses are intended to be indicative only. The A1B scenario projections for rainfall and temperature lie towards the middle of the range of projected rainfall and temperature at 2030, 2050 and 2070. Thus in considering the results for the A1B scenario presented in this report, it is important to bear in mind that if the world progresses down a different development pathway from that described by the A1B scenario, changes in temperature and precipitation could be bigger or smaller than those described in this report. It is also important to bear in mind that the reported results are for 2030, and that further increases in both temperature and precipitation are possible beyond this timeframe.

CONTENTS

Contents	xv
1. Introduction	1
1.1. Background and aims of the research	1
1.2. Climate Change	1
1.3. Previous studies on climate change in the Mekong Basin	3
1.4. Water resources assessment using the water account model	3
2. Description of the Mekong Basin.....	4
2.1. Basic hydrology of the Mekong Basin.....	4
2.2. Land use	7
2.3. Population.....	11
2.3.1. Methods of estimating population in 2000 and 2030	11
2.3.2. Mekong Basin populations for 2000 and 2030.....	14
3. Climate Analyses.....	17
3.1. Observed data	17
3.2. Simulated data	17
3.3. GCM selection and methodology for future climate projections	17
3.4. Projected changes in temperature for the Mekong Basin.....	19
3.4.1. Projected changes in basin-wide temperature.....	19
3.4.2. Projected changes in temperature for Mekong catchments.....	19
3.5. Projected changes in precipitation for the Mekong Basin.....	23
3.5.1. Projected changes in basin-wide precipitation.....	23
3.5.2. Projected changes in precipitation for Mekong catchments.....	24
3.5.3. Uncertainty in projected (2030) precipitation for Mekong catchments	28
3.6. Projected changes in potential evaporation for catchments of the Mekong Basin. 30	
3.6.1. Projected changes in basin-wide potential evaporation.....	30
3.6.2. Projected changes in potential evaporation for Mekong catchments.....	31
4. Surface water availability	34
4.1. Modelling the basin water balance using the water account model	34
4.2. Runoff	35
4.2.1. Projected changes in basin runoff	35
4.2.2. Projected changes in runoff for Mekong catchments.....	36
4.2.3. Uncertainty in projected (2030) runoff for Mekong catchments	39
4.3. Impact of glacier melt and snowmelt	41
4.4. Water uses.....	43
4.5. Water Stress	47
5. Groundwater Availability	51
5.1. Introduction	51
5.2. Groundwater resources – a country based overview of the resource	51
5.2.1. Cambodia	51
5.2.2. Vietnam	52
5.2.3. Thailand.....	53
5.2.4. Myanmar	54
5.2.5. Lao PDR.....	54
5.3. Groundwater quality.....	56
5.3.1. Cambodia	56
5.3.2. Vietnam	57

5.3.3.	Thailand.....	57
5.3.4.	Myanmar	57
5.3.5.	Lao PDR.....	57
5.4.	Conclusions	58
5.5.	Implications for climate change impacts.....	59
5.6.	Knowledge/information gaps.....	59
6.	Flooding and Saline Intrusion in the Mekong Delta.....	62
6.1.	Mean monthly discharge at Kratie	62
6.2.	Frequency of flood events of different magnitudes.....	63
6.3.	Flood mapping and area of inundation	64
7.	Responses of the Tonle Sap Lake	68
8.	Impact of Climate Change on Agricultural Productivity.....	72
8.1.	Introduction	72
8.2.	Method.....	73
8.2.1.	Soil-Water Balance Simulation Model	73
8.2.2.	Crop-Water Production Function.....	74
8.2.3.	Yield impact on rain fed crops	74
8.2.4.	Yield impact on irrigated crops	75
8.2.5.	Data Sources.....	75
8.3.	Impact of climate change on growing season rainfall.....	78
8.4.	Impact of climate change on crop productivity	81
8.4.1.	Rain fed rice	81
8.4.2.	Upland/flood-prone Rice.....	82
8.4.3.	Sugarcane	82
8.4.4.	Maize	83
8.4.5.	Soybean	84
8.4.6.	Irrigated rice.....	84
8.4.7.	Irrigation requirements.....	85
8.4.8.	Total productivity estimates	86
8.4.9.	Discussion of productivity responses.....	89
9.	Indicative climate change responses for alternative IPCC scenarios.....	92
10.	Recommendations	94
11.	Appendix 1	95
11.1.	Global climate change model selection	95
11.1.1.	Assessment of climate change model performance	95
12.	Appendix 2	102
Mapping water extent and change for the Mekong Delta and the Tonle Sap using Optical and Passive Microwave Remote Sensing		102
12.1.	Introduction to observing surface water using remote sensing	102
12.2.	Mapping Floods using Optical	102
12.2.1.	Mapping Floods using Optical Remote Sensing.....	102
12.2.2.	MODIS background.....	102
12.2.3.	Method.....	103
12.2.4.	Results.....	105
12.2.5.	Discussion	107
12.3.	Mapping Floods using Passive Microwave.....	108
12.3.1.	TRMM background.....	108
12.3.2.	Method	108
12.3.3.	Results	110

12.3.4. Discussion	113
12.4. Potential of combining Optical and Passive Microwave remote sensing for mapping water extent and change for the Lower Mekong River	113
12.4.1. Summary	116
13. Appendix 3	117
Current and recent trends in agricultural productivity	117
14. References	123

LIST OF FIGURES

Figure 1. Historical (1951-2000) and future (2030) monthly runoff.....	vii
Figure 1.1. Figure 3.1 from IPCC (2007). Scenarios for greenhouse gas emissions from 2000 to 2100 in the absence of additional climate policies.....	2
Figure 2.1. The Mekong Basin with the 18 catchments used in the water use account.	5
Figure 2.2. Monthly average rain and potential evapotranspiration in the Mekong Basin: a. Upper Mekong; b. Se Bang Hieng in central Laos; c. Chi in NE Thailand; d. Lower Mekong around Phnom Penh.....	6
Figure 2.3. Annual rainfall 1951-2000.....	7
Figure 2.4. Land cover/land use map.....	8
Figure 2.5. Mapped irrigation areas reclassified to 3 broad categories.....	9
Figure 2.6. Land use map based on USGS land cover/land use data. Classes aggregated for modelling purposes.....	10
Figure 2.7. 2000 Population distribution.....	12
Figure 2.9. Urban and rural population in 2000 and future (2030) populations estimated using UNDP and SEDAC growth rates for catchments of the Mekong Basin.	15
Figure 2.10. Population density in 2000 and projected (SEDAC) population density in 2030 for catchments of the Mekong Basin.	16
Figure 3.1. Baseline (1951-2000) versus future (2030) monthly mean temperature.	19
Figure 3.2. Spatial distribution of the projected change in mean temperature at 2030 compared with historical (1951-2000) mean temperatures.	20
Figure 3.3. Baseline (1951-2000) versus future (2030) monthly mean temperature for catchments of the Upper Mekong basin: Upper Mekong and Chiang Saen.....	21
Figure 3.4. Baseline (1951-2000) versus future (2030) monthly mean temperature for Moug Nouy, Luang Prabang, Vientiane, Tha Ngon, Nakhon Phanom, Mukdahan, Ban Keng Done and Yasothon catchments.	22
Figure 3.5. Baseline (1951-2000) versus future (2030) monthly mean temperature for Ubon Ratchathani, Pakse, Se San, Kratie, Tonle Sap, Phnom Penh, Border and Delta catchments.	23
Figure 3.6. Baseline (1951-2000) versus future (2030) monthly mean precipitation.	24
Figure 3.7. Spatial distribution of the projected change in mean annual precipitation at 2030 compared with historical (1951-2000) mean precipitation.	25
Figure 3.8. Spatial distribution of the projected change in precipitation during the wet season (May to October) at 2030 compared with historical (1951-2000) mean precipitation.	26
Figure 3.9. Spatial distribution of the projected change in precipitation during the dry season (November to April) at 2030 compared with historical (1951-2000) mean precipitation.	27
Figure 3.10 Baseline (1951-2000) versus future (2030) monthly mean precipitation for catchments of the Upper Mekong basin: Upper Mekong and Chiang Saen.....	28
Figure 3.11. Baseline (1951-2000) versus future (2030) monthly mean precipitation for Moug Nouy, Luang Prabang, Vientiane, Tha Ngon, Nakhon Phanom, Mukdahan, Ban Keng Done and Yasothon catchments.....	29
Figure 3.12. Baseline (1951-2000) versus future (2030) monthly mean precipitation for Ubon Ratchathani, Pakse, Se San, Kratie, Tonle Sap, Phnom Penh, Border and Delta catchments.	30
Figure 3.13. Baseline (1951-2000) versus future (2030) monthly potential evaporation.	31
Figure 3.14. Baseline (1951-2000) versus future (2030) monthly potential evaporation for catchments of the Upper Mekong basin: Upper Mekong and Chiang Saen.....	31
Figure 3.15. Baseline (1951-2000) versus future (2030) monthly potential evaporation Moug Nouy, Luang Prabang, Vientiane, Tha Ngon, Nakhon Phanom, Mukdahan, Ban Keng Done and Yasothon catchments.....	32

Figure 3.16. Baseline (1951-2000) versus future (2030) monthly potential evaporation for Ubon Ratchathani, Pakse, Se San, Kratie, Tonle Sap, Phnom Penh, Border and Delta catchments.	33
Figure 4.1. Historical (1951-2000) and future (2030) monthly runoff.....	35
Figure 4.2. Spatial distribution of the projected change in mean annual runoff at 2030 compared with historical (1951-2000) mean annual runoff for catchments of the Mekong Basin.....	37
Figure 4.3. Spatial distribution of the projected change in dry season (November to April) runoff at 2030 compared with historical (1951-2000) dry season runoff.....	38
Figure 4.4. Historical (1951-2000) and future (2030) monthly runoff for catchments of the Upper Mekong basin: Upper Mekong and Chiang Saen.	39
Figure 4.5. Historical (1951-2000) and future (2030) monthly runoff for Moung Nouy, Luang Prabang, Vientiane, Tha Ngon, Nakhon Phanom, Mukdahan, Ban Keng Done and Yasothon catchments.	40
Figure 4.6. Historical (1951-2000) and future (2030) monthly runoff for Ubon Ratchathani, Pakse, Se San, Kratie, Tonle Sap, Phnom Penh, Border and Delta catchments.....	41
Figure. 4.7. The extent of glaciers in the Upper Mekong catchment	42
Figure 4.8. Historical (1951-2000) and future (2030) seasonal discharge at Chiang Saen into the Lower Mekong Basin.	43
Figure 4.9. Historical (1951-2000) and future (2030) water uses.	44
Figure 4.10. Historical (1951-2000) and future (2030) industrial (a), domestic (b) and irrigation (c) water. 2030 irrigation applications for median, wet and dry projected climate ranges are shown.	46
Figure 4.11. The annual water stress index (ratio of withdrawals to water available) under historic and future (2030) climate scenarios. Values of the index < 0.1 indicate low stress; between 0.1 and 0.2 indicates moderate water stress; between 0.2 and 0.4 indicates medium-high stress; and > 0.4 indicates high water stress.	47
Figure 4.12. The number of people experiencing high, medium-high moderate and low levels of water stress in the Mekong basin under historic climate and 2030 climate projections. ...	48
Figure 4.13. Water availability/capita under historic and future (2030) climate scenarios.....	49
Figure 4.14. Dry season water stress index (ratio of withdrawals to water available) under historic and future (2030) climate scenarios. Values of the index < 0.1 indicate low stress; between 0.1 and 0.2 indicates moderate water stress; between 0.2 and 0.4 indicates medium-high stress; and > 0.4 indicates high water stress.....	49
Figure 5.1. Southern parts of the Mekong Basin showing countries, regions and provinces.	55
Figure 5.2. Central parts of the Mekong Basin showing countries, regions and provinces. .	55
Figure 5.3. Northern parts of the Mekong Basin showing countries, regions and provinces.	56
Figure 6.1. Historical (1951-2000) and future (2030) mean monthly discharge at Kratie.	62
Figure 6.2. Historic (1951-2000) and future (2030) minimum monthly flow at Kratie	63
Figure 6.3. Historical (1951-2000) and future (2030) frequency of floods of different magnitude at Kratie.....	64
Figure 6.4. Scatterplot of TRMM (1998-2002) and MODIS (2000-2002) annual maximum flood extent for the Delta verses modelled Kratie annual water volume	65
Figure 6.5. Historical (1951-2000) and future (2030) flooded area in the Mekong delta.	66
Figure 6.6. TRMM scenes of the Lower Mekong River for a dry month (Feb 1998) and the maximum flood months for 1998 – 2002. Dark areas indicate water.....	67
Figure 6.7. MODIS scenes of the Lower Mekong River for the flood season of 2001. Light areas indicate water.....	67
Figure 7.1. Scatterplot of the combined MODIS (2000-2002) and scaled TRMM (1998-2002) monthly flood extent for the Tonle Sap Lake verses modelled monthly water volume.	68
Figure 7.2. Relationship between modelled water volume in the Tonle Sap lake, and water levels in the lake derived from Baran <i>et al.</i> 2007.....	69
Figure 7.3. Historical (1951-2000) and future (2030) maximum and minimum area of Tonle Sap Lake.....	70

Figure 7.4. Historical (1951-2000) and future (2030) maximum and minimum annual water level of Tonle Sap Lake.	70
Figure 7.5. Historical (1951-2000) and future (2030) seasonal fluctuation in area and water level of Tonle Sap Lake.	71
Figure 8.1. Overlay of provincial administrative boundary with the sub-basin boundary. Coloured and numbered polygons are the provinces (1-18 are in Laos, 19-40 are in Thailand, 41-60 are in Cambodia and 61-76 are in Vietnam). Black lines are the sub-basin boundary.	77
Figure 8.2. Projected and historical rainfall during the growing season of rice crops.	79
Figure 8.3. Projected and historical rainfall during the growing season of sugarcane, maize and soybean crops.	80
Figure 8.4. Projected and historical relative yield of rain fed lowland rice.	81
Figure 8.5. Projected and historical relative yield of upland/flood-prone rice.	82
Figure 8.6. Projected and historical relative yield of sugarcane.	83
Figure 8.7. Projected and historical relative yield of maize.	83
Figure 8.8. Projected and historical relative yield of soybean.	84
Figure 8.9. Projected and historical relative yield of irrigated rice.	85
Figure 8.10. Projected and historical irrigation requirements of irrigated rice.	85
Figure 8.11. Change in total water diversion for irrigation due to climate change.	86
Figure 8.12. Historical (1951-2000) and future (2030) productivity.	87
Figure 8.13. Historical (1951-2000) and future (2030) productivity per capita.	88
Figure 8.14. Historical (1951-2000) and future (2030) production in excess of demand. Negative values indicate production is insufficient to meet demand.	89
Figure 9.1. Projected mean temperature and mean annual precipitation for the Mekong Basin for different IPCC scenarios at 2030, 2050 and 2070.	92
Figure 11.1. Pattern correlation and RMS error for observed versus simulated monthly.	96
Figure 11.2. Pattern correlation and RMS error for observed versus simulated monthly temperature for July to December.	97
Figure 11.3. Pattern correlation and RMS error for observed versus simulated monthly precipitation for January to June.	98
Figure 11.4. Pattern correlation and RMS error for observed versus simulated monthly precipitation for July to December.	99
Figure 11.5. Pattern correlation and RMS error for observed versus simulated seasonal temperature for wet (May to October) and dry (November to April) seasons.	100
Figure 11.6. Pattern correlation and RMS error for observed versus simulated seasonal precipitation for wet (May to October) and dry (November to April) seasons.	101
Figure 12.1. Scatterplot of the Global Vegetation Moisture Index (GVMI) and the Enhanced Vegetation Index (EVI) in Australia. Point colour indicates vegetation type (inset map) as: blue=water, green=forests, red=grasslands and croplands, yellow=shrublands and brow=woodlands. The dotted line indicates the criteria for separating the open water from the vegetation domain.	103
Figure 12.2. Relationship between the open water likelihood.	104
Figure 12.3. Changes in inundated area shown by a time series of Modis images in 2001.	105
Figure 12.4. Modelled flood volumes at Kratie and Modis flood areas for 2000 to 2002.	106
Figure 12.5. Modelled Tonle Sap Lake monthly storage and Lake Area 2000 to 2002.	106
Figure 12.6. Comparison of RADARSAT derived map and Modis image for the Tonle Sap Lake.	108
Figure 12.7. Scatterplot of TRMM Digital Number verses proportion of water (from MODIS) for the Tonle Sap and Kratie area for the 16-day period starting 2 nd December 2000.	109
Figure 12.8. Scatterplot of modelled annual flood volumes for Kratie verses TRMM mapped flood extent for the Delta for 1998 to 2002.	110
Figure 12.9. TRMM scenes of the Lower Mekong River for a dry month (Feb 1998) and the maximum flood months for 1998 – 2002. Dark areas indicate water.	111
Figure 12.10. Percentage of water within TRMM pixels showing flood extent for the 2001 wet season for Tonle Sap and the Mekong Delta.	112

Figure 12.11. Scatterplot of monthly storage volume for Tonle Sap verses TRMM flood extent for 1998-2002.....	112
Figure 12.12. Scatterplot of TRMM (1998-2002) and MODIS (2000-2002) mapped flood extent verses modelled monthly storage water volume for Tonle Sap Lake.	113
Figure 12.13. Scatterplot of TRMM (1998-2002) and MODIS (2000-2002) annual maximum flood extent for the Delta verses modelled Kratie annual water volume.....	114
Figure 12.14. Scatterplot of Tonle Sap Lake monthly maximum flood extent for TRMM verses MODIS for 2000-2002.....	114
Figure 12.15. Scatterplot of the combined MODIS (2000-2002) and scaled TRMM (1998-2002) monthly flood extent for the Tonle Sap Lake verses modelled monthly water volume.	115
Figure 13.1. Spatial and temporal variability of average yield (tonne/ha) of rice in the lower Mekong Basin.....	118
Figure 13.2. Regional average yield of rice	119
Figure 13.3. Regional average yield of main rain fed rice	119
Figure 13.4. Regional average yield of irrigated rice	119
Figure 13.5. Regional average yield of upland/flood-prone rice	120
Figure 13.6. Regional average yield of sugarcane	121
Figure 13.7. Regional average yield of maize	121
Figure 13.8. Regional average yield of soybean	122

LIST OF TABLES

Table 1. Summary of potential impacts of climate change on catchments of the Mekong Basin.....	xii
Table 2.1 Catchments in the Mekong Basin with their areas.....	6
Table 2.2. Quinquennial rural and urban growth rates for Mekong Basin countries used to calculate population projection for 2030.	11
Table 3.1. List of GCMs recommended by the Intergovernmental Panel on Climate Change (IPCC). Models selected for the construction of climate scenarios for the Mekong basin are shown in bold letters.	18
Table 8.1. List of crops considered with their growing season and growing period.....	76
Table 12.1. TRMM Digital Number ranges used to represent proportion of water within each pixel.	110
Table 13.1. Harvested area of different crops grown in the basin as percentage of the total harvested area, 1995-2003.....	117
Table 13.2. Inter-provincial coefficient of variation (CV) of the yield of main rain fed rice ...	120
Table 13.3. Inter-provincial coefficient of variation (CV) of the rainfall during the growing season of main rain fed rice.....	120
Table 13.4. Distribution (%) of total rice production in the lower Mekong Basin by region and type of rice	121

1. INTRODUCTION

1.1. Background and aims of the research

From a world perspective, the Mekong basin appears well-endowed with water resources, with the Mekong River having the eighth largest discharge in the world. There are, however, competing demands on the resource causing water shortages which impact more widely on the livelihoods of the population and the regional economies. Examples of these demands and impacts are seasonal water shortages in northeast Thailand, hydropower development in the Upper Mekong in China, increasing forest clearing intensity in the uplands of Laos, concerns about fishery sustainability in the Tonle Sap and elsewhere, and water quality deterioration and salt intrusion in the delta. The situation is unlikely to improve, as projected rapid population and economic growth will increase energy and food demands. Furthermore, climate change will likely change rainfall amounts and patterns and the frequency and extent of extreme weather events. These may have serious consequences for growth and sustainable development in the basin.

AusAID has developed a strategy to promote integration and co-operation in the Greater Mekong Subregion (AusAID, 2007). One objective of the strategy is to improve water resource management in the Mekong basin. Integral to achieving this objective is knowledge of the spatial and temporal availability and uses of the resource, and how this is likely to change under the influence of climate change. The research outlined in this report quantifies water resource availability across the Mekong basin, and its seasonal distribution. It also evaluates the likely response in precipitation and temperature to climate change, and the impact on water resources across the basin. This short term, integrated assessment of water resource response to climate change identifies critical regions and issues, and will provide a basis for future in depth analyses, targeted at developing solutions and potential adaptation strategies.

The aims of the research were to:

- 1) Assess at a sub-basin scale the most likely response in precipitation and temperature to different climate change scenarios for 2030.
- 2). Quantify the likely impact of climate change on water resources availability, water flows and storages, flooding and major water-bodies/wetlands
- 3). Quantify the impact of climate change on agricultural productivity and quantify any potential change in water uses for irrigation to sustain production to meet the needs of the population.
- 4) Relate the climate change impacts to population and its distribution in the basin, including projections for population growth.

1.2. Climate Change

There is agreement and much evidence that green house gas (GHG) emissions will continue to increase over the next few decades under current climate change and sustainable development initiatives. However there is uncertainty over the rate at which emissions will increase, and their impact on the global climate. In 2000, the Intergovernmental Panel on Climate Change (IPCC) published a Special Report on Emissions Scenarios (SRES, 2000) which described different developmental pathways for the world. The scenarios are grouped into 4 families (A1, A2, B1 and B2), each describing a scenario of different demographic, economic and technological driving forces, and resulting GHG emissions. These scenarios are widely used in climate change studies to describe the range of possible future conditions and potential impacts. The A1 storyline describes world of rapid economic growth, with a global population that peaks in the middle of the century, together with rapid introduction of new efficient technologies. The A1 is divided into 3 groups which assume reliance on different energy sources, fossil intensive (A1F1), non-fossil energy sources (A1T), and a

balance across all sources (A1B). The B1 scenario describes a convergent world with the same population as A1, but with rapid changes towards a service and information economy. B2 describes a world with intermediate population and economic growth, but including local solutions to economic, social and environmental sustainability. A2 describes a heterogeneous world with high population growth, slow economic development and a low rate of technological change. The simulated impact of these various scenarios on GHG emissions are shown in Figure 1.1.

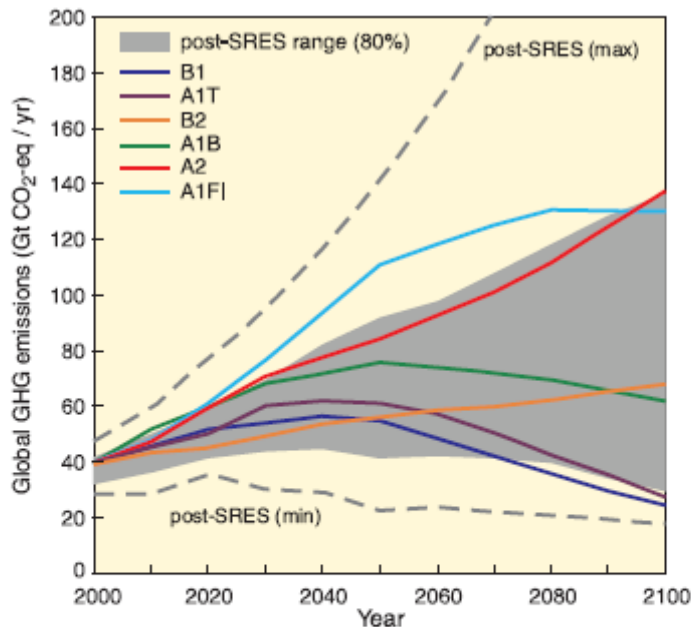


Figure 3.1. Global GHG emissions (in GtCO₂-eq per year) in the absence of additional climate policies: six illustrative SRES marker scenarios (coloured lines) and 80th percentile range of recent scenarios published since SRES (post-SRES) (gray shaded area). Dashed lines show the full range of post-SRES scenarios. The emissions include CO₂, CH₄, N₂O and F-gases. {WGIII 1.3, 3.2, Figure SPM.4}

Figure 1.1. Figure 3.1 from IPCC (2007). Scenarios for greenhouse gas emissions from 2000 to 2100 in the absence of additional climate policies.

Thus there is uncertainty in the future developmental pathway of the world, and the resulting GHG emissions. For this study, which assesses the impacts of climate change on water resources and productivity of the Mekong Basin, we have selected the A1B scenario for in-depth investigation. We have chosen this as it represents a mid-range scenario in terms of development impacts on GHG emissions. Investigation of the impacts of all six scenarios to cover a greater range of uncertainty in future emissions and climate impacts is beyond the scope of this study.

Global Climate Models (GCMs) are used to simulate future climate conditions under the different emission scenarios. A further cause of uncertainty in climate change studies is the variability in simulations by different GCMs. These models differ considerably in their estimates of the strength of different feedbacks in the climate system (including cloud feedbacks, ocean heat uptake and carbon cycle feedbacks). In this study, 24 GCMs were assessed, and models selected to develop future climate projections, based on their capacity to simulate historic climate patterns over the Mekong Basin.

Confidence in GCM projections is higher for some variable (e.g. temperature) than for others (e.g. precipitation). Confidence is also higher for longer time-averaging periods and larger spatial scales. Climate change projections beyond about 2050 are strongly scenario- and model-dependent. Impacts research is hampered by uncertainties surrounding regional

projections of climate change, particularly precipitation. Understanding of low-probability/high impact events and the cumulative impacts of sequences of smaller events, which is required for risk-based approaches to decision making, is generally limited.

IPCC broad projections for climate change in the 21st century suggest that both temperature and precipitation will increase across Asia. In the tropical Asia region, the frequency and magnitude of extreme events are also projected to increase, potentially affecting the Mekong Basin. It is important to understand both the magnitude of these projected changes, and how they may vary across the basin, so that the potential impacts may be assessed. Much of the population of the basin depends on agriculture or fisheries for their livelihoods and these are likely to be impacted (either positively or negatively) by changing temperatures and precipitation. Annual flooding is a regular and essential part of life in many parts of the basin, with the floodwaters bringing positive or negative impacts depending on the extent and duration of each season's flood event. Because of the strong seasonality of rainfall, drought is also a feature of life in the basin, with some regions more prone to drought conditions than others. Both the frequency and intensity of drought and flood may be impacted by a changing climate.

1.3. Previous studies on climate change in the Mekong Basin

Other studies have investigated the impact of climate change on future climate and water resource availability in the Mekong Basin (Hoanh et al., 2003; Snidvongs et al. 2003; The Government of Vietnam 2003; Chinavanno, 2004a; Snidvongs et al. 2006; Kiem et al. 2008). However, most of these studies have used a single or only a limited number of global climate model simulations to represent the future climate. Thus they have not quantified the uncertainty around future climate projections. None of these studies compares the GCMs from the IPCC 4th Assessment to determine which best represent the climate of the Mekong basin through comparison with historic climate data. The results from these studies indicate broadly similar responses in future climate. Temperatures are projected to increase across the basin by varying amounts. In general, wet season rainfall is projected to increase, and dry season rainfall to decrease in some months in some areas.

1.4. Water resources assessment using the water account model

We assessed the impacts of climate change on water resources in the Mekong Basin using a water account model (Kirby et al. 2008a). We have applied this accounting method to several major river basins including the Murray-Darling, Yellow River, Indus, Ganges, Karkheh, Nile, Limpopo, Niger, Sao Francisco and Volta basins. Water use accounts provide an understanding of basin function. The water accounts are dynamic, with a monthly time step, and thus account for seasonal and annual variability. They can also examine dynamic effects such as climate change, land use change, changes to dam operation, etc. The accounts are simple to modify and customise to suit the particular situation in a basin, or to investigate the response of related variables. For example, the Mekong Basin account has been customised to allow simulation of the reverse flows in the Tonle Sap River, and the melting of snow and glaciers in the Upper Mekong. It has also been modified to estimate flood volumes and duration of flooding from modelled flows.

There are other models of the Mekong Basin. They include:

- SWAT / IQQM / ISIS suite (Podger et al, 2004)
- MIKE11, lower floodplains only (Fujii et al, 2003; Morishita et al, 2004)
- SLURP (Kite, 2001)
- RAM (relies on SWAT/IQQM inputs, and only perturbs them) (Johnston and Rowcroft 2003)
- Economic – hydrology model of Ringler (2001).

The first three models are the most comprehensive models of basin hydrology, and are suitable for detailed studies. However, they require considerable effort and are less suited to the quick scoping study reported here. They also require some modifications to simulate climate change in the upper basin. The MIKE11 model does not deal with the whole of the basin. The last two models integrate water use and hydrology with economics, but do not deal with all aspects of the water use. The RAM model deals mainly with flows, with the runoff inflows supplied by the SWAT/IQQM suite. Thus, it cannot deal with the climate change scenarios, for example, unless the scenario is first run with the comprehensive suite, and the results used as an input to the RAM. The economic - hydrology model of Ringler (2001) deals only with average conditions and does not deal with runoff inflows.

Given the short timeframe of the project and the objective of identifying critical regions and issues, the water account model was judged to be an appropriate tool for rapid preliminary analyses of the likely impacts of climate change on water resources in the Mekong basin. Analyses with a more complex model would preclude the use of outputs from a number of GCMs, required to quantify the uncertainty around future climate projections.

2. DESCRIPTION OF THE MEKONG BASIN

The Mekong River Basin includes the Mekong River and its network of tributaries and drains in parts of six countries namely Cambodia, China, Lao PDR, Myanmar, Thailand and Vietnam. The river originates in the Tangelo mountain range in Qinghai province of China. Its length within China is around 2161 km. Below China, the river flows through countries of the Southeast Asian peninsula to the south of Ho Chi Minh City where it discharges to the South China Sea. The part of the Mekong River Basin within China and the eastern end of Myanmar is known as the Lancang or Upper River Basin (UMRB) and lower part is known as the Lower Mekong River Basin (LMRB). The UMRB is largely mountainous whereas LMRB is predominantly lowlands and floodplains. The LMRB covers approximately 70% of the basin and is the most important region both economically and environmentally. Out of total catchment area of 795,000 km², around 25% lies in the Lao PDR, 23% in Thailand, 21% in Yunnan (China), 20% in Cambodia, 8% in Vietnam and only 3% is part of the Myanmar.

2.1. Basic hydrology of the Mekong Basin

The hydrology of the Mekong Basin is described in greater detail in MRC (2005). Here we give a brief summary. The Mekong Basin covers about 790,000 km², and is drained by the 4200 km long River Mekong. The basin is mostly long and thin, particularly in the upper, Chinese part, and the Mekong is fed mostly by many short tributaries draining small catchments (Figure 2.1 and Table 2.1). The largest catchments are the Mun-Chi (about 107,000 km²), the Se San (73,000 km²) and the Tonle Sap (87,000 km²).

The climate of the region ranges from cold temperate and tundra in the UMRB to typically tropical monsoonal in the LMRB. The source of the Mekong is fed by snowmelt, though precipitation is much less than throughout the Lower Mekong (Figure 2.2). The Lower Mekong is fed by runoff, characterised by a pronounced wet and dry season. The peak flow from the Upper Mekong more or less coincides with the peak inflows from runoff into the Lower Mekong. Furthermore, the wet season affects the whole of Lower Mekong more or less simultaneously (Figure 2.2).

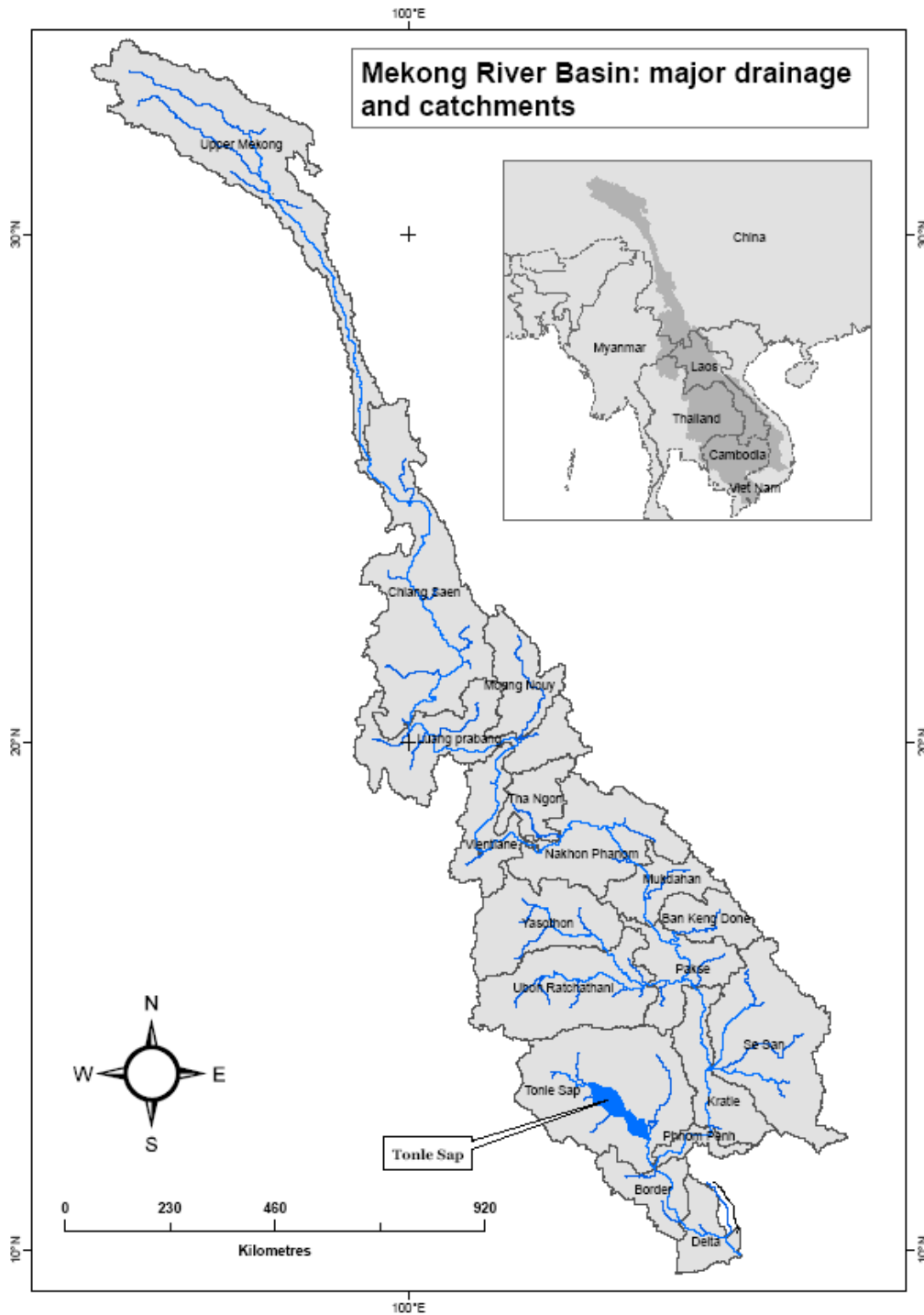


Figure 2.1. The Mekong Basin with the 18 catchments used in the water use account.

Table 2.1 Catchments in the Mekong Basin with their areas.

Catchment	Location	Area, km ²
Mekong	Upper Mekong	90771
Mekong	Chiang Saen	102936
Moung Nouy	Moung Nouy	26044
Mekong	Luang Prabang	56801
Mekong	Vientiane	28349
Nam Ngum	Tha Ngon	17695
Mekong	Nakhon Phanom	53085
Mekong	Mukdahan	21081
Se Bang Hieng	Ban Keng Done	18050
Chi	Yasothon	45368
Mun	Ubon Ratchathani	61812
Mekong	Pakse	29224
Se San	Se San	73232
Mekong	Kratie	31103
Mekong	Tonle Sap	87192
Mekong	Phnom Penh	7901
Mekong	Border	20167
Mekong	Delta	17362
Total		788173

Note: the area of the Mekong Basin is often given as 795,000 km², though the exact area depends on what is classified as inside the basin in the area around the delta. Different maps show different areas around the delta. The area of 788,173 km² given in the table is the area used in the water use account spreadsheets.

The rainfall is greater in the eastern, mountainous regions of Lao PDR, from which a major portion of the runoff and flow is generated. The rainfall in NE Thailand is less, and the potential evapotranspiration somewhat greater than the rest of the basin, and this area contributes the smallest portion of the runoff and flow.

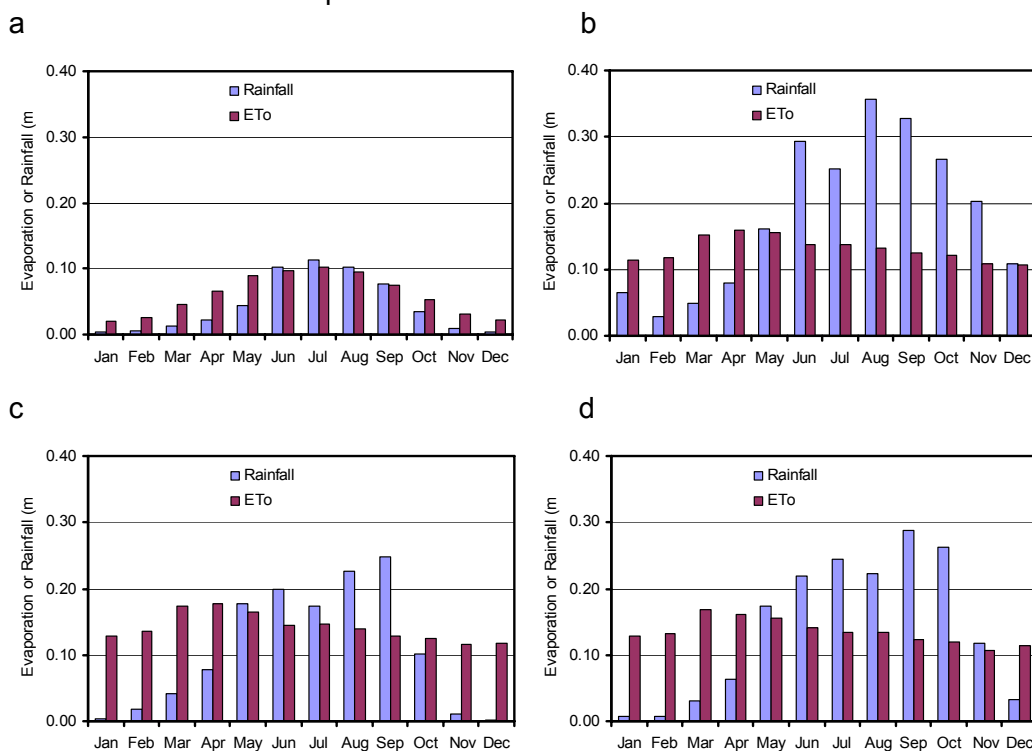


Figure 2.2. Monthly average rain and potential evapotranspiration in the Mekong Basin: a. Upper Mekong; b. Se Bang Hieng in central Laos; c. Chi in NE Thailand; d. Lower Mekong around Phnom Penh.

In addition to the spatial variability of precipitation, there is considerable year-to-year variability (Figure 2.3).

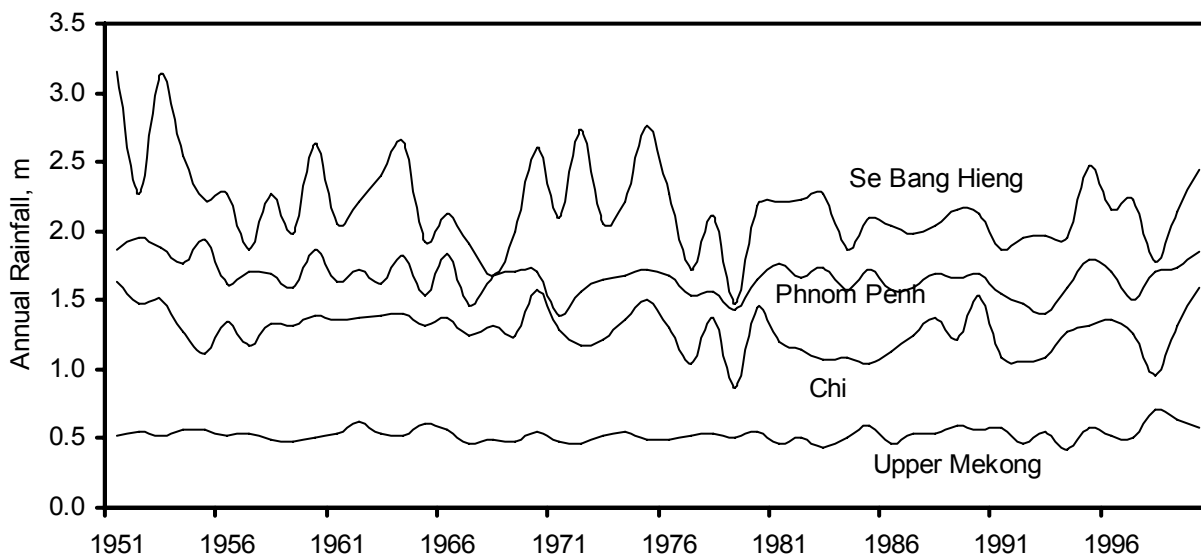


Figure 2.3. Annual rainfall 1951-2000.

2.2. Land use

Due to the contrasting landforms and climate, land use shows considerable diversity across the Mekong Basin. We estimated the area under different land uses using a combination of data sources, so that we could account for the water use of different land use classes. The area of all land use classes except irrigated agriculture was derived from the USGS land use/land cover classification (<http://edcsns17.cr.usgs.gov/glcc/>) (Figure 2.4). We assumed that the area of irrigated land in the USGS land use/land cover was inaccurate, since it was much greater than the area estimated by other credible local sources e.g. The State of the Basin report (MRC, 2003). We used a Global Irrigation Area Map (GIAM - <http://www.iwmiqiam.org/info/main/index.asp>) to estimate the area of irrigated land in different classes (surface water irrigated; groundwater irrigated; irrigated by conjunctive use of surface and groundwater (Figure 2.5). Areas recorded as irrigated land by the USGS data but not mapped by GIAM were recoded to the rain fed agriculture class. Additional areas mapped by GIAM as “conjunctive use” were also recoded to the rain fed agriculture class as the area of conjunctive use was much greater than the area using groundwater for irrigation estimated by other credible local sources e.g. The State of the Basin report (MRC, 2003). A final aggregation of land use classes was performed to produce the simple land use classification used in the water accounting model (Figure 2.6). The classes include Forest, Irrigated agriculture; Rain fed agriculture, Woodland/grassland, Water/wetland and Other.

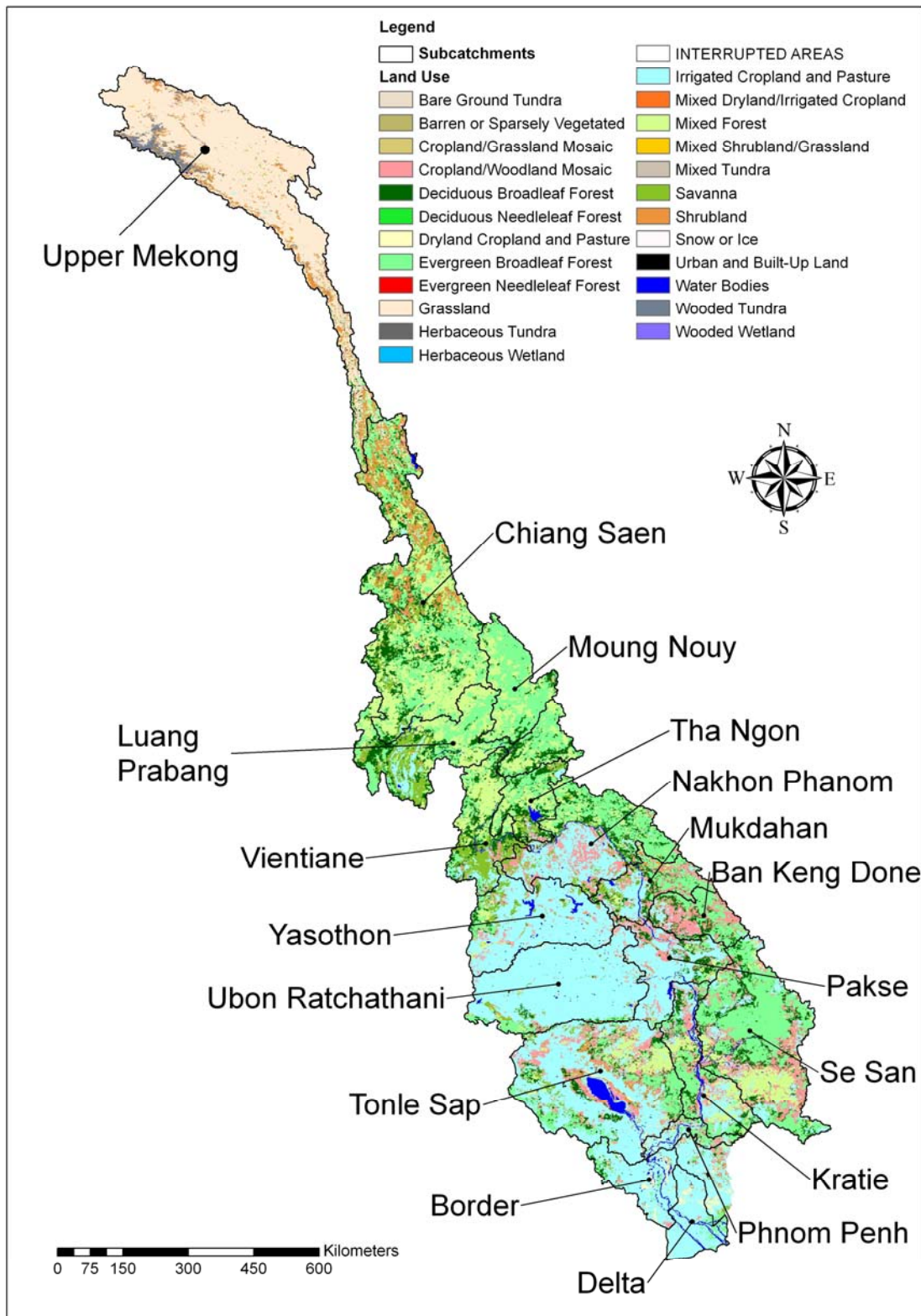


Figure 2.4. Land cover/land use map

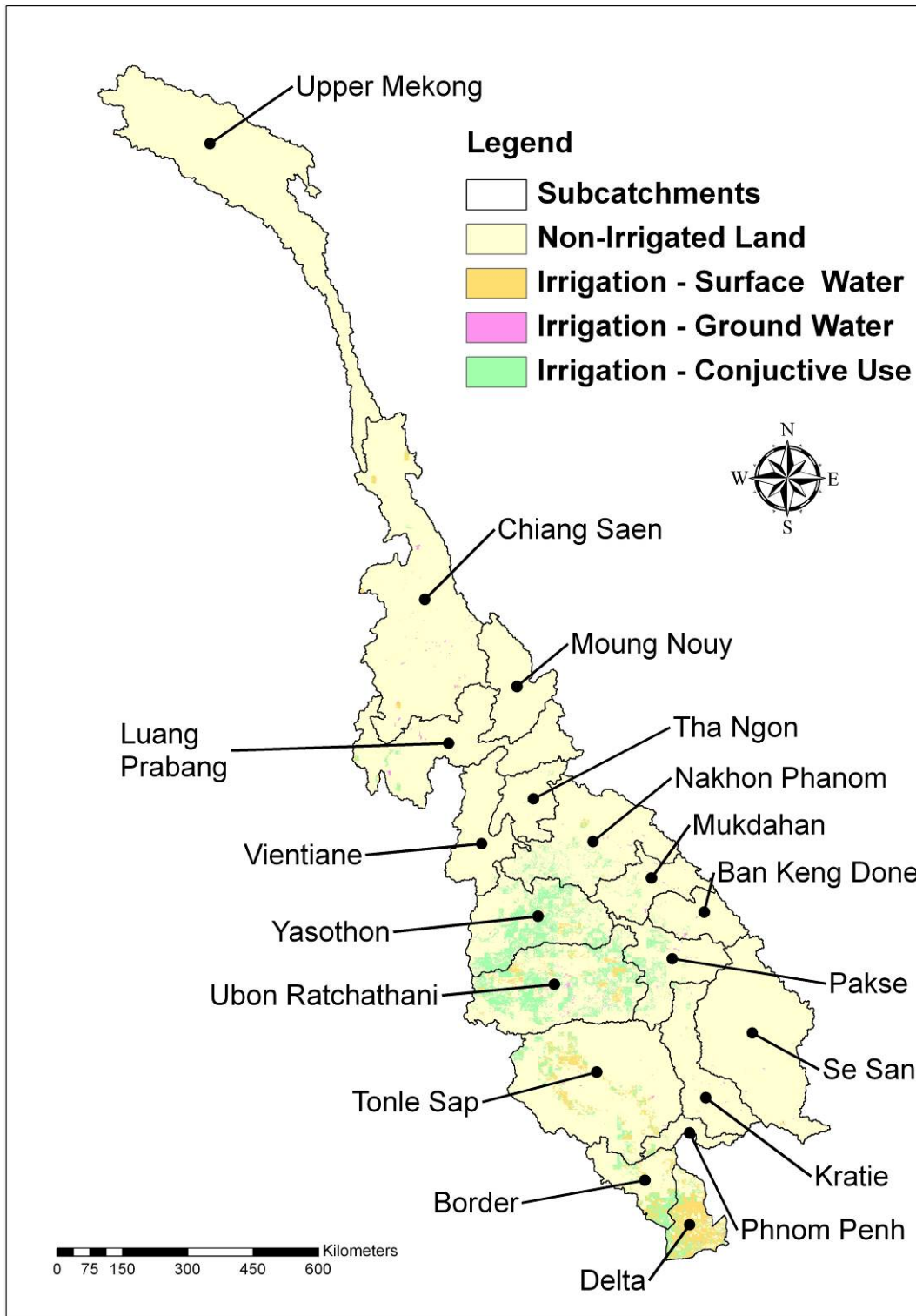


Figure 2.5. Mapped irrigation areas reclassified to 3 broad categories.

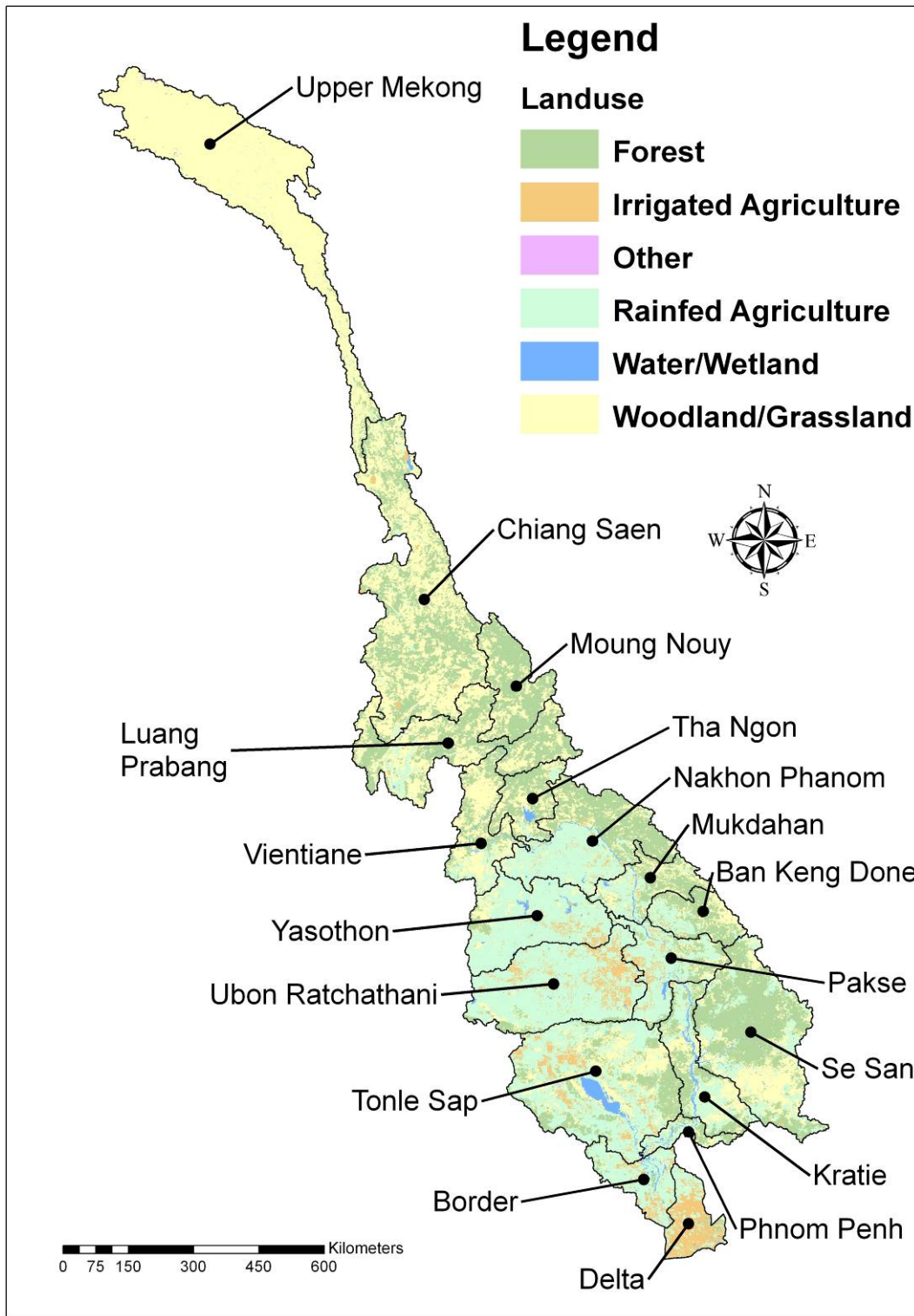


Figure. 2.6. Land use map based on USGS land cover/land use data. Classes aggregated for modelling purposes

2.3. Population

The estimates of the population in the Mekong Basin around the year 2000 range from 58 to 73 million people. Kristensen (2001) estimates the population of the Mekong basin as 73 million and predicts that will grow to 120 million by 2025. Pech and Sunada (2008) note the uncertainty in population growth in the region and estimate that population grew from 63 million in 1995 to 72 million in 2005. Given this rate they expect population to at least double by 2050. Hoanh et al. (2003) approximate the population of the Mekong Basin as 65 million in 1995-2000 with about 55 million of these in the Lower Mekong Basin (LMB). Based on a 2% growth rate they conclude that the population will reach 132 million by 2030. Similarly, Hirsch and Cheong (1996) estimate the population at 60 million with 50 million residing in the LMB. This uncertainty is not surprising given that the Basin covers 6 different countries and many administrative areas which may lead to a lack of consistency in census data collection and frequency. Estimates can also vary due to the extent of the basin boundary in the Mekong Delta region where drainage is ill defined and population density is highest.

2.3.1. Methods of estimating population in 2000 and 2030

For this study, we quantified the population for catchments of the basin for the year 2000 (Figure 2.7) using Gridded Population of the World, Version 3 (GPWv3) data obtained from the Social Economic Data and Applications Center (SEDAC) website (<http://sedac.ciesin.columbia.edu/gpw/country.jsp?iso=GNQ>). We used SEDAC data from their Global Rural-Urban Mapping Project (GRUMP) to quantify urban and rural populations in each country for each catchment (Figure 2.8).

We used two approaches to estimate the 2030 population for each catchment of the basin. In the first, we used United Nations Population Division (UNPD) data on urban and rural growth rates (Table 2.2) for each country (<http://esa.un.org/unup/index.asp?panel=1>). These growth rates attempt to account for urbanisation and the migration of rural populations to urban populations as well as factors such as AIDS, fertility, ageing and death rates and abortion and contraceptive use. We applied these growth rates to our 2000 estimate of urban and rural population for each country in each catchment to estimate populations in 2030.

Table 2.2. Quinquennial rural and urban growth rates for Mekong Basin countries used to calculate population projection for 2030.

Country	Population Type	2000-2005	2005-2010	2010-2015	2015-2020	2020-2025	2025-2030
	Burma	Rural	0.15	-0.11	-0.31	-0.51	-0.71
	Urban	2.68	2.88	2.7	2.51	2.31	2.08
Cambodia	Rural	1.07	0.96	0.91	0.72	0.42	0.1
	Urban	4.84	4.64	4.48	4.19	3.79	3.42
China	Rural	-0.83	-1	-1.08	-1.17	-1.28	-1.5
	Urban	3.1	2.7	2.37	2.03	1.67	1.36
Laos	Rural	0.18	0.06	-0.14	-0.32	-0.47	-0.6
	Urban	6.02	5.56	4.8	4.07	3.36	2.7
Thailand	Rural	0.42	0.17	-0.18	-0.52	-0.88	-1.14
	Urban	1.49	1.66	1.75	1.83	1.88	1.73
Viet Nam	Rural	0.88	0.65	0.41	0.13	-0.17	-0.48
	Urban	3.13	3.08	3.02	2.91	2.79	2.6

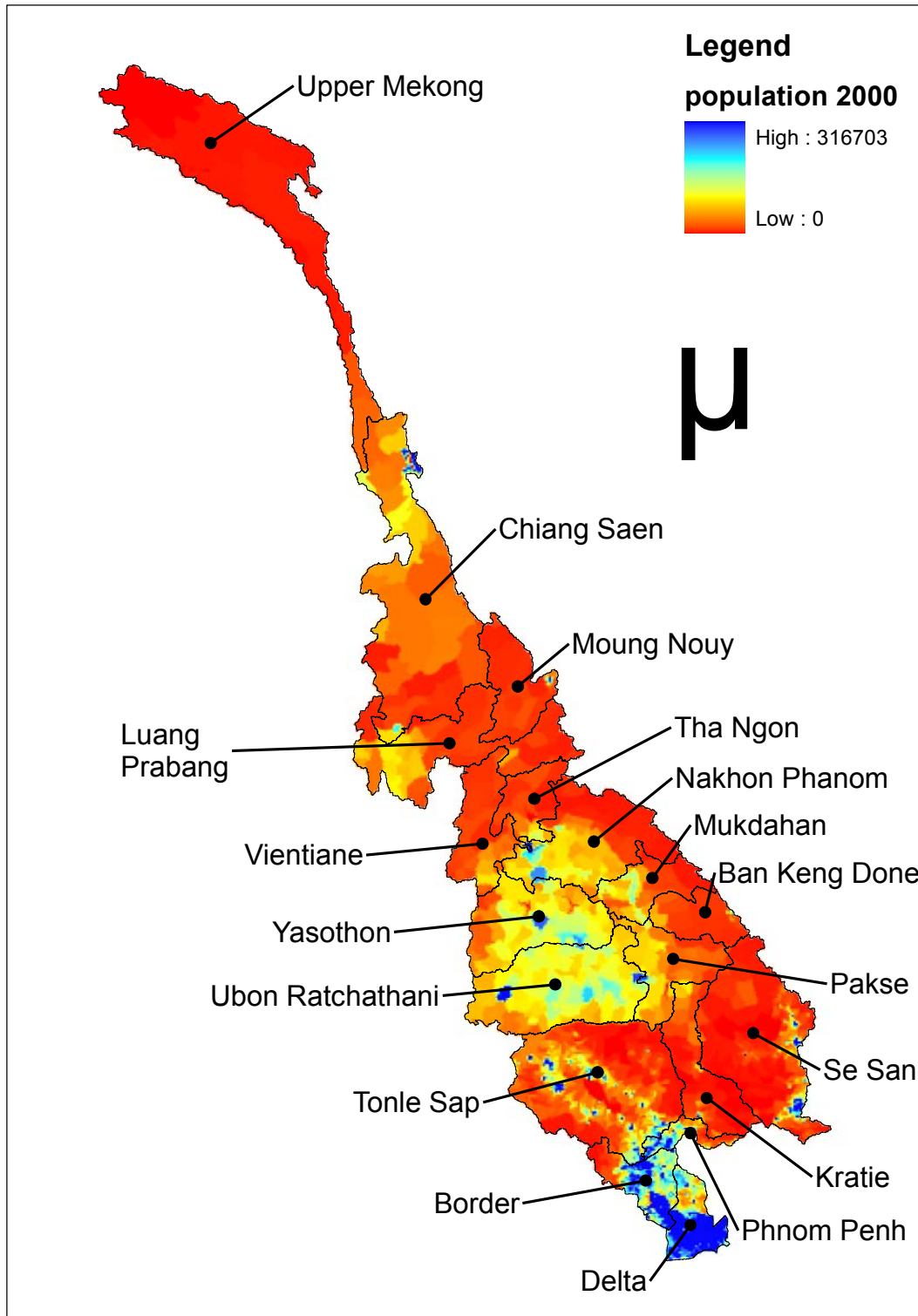


Figure 2.7. 2000 Population distribution

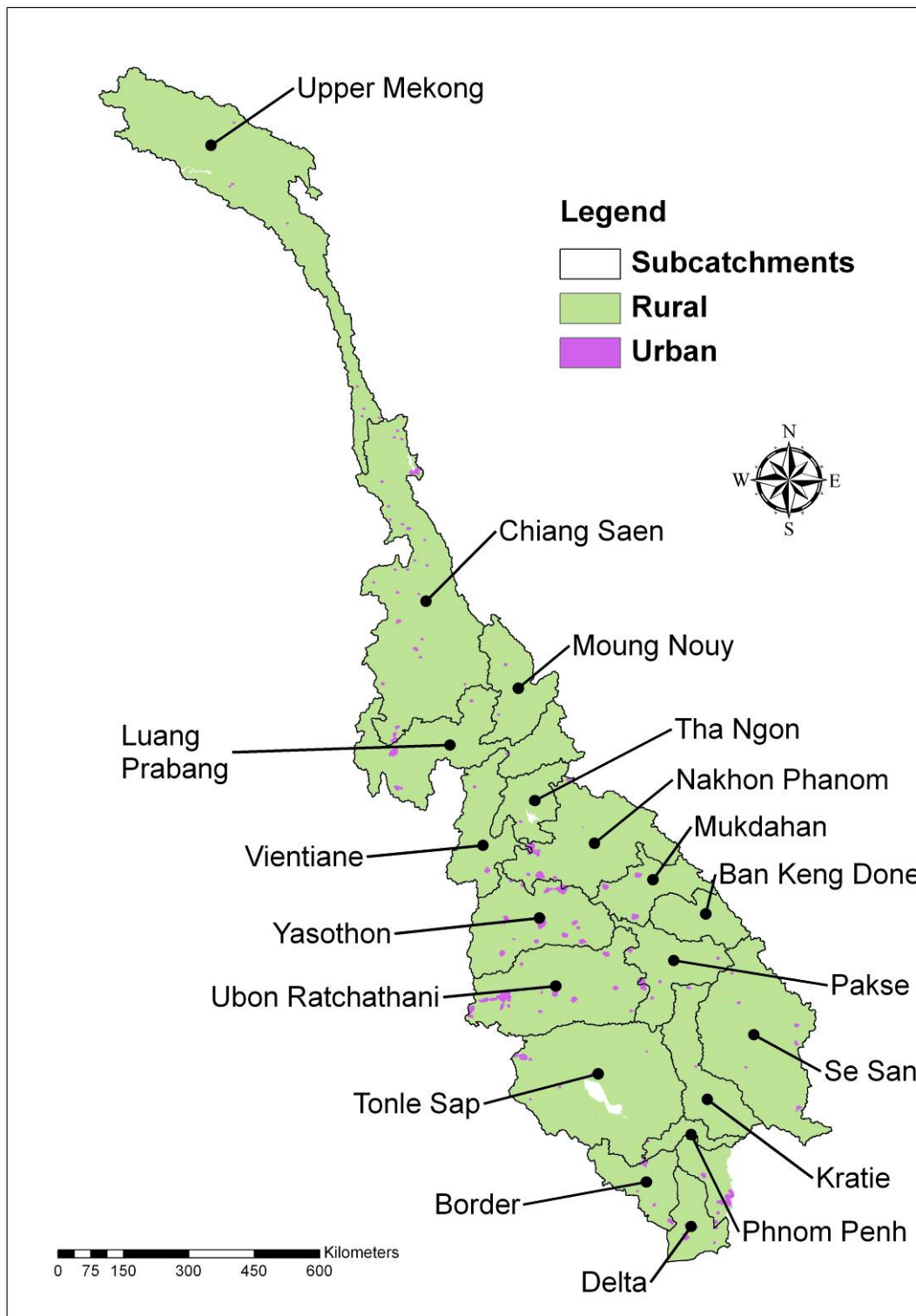


Figure 2.8. 2000 Population distribution for urban and rural areas

In the second approach to estimating 2030 population, we used the SEDAC data for the year 2015 (the last year of their projections) to estimate urban and rural populations at 2015 in each country and catchment. For the projections we used past population growth rates (pre 2015) as the basis for future population estimates. We used different growth rates for each category of population (country and urban or rural for each catchment).

2.3.2. Mekong Basin populations for 2000 and 2030

Our estimate of total populations for the Mekong basin for 2000 estimated from SEDAC data is ~ 58 million. The estimate for the Lower Mekong Basin is ~ 52 million, comparable to the population reported in 2003 as 55 million (MRC 2003). Our estimates of 2030 populations using the two approaches are quite different. Using the UNPD growth rates, our estimate of total basin population in 2030 is ~64 million, compared with ~ 111 million using the SEDAC data and method. Population projections for the Lower Mekong Basin are ~ 59 million for the UNDP based estimates, and ~ 104 million for the SEDAC based estimates. The difference in these estimates arises primarily from the different growth rates applied. The higher population estimate of ~ 111 million results from the application of past growth rates which were positive for both urban and rural populations. In contrast, UNDP growth rates show differential responses in rural and urban populations. In all of the countries of the basin except Cambodia, negative growth rates are projected for rural populations for some intervals between 2000 and 2030 (Table 2.2). In contrast, urban populations are projected to increase in all countries throughout this thirty year period. Since our analyses for 2000 shows that urban populations account for only 9% of the total population, the future estimate for 2030 shows only modest growth using this approach. The disparity in the two estimates may also arise because UNDP growth rates are based on country level data. There may be regional differences in growth rates within a country, with the portion within the Mekong Basin responding differently to the country-wide growth rate. The SEDAC based estimates of 2030 population were used in future (2030) analyses of impacts of climate change, since this estimate was closer to other published population projections for the basin. For example, the Mekong River Commission estimates the population to increase to 90 million by 2025 (MRC 2003).

There is large variability between catchments of the basin in both urban and rural populations in 2000, and in projected populations in 2030 (Figure 2.9). Our analyses show that the population will increase in all catchments of the basin by 2030, with urban populations generally showing greater growth than rural populations. There is great variation between catchments in both the total population and population densities (Figure 2.1) in 2030. Population density in catchments of the basin ranges from ~8 people/km² in the Upper Mekong to ~460 people/km² in the Delta in 2000. Population growth is the greatest in the catchments towards the south of the basin (Tonle Sap, Phnom Penh, Border and Delta). By 2030, the variation between catchments in population density is estimated to be more extreme, with 11 catchments having low population density (< 100 people/km²), whilst population density in the downstream delta catchment reaches ~1800 people/km².

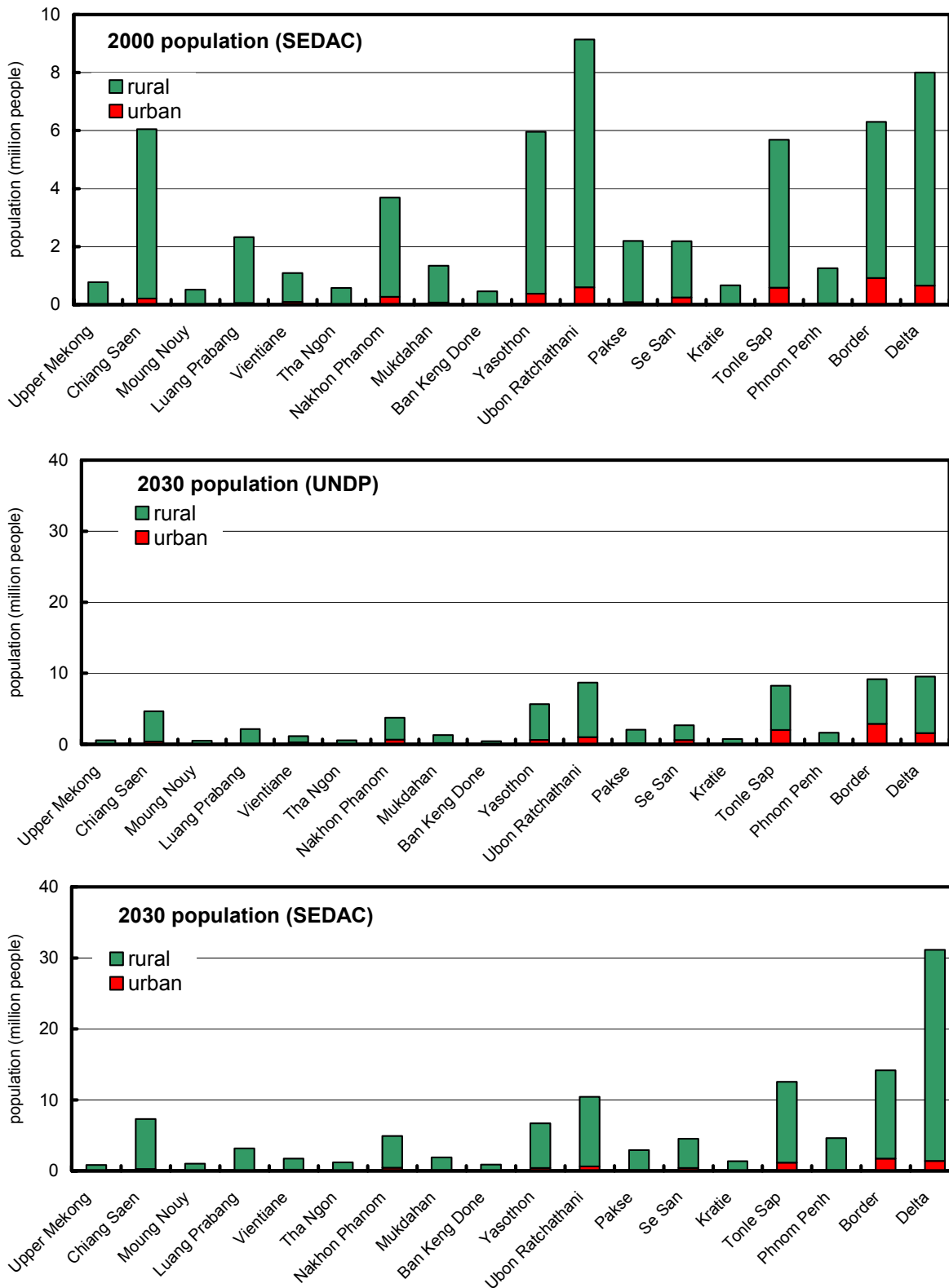


Figure 2.9. Urban and rural population in 2000 and future (2030) populations estimated using UNDP and SEDAC growth rates for catchments of the Mekong Basin.

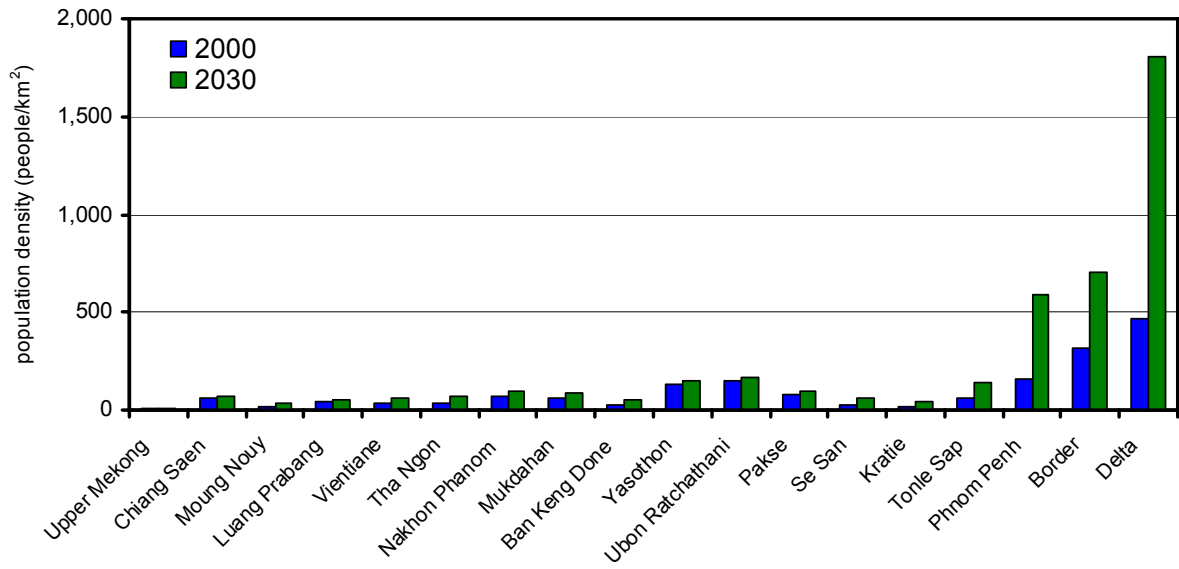


Figure 2.10. Population density in 2000 and projected (SEDAC) population density in 2030 for catchments of the Mekong Basin.

3. CLIMATE ANALYSES

3.1. Observed data

Historical monthly time series of precipitation and temperature for the Mekong Basin were extracted from the CRU_TS_2.10 dataset of the Climate Research Unit at the University of East Anglia, available at <http://www.cru.uea.ac.uk/cru/data/> website. This is a global dataset on a 0.5°x 5° grid (about 50 km resolution), for 1901 to 2002. The dataset was constructed by interpolating observed values. We extracted data on the grids over the Mekong Basin to construct monthly area-averaged time series of precipitation and temperature from the temporal surfaces of data for 18 major catchments in the Mekong River Basin. The Hargreaves method was used to estimate monthly potential evapotranspiration from temperature data (Hargreaves and Samani, 1982). The method is described in more detail in Kirby et al. (2007).

3.2. Simulated data

Simulations of monthly time series of precipitation and temperature for the 20th century (1901-2000) and for the 2001-2100 climate under global warming by the mid-range emission scenarios (SRES A1B) were used. Data from 24 Global Climate Models (GCMs) listed in Table 3.1 were downloaded from the website of the Programme for Climate Model Diagnosis and Intercomparison (PCMDI), (<https://esg.llnl.gov.8433/index.jsp>). We extracted data for grids over the Mekong Basin. The 1960-1999 data were spatially averaged over 18 major catchments to constitute catchment mean monthly precipitation and temperature time series for respective catchments. The simulated historical data were used in conjunction with observed data in the assessment of the performance of GCMs for model selection and the 1901-2100 gridded data were used in the derivation of patterns of change in precipitation and temperature.

3.3. GCM selection and methodology for future climate projections

Global Climate Models are the best tools available for making climate change projections. Patterns of climate change for the Mekong Basin are readily obtainable from GCMs' simulations. However, there are significant differences between GCMs with regard to climate changes simulated at the regional scale, particularly for precipitation. Thus to represent this uncertainty results from a range of GCMs are commonly used in the construction of regional projections. To select a suitable set of GCMs from 24 GCMs used in the AR4 report of the Intergovernmental Panel on Climate Change (IPCC), we used statistical methods to objectively quantify the relative ability of each model in simulating climate over the Mekong Basin. The methodology we applied in selecting climate change models, and data to support our selection are described fully in Appendix 1.

Models were selected on their capacity to represent seasonal temperature and precipitation for wet (May to October) and dry (November to April) seasons (Figures 11.5 and 11.6). A total of 11 models were selected (ncar_ccsm3_0; miub_echo_g; micro3_2_medres; micro3_2_hires; inv_echam4; giss_aom; csiro_mk3_0, cnrm_cm3, cccma_cgcm3_1_t63; cccma_cgcm3_1 and bccr_bcm2_0) and used to make climate changed projections described in the chapters which follow.

Table 3.1. List of GCMs recommended by the Intergovernmental Panel on Climate Change (IPCC). Models selected for the construction of climate scenarios for the Mekong basin are shown in bold letters.

Country and groups of origin	GCM Model	Horizontal resolution (km)
Bjerknes Centre for Climate Research, Norway	bccr_bcm2_0	~200
Canadian Climate Centre, Canada	cccma_cgcm3_1	~300
Canadian Climate Centre, Canada	cccma_cgcm3_1_t63	~200
Meteo-France, France	cnrm_cm3	~200
CSIRO, Australia	csiro_mk3_0	~200
CSIRO, Australia	csiro_mk3_5	~200
Geophysical Fluid Dynamics Lab, USA	gfdl_cm2_0	~300
Geophysical Fluid Dynamics Lab, USA	gfdl_cm2_1	~300
NASA/Goddard Institute for Space Studies, USA	giss_aom	~300
NASA/Goddard Institute for Space Studies, USA	giss_model_e_h	~400
NASA/Goddard Institute for Space Studies, USA	giss_model_e_r	~400
LASG/Institute of Atmospheric Physics, China	iap_fgoals1_0_g	~300
National Institute of Geophysics and Volcanology, Italy	ingv_echam4	~300
Institute of Numerical Mathematics, Russia	inmcm3_0	~400
Institute Pierre Simon Laplace, France	ipsl_cm4	~300
Centre for Climate Research, Japan	miroc3_2_hires	~125
Centre for Climate Research, Japan	miroc3_2_medres	~300
Meteorological Institute of the University of Bonn, Meteorological Research institute of KMA, Germany/Korea	miub_echo_g	~400
Max Planck Institute for Meteorology DKRZ, Germany	mpi_echam5	~200
Meteorological Research Institute, Japan	mri_cgcm2_3_2a	~300
National Centre for Atmospheric Research, USA	ncar_ccsm3_0	~150
National Centre for Atmospheric Research, USA	ncar_pcm1	~300
Hadley Centre, UK	ukmo_hadcm3	~300
Hadley Centre, UK	ukmo_hadgem1	~125

Scenarios of change in temperature and precipitation for the period centred 2030 for the A1B SRES were constructed from simulations by the selected 11 GCMs using a simple pattern scaling approach similar to that used by Whetton *et al.* (1994). Since it is simple to implement, the method may be applied to outputs from a number of GCM simulations allowing assessment of the uncertainty associated with global warming and local climate change projections. Analysis of GCM rainfall and temperature simulations have shown that patterns of regional climate change tend to scale linearly with global warming for different emission scenarios (Whetton *et al.* 2005, Ruosteenoja *et al.* 2003). We analysed each of the selected 11 GCM simulations to extract patterns of mean temperature change and precipitation change over the Mekong Basin. The climate response was calculated at each grid point in terms of local temperature change (or per cent rainfall change with respect to 1961-1990) per degree of global warming using the 1901-2100 simulations. This was done by linearly regressing the local monthly mean temperature (or rainfall) against global average temperature and taking the slope of the relationship at each grid point as the estimated response. The grid point values were then averaged across each of the 18 major catchments to obtain respective patterns of change. Thus a change per degree of global warming multiplied by the global warming projected for 2030 gives a scaling pattern of change (factor). The IPCC estimated a global warming of 0.9 °C under the A1B scenario for the period centred 2030 (in Figure SMP-3 of the IPCC (2007) report).

We constructed scenarios of monthly time series of catchment temperature and precipitation for the period centred 2030 by scaling the historical monthly precipitation and temperature series of 1951-2002 period. Scenarios of potential evaporation were derived from temperature scenarios using the Hargreaves method (Hargreaves and Samani, 1982),

assuming the projected changes in maximum and minimum temperatures were the same as changes in the mean temperatures. It is important to note that using this using this downscaling approach, the future temporal distribution of precipitation and temperature depend on their distribution in the historical data. Thus the method does not allow investigation of the changing probability of extreme weather events due to climate change.

3.4. Projected changes in temperature for the Mekong Basin

3.4.1. Projected changes in basin-wide temperature

An increase in temperature of 0.68 to 0.81 is projected for 2030 over the Mekong basin as a whole (Figure 3.1). The best estimate in of the average increase of temperature over the Mekong basin represented by the median of GCM simulations is 0.79°C. This reflects a change in average temperature from 21.2 to 22.0 °C. The increase in temperature projected for different months ranges from 0.73 °C in October to 0.88 °C in March. Projected increases are generally smaller (< 0.75 °C) for the months of July to November, and more than 0.79 °C for the remaining months. There is some uncertainty in projections for basin temperatures, but all models indicate that temperatures will increase in all months compared with baseline temperatures.

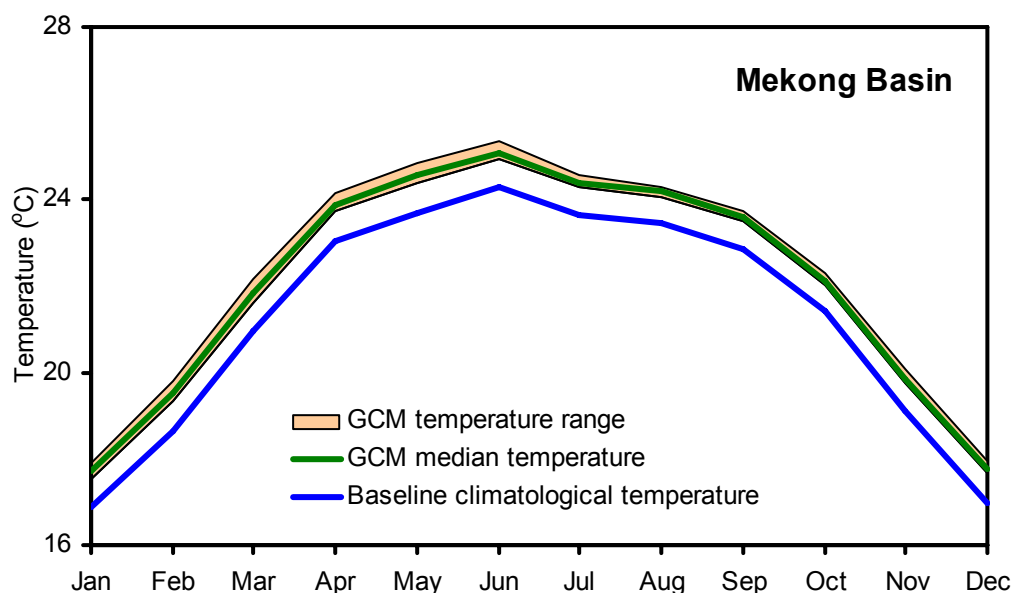


Figure 3.1. Baseline (1951-2000) versus future (2030) monthly mean temperature.

3.4.2. Projected changes in temperature for Mekong catchments

The spatial distribution of the response in mean temperature under the most likely climate projections for 2030 indicates a temperature increase of 0.7-0.8°C for the majority of catchments (Figure 3.2). Temperature increases tend to be greater towards the northern part of the basin, with the greatest increase (>1.0 °C) in the coldest Upper Mekong catchment, and increases from 0.8 to 0.9 °C in catchments of Northern Thailand and Laos. The smallest increases in projected temperature (0.8 to 0.9 °C) are for the Ban Keng Done and Mukdahan catchments.

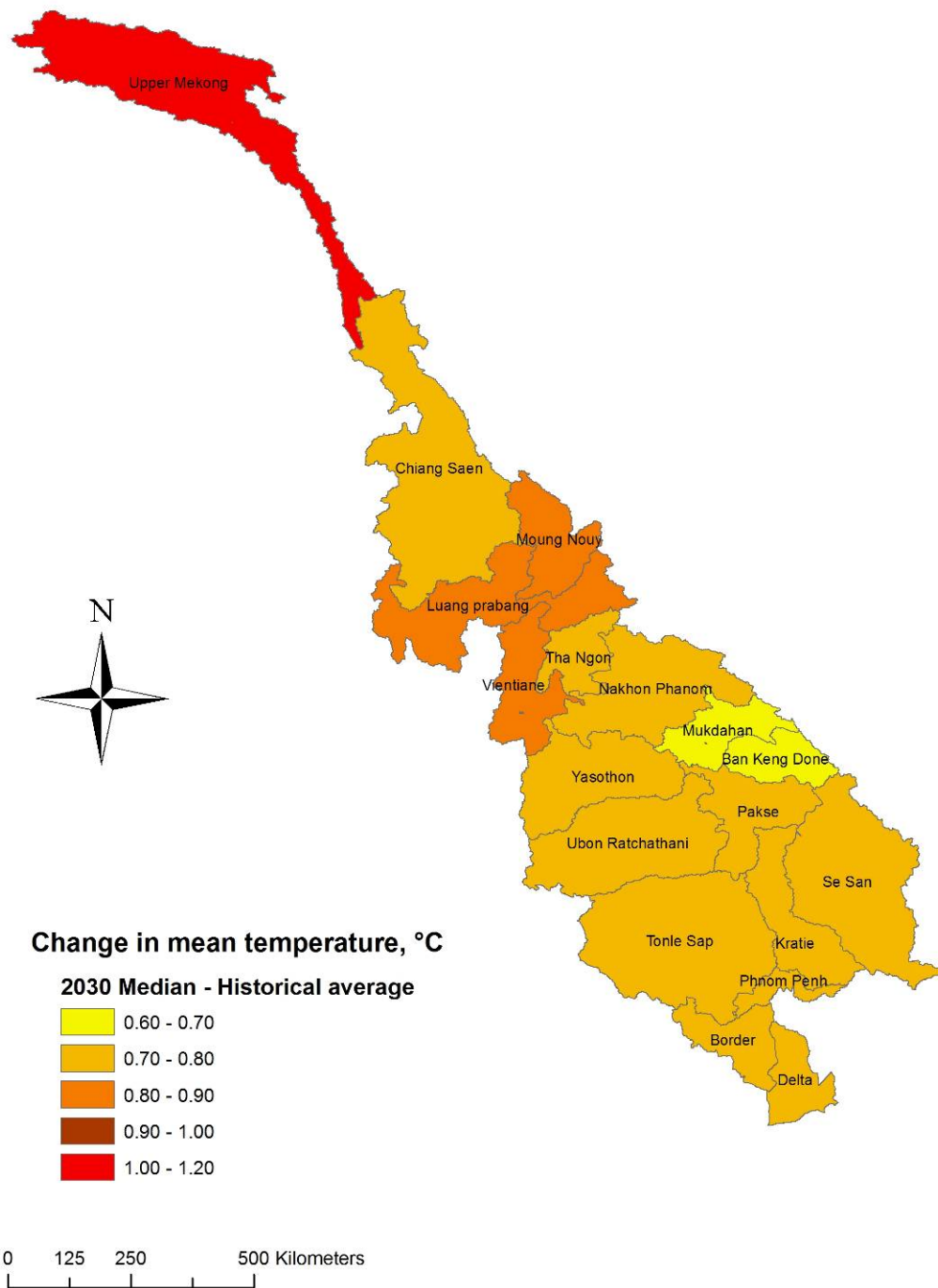


Figure 3.2. Spatial distribution of the projected change in mean temperature at 2030 compared with historical (1951-2000) mean temperatures.

The projected seasonal response in average temperature is generally similar across the catchments of the basin, with generally smaller increases in the months from July to November, and larger increases for the remaining cool/cold months (Figures 3.3 to 3.5). Thus the amplitude in seasonal variation in temperature will tend to be reduced. In all catchments of the basin, the range in projected temperatures is greater for all months than historic figures (Figures 3.3 to 3.5).

The largest most likely increase in monthly temperature by 2030 is in the Upper Mekong where the November temperature is projected to increase by 1.31 °C. Temperature increases are smaller for all other catchments of the basin, and there is less variation between the catchments in temperature increases. Projected increases are <1 °C for all months in all other basin catchments (Figures 3.3 to 3.5). The smallest temperature increases are for the Ban Keng Done catchment, where the largest projected increase in any month is less than 0.8 °C (Figure 3.4).

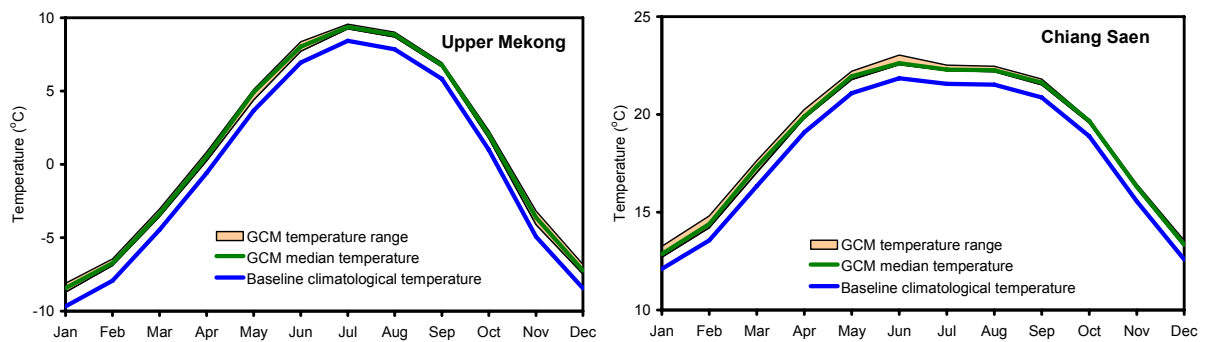


Figure 3.3. Baseline (1951-2000) versus future (2030) monthly mean temperature for catchments of the Upper Mekong basin: Upper Mekong and Chiang Saen.

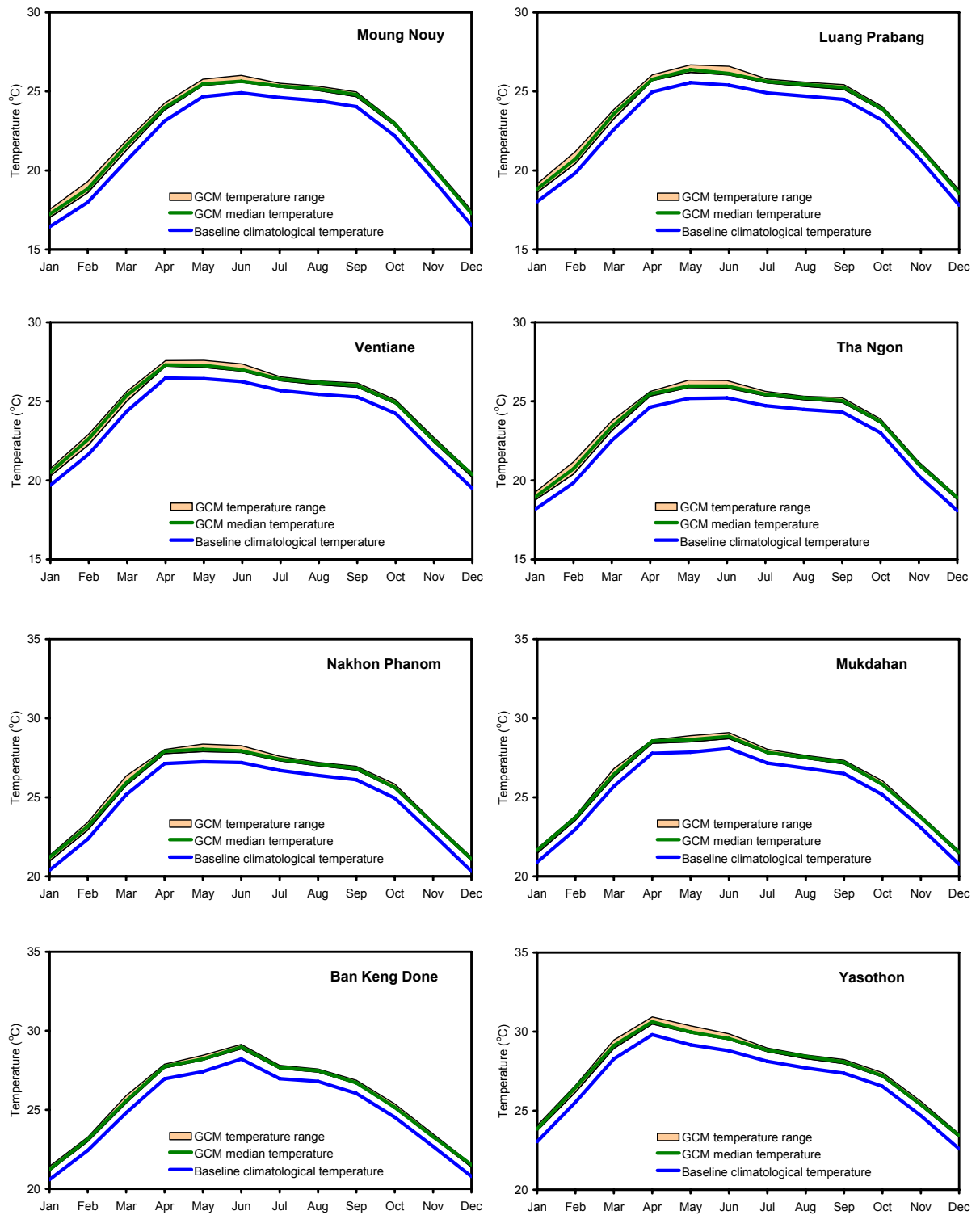


Figure 3.4. Baseline (1951-2000) versus future (2030) monthly mean temperature for Moung Noy, Luang Prabang, Vientiane, Tha Ngon, Nakhon Phanom, Mukdahan, Ban Keng Done and Yasothon catchments.

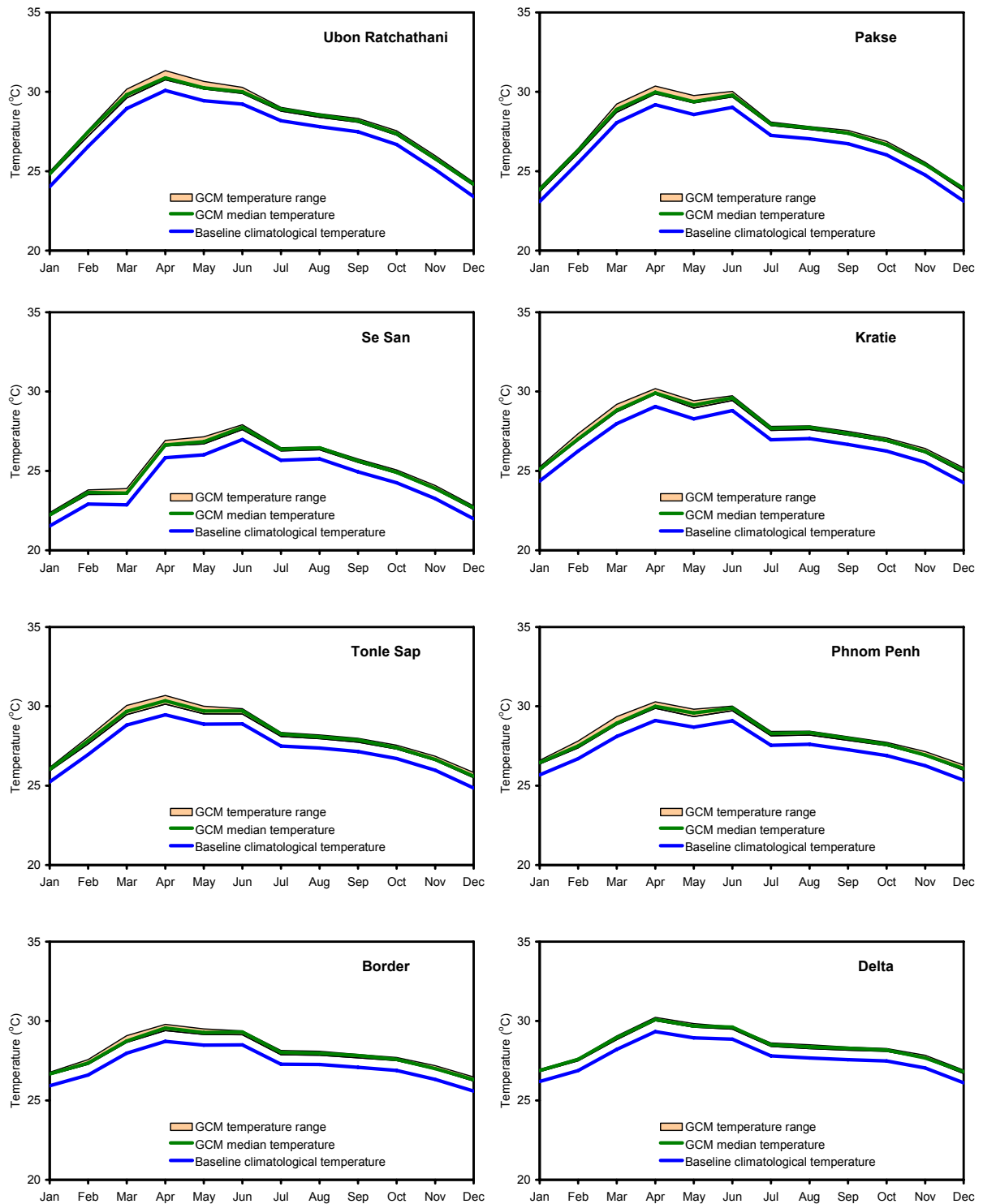


Figure 3.5. Baseline (1951-2000) versus future (2030) monthly mean temperature for Ubun Ratchathani, Pakse, Se San, Kratie, Tonle Sap, Phnom Penh, Border and Delta catchments.

3.5. Projected changes in precipitation for the Mekong Basin

3.5.1. Projected changes in basin-wide precipitation

The most likely projected change in annual precipitation for the Mekong Basin as a whole by 2030 is an increase from the historical mean of 1.509 m to 1.712 m (a 13.5% increase).

There is some uncertainty in the modelling results with the projections ranging from a 0.5% to a 36% increase in annual rainfall. The greatest changes are projected for the wet season months of May to September, when the 2030 median shows increased monthly precipitation ranging from 0.016 m in May to 0.056 m in September (Figure 3.6). The range in modelled precipitation is large for the wet season months, with decreases of up to 27% in some months or increases as large as 88% in others. The projected changes in dry season precipitation are much smaller, but the median projection indicates small decreases (<0.003 m) in mean monthly precipitation in February, March and November. No change in precipitation is projected for January and December, and a small increase of 0.002 m or 3% is projected for April. The drier extremes of the model projections indicate precipitation decreasing in all months in the dry season, with decreases of up to 25% from historic values. Other projections indicate precipitation increases in dry months of up to 22%.

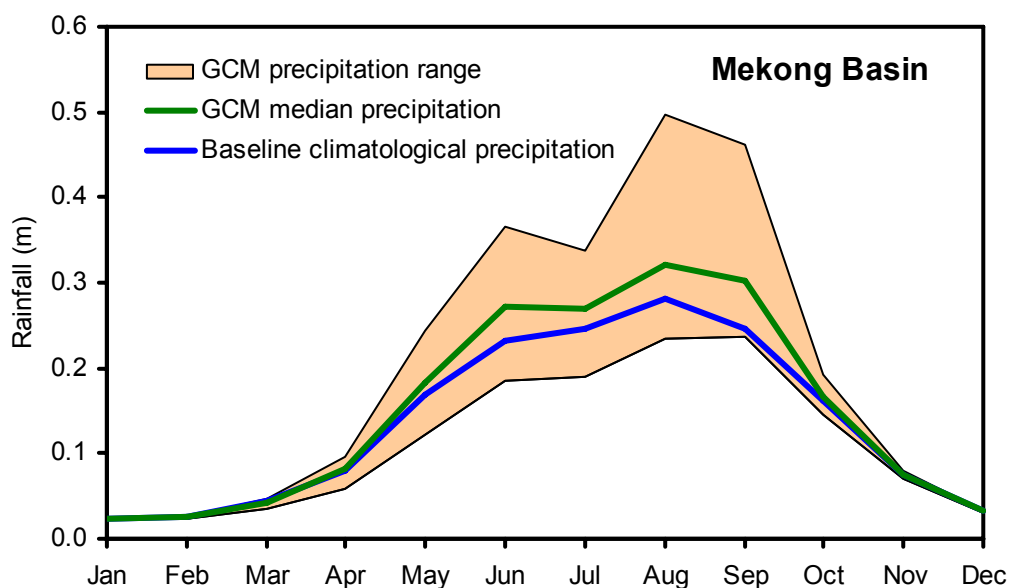


Figure 3.6. Baseline (1951-2000) versus future (2030) monthly mean precipitation.

3.5.2. Projected changes in precipitation for Mekong catchments

Although there is uncertainty in the modelling results, mean annual precipitation is likely to increase in all catchments of the basin under 2030 projections. The size of the projected increase shows considerable variation across catchments of the basin, ranging from the smallest increase of 0.03 m in Moug Nouy to the largest of 0.359 in Yasothon (Figure 3.7).

Projected increases in annual precipitation for all catchments result chiefly from an increase in precipitation during the wet season (May to October, Figure 3.8), which shows large variation across the basin (Figure 3.7). The response in projected dry season (November to April) rainfall is also spatially variable, but there is a trend of increasing dry season precipitation in the northern catchments of the basin and decreasing precipitation in the south (Figure 3.9). The disparity between wet and dry season precipitation will be accentuated for all catchments, but particularly for some of the catchments towards the south where both decreases in dry season and increases in wet season precipitation are greatest.

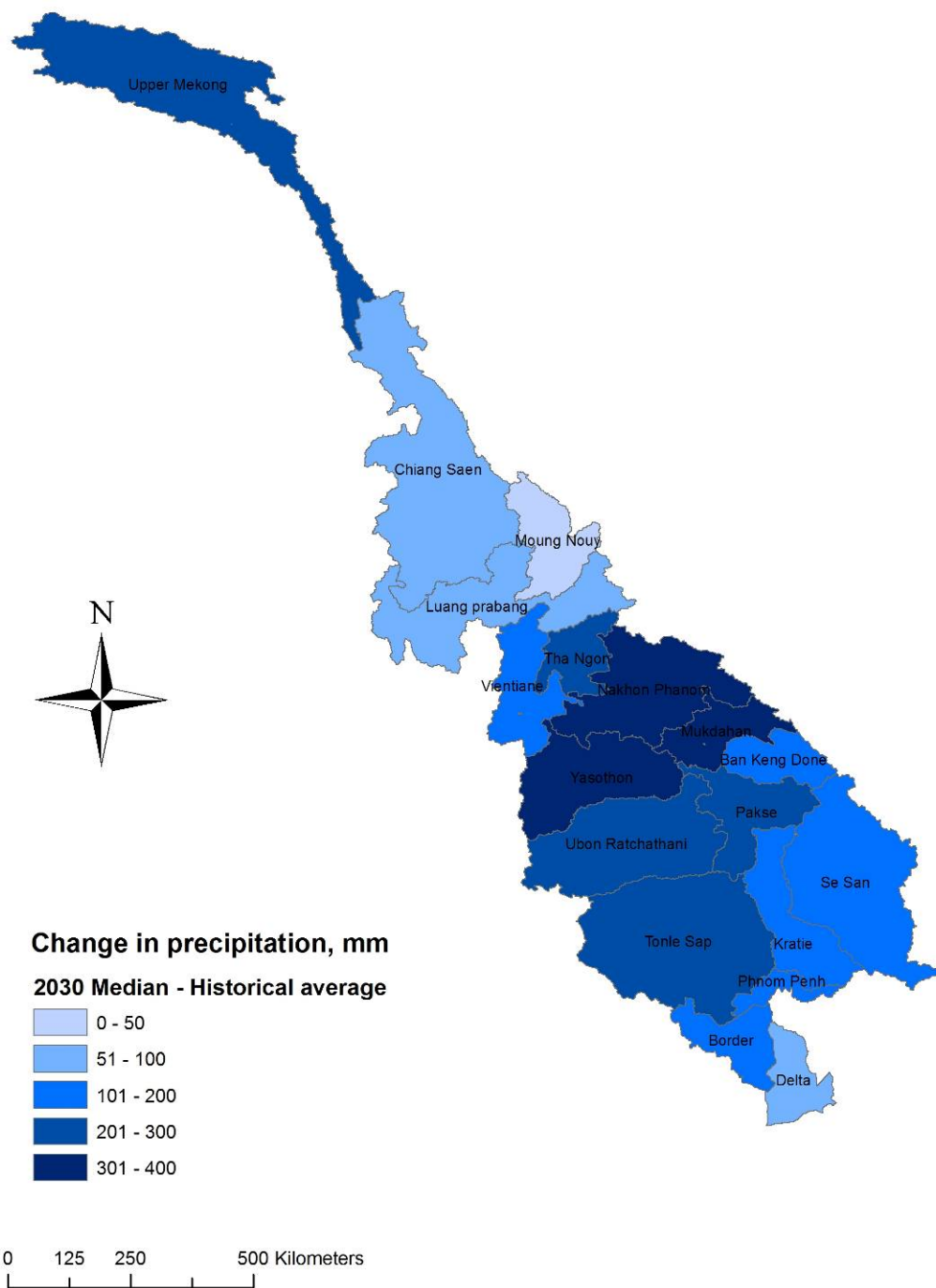


Figure 3.7. Spatial distribution of the projected change in mean annual precipitation at 2030 compared with historical (1951-2000) mean precipitation.

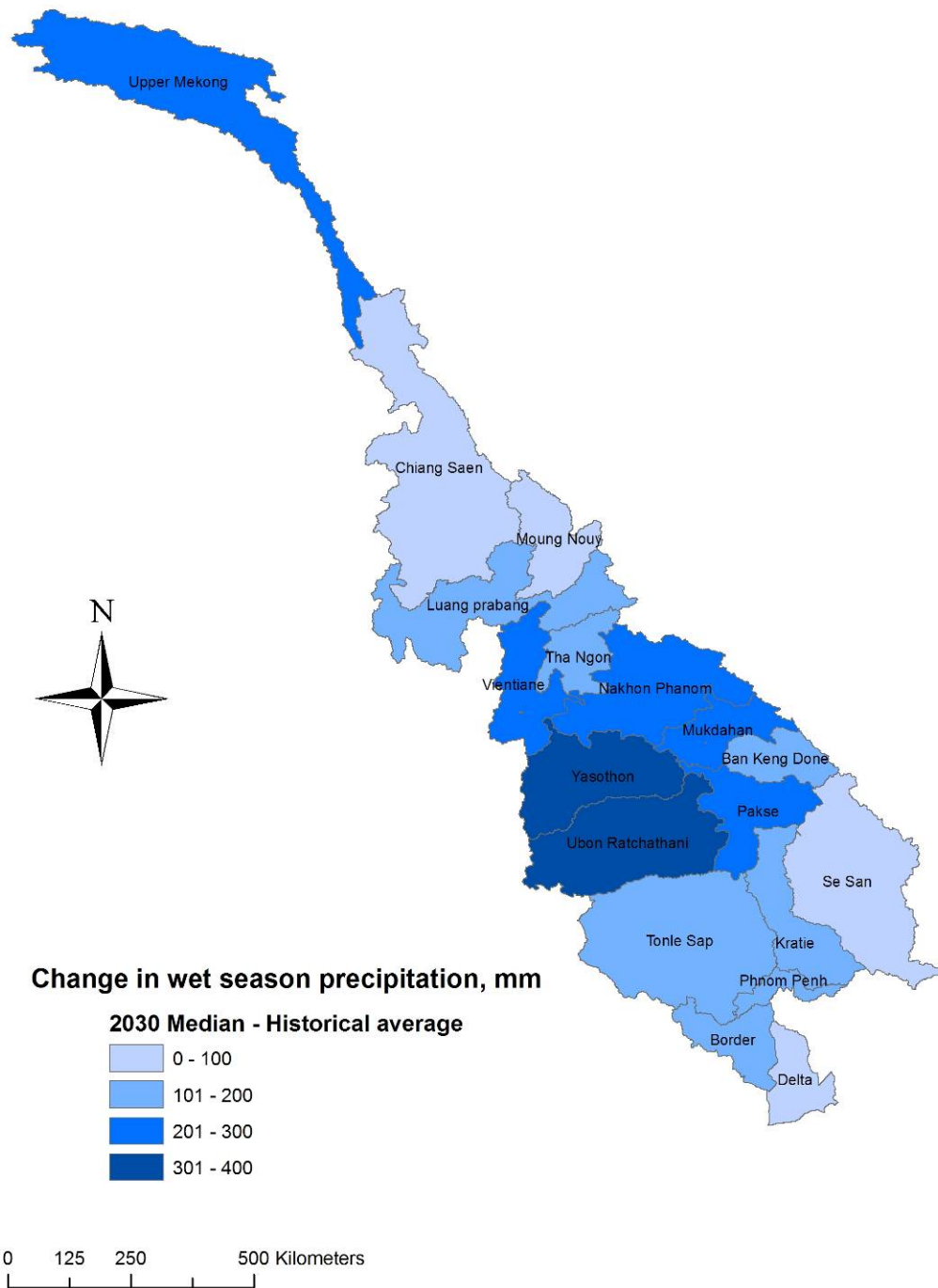


Figure 3.8. Spatial distribution of the projected change in precipitation during the wet season (May to October) at 2030 compared with historical (1951-2000) mean precipitation.

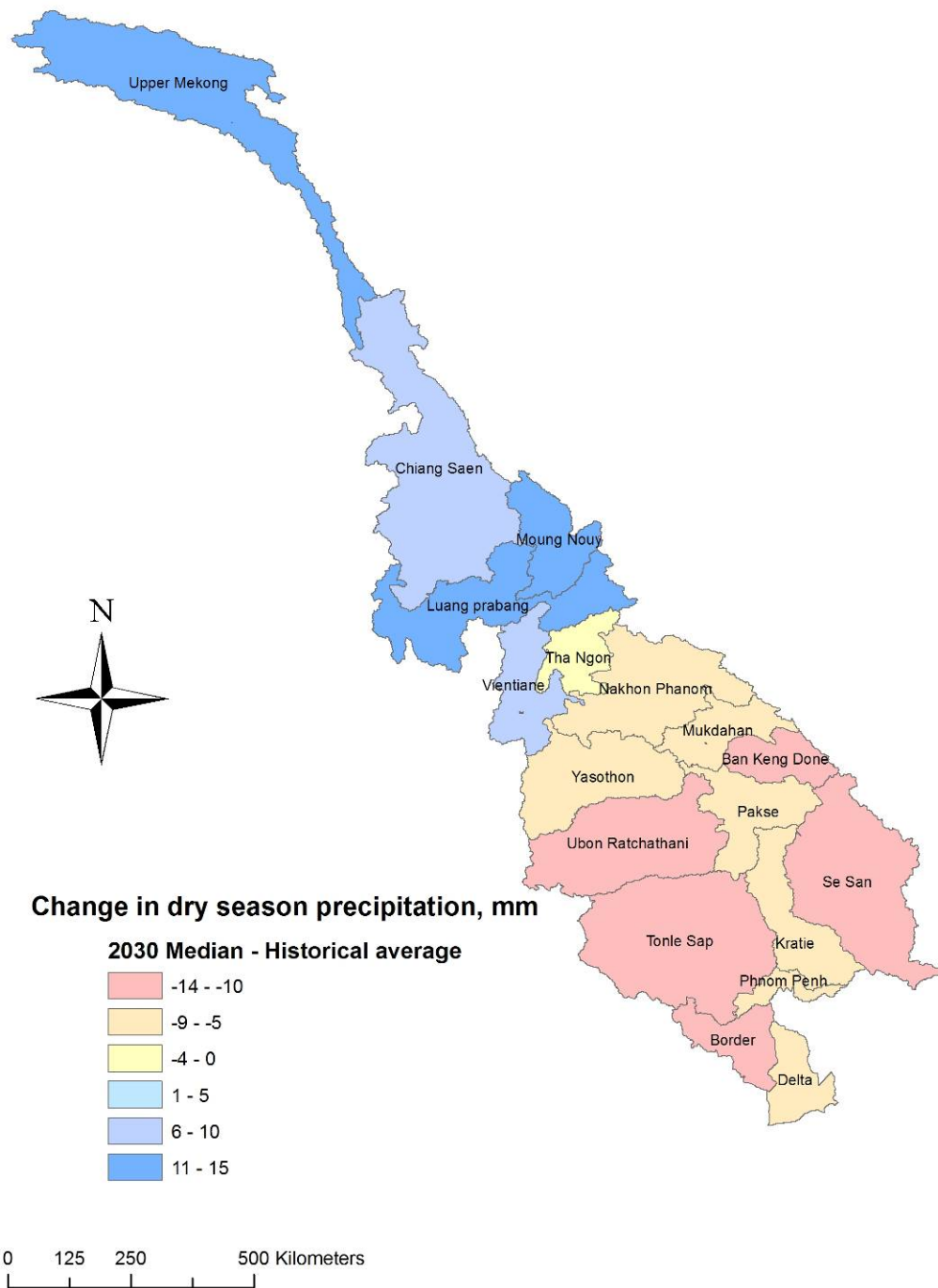


Figure 3.9. Spatial distribution of the projected change in precipitation during the dry season (November to April) at 2030 compared with historical (1951-2000) mean precipitation.

3.5.3. Uncertainty in projected (2030) precipitation for Mekong catchments

There is some uncertainty around the projected (2030) precipitation for each of the catchments (Figures 3.10 to 3.12). For the Chiang Saen, Moug Nouy, Luang Prabang, Tha Ngon, Se San and Delta catchments, annual precipitation is projected to decrease under the dryer range of GCM simulations. These projected decreases are associated with decreases in wet season precipitation. For the remaining catchments, all simulations indicate that annual precipitation will increase.

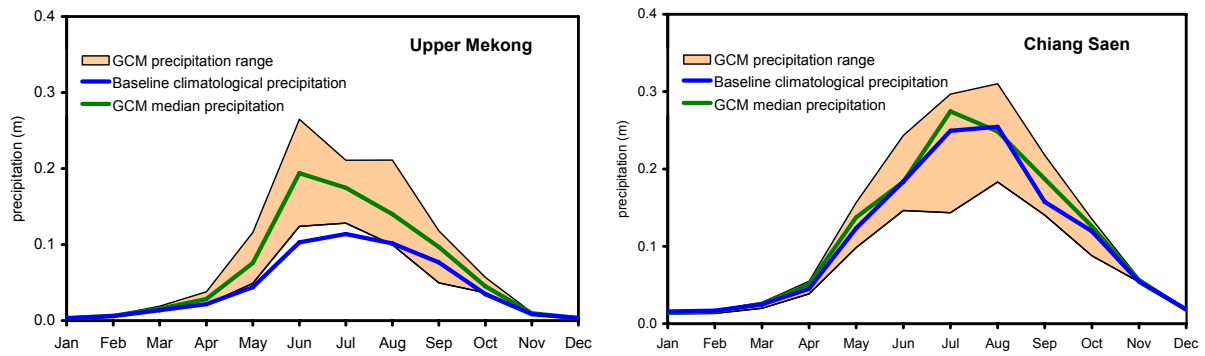


Figure 3.10 Baseline (1951-2000) versus future (2030) monthly mean precipitation for catchments of the Upper Mekong basin: Upper Mekong and Chiang Saen.

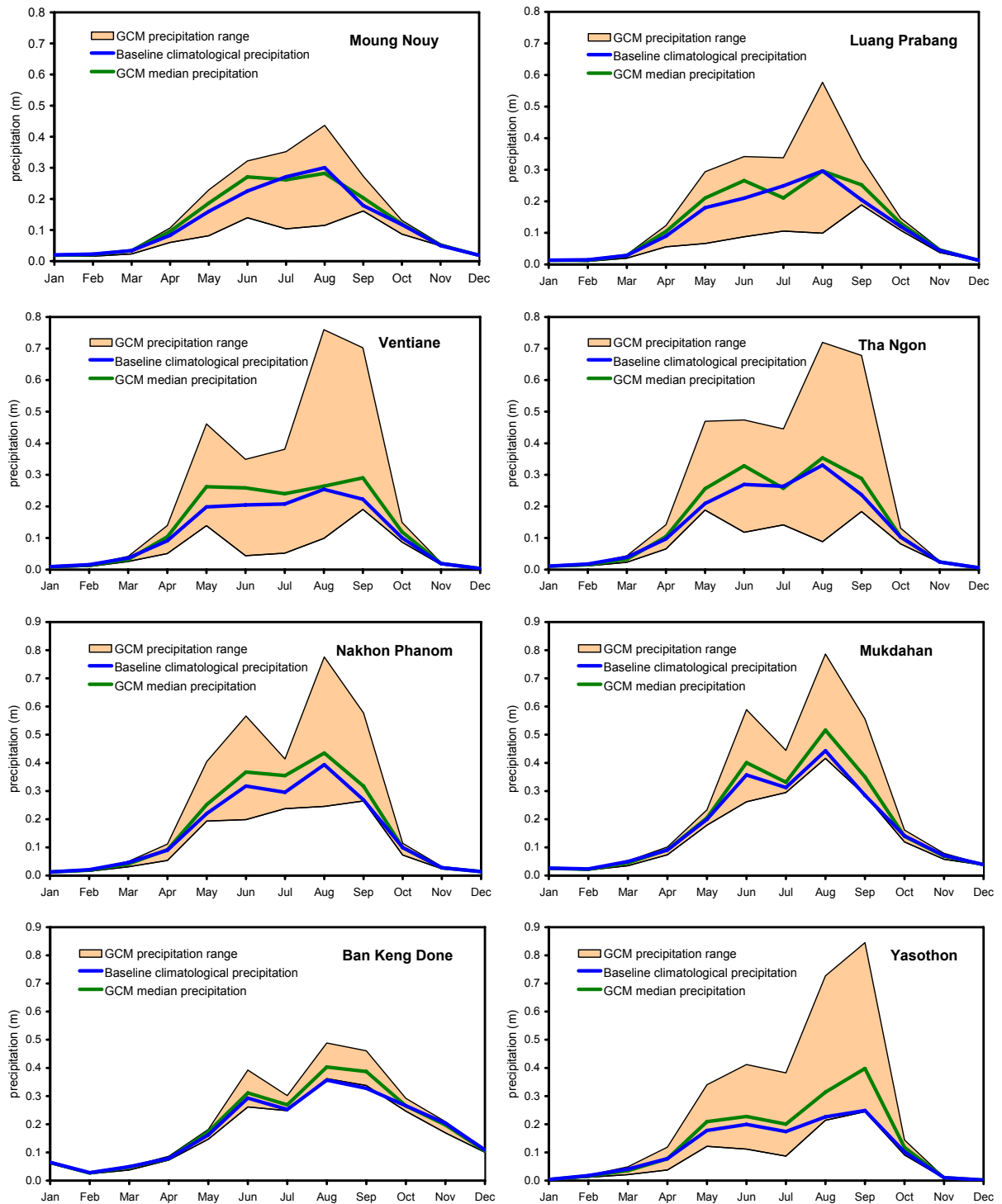


Figure 3.11. Baseline (1951-2000) versus future (2030) monthly mean precipitation for Moung Nouy, Luang Prabang, Vientiane, Tha Ngon, Nakhon Phanom, Mukdahan, Ban Keng Done and Yasothon catchments.

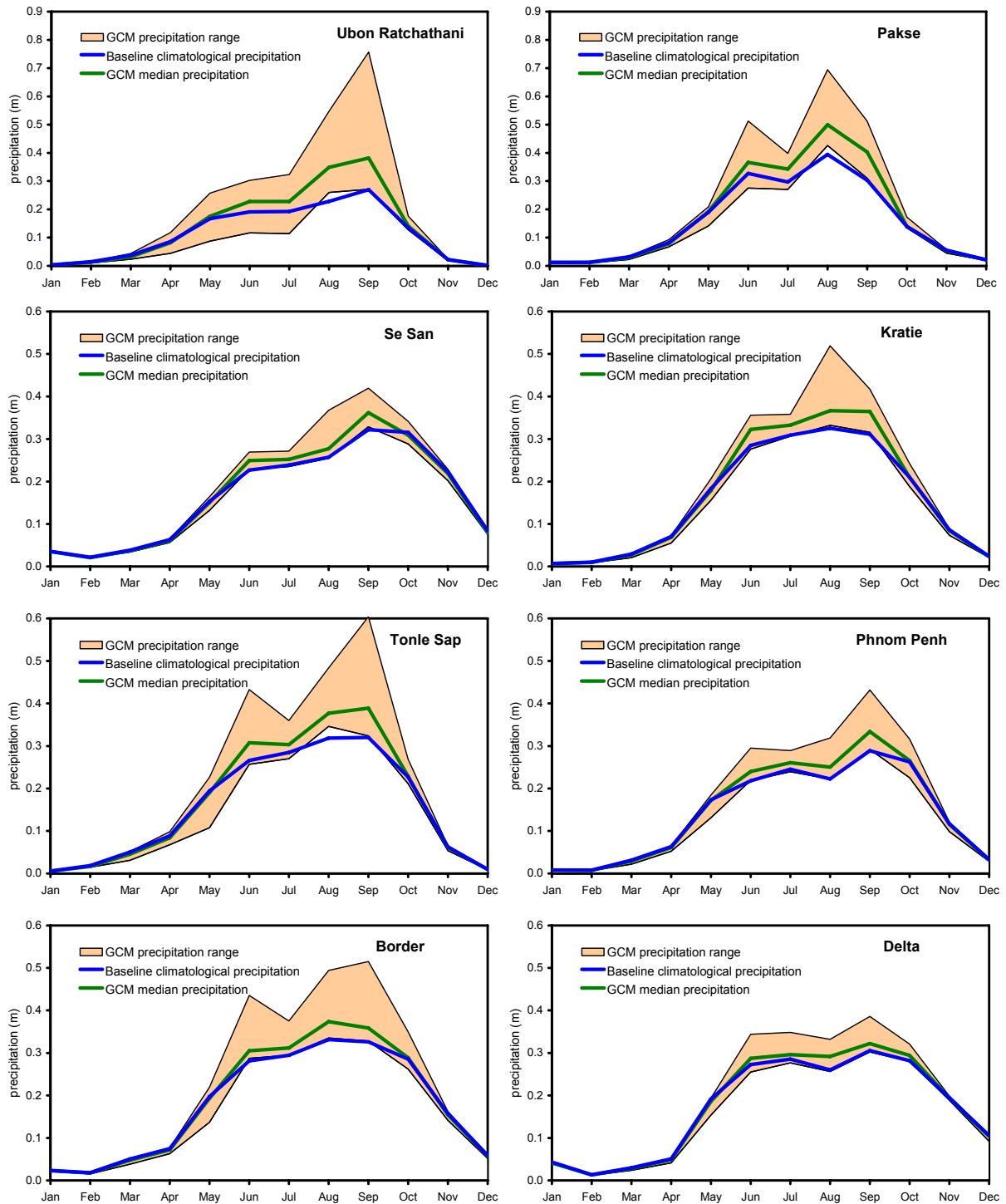


Figure 3.12. Baseline (1951-2000) versus future (2030) monthly mean precipitation for Ubon Ratchathani, Pakse, Se San, Kratie, Tonle Sap, Phnom Penh, Border and Delta catchments.

3.6. Projected changes in potential evaporation for catchments of the Mekong Basin

3.6.1. Projected changes in basin-wide potential evaporation

Consistent with the trend in projected temperature, potential evaporation is projected to increase by 2030 in all months and all catchments. The projected increase in annual

potential evaporation averaged across the basin ranges from 1.451 m to 1.48 m, a change of 2%. Projected increases in monthly potential evaporation are 0.003 m from February to June, and 0.002 for the remaining months (Figure 3.13)

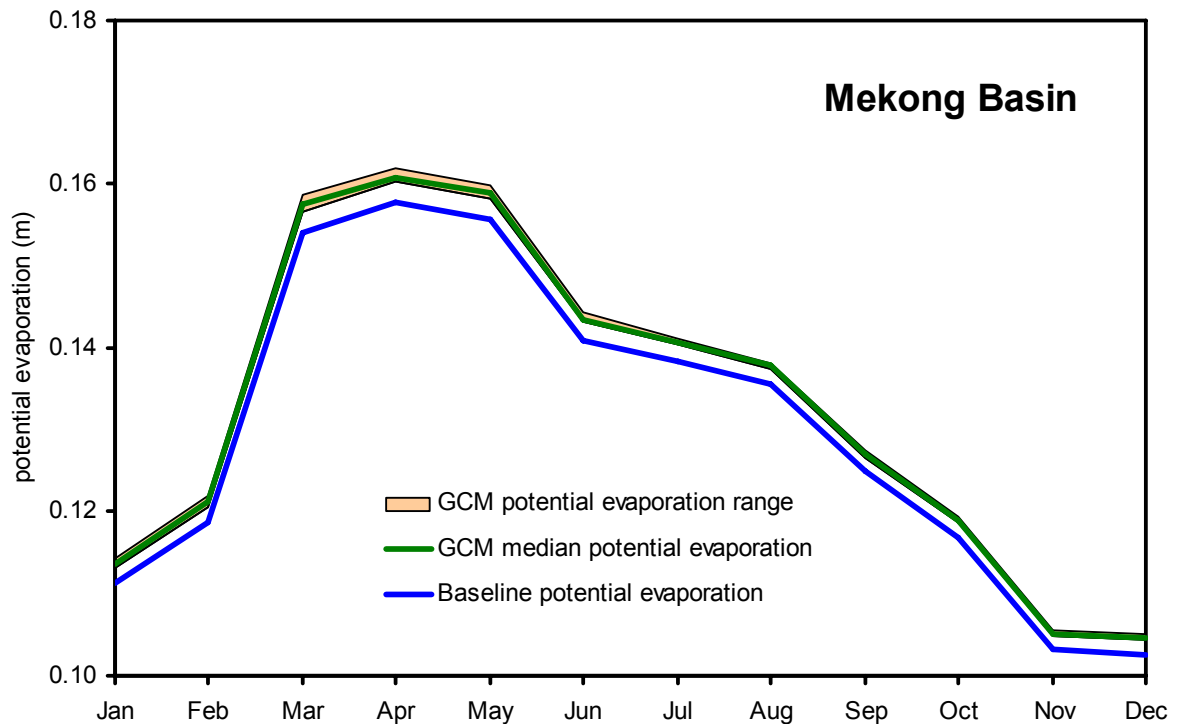


Figure 3.13. Baseline (1951-2000) versus future (2030) monthly potential evaporation.

3.6.2. Projected changes in potential evaporation for Mekong catchments

The projected increase in annual potential evaporation is greatest for the Upper Mekong (0.043 m), an increase of 6% (Figure 3.14). Projected increases in annual potential evaporation are less than 2.1% for all the remaining catchments of the basin (Figures 3.14 to 3.16). The range in projected potential evaporation is low for all months and for all catchments, being 0.002 m or less for all months in all catchments except the Upper Mekong where the range in projected potential evaporation is 0.003 m for May.

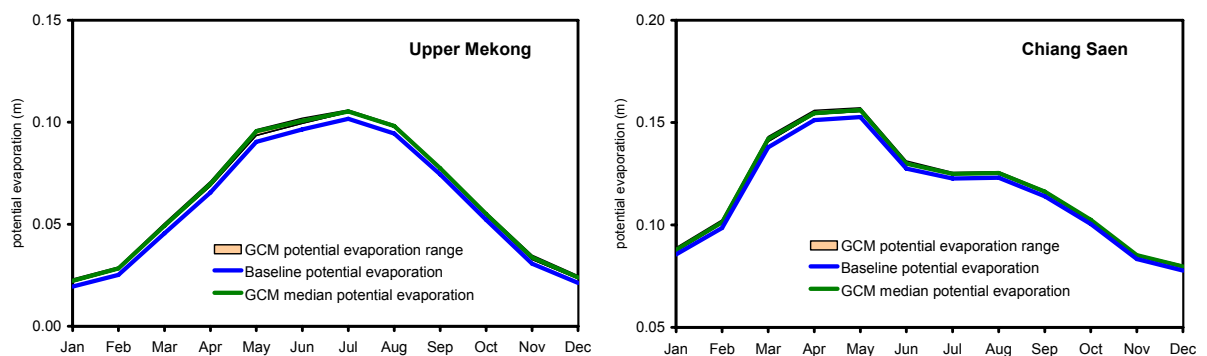


Figure 3.14. Baseline (1951-2000) versus future (2030) monthly potential evaporation for catchments of the Upper Mekong basin: Upper Mekong and Chiang Saen.

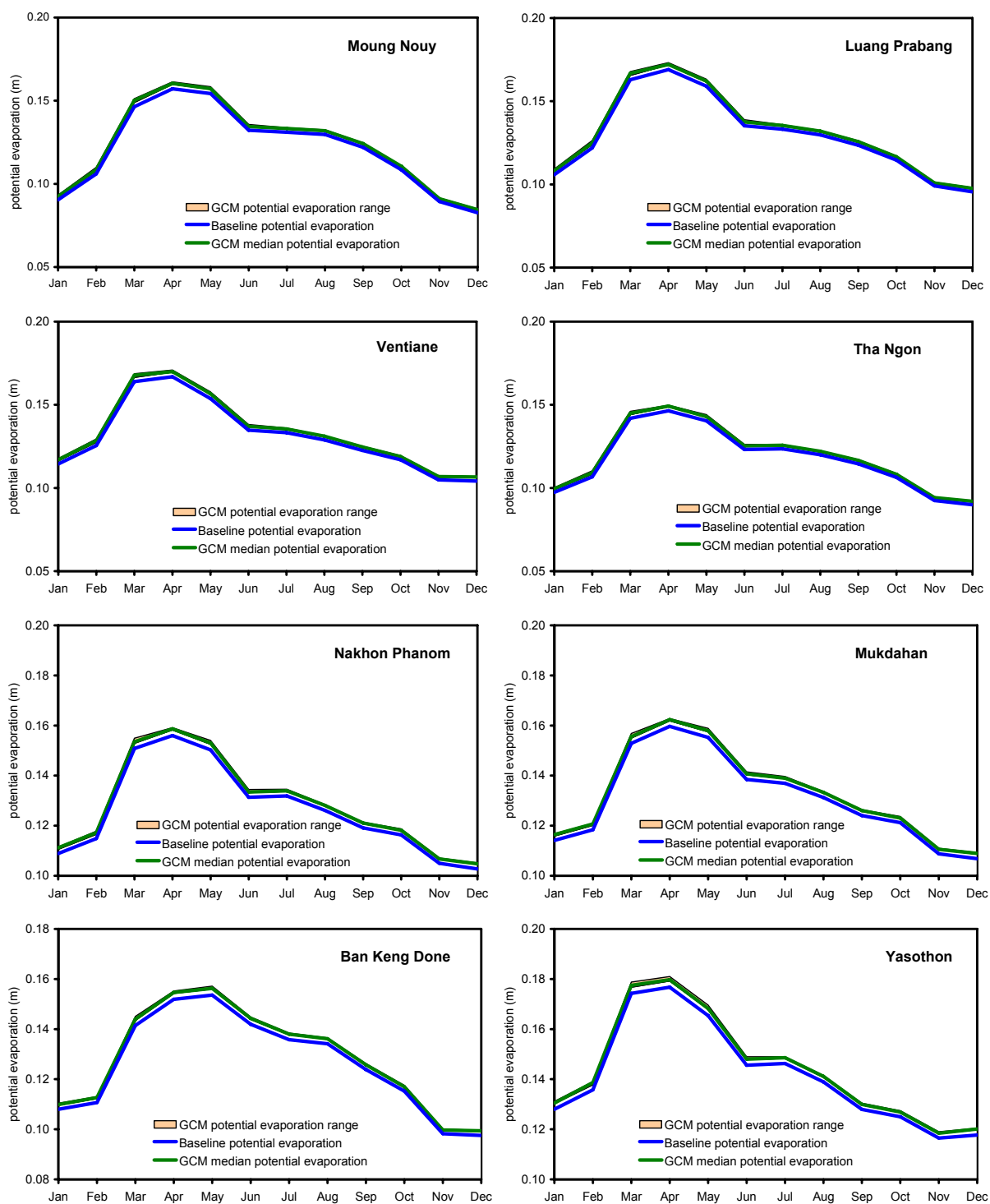


Figure 3.15. Baseline (1951-2000) versus future (2030) monthly potential evaporation Moug Nouy, Luang Prabang, Vientiane, Tha Ngon, Nakhon Phanom, Mukdahan, Ban Keng Done and Yasothon catchments.

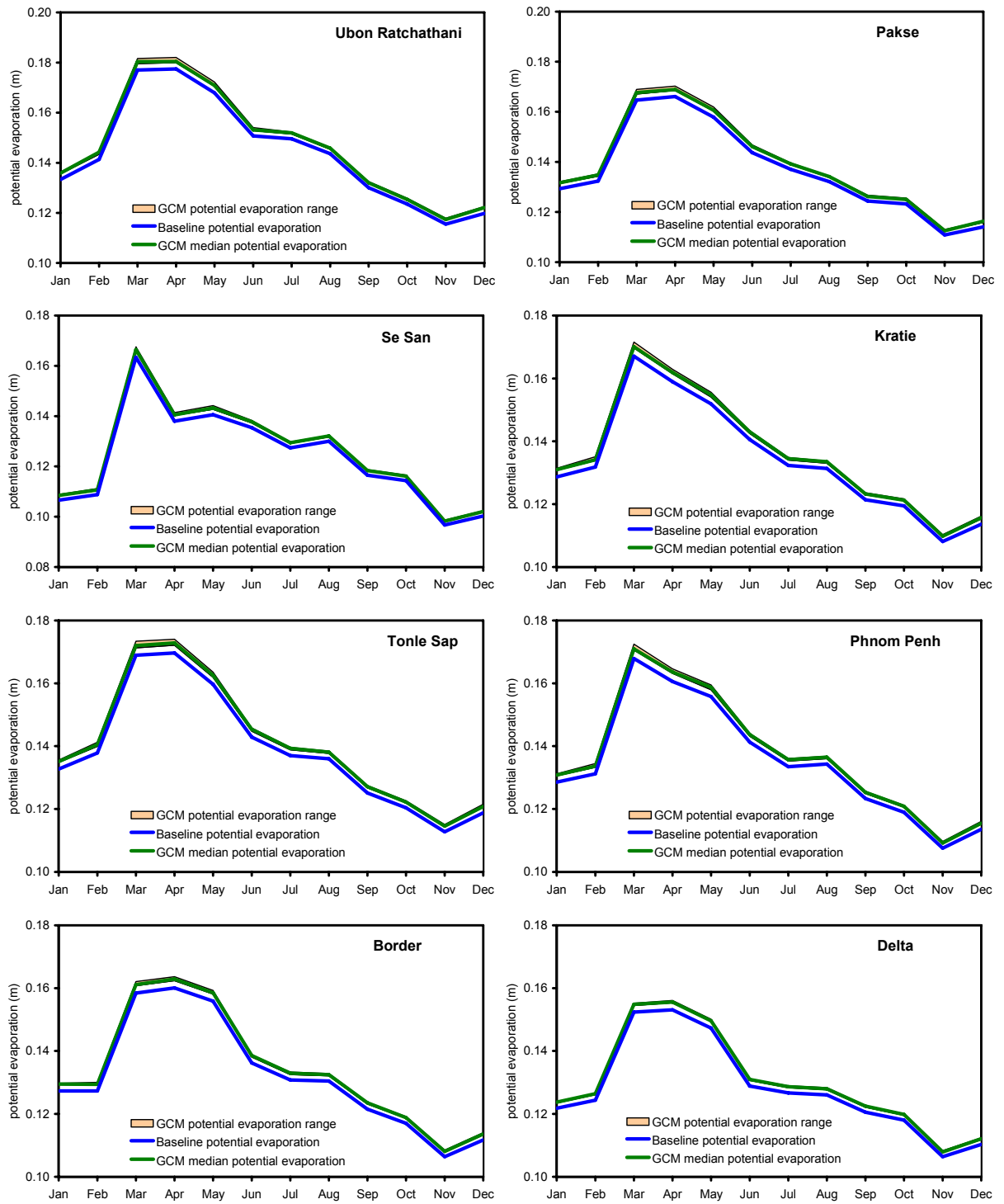


Figure 3.16. Baseline (1951-2000) versus future (2030) monthly potential evaporation for Ubon Ratchathani, Pakse, Se San, Kratie, Tonle Sap, Phnom Penh, Border and Delta catchments.

4. SURFACE WATER AVAILABILITY

4.1. Modelling the basin water balance using the water account model

The impact of the projected changes in climate on water resource availability and flows was evaluated using a water account model (Kirby et al 2008a). The hydrological account is based on a monthly time step, this being considered adequate for our purpose. The account is a top-down model (Sivapalan et al., 2003), based on simple lumped partitioning of rainfall into runoff and infiltration into a generalised surface store. This is done at the catchment level, with no attempt to model the spatial distribution of hydrological processes and storages within a catchment. Total catchment evapotranspiration is estimated from potential evaporation and water supply from the surface store, and partitioned between rain fed and irrigated land uses based on the ratio of their areas. The rain fed component of evapotranspiration is further partitioned between land uses/vegetation types (agriculture, forest/woodland, grassland, other) based on the ratio of their areas and using crop factors to scale their evapotranspiration relative to other land uses.

Flows that derive from snow melt and glacier melt are modelled separately in the water account. The proportion of monthly precipitation falling as snow (R) is estimated from the average monthly temperature (T_a) using the following relationship derived by Legates (1987):

$$R = 1 / (1 + 1.61(1.35)^{T_a}) \quad \text{Equation (4.1)}$$

Precipitation falling as snow is added to snow and glacier storages. The snow and glacier storages are reduced by losses by snow and glacier melt respectively using a simple degree day factor approach (Hock, 2003). Snow and glacier melt each month is added to the proportion of precipitation falling as rain in that month, and partitioned into runoff and infiltration as described above. The model was calibrated using the change in mean storage of glaciers in the vicinity of the Upper Mekong (the Meikuang, Xiaodongkemadi and Hailogou glaciers), since data on the Mekong glaciers was inaccessible. Data on the Meikuang, Xiaodongkemadi and Hailogou glaciers was available for 1989 to 1998 published in Dyurgerov and Meier (2005).

Runoff flows into the tributaries and into the Mekong, with downstream flow calculated by simple water balance. The contribution of baseflow from groundwater to the river system is estimated as a proportion of water discharging from a groundwater store. Deep drainage to the groundwater store is estimated as a proportion of the surface water store. Channel storages and losses from the river are estimated as a function of flows. Inflows are stored in reservoirs, and are balanced by evaporation and discharge at the dam. Water is spilled if the capacity of the dam is exceeded.

Crops in each catchment may be irrigated from both surface water and groundwater sources. Extractions from groundwater and surface water diversions for irrigation are based on crop water requirements calculated from cropped areas, crop factors, potential evaporation and irrigation efficiencies. Maximum irrigated areas are defined based on land use data, but the area irrigated from surface water may be reduced in any year to match supply if the volume stored in the reservoir at the beginning of the season is insufficient to meet crop water requirements. If reservoir storage becomes insufficient to meet crop demand during the season, irrigation applications are reduced to match supply. Irrigation is assumed to be inefficient, and a proportion of the water applied returns to the groundwater store, and a further amount lost by evaporation.

The general form of the model is described in detail in Kirby et al., 2008a. Features specific to the Mekong basin, such as flow to and from the Tonle Sap to the Mekong River are described more fully in Kirby et al., 2008b. Here we describe only the additional part of the model which relates to snow and glacier melt from the Upper Mekong.

Units:

Rain, evapotranspiration and potential evapotranspiration are given in mm. River flows and storages, and lake storage, are given in mcm (million cubic metres). 1 mcm is equivalent to one metre over one square kilometre. 1000 mcm = 1 bcm (billion cubic metres) = 1000 m over 1 km² = 1 km³.

The model was calibrated against reach flows taken from a dataset called dss522.1, available on the internet (<http://dss.ucar.edu/catalogs/free.html>) (Bodo, 2001). The dataset also gives contributing drainage areas for each flow gauge. Flow records were not available for all the catchments, particularly those downstream of Pakse. For downstream catchments, the flow results used in the RAM (Johnston and Rowcroft 2003) were used here. For some catchments, no flow records or estimates were available: these included the Upper Mekong (the upper part of the Lancang in China, the lower part of the Lancang being gauged at Chiang Saen), the Se San, and the delta region.

4.2. Runoff

4.2.1. Projected changes in basin runoff

Mean annual runoff from the Mekong Basin as a whole under the historical climate scenario is ~512,000 mcm. Runoff is greatest in the wet season from May to October, and low in the remaining months (Figure 4.1), following the pattern of monthly precipitation distribution for the basin (Figure 3.6).

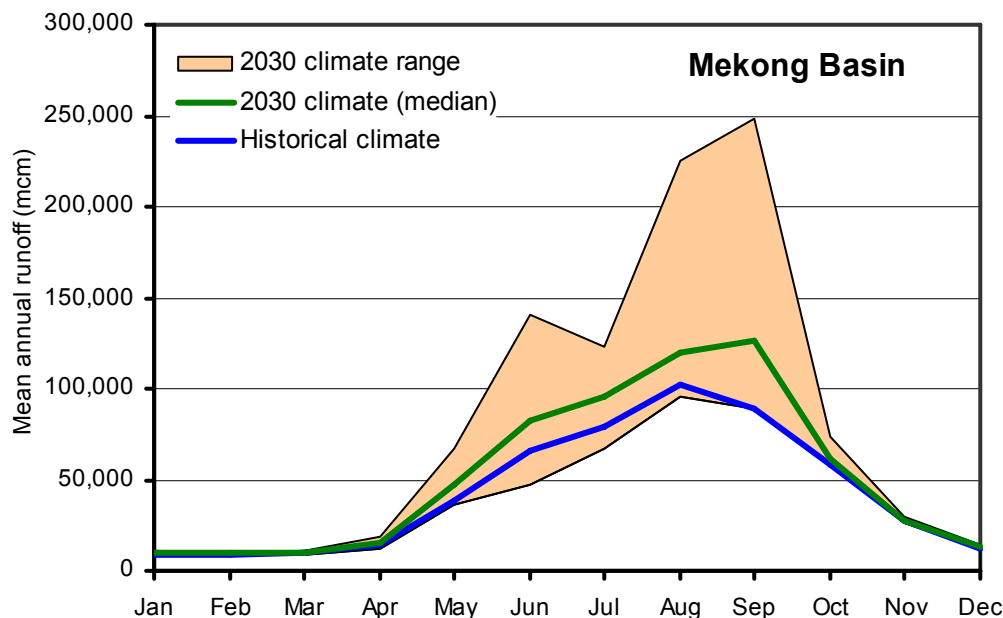


Figure 4.1. Historical (1951-2000) and future (2030) monthly runoff

Figure 4.1 indicates that there may be a significant potential impact of climate change on runoff from the basin. Although there is uncertainty in the estimates, the results indicate that annual runoff is likely to increase under the projected climate in 2030. The best estimate of runoff from the Mekong basin, represented by the median runoff response from GCM simulations is ~619,000 mcm, an increase of ~107,000 mcm (21%). The range in projected

change in mean annual runoff varies from a decrease of ~41,000 mcm (8%) to an increase of ~460,000 mcm (90%). The median runoff projections for 2030 suggest that total basin runoff will increase in all months of the year. The largest increases are projected to occur in the months of May to September, with runoff increases of 17% or greater. The lower range of GCM projections indicates decreasing runoff for all months except January, February and October. The upper range of projections indicate increases of 9% or greater in monthly runoff for all months, with runoff increases greater than 100% for June, August and September.

4.2.2. Projected changes in runoff for Mekong catchments

The most likely response in runoff to projected (2030) climate is an increase in runoff in all catchments of the basin (Figure 4.2). The size of the most likely projected increase varies across the catchments of the basin. When changes in annual runoff changes are expressed as equivalent ponded depth of water to allow comparison between catchments with different areas (Figure 4.2), projected increases range from 0.055 m in the Delta catchment to 0.251 m at Pakse. Expressed on a volumetric basis, likely annual runoff increases range from ~500 to ~1300 mcm. Percentage changes in annual runoff for different catchments vary from likely increases of 7 to 111 %. The largest percentage increase in annual runoff is for the Upper Mekong catchment, where it is likely to increase by 111% in 2030, a change of ~13,000 mcm (Figure 4.4). Other catchments where large percentage increases in runoff are likely are Yasothon (92%), Phnom Penh (65%), Ubon Ratchathani (53%) and Vientiane (40%). An increase of 20% or greater is also likely for Mukdahan, Pakse and Tonle Sap catchments. Increases between 10 – 20% are likely for Moung Nouy, Luang Prabang, Tha Ngon, Nakhon Phanom, Ban Keng Done, Kratie and Border catchments.

Increases in wet season runoff are likely for all catchments of the basin, but the response in dry season runoff is projected to vary across the basin (Figure 4.3). Under the most likely future climate, dry season runoff is projected to increase in 11 catchments of the basin, with the largest increase of 0.04 m in Ubon Ratchathani. In the Ban Keng Done, Se San and Border catchments, dry season runoff is likely to decrease by 0.003 m, and by 0.006 m in the Delta. In Nakhon Phanom, Kratie and Tonle Sap, dry season runoff is likely to remain the same.

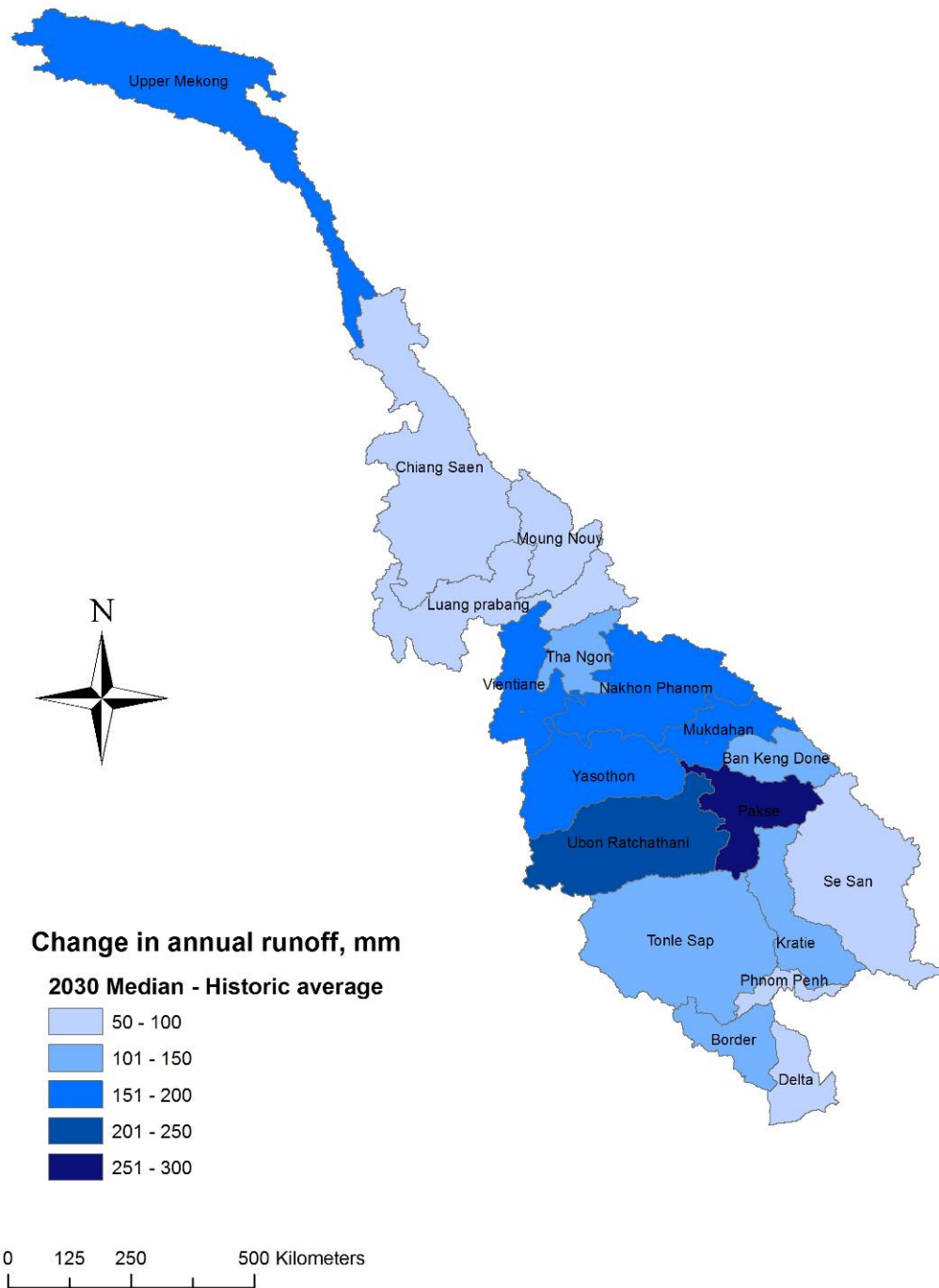


Figure 4.2. Spatial distribution of the projected change in mean annual runoff at 2030 compared with historical (1951-2000) mean annual runoff for catchments of the Mekong Basin.

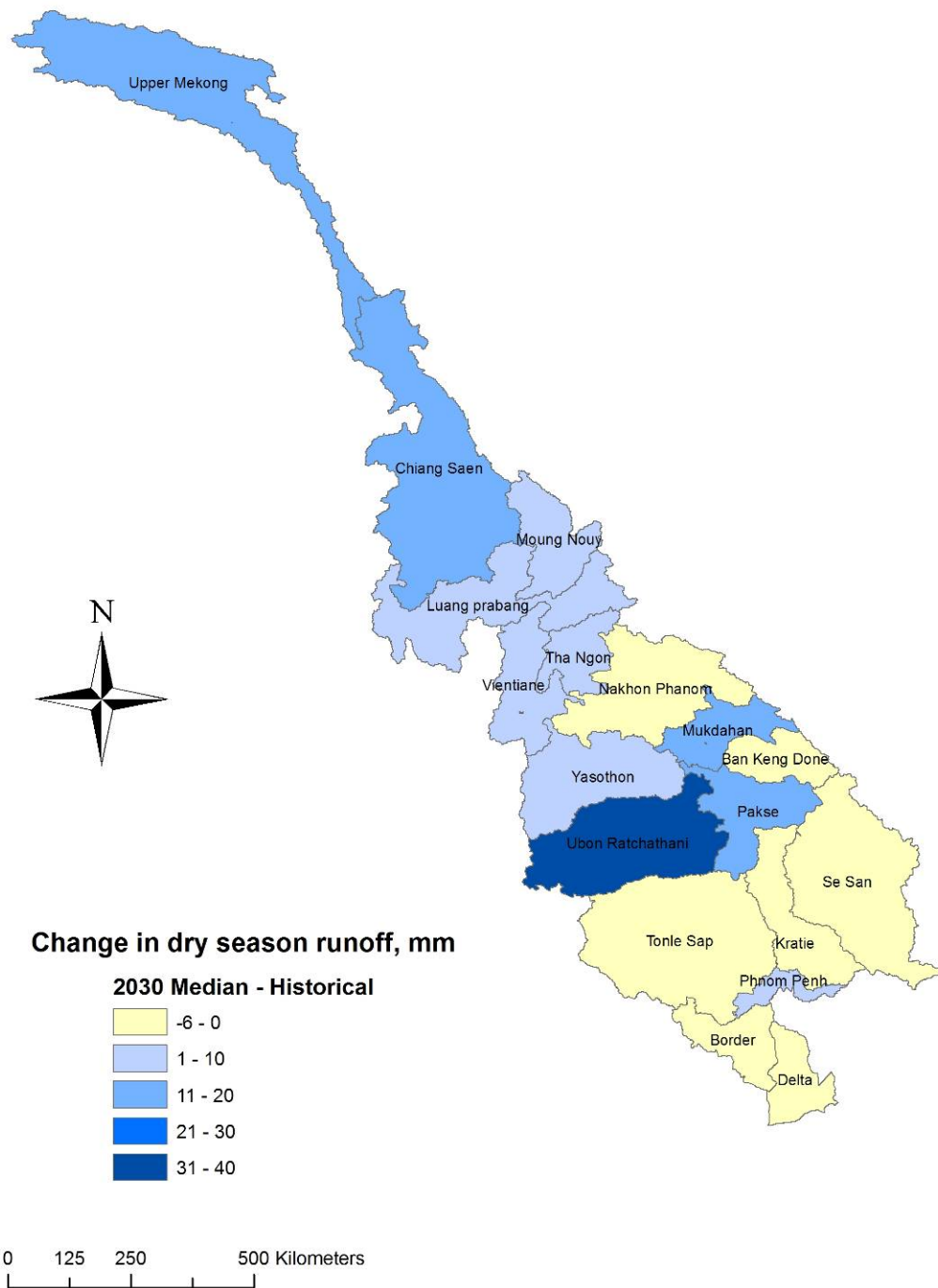


Figure 4.3. Spatial distribution of the projected change in dry season (November to April) runoff at 2030 compared with historical (1951-2000) dry season runoff.

4.2.3. Uncertainty in projected (2030) runoff for Mekong catchments

Uncertainty in runoff projections is large for most catchments, with the smallest range in annual runoff from GCM projections found for the Ban Keng Done, Se San and Delta catchments. For the Upper Mekong, Ubon Ratchathani, and Phnom Penh catchments all model projections show an increase in annual runoff. For the remaining catchments, a decrease in runoff in 2030 is projected by some models. The 2030 annual runoff projections for the wetter GCM simulations (shown by the range maxima in Figures 4.4 to 4.6) indicate increases ranging from 26% in Se San to 630% in Yasothon. The 2030 projections for the drier GCM simulations (shown by the range minima in Figures 4.4 to 4.6) indicate increases of less than 6% in annual runoff for the Upper Mekong, Ubon Ratchathani, and Phnom Penh catchments, and decreases of up to 63% for the remaining catchments.

Although runoff projections for 2030 indicate a likely increase in annual runoff for all catchments of the basin, for some catchments runoff is likely to decrease in some months of the year. For the Upper Mekong, Mukdahan, Yasothon, Ubon Ratchathani, Pakse and Phnom Penh catchments, runoff is likely to increase in every month. However, protracted reductions in runoff are likely in Ban Keng Done, Tonle Sap and Border catchments, where runoff decreases are likely in 6 months of the year, and in 5 months in Moug Nouy, Se San and Kratie catchments. These likely decreases occur predominantly in the dry months between November and April. Runoff reductions during the dry season are also likely to occur for between 1-3 months in the Moug Nouy, Tha Ngon, Nakhon Phanom and Delta catchments.

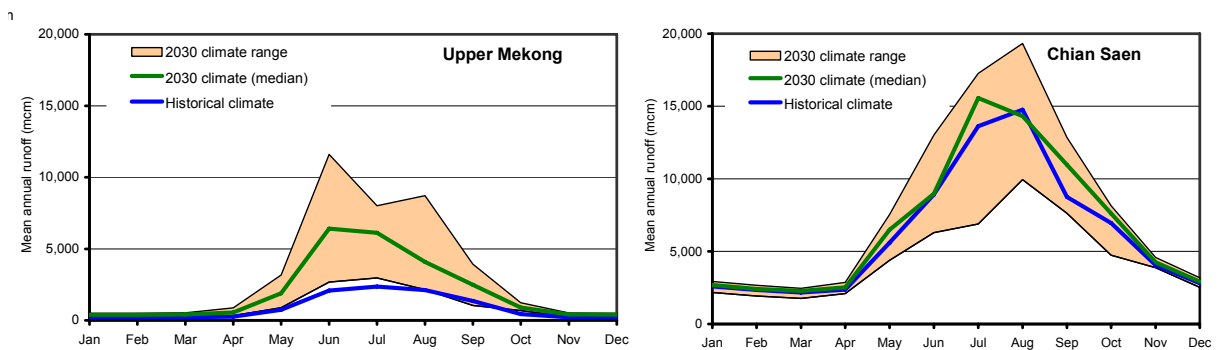


Figure 4.4. Historical (1951-2000) and future (2030) monthly runoff for catchments of the Upper Mekong basin: Upper Mekong and Chiang Saen.

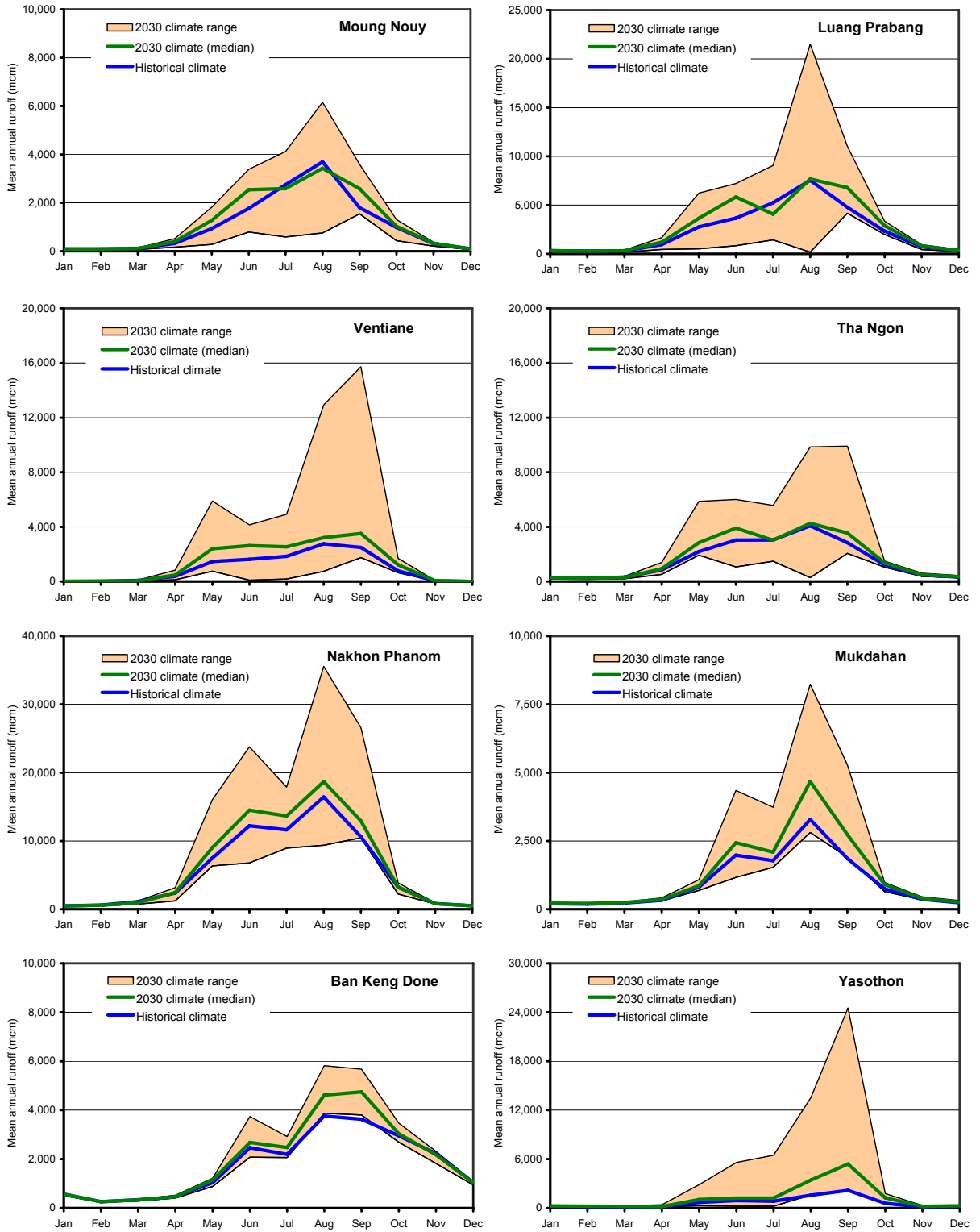


Figure 4.5. Historical (1951-2000) and future (2030) monthly runoff for Moung Nouy, Luang Prabang, Vientiane, Tha Ngong, Nakhon Phanom, Mukdahan, Ban Keng Done and Yasothon catchments.

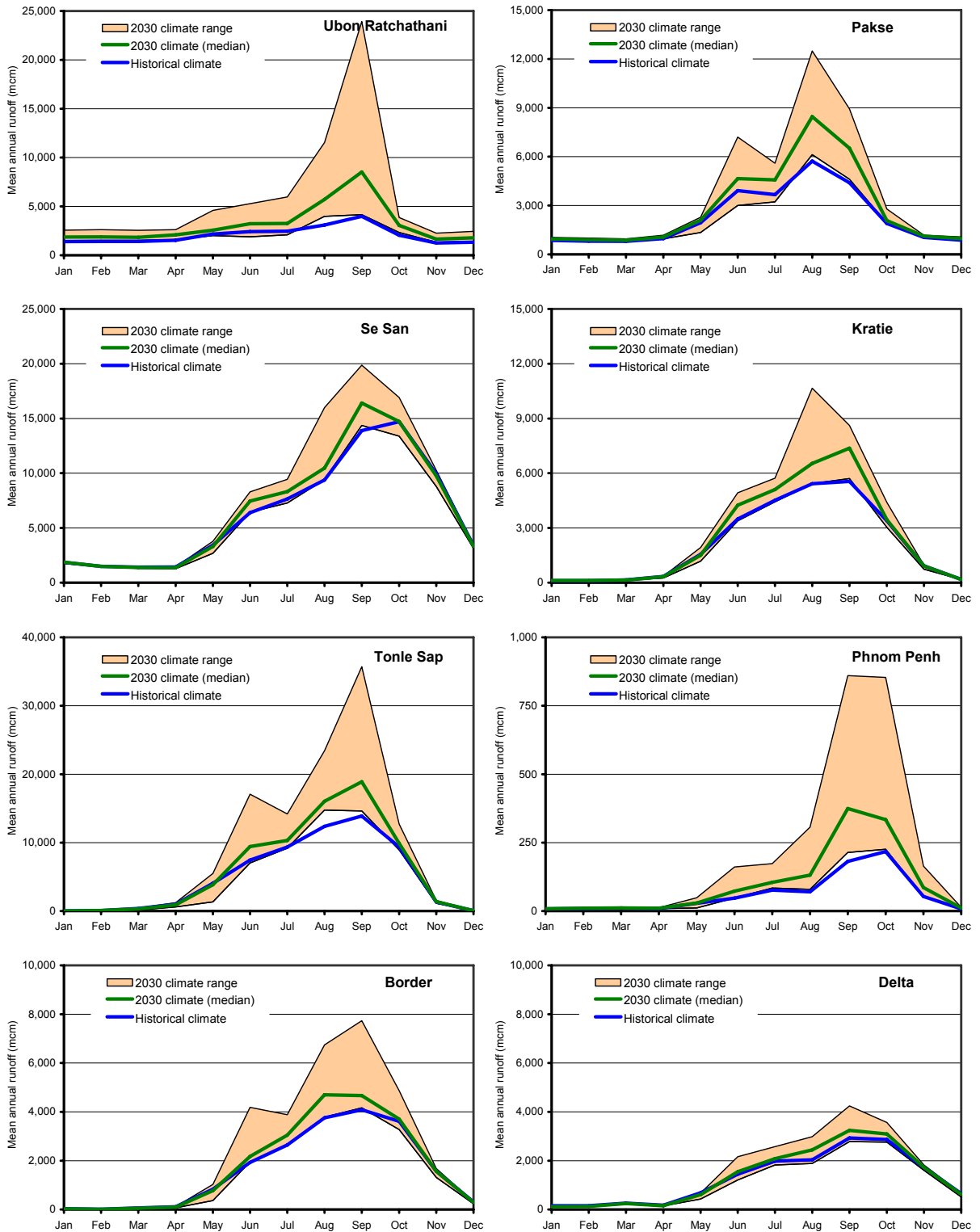


Figure 4.6. Historical (1951-2000) and future (2030) monthly runoff for Ubon Ratchathani, Pakse, Se San, Kratie, Tonle Sap, Phnom Penh, Border and Delta catchments.

4.3. Impact of glacier melt and snowmelt

Defining the area of glaciers within the Mekong Basin is important for modelling the contribution of melting glaciers to flows from the UMRB. Data on the area and volume of

glaciers were obtained from the World Data Center for Glaciology and Geocryology, Lanzhou (http://wcdgg.westgis.ac.cn/DATABASE/Glacier/glacier_inventory.asp).

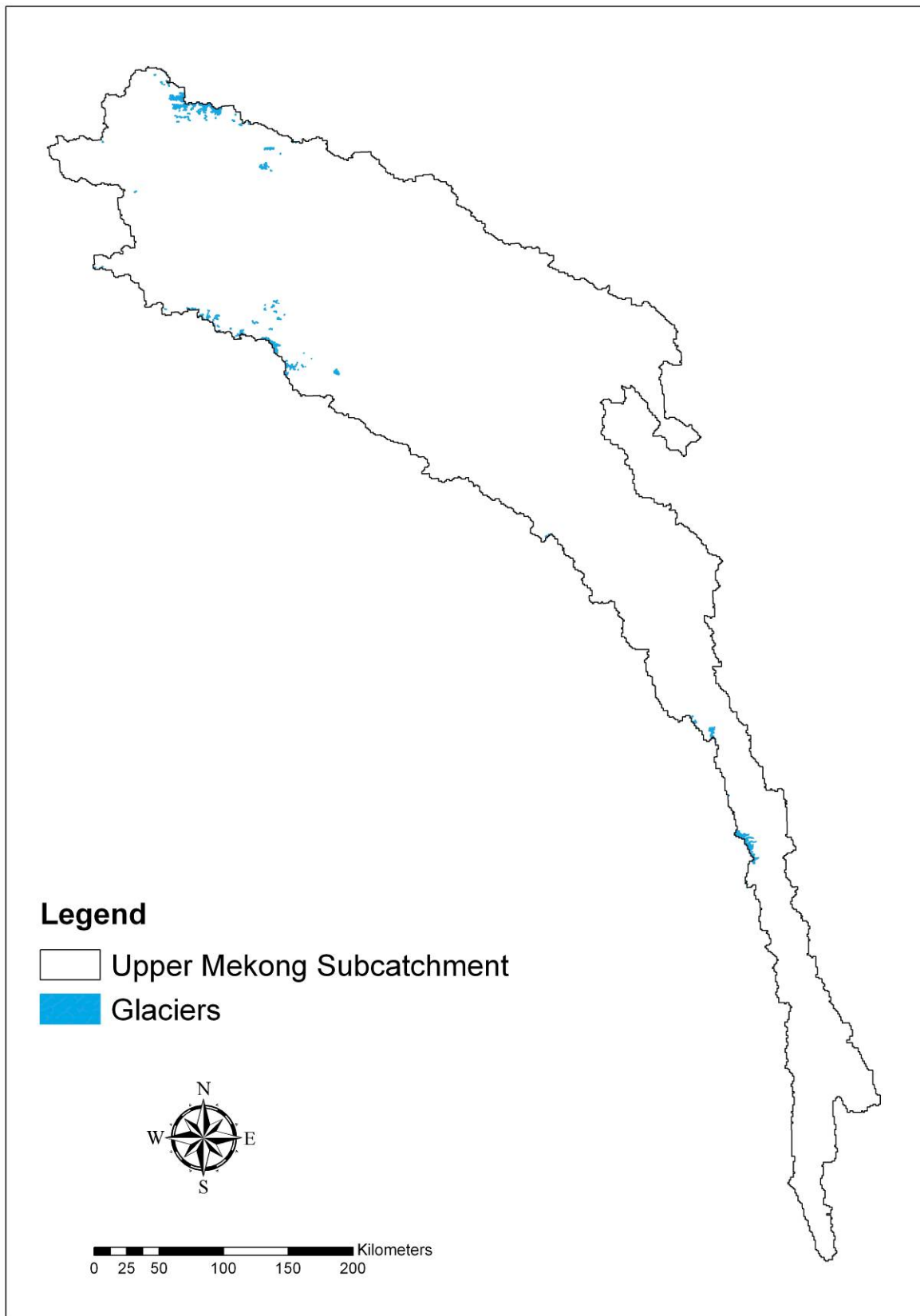


Figure 4.7. The extent of glaciers in the Upper Mekong catchment

The area of glaciers in the basin is small and confined to the Upper Mekong catchment (Figure 4.7) where the Mekong River arises. The total glacial area is 316.3 km², and their total volume 17.3 km³. Since the area of glaciers is small, the annual contribution of glacial melt to discharge at Chiang Saen into the Lower Mekong basin under historic climate conditions is only 0.1 % of the mean annual discharge (118 mcm/year). In contrast, snow cover constitutes 5.1 % of the Mekong River Basin Area (Kiem et al, 2005), or approximately 40,000 km² from November to March, and snow melt contributes ~6,700 mcm or 8% of the mean annual discharge from Chiang Saen under the historical climate.

In recent years, glaciers on the Qinghai-Tibetan plateau have been shrinking (Ding et al 2007), with regions towards the exterior of the plateau (including the source of the Mekong river) showing greater rates of shrinkage. The modelled change in volume under the historic climate reflects this reduction in volume. The rate of decrease in glacier volume under the most likely climate projections for 2030 is 0.11 km³ each year. At that rate, the glaciers which currently exist in the source areas of the Mekong River will take 163 years to disappear. Under the most likely projected impacts of climate change in 2030, the mean annual contribution of melting glaciers and snow will increase to 142 and ~7,700 mcm respectively – an overall annual increase of about 1000 mcm. The most likely (median) projection for mean annual discharge at Chiang Saen in 2030 from combined runoff and glacier and snowmelt is ~103,000 mcm, an increase of ~ 19,000 mcm. Thus the contribution of melting glaciers and snowmelt to flows in the Mekong Basin is small relative to that from runoff under both historic conditions and under the most likely projections for 2030.

Although there is uncertainty in climate change projections, the discharge from the Upper Mekong basin at Chiang Saen is likely to increase in all months of the year compared with historical climate conditions (Figure 4.8). The increase in discharge each month is greater than the contribution to flows from glacial melt. This suggests that after the glaciers have disappeared, flows into the Lower Mekong basin at Chiang Saen will still exceed flows under historical climate in all months of the year.

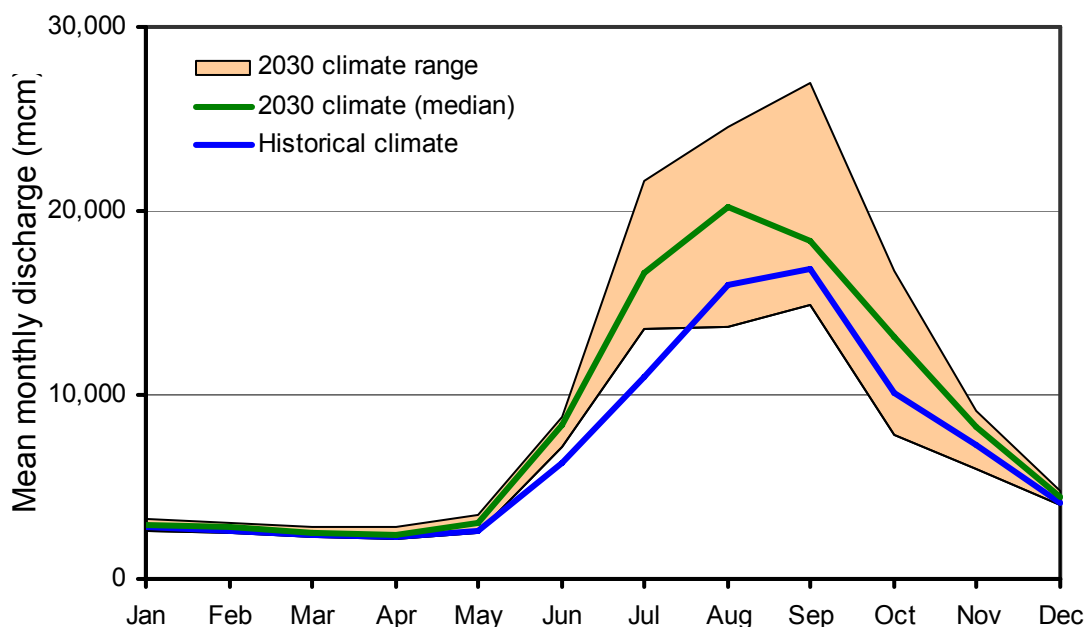


Figure 4.8. Historical (1951-2000) and future (2030) seasonal discharge at Chiang Saen into the Lower Mekong Basin.

4.4. Water uses

Under the historic climate, the mean annual input by precipitation to the Mekong basin totals ~1,192,000 mcm. Figure 4.9 summarizes how this water is partitioned amongst the major

water uses in the basin. Net runoff comprises the runoff remaining after all the water uses in the basin have been satisfied, and includes all other storage changes and losses. Net runoff from the basin under the historic climate is about ~ 509,000 mcm or 43% of the total precipitation input (Figure 4.9.a). Under each of the median, wet and dry scenarios for 2030, net runoff is projected to increase. The most likely net runoff in 2030 will be ~673,000 mcm, an increase of 32 %.

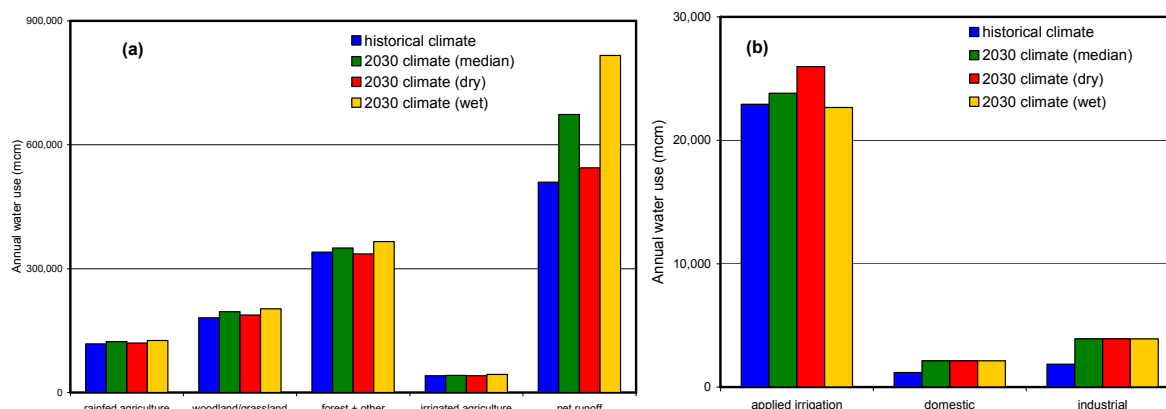


Figure 4.9. Historical (1951-2000) and future (2030) water uses.

Median and wet and dry climate ranges are shown for 2030. Figure 4.9a shows annual water use by evapotranspiration from different rain fed land uses and net runoff. Figure 4.9b shows, at an enlarged scale, annual water applied as irrigation and domestic and industrial consumption.

Under the historic climate, the major water use of the basin is by evapotranspiration from the ‘forest and other’ land use, which uses 29% of the basin precipitation. Water use from ‘rain fed agriculture’ is 10% of basin precipitation and less than both of the other rain fed land uses (‘forest and other’ and ‘woodland and grassland’). Since irrigated agriculture is the least extensive land use of the basin (<5% of the basin area), it uses less water than any of the rain fed land uses.

Under the most likely (median) 2030 climate scenario, water use by evapotranspiration from all land uses is projected to increase under the greater annual precipitation projected for the basin. However there is some uncertainty in projections of 2030 water use by evapotranspiration from different land uses. Under all model projections, water use of rain fed and irrigated agriculture and ‘woodland and grassland’ will increase, but the water use of ‘forest and other’ is projected to be less than historic amounts for some models. This may reflect the impact of a decrease in dry season precipitation under some model projections, reducing the water use of perennial vegetation.

Water applied as irrigation, domestic and industrial water uses are much smaller components of the total water used in the basin (Figure 4.9b). Under the historic climate, domestic and industrial water consumption are significantly less than the amount of water applied as irrigation, being 5 % and 8 % respectively of the water applied as irrigation. Domestic and industrial water consumption will increase by 2030, a response to the increasing basin population. The amounts used are insignificant compared with the available water, being less than 1% of the net runoff from the basin. Under the most likely (median) climate projection for 2030, the amount of water applied as irrigation will increase by 4%. Increased irrigation requirement in 2030 results from the reduction in projected rainfall during dry months in some catchments, and increasing potential evaporation arising from projected temperature increases across the basin. There is some uncertainty around the estimate of irrigation water use in 2030, with water applications increasing by as much as 13% in some

model projections, and others decreasing by up to 1% compared with applications under the historic climate.

There is variability across the catchments of the Mekong basin in the amounts of water used for irrigation, domestic and industrial uses (Figure 4.10). Domestic and industrial water use in all catchments will increase by 2030, because of the increasing population. The rate of change varies between catchments because of the changing proportion of people from different countries (with different domestic and industrial consumption) in the catchment. In the majority of catchments, water applied as irrigation is larger than domestic and industrial consumption, both under historic and projected 2030 climate conditions (Figure 4.10). Under the most likely 2030 climate projections, irrigation applications are likely to increase in all catchments except Yasothon and Ubon Ratchathani. There is some uncertainty around 2030 projections, with irrigation applications increasing in all catchments under the drier climate projections. Increased applications are also indicated under the wetter climate projections, except in Yasothon and Ubon Ratchathani, where applications are projected to decrease.

Irrigation withdrawals are greatest in the Ubon Ratchathani catchment, both under current and 2030 climate scenarios. Tonle Sap and Delta catchments also have large irrigation withdrawals relative to other catchments, with irrigation water applications greater than 3500 mcm/year. Both domestic and industrial water use are greatest from the Delta catchment.

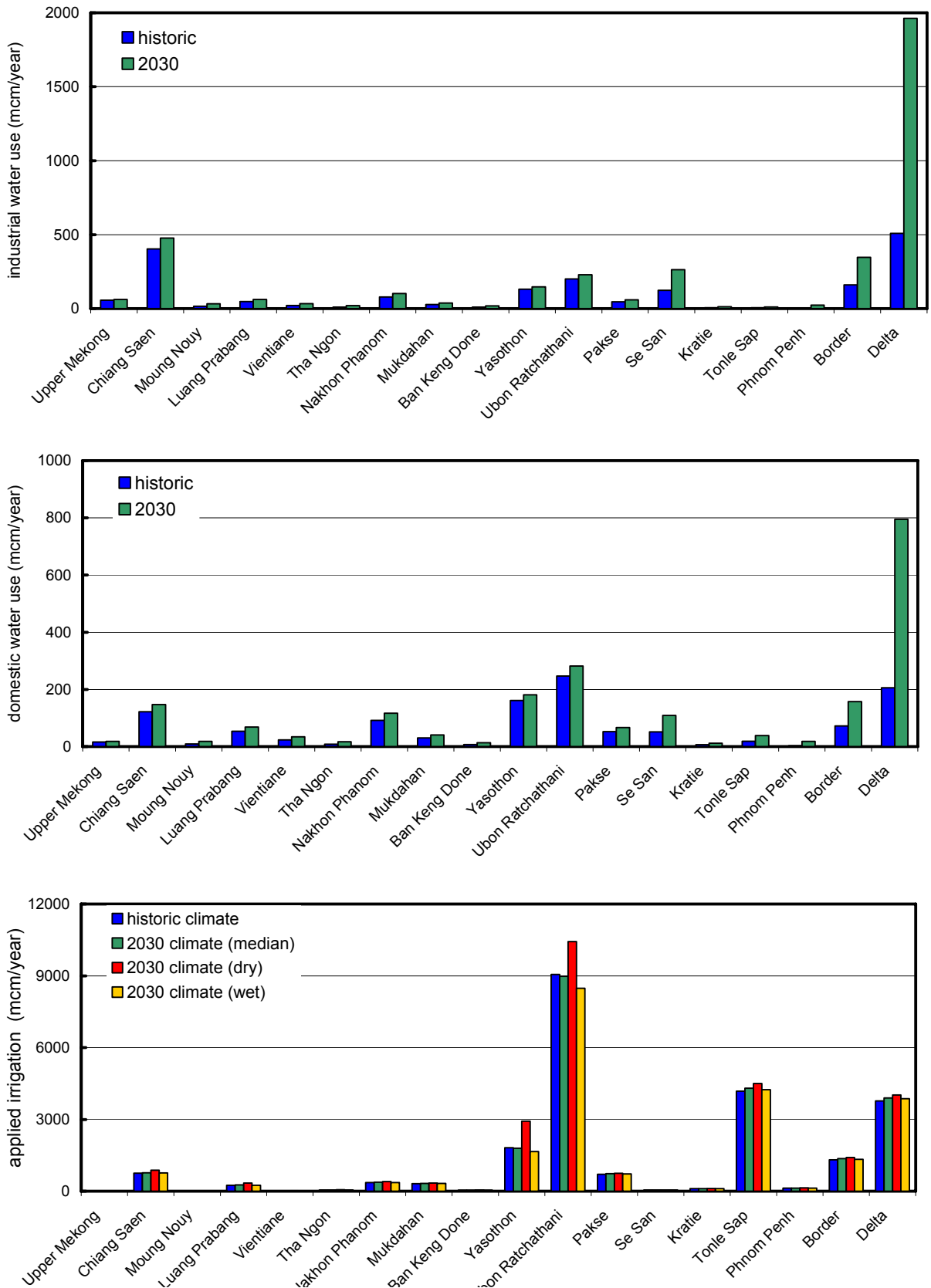


Figure 4.10. Historical (1951-2000) and future (2030) industrial (a), domestic (b) and irrigation (c) water. 2030 irrigation applications for median, wet and dry projected climate ranges are shown.

4.5. Water Stress

The degree of water stress experienced by the catchments of the basin may be quantified by two indices: water stress index; and water availability per capita. The first includes the ratio of total water withdrawals (irrigation + industrial + domestic) to water available (runoff + inflows from upstream) in each catchment, called the water stress index. The index has been described by SEI (1997), with the size of the ratio indicating the degree of water stress. If the ratio of water withdrawals is less than 0.1, water stress is unlikely to occur, and the degree of stress is ranked as low. Ratios in the range of 0.1 to 0.2 indicate that availability is becoming a limiting factor, and moderate water stress conditions prevail. Significant efforts and investment are needed to reduce demand and increase supply. At ratios from 0.2 to 0.4, the degree of water stress is moderate, requiring management of both supply and demand to ensure that use is sustainable. At ratios greater than 0.4, water stress is high indicating serious scarcity and an urgent need for intensive management of supply and demand.

At a basin level, the annual water stress index for the Mekong is 0.05 under the historic climate, indicating a low water stress. Under the most likely climate projection for 2030, the annual water stress index for the basin will decrease to 0.04 (range 0.04 to 0.05). Thus at a basin level, annual water stress is minimal. However, there is variation amongst the catchments of the basin in both the amount of water available from runoff (Figure 4.2), and water withdrawals for irrigation, domestic and industrial uses (Figure 4.10). Thus the degree of water stress varies across catchments of the basin, both for historic climate conditions, and for 2030 climate projections (Figure 4.11).

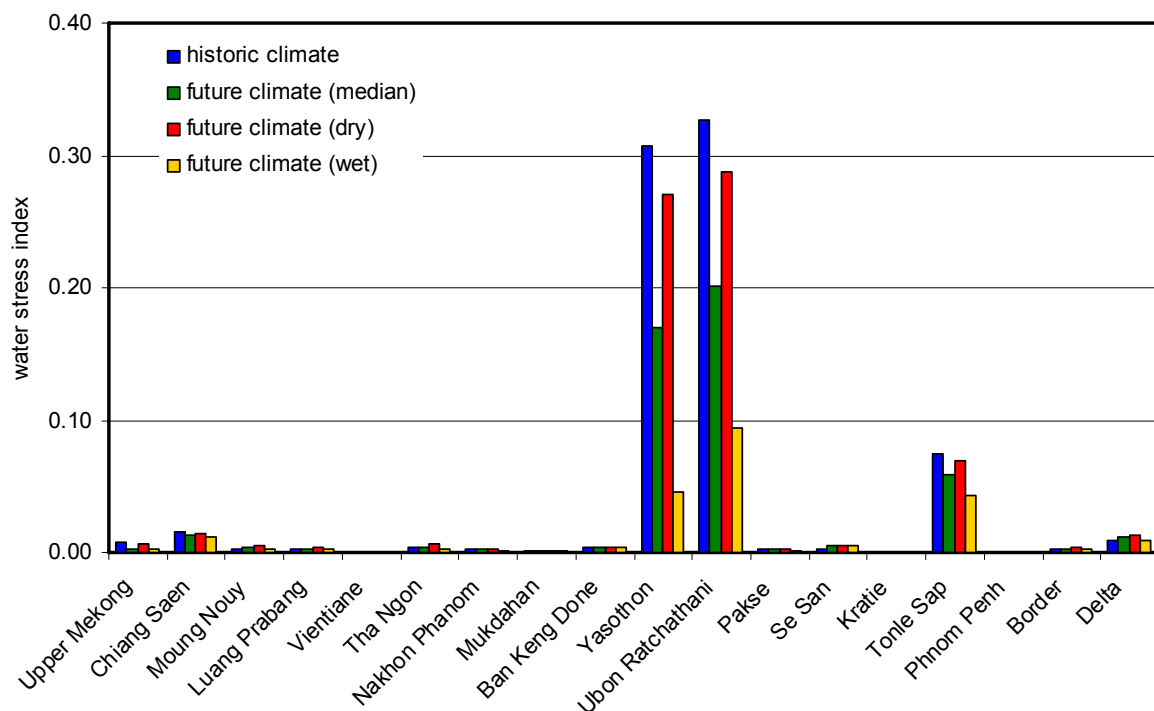


Figure 4.11. The annual water stress index (ratio of withdrawals to water available) under historic and future (2030) climate scenarios. Values of the index < 0.1 indicate low stress; between 0.1 and 0.2 indicates moderate water stress; between 0.2 and 0.4 indicates medium-high stress; and > 0.4 indicates high water stress.

Under historic climate conditions, the index shows low levels of water stress in all catchments except Yasothon and Ubon Ratchathani, where there is medium-high water stress under the historic climate conditions. Although there is uncertainty in the climate projections, under the most likely climate projections for 2030, and under the range of

projected climate, the level of stress will remain low in all catchments that were previously under low stress. Water stress levels are likely to decline by 2030 in both the Yasothon and Ubon Ratchathani catchments, and water stress in Yasothon is likely to reduce to moderate. However, it is likely that Ubon Ratchathani will still experience medium-high levels of stress. At the dry end of the range of climate projections for 2030, the water stress index is > 0.2 for Yasothon and Ubon Ratchathani, indicating medium-high stress levels for these catchments. At the wet end of the range of climate projections, water stress is low (< 0.1) in all catchments. No catchments suffer severe levels of water stress under the historic climate or for the projected range of 2030 climate.

We can examine the impact of water stress in the basin under historic and future climate projections, by quantifying the number of people experiencing varying degrees of stress in the basin under the different climate and population conditions (Figure 4.12).

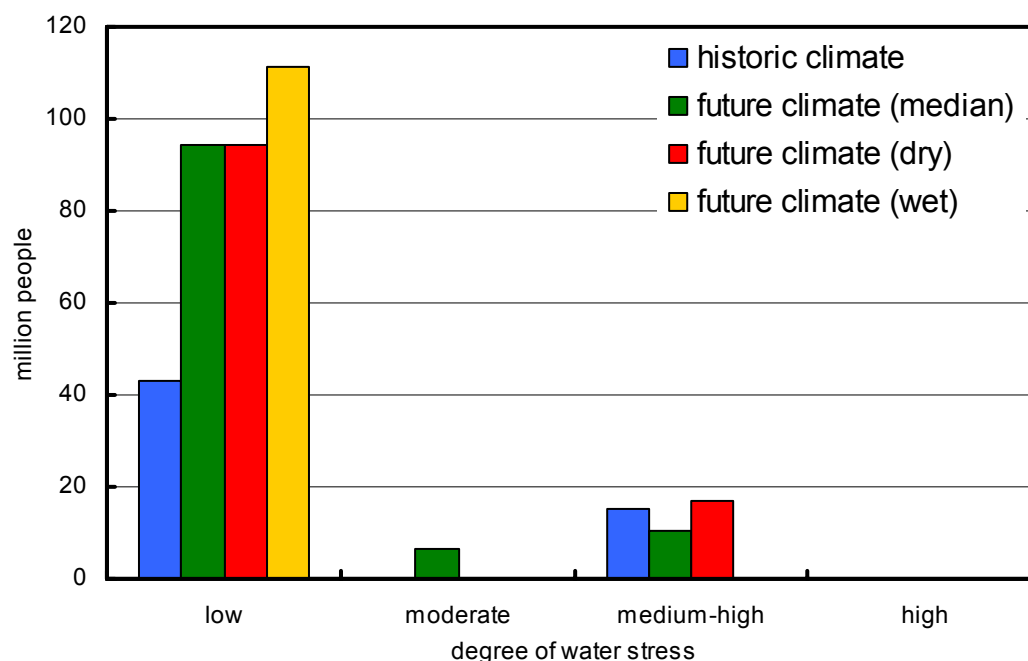


Figure 4.12. The number of people experiencing high, medium-high moderate and low levels of water stress in the Mekong basin under historic climate and 2030 climate projections.

Under the historic climate and population, there are ~15 million people experiencing a medium-high water stress in the Yasothon and Ubon Ratchathani catchments, with the remainder of the basin under low stress levels. Under the most likely climate (median) projections for 2030, the impact of water stress will be somewhat reduced, but ~10 million people will still experience medium-high stress in Ubon Ratchathani, and ~7 million people in Yasothon experiencing moderate stress. There is uncertainty around the climate projections with all the population experiencing low stress under the wet end of the range in climate projections. Under the dry range of projections, ~17 million people in Yasothon and Ubon Ratchathani will experience medium-high stress.

A second index for quantifying water stress is the water availability per capita in $\text{m}^3/\text{capita}/\text{year}$. This has been described by Falkenmark and Lindh (1976), and a threshold stress level of $< 1700 \text{ m}^3/\text{capita}/\text{year}$ defined as a level below which a population may be said to be experiencing water stress. At a basin level, the water availability per capita is high ($\sim 9000 \text{ m}^3/\text{capita}$). However, because of variation in both the availability of water and the population distribution across the basin, the water available per capita varies for different catchments.

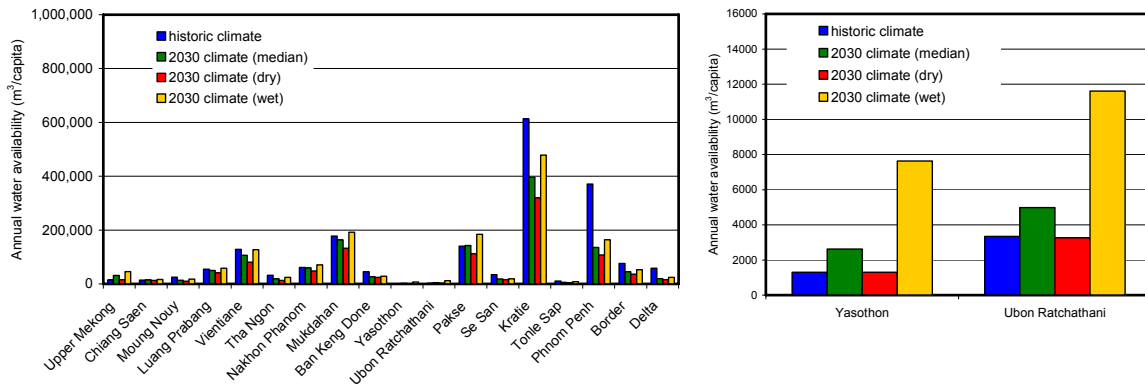


Figure 4.13. Water availability/capita under historic and future (2030) climate scenarios.

Under the historic climate, water availability is high, and above the threshold level of 1700 m³/capita for all catchments of the basin except the Yasothon catchment. The Ubon Ratchathani catchment also has a relatively low water availability per capita (3340 m³/capita) compared with other catchments where water availability is 10,000 m³/capita or greater. The most likely climate projection for 2030 indicates increased water availability in Yasothon to a level above the threshold level for water stressed (2621 m³/capita). However, there is uncertainty in the 2030 climate projections, with greater water availability in Yasothon under the wet end of the range of projections (7627 m³/capita), and greater water stress conditions projected at the dry end of the range (1307 m³/capita). For all other catchments of the basin, water availability is high under the range of projected climate conditions for 2030.

We have shown the likely impacts of climate change on water stress indices and water availability per capita expressed on an annual basis. However, seasonal differences in water availability and water withdrawals cause higher levels of water stress during the dry season for some catchments. We have calculated the ratio of withdrawals to water available for the dry season (November to April) for each catchment as an indicator of the potential for dry season water stress (Figure 4.14).

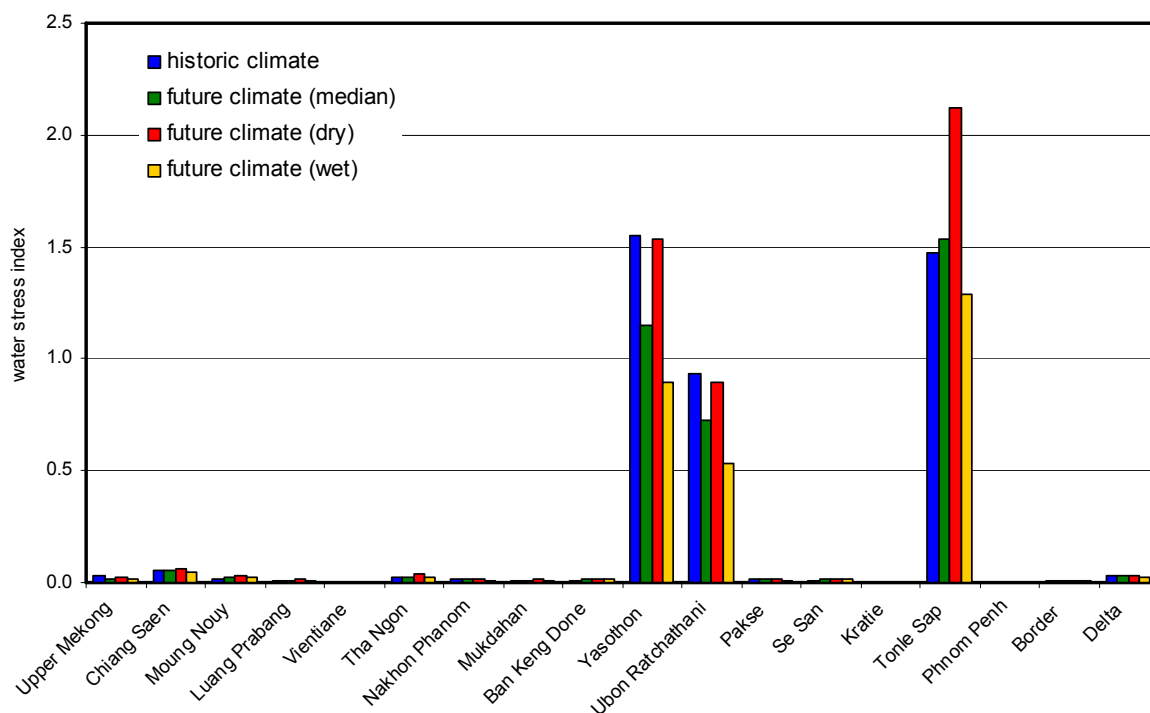


Figure 4.14. Dry season water stress index (ratio of withdrawals to water available) under historic and future (2030) climate scenarios. Values of the index < 0.1 indicate

low stress; between 0.1 and 0.2 indicates moderate water stress; between 0.2 and 0.4 indicates medium-high stress; and > 0.4 indicates high water stress.

The index indicates the potential for high water stress during the dry season for the Yasothon, Ubon Ratchathani and Tonle Sap catchments both under the historic climate, and the most likely projected (2030) climate. Even under the wettest climate projections for 2030 the ratio indicates high levels of stress in these catchments. These high levels of stress relate to generally greater water withdrawals for dry season irrigation in these catchments compared with other catchments (with the exception of the Delta catchment where water withdrawals are also relatively large, but water availability is also high in the dry season). The ratio of withdrawals to water availability in the dry season is greater than 1 for the Yasothon and Tonle Sap catchments, implying that withdrawals are greater than water available from runoff and inflows from upstream. This is possible since water storages provide water collected from runoff during the wet season, which is subsequently used for dry season irrigation. Irrigation withdrawals from groundwater also contribute to the high ratio of withdrawals to availability in the Yasothon, Ubon Ratchathani and Tonle Sap catchments.

5. GROUNDWATER AVAILABILITY

5.1. Introduction

There are believed to be extensive groundwater resources in the Mekong River Basin but these have not been adequately assessed (MRC, 1997). Aquifers of recent alluvium, recharged mainly by rainfall seepage, flank the Mekong River in northeast Thailand and the Mekong River Delta. Over 6,000 groundwater wells have been constructed in these and other aquifers of the Mekong River Basin (MRB) since 1980. This part of the project assessed both the quantity and quality of groundwater resources of the MRB including identification of knowledge and/or information gaps. The aim of this part of the project was to assess groundwater quantity and quality of the MRB. The objectives were to:

- present a country based overview of the groundwater resources of the Mekong Basin;
- provide an overview of the groundwater quality in various parts of the Mekong Basin; and
- outline information/knowledge gaps about the groundwater resources of the MRB.

5.2. Groundwater resources – a country based overview of the resource

5.2.1. Cambodia

The agricultural land in Cambodia is around 20% of its total area of 181,035 km². It is an agricultural country with 84% of the total population being rural and 80% are farmers. The length of the Mekong River through Cambodia is around 480 km with catchment covering around 86% of the land area of the country and contributing around 475,000 million m³ as surface runoff to the Mekong River.

An important feature of the Mekong system in Cambodia is Tonle Sap Lake which regulates around 20% of the whole Mekong River floods and acts as a natural flood stabilizer during the rainy season. During rainy season relatively large areas of Cambodia around the Tonle Sap, Tonle Bassac and Mekong Rivers are flooded. Cambodia's upper part of delta has about 2,000 km² of irrigation (central parts of delta region in Figure 5.1). Its hydrology is dominated by the Tonle Sap and Cambodia's Great Lake (White, 2002).

Groundwater in Cambodia is mainly used for both domestic supply and irrigation. In general, the groundwater resources are not sufficient for any large scale irrigation. In other words the groundwater sources of sufficient potential for any large scale irrigation have not been found (Sinath, 2001).

There are estimates of over 6,000 wells drilled post 1980 in the Mekong delta for domestic water supply and small scale irrigation of vegetables and fruit trees. The groundwater use has increased from 120,000 m³/day in 1997 to 290,000 m³/day in 2000 (Hoanh *et al.*, 2003). According to Seng *et al.*, (2006) over 12,000 tube wells in Siem Reap, Battambang and Kampong Chhnang provinces of the Tonle Sap region; Kampong Cham province of the Phnom Penh region; and Prey Veng, Takeo, and Kandal provinces of the Border region (Figure 5.1) of Cambodia have been used to abstract the groundwater for irrigation. The area irrigated by these wells was around 19,000 ha. The average area served by each tube well was around 1.6 ha. The fresh shallow aquifers that exist around the Tonle Sap Lake and beside the Bassac (central parts of Border region) and Mekong Rivers in Cambodia have strong interactions with these surface water bodies. Water levels up to 30 km each side of the Bassac River closely follow stage heights in the river (CIAP, 1999) indicating a continuous recharge from the river. Farmers along the Bassac River have installed shallow tube wells for irrigating 1 to 2 ha of dry season crops. Due to relatively low recharge rates the farmers in some intensively irrigated areas run short of water during peak periods.

There have not been any comprehensive investigations of the groundwater resources of Cambodia. The Mekong lowlands in general have alluvial material overlying shale, slate and sandstone bedrock (border region in the Figure 5.1). Whereas low hills and plateau are generally underlain by igneous rocks and limestone. The alluvium has very low hydraulic conductivity and yield (0.2 L/sec) except sandy beds and lenses where yields are higher (1 L/sec) (Peng and Pin, 2000). Cambodia can be divided into three regions on the basis of landforms, geology and occurrence of groundwater. These regions are:

The Mekong lowlands;

The South-western highlands; and

The Coastal Plain of South-western Cambodia.

The Mekong lowlands are underlain by a series of consolidated sediments of shale, slate, sandstone and limestone of Triassic and older age. The South-western highlands have several massive mountain ranges. The highlands consist of a series of metamorphosed sandstone, slate, schist and quartzite units. The alluvium units, generally composed of sand, silt and clay and mixtures of these constituents, contain some of the most important sources of groundwater. A large area in the Kompong Cham province (south-western parts of the Phnom Penh region) is underlain by basalt with yield of 30-50 m³/hr. The Post-Triassic Sandstone and conglomerate underlie a large part of the highland area and a large area between Kompong Cham and Pursat Province (southern parts of Phnom Penh and Tonle Sap regions). However the storage capacity of these formations has not been investigated. Similarly the water holding capacity of the sandstone is unknown although it is generally believed that it can yield substantial quantities of the water. The productivity of aquifers in the eastern part (Kratie region) of the country is high and in the western parts of the Tonle Sap region it is low (Figure 5.1).

The groundwater recharge occurs through seepage from rainfall and seepage from areas inundated with flood waters during rainy season. Kazama *et al.*, (2007) conclude that the inundation areas in the Cambodian part (south-western parts of the Tonle Sap region) of the Mekong River have relatively large impacts on the groundwater recharge and storage. During 1993 the total area of inundation was around 5,200 km² and the groundwater storage was estimated at 52 km³. During 1997 a 19% reduction in the area of inundation due to low rainfall and flood waters in the Mekong River resulted in 31% reduction in the groundwater storage. During 1998 the inundation area was reduced to 44% of that during 1993 and it resulted in 42% reduction in the groundwater recharge.

5.2.2. Vietnam

There are abundant groundwater resources in the Mekong delta (delta region in the Figure 5.1) however groundwater resources are limited in the North Central Region (WEPA, no date-A). The groundwater is mainly used for domestic and industrial consumption. The potential capacity of the groundwater is estimated at 60 million m³/day. The actual rate of groundwater extraction is estimated at 420,000 m³/day (Hoanh *et al.*, 2003) most of which occurs in the central highlands (eastern parts of Se San region in the Figure 5.2) and Vietnamese part of the Mekong Delta (delta region in the Figure 5.1). In 1997 the estimated groundwater use was around 244,000 m³/day of which about 150,000 m³/day was used in the urban areas.

The groundwater abstraction varies across the country. In the central Highlands, it has been over-exploited for irrigation of cash crops resulting in shortages of water in parts of his region (eastern parts of Se San region in the Figure 5.2). In this region the main reason for over exploitation of the groundwater is to support the coffee production. Regardless of drought related water shortage issues the area under coffee has increased dramatically in recent years in response to population resettlement programmes. There are currently about 300,000 ha of coffee grown in the central highlands of Vietnam. The water application frequency to coffee crop is every 9 days during the dry season (SRMP, 1999). This equates to around 6.5 ML/ha. The groundwater recharge in this area is low and the groundwater

levels have declined due to over-exploitation of the resource for cash crops (MRC and UNEP, 1997).

The portion of the Mekong delta (all of the delta region and southern parts of Border region in the Figure 5.1) that lies within the Vietnam covers about 39,000 km² of which 24,000 km² are used for aquaculture and agriculture and 4,000 for forestry. Primary products from Delta contribute over 30% to the Gross Domestic Product. It is Vietnam's rice bowl, producing 50% of the nation's rice (NEDECO, 1993). The groundwater has been used for almost 100 years in the Mekong Delta, however its assessment only started since 1975 (Ghassemi and Brennan, 2000). Due to increasing development, pollution of surface water from salinity, acidity, domestic wastes and suspended sediment and longer dry season in the southwest, the groundwater use in the Delta (delta and southern parts of the border regions) is increasing. A large number of pumps exist in the Mekong delta in Vietnam. These pumps are used to lift the river water or extract the groundwater for domestic and irrigation consumption. The number of these pumps has increased dramatically within the last 10-15 years. According to IWMI (2006), there were around 175,000 pumps in the Mekong delta in Vietnam in 1990. By 1999 these were increased to around 800,000 pumps. The current rate of groundwater abstraction is estimated at 430,000 m³/day serving about 4.5 million people out of the Delta's population of 14 million. Saline groundwater is also abstracted for shrimp and fish aquaculture. The groundwater is increasingly being used for domestic water supplies in the Mekong Delta. UNICEF helped install many groundwater wells of 40 to 400 mm diameter which extract groundwater from deeper confined aquifers ranging in depth from 100 to 480 m. Currently there are no constraints on the extraction rates. The groundwater is viewed as a possible source for industrial enterprises and dry season irrigation. However there are no estimates of groundwater recharge and therefore sustainable yield from these confined aquifers.

There are five major aquifers in the Delta. They range in age from Holocene through to Upper Miocene. The eastern, southern and western boundaries of these aquifers are unknown but oil exploration wells suggest they run hundreds of kilometres offshore. Burnett and Bokuniewicz (2002) suggest that there might be substantial submarine groundwater discharge of the coast of the Mekong. The confined aquifers are the most important fresh groundwater resources in the Delta. The groundwater reserves are considered to be large in these confined aquifers (Haskoning, 2000).

Some wells tapping the medium depth aquifers that were artesian or sub-artesian 10 to 20 years ago, are already suffering from over-exploitation and rapidly declining water levels. In part of the Delta, the shallow groundwater aquifers have already exhausted due to over abstraction and construction of extensive surface drainage system during the 1990s. In the Mekong Delta, the only major areas consuming groundwater for agricultural production are located between and along the Bassac and Mekong rivers (south-eastern parts of the delta region in the Figure 5.1). An over-exploitation of the groundwater resource has been occurring in Mekong River Delta (delta region in the Figure 5.1) resulting in falling water tables, land subsidence and salinity intrusion (WEPA, no date-A).

5.2.3. Thailand

There are relatively large groundwater resources in Thailand. Aquifers yield a large quantity of water throughout Thailand, with the exception of the eastern region. According to Pattanee (2002) around 75% of domestic water supply in Thailand comes from groundwater resources, serving around 35 million people in villages and urban areas. Groundwater irrigation is mainly in the north of the country (Nakhon Phanom, Vientiane, Yasothon, and Mukdahan regions in the Figure 5.2). In the Northeast Thailand (Nakhon Phanom, Mukdahan, Yasothon and Ubon Ratchathani regions in the Figure 5.2) aquifers of recent alluvium ranging in thickness from 1 to 10 m flank the main Mekong River. The main source of recharge to these aquifers is through seepage from rainfall and it is estimated that around 5-6% of total rainfall is recharged to the groundwater (Hoanh *et al.*, 2003). Williamson *et al.*, (1989) assessed that the shallow groundwater recharge estimates were lower (9 to 15% of total rainfall) in the north and south uplands and higher (14 to 31% of total rainfall) in the southwest uplands located about 20 km northwest of Nakhon Ratchasima (western parts of

the Ubon Ratchathani region in the Figure 5.2) in the Northeast Thailand. The groundwater extraction is mainly for domestic supply and irrigation and has not been large enough to cause any continued aquifer depletion in the past. Fresh groundwater can be found in the Northeast Thailand among saline aquifers, the quantities of this fresh groundwater resource are not enough to support wide-scale irrigated agriculture (MRC, 2005).

5.2.4. Myanmar

Myanmar is endowed with abundant surface and groundwater resources. Potential groundwater resource volume annually is around 495 km³. Around 90% of the total water use in this country is for agriculture while the remaining 10% is used for industry and domestic supply. Due to population growth there is an increased demand on the use of both surface and groundwater (WEPA, no date). An efficient management of surface and groundwater resources is therefore required for the sustainable development of the country in future. No other information about the location, size and use of groundwater from within the Mekong Basin was available from the literature.

5.2.5. Lao PDR

The groundwater is considered as a large and generally untapped resource in the Lao PDR. The knowledge of groundwater occurrence, monitoring and use in the Lao PDR is very limited. The country is divided into two geological areas: the Annamian Strata occupying most of northern (northern parts of Moung Nouy and Luang Prabang regions in the Figure 5.3) and eastern parts (Moung Nouy and Tha Ngon regions in the Figure 5.3) of the country and the Indosinian sediments mainly along the Mekong River (Luang Prabang and central and northern parts of Vientiane regions in the Figure 5.3). There are three different aquifer systems (the Annamian aquifers, Indosinian group of aquifers and alluvial aquifers). The Annamian aquifers occur randomly. These are local systems that discharge locally into the river or its tributaries. The potential groundwater supply from this aquifer system in the northern parts (northern parts of Moung Nouy and Luang Prabang regions in the Figure 5.3) of the country is considerable. The Indosinian group (Luang Prabang and central and northern parts of Vientiane regions in the Figure 5.3) of aquifers are regional groundwater systems and are mostly freshwater sediments. Yields of 12-24 L/sec can be developed from these aquifer systems. The alluvial aquifers associated with the sedimentary deposits of the Mekong River are not rated highly as aquifers. Limestone in the central Lao PDR is part of the Indosinian flow system and is known to have enormous groundwater resources. The groundwater is likely to remain the main source of rural and small town water supply, especially in lowland areas located far from the surface water sources such as southern and western parts of the Champassack Province (central part of the Kratie region in the Figure 5.2). Milne-Home *et al.*, (no date) found evidence of the interactions between the shallow and regional deep aquifers in the Champone District (Ban Keng Done region in the Figure 5.2) in the southern region of the Lao Peoples Democratic Republic.

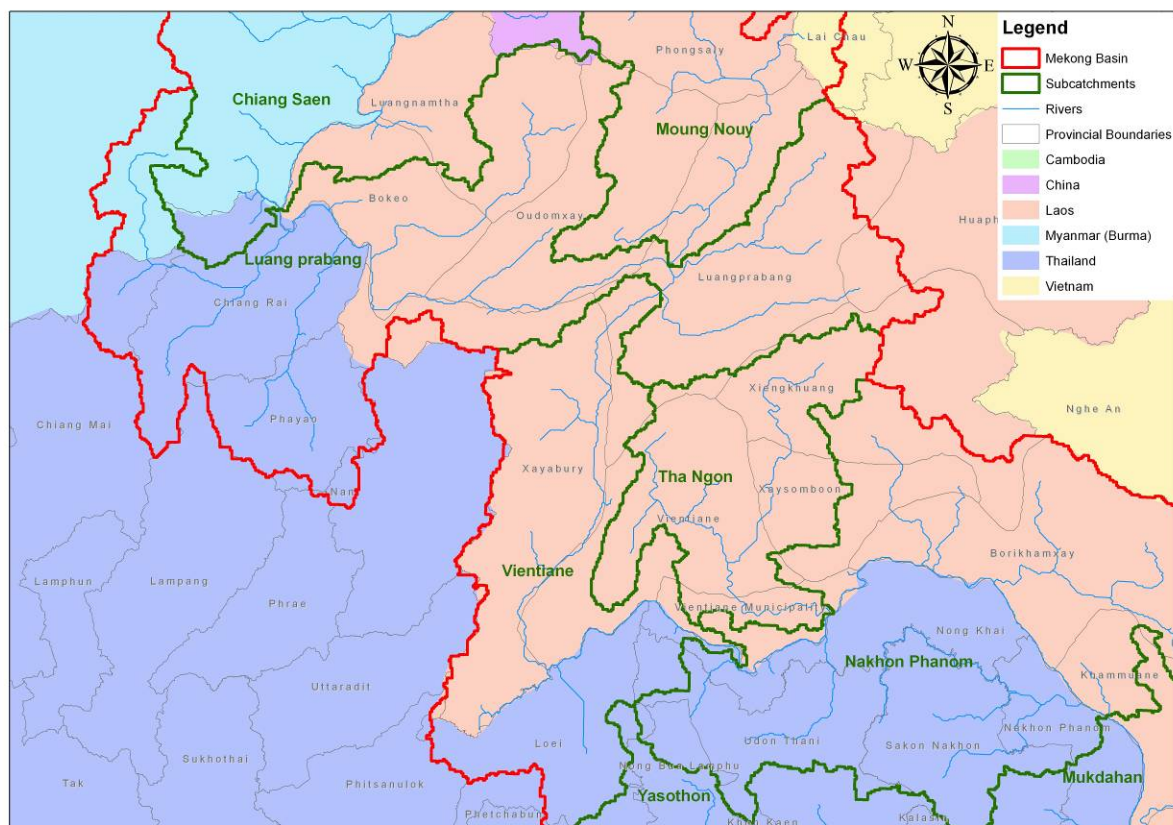


Figure 5.3. Northern parts of the Mekong Basin showing countries, regions and provinces.

5.3. Groundwater quality

5.3.1. Cambodia

The quality of groundwater extracted from alluvium is generally good and fit for most purposes. In many areas the dug wells are used for domestic water supply. The data are too limited to draw global conclusions and suggest advisory guidelines on limits to drainage density. The groundwater is extensively used for drinking water supplies in the Mekong Delta in the Cambodia (southern parts of the delta region in the Figure 5.1). The family-based groundwater wells have been becoming popular during the last 10 years in this region due to bacterial diseases from using the surface water. Arsenic contamination of groundwater in this area was first identified in 2000 by Feldman *et al.*, (2001). Later on it was found that there is a wide spread arsenic contamination of groundwater resources in the Mekong flood plain or Delta where some 100,000 family-based wells exist for drinking water supply (Polya *et al.*, 2003; Polya *et al.*, 2005; Stanger *et al.*, 2005; and Trang *et al.*, 2005). Buschmann *et al.* (2007) conducted a comprehensive survey in an area of 3700 km² in the Mekong River floodplain (border region in the Figure 5.1) and found a wide-spread arsenic contamination ranging from 1 to 1340 µg/L (average 163 µg/L) with 48% exceeding 10 µg/L. Around 350 people per km² are potentially exposed to chronic arsenic poisoning. These elevated levels of arsenic are sharply restricted to the Bassac and Mekong River banks and the alluvium braided by these rivers. Regions of low to elevated levels of arsenic in the groundwater are in co-incident with the present low relief topography featuring gently increasing elevation to the west and east of a shallow valley-understood as a relict of pre-Holocene topography. There is also additional threat from elevated levels of manganese in the groundwater.

5.3.2. Vietnam

The groundwater quality is good in many parts of the country. In the Vietnamese delta (delta region in the Figure 5.1) the groundwater is affected by acid sulphate leaching from acid sulphate soils. According to Berg *et al.*, (2007) there was evidence of groundwater arsenic contamination in the southern Vietnam (southern parts of delta region in the Figure 5.1) where its average concentration was around 159 µg/L. It is estimated that around 0.5-1 million population of the Mekong Delta (delta region and southern parts of border region in Vietnam) is at the risk of arsenic poisoning from arsenic contamination of the groundwater.

There is an acute problem of sea water intrusion in the Mekong River delta (WEPA, no date-A) and the sea water is registered in almost half of the area. Elevated levels of nitrogen and iron have also been found in some observation wells in the Mekong delta. There is evidence of pollution from poorly maintained septic tanks, garbage dumping, and industrial effluents in part of the Mekong River Delta.

There are large groundwater reserves in the confined aquifers of the Mekong Delta but most are either brackish or saline (Haskoning, 2000). As much of the water is either brackish or saline care is needed for their exploitation as their recharge characteristics are poorly understood. The Upper Middle Pleistocene, coarse to fine sand confined aquifer in the north and south of Delta, contain good quality water with TDS less than 1000 mg/L. The Lower Pleistocene below the Upper Pleistocene contains even better quality groundwater over 60% of the Delta. The Upper Pleistocene aquifer outcrops near the Cambodian border. The interactions between annual surface flooding and groundwater recharge are yet to be investigated. There is a possibility of groundwater acidification from pumping-induced oxidation of sulfidic sediments and the subsequent solution and mobilisation of heavy metals.

5.3.3. Thailand

Most of the aquifers in the Northeast Thailand (Nakhon Phanom, Mukdahan, Yasothon and Ubon Ratchathani regions in the Figure 5.2) are saline and are not suitable either for domestic or irrigation use. The main sources of groundwater pollution in Thailand are agricultural run-off, coastal aquaculture, industrial effluents and domestic sewage. National level information about groundwater abstraction rates and the extent of contamination is limited. Deforestation in the northeast Thailand is the main cause of rising water tables and salinity problems (Hirsch and Cheong, no date). The groundwater salinisation in this northeast Thailand region is mainly induced by a rock salt layer that underlies this region (Imaizumi *et al.*, no date). The salinity is also expected to increase in this region due mainly to irrigation development. Ichikawa *et al.* (2007) found that the groundwater levels in the Nam Kam River catchment (south-eastern parts of the Nakhon Phanom region in the Figure 5.3), a tributary of the Mekong River, located in the northeast of Thailand are significantly influenced by the stage heights in the river. River recharges the shallow aquifers during flood periods. Afterwards the groundwater levels fall 5 to 6 m due to groundwater abstractions. The groundwater exploitation often causes depletion of the shallow groundwater such that its level drops below the deeper saline groundwater level. This reversal of groundwater levels causes salinity problems in the shallow aquifers.

5.3.4. Myanmar

This country has huge groundwater resources. The detailed investigations about its use, sustainability and quality were not available from the literature and probably have not been carried out yet. The groundwater quality issues in catchments of the Mekong River in Myanmar are largely unknown.

5.3.5. Lao PDR

The water quality from the Annamian aquifers (northern parts of Moung Nouy and Luang Prabang regions in the Figure 5.3) is reasonably good. It is considered potable in the most parts but rich in iron. The Indosinian group of aquifers (Luang Prabang and central and northern parts of Vientiane regions in the Figure 5.3) are mostly freshwater sediments. Horizons of brackish water also exist and there is one major zone of saline water. There is

evidence of groundwater contamination from poor sanitation and sewerage facilities in the rural areas of the Lao PDR both within and outside the Mekong Basin.

5.4. Conclusions

Generally the groundwater resources of the Mekong Basin have not been investigated in detail. Very limited information about the groundwater resource size, use, sustainability and quality is available from the literature. Only a few studies, focusing on some local areas within the Mekong Basin, exist where they have made some assessments of the resource, use and/or quality.

In Cambodia, the groundwater is mainly used for both domestic supply and irrigation of vegetable and fruit crops. The groundwater use was around 290,000 m³/day in 2000. Cambodia can be divided into three regions (namely the Mekong lowlands, the South-western highlands and the Coastal Plain of South-western Cambodia) on the basis of landforms, geology and occurrence of groundwater. The storage capacity and sustainable yield of formations underlying these regions have not been investigated. The groundwater recharge occurs through seepage from rainfall and seepage from areas inundated with flood water during rainy season. There are no reliable groundwater recharge estimates available except a few local yield estimates.

There is abundant groundwater resource in the Mekong Delta of Vietnam. A large number of wells have been installed in the Mekong Delta to extract groundwater for domestic supply and irrigation. The saline groundwater is also extracted to support aquaculture. The groundwater extraction rate was estimated at 420,000 m³/day in 2002. In the central highlands (eastern parts of the Se San region) the groundwater is over-exploited to support coffee crop. In this region the coffee crop areas has increased dramatically within the last few years however there have not been any detailed investigations about the groundwater resource availability and impacts on its sustainability and quality from over-exploitation.

There are relatively large groundwater resources and aquifers yield a large quantity of water throughout Thailand. The groundwater irrigation is mainly in the north and northeast of country. In the northeast the aquifers of recent alluvium of 1 to 10 m thickness flank the main Mekong River. The main resource of recharge to these aquifers is through seepage from rainfall and it is estimated that around 5-6% of total rainfall is recharged to the groundwater.

There are abundant groundwater resources in the Myanmar. However the pressure on both surface and groundwater resources of the country is increasing due to population growth and increase cropped areas. To date there have been no detailed investigative studies of the groundwater resources of the Myanmar.

The groundwater is considered as a large and generally untapped resource in the Lao PDR. The knowledge of groundwater occurrence, monitoring and use is very limited. The country can be divided into two geological areas: the Annamian Strata occupying most of the northern and eastern parts and the Indosinian sediments mainly along the Mekong. Yields of 12-24 L/sec can be developed from Indosinian aquifer systems. The groundwater is mainly used for irrigation and rural and town supplies. The groundwater from some of the fresh aquifers, located along the mountainous region of Lao PDR is used to irrigate around 42,000 ha of coffee crop.

In the Mekong Delta the groundwater has been used for over 100 years. In the recent years, due to pollution of surface water resources, the groundwater use is increasing. In the Mekong Delta, the current rate of groundwater abstraction is about 430,000 m³/day serving around 14 million population of the region. Currently there are no constraints on the extraction rates. In part of the Delta, the shallow groundwater aquifers have already exhausted due to over abstraction and construction of extensive surface drainage system during the 1990s. The groundwater is viewed as a possible source of industrial enterprises and dry season irrigation. The interactions between annual surface water flooding and groundwater recharge are yet to be investigated.

The groundwater quality varies across the Mekong Basin. Some superficial and confined aquifer systems of the Mekong Basin have good quality water while in other parts these resources are contaminated. In the Cambodian part of the Mekong Delta, there is widespread arsenic contamination in areas around Bassac and Mekong River banks and the alluvium braided by these rivers. In the Vietnam part of the Mekong Delta, there is also evidence of groundwater arsenic contamination. In this part of the Vietnam around 0.5-1 million people are at risk of arsenic poisoning from arsenic contamination of the groundwater. There is also sea water intrusion in almost half of the Vietnam part of the Mekong Delta.

The groundwater salinity problems are increasing in some areas of the Mekong Basin in Thailand due to rising water tables from deforestation and dissolution of rock salt from underlying salt domes. In some parts of the Mekong Delta in Vietnam the salinisation of the shallow aquifers is occurring due to lowering of shallow water tables below the deep confined aquifers from excessive abstractions and leakage from deeper saline confined aquifers into the shallow aquifers. In Lao PDR the contamination of the groundwater resource is occurring from poor sanitation and sewerage facilities in the rural areas.

The detailed investigative studies about the extent and distribution of groundwater contamination sources and their impacts on the groundwater quality have not been carried out in the Mekong Basin. There are hardly any guidelines about the monitoring and evaluation of the groundwater contamination in the Mekong Basin. Similarly there are no detailed assessments of the sustainable groundwater yields that help restrict or limit groundwater contamination in the Mekong Basin. The detailed investigations about the groundwater resources of the Mekong Basin are required as outlined in the information/knowledge gaps section below.

5.5. Implications for climate change impacts

Generally the groundwater resources of the Mekong Basin have not been investigated in detail. Very limited information about the groundwater resource size, use, sustainability and quality is available from the literature. Only a few studies, focusing on some local areas within the Mekong Basin, exist where they have made some assessments of the resource, use and/or quality. Therefore, little can be said about potential climate change impacts. However, some general remarks may be made.

Climate change may affect both the recharge to and the demand from aquifers. Since wet season rain is expected to increase, this may lead to greater recharge. For those aquifers along the rivers (in lower Cambodia especially) which are well connected to the rivers, the changed flow regime will presumably be reflected in changed aquifer levels. Larger wet season flows and floods and possibly higher dry season flows may result in higher aquifer water levels and, thus potentially a greater water resource for use.

Greater water demand in the dry season will result from the projected greater potential evapotranspiration. This will add to the likely greater demand due to increasing population and the preference in some areas for groundwater since, unlike surface water, it is less contaminated by bacteria and the like. Where arsenic contamination is a problem, such as in southern Cambodia, this may be exacerbated by greater groundwater use. Such an outcome would be a serious problem and should be avoided.

Quantifying these effects, and avoiding the serious potential arsenic contamination problems, will require addressing the knowledge and information gaps described in the next section.

5.6. Knowledge/information gaps.

Very limited reliable information about the groundwater resources of the Mekong Basin exists in the literature. Due to increasing population, the pressures on the groundwater resources of the Mekong Basin are increasing by the day. However, there is no detailed knowledge of the:

- number and/or characteristics of superficial and confined aquifer systems;

- volume of groundwater resource in aquifers systems in various parts of the Mekong Basin in various countries;
- current groundwater volumes being abstracted for various uses;
- likely future increase of the groundwater abstractions for agriculture, industrial and domestic use,
- sustainable extraction rates that guarantee or avoid groundwater contamination and or salinisation;
- sources of groundwater contamination;
- extent and distribution of groundwater contamination and salinisation; and
- impacts of groundwater contamination and salinisation on agriculture, humans, industry and economy.

To understand aquifer characteristics of the shallow and confined aquifer systems of the Mekong Basin, the detailed hydrogeological and geophysical investigations are required in various countries and regions of the Mekong Basin. This together with the groundwater monitoring network will be required for developing regional models of the groundwater systems. These regional groundwater models will help quantify the groundwater resources in various parts of the Mekong Basin. Once developed these models can be used to:

- determine volumes of the groundwater resources in both shallow and deep aquifer systems;
- determine groundwater recharge rates from flooding and rainfall under the current and future climate conditions;
- determine the sustainable groundwater extraction rates under various current and likely future land use conditions;
- assess impacts of the current and likely future climate change conditions on the groundwater resources in various parts of the Mekong Basin;
- predict impacts of the current and future abstractions on groundwater salinisation;
- assess interactions between and groundwater systems;
- assess impacts of groundwater abstractions on groundwater dependent ecosystems and environment.

It is evident from literature review that the detailed evaluations of the groundwater resources and quality of the Mekong Basin are almost non-existent. Various studies pointed out the following knowledge gaps about the groundwater resources and quality in various countries and regions of the Mekong Basin.

The interactions between surface and groundwater in the Mekong delta have not yet been investigated (White, 2003). The availability and sustainability of the groundwater resources in the Mekong Delta are largely unknown (White, 2003). There are great concerns about the quality and availability of rural water supply in the Cambodian part of the Mekong Delta. Detailed investigations are required to determine the extent and location of plantations and other engineering measures for lowering the rising water tables in the Northeast Thailand where they bring salt to the soil surface impacting on crop productivity.

The sustainability of the shallow groundwater aquifers along the Bassac River need detailed investigations to determine the optimal pumping rates and pump locations to avoid dry season extensive drawdowns and water shortages.

The aquifer systems in the central highlands of Vietnam are over-exploited. The sustainable yield of these aquifers systems needs to be determined to avoid depletion of the resource. Depletion of the groundwater resource in this area has huge implications for the coffee crop

in this area. New resources also need to be identified in this area due to vast expansion of areas under coffee crops during the last two decades.

The use of groundwater in the rain fed lowland environments of Cambodia for increased crop productivity may not be sustainable if the groundwater discharge rates exceed the recharge rates. Under current climate and land use conditions the recharge and discharge rates are well balanced and there is no net decline in the groundwater levels over time. The situation will be quite different when the discharge rates will exceed the recharge rates due to increased use of the groundwater resource over time. Detailed studies need to be initiated to assess the total volumes of the groundwater resource available, its current and likely future consumption under population growth and/or climate change scenarios and determination of sustainable yields in various provinces of the country.

Much of the groundwater in all of the Mekong Basin watersheds may contain high levels of iron, calcium and sometimes arsenic. Investigative studies should be undertaken to determine the type and levels of groundwater contamination in the Mekong Basin so that the guidelines about its use, especially for drinking purposes, can be developed. Drinking of arsenic contaminated water, for example, in the Mekong Basin is already causing very serious health problems among its rural population.

Very limited hydro-chemical and/or hydrological evaluations exist about the groundwater resources in many areas of Cambodia. There is evidence of arsenic contamination in some areas but there is no systematic program of sampling and testing this type of contamination. A national focal point is required for the detailed hydrogeological evaluations and monitoring of the groundwater resources of Cambodia.

Since most of the groundwater aquifers are either brackish or saline in the northeast Thailand, strategies for mixing of surface and groundwater should be assessed for the productive use of saline shallow aquifers.

Groundwater quality problems from tube wells vary in various provinces. The identification of the location of poor quality groundwater areas needs to be carried out to avoid any land degradation, productivity and environmental impacts. Regular monitoring of groundwater quality, especially in the peri-urban agricultural areas, should be undertaken to monitor any water quality changes over time and its contamination from heavy application of fertilisers and pesticides. Both the groundwater and surface water use planning should be carried out together; both sources are closely linked and their integrated management is required to ensure sustainable use and agricultural productivity.

6. FLOODING AND SALINE INTRUSION IN THE MEKONG DELTA

The Mekong delta is the most highly productive and densely populated part of the Basin. The area is prone to flooding in the wet season and to intrusion of seawater during dry months when discharge is low. Given the potential vulnerability of the population and economic activities in the delta to projected hydrological impacts of climate change, we assessed the response in flooding and indicators of saline intrusion to climate change.

6.1. Mean monthly discharge at Kratie

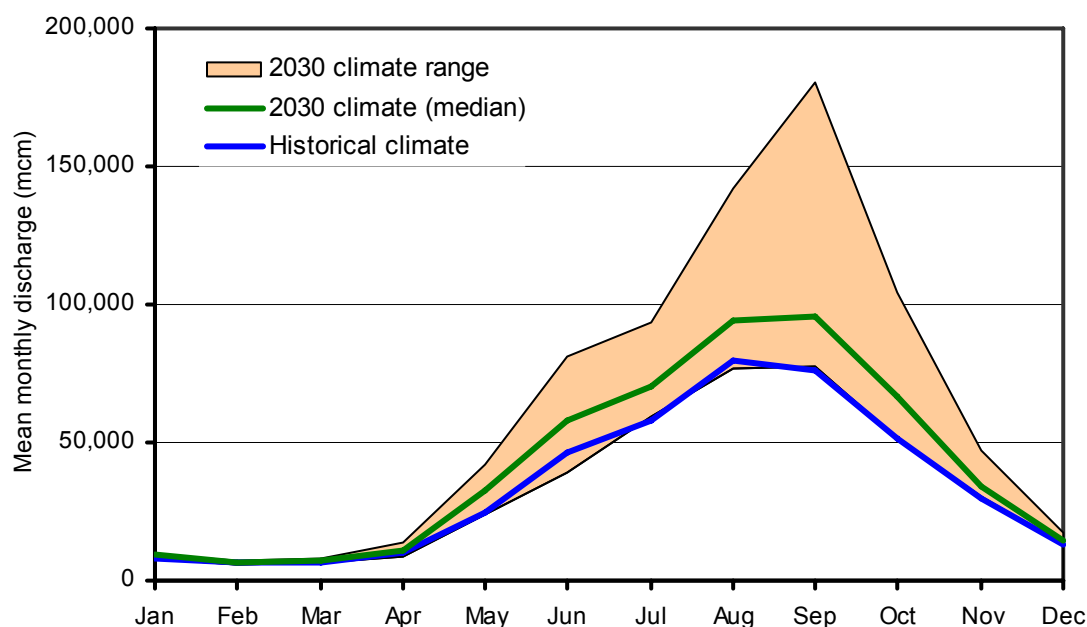


Figure 6.1. Historical (1951-2000) and future (2030) mean monthly discharge at Kratie.

Figure 6.1 indicates that there may be a significant potential impact of climate change on discharge at Kratie. The results indicate that discharge is likely to increase in all months of the year under the projected climate in 2030. The best estimate of annual discharge at Kratie, represented by the median discharge response from GCM simulations is ~500,000 mcm, an increase of 22%. There is uncertainty in discharge estimates, but most models predict increases in annual discharge at Kratie. The projected increase in monthly discharge is greatest during the wet season and smallest during the drier months. There may be positive impacts of projected increases in discharge during dry months. Low flows at Kratie influence intrusion of salt water into the Delta, with lower rates of flow increasing the area of saline intrusion. Minimum monthly flow each year is likely to increase under the projected climate in 2030, with an average increase of 580 mcm under the most likely (median) projection (Figure 6.2). The potential impact of increased minimum flows on the area of saline intrusion in the delta is unknown. This may be assessed using an hydraulic model, also considering any impact of climate change on sea level rise. Assessing the potential impact is important, since the productivity of both agriculture and aquaculture in the highly productive and populous delta area depend on salinity levels, their areal extent and their duration.

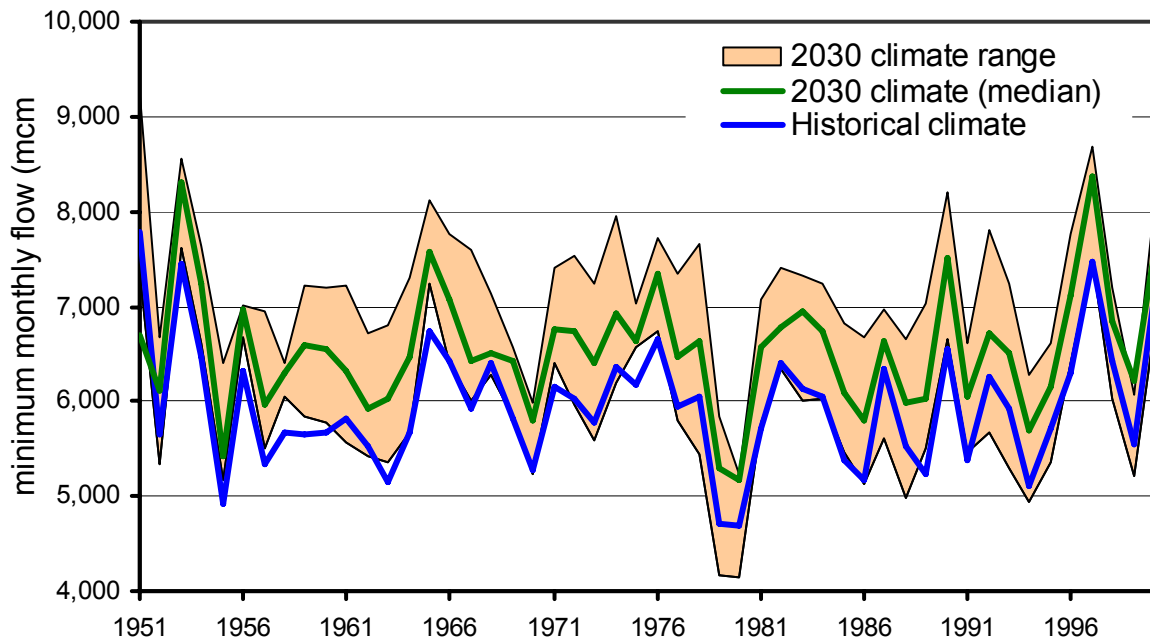


Figure 6.2. Historic (1951-2000) and future (2030) minimum monthly flow at Kratie

6.2. Frequency of flood events of different magnitudes

The annual flood volume each year at Kratie was calculated as the sum of monthly flows for months when flow exceeded the mean annual discharge at Kratie. For consistency with Mekong River Commission analyses, the mean annual discharge was taken as $13600 \text{ m}^3\text{s}^{-1}$, the mean annual discharge at Kratie from 1924-2006 (MRC, 2007). The annual Mekong flood in any year may be above or below 'normal', and the MRC have characterised flood volumes above or below the 'normal' range as significant or extreme (MRC, 2007). They define 'normal' flood years as those when the flood volume lies within the 1:10 year range, equivalent to a 10% or greater annual probability of occurrence. They define 'significant' flood years as those with an annual recurrence interval greater than 10 years, and 'extreme' years as those with an annual recurrence greater than 20 years (equivalent to annual probability occurrences of 10% and 5% respectively). Flood years may be classified as 'extreme dry', 'significant dry', 'extreme wet' and 'significant wet', depending on whether they lie in the lower or upper 5% and 10% percentiles of flow volumes. We used these MRC definitions of flooding to define flood volumes for annual probabilities of 10% and 5% for 1951-2000 modelled flows. We used the same flood volumes for annual probabilities of 10% and 5% derived from the historic data to classify modelled flood volumes estimated using 2030 climate projections, so that we could evaluate the potential impacts of climate change on flooding (Figure 6.3). Figure 6.3 indicates that there may be a significant decrease in the frequency of 'normal', 'significant dry' and 'extreme dry' flood seasons, and an increase in 'significant wet' and 'extreme wet' seasons. Although there is uncertainty around the projections, under the most likely (median) climate scenario, 'extreme wet' flood events will increase to an annual probability of 76%. Under the dry end of the climate projections, the probability of 'normal wet', 'significant wet' and 'extreme wet' events will increase. Under the wet projections, the probability of 'extreme wet' events is 96%.

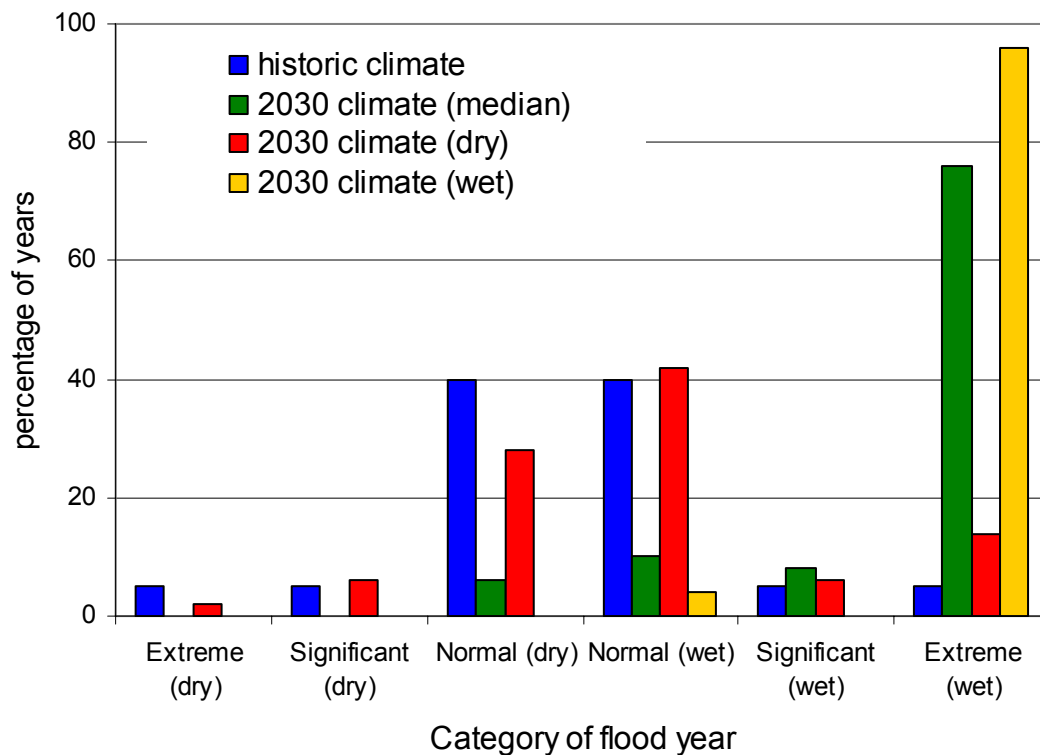


Figure 6.3. Historical (1951-2000) and future (2030) frequency of floods of different magnitude at Kratie.

The increased frequency of ‘significant wet’ and ‘extreme wet’ events projected for 2030 result from both longer duration of flooding, and greater peak discharge at Kratie, compared with historical data. The mean annual duration of flooding under historical climate conditions is 5.1 months, compared with 5.7 months duration projected for 2030. Mean annual peak monthly discharge is ~85,000 mcm under historical climate conditions, compared with ~111,000 mcm projected for 2030.

6.3. Flood mapping and area of inundation

We used remote sensing techniques to quantify the area of land flooded in the delta area each year, and it’s changes during the wet season. Two types of remote sensing instruments were used, the Tropical Rainfall Measuring Mission’s (TRMM) Microwave Imager (TMI) and the MODIS (Moderate Resolution Imaging Spectroradiometer), the latest instrument in use as part NASA’s Earth Observation System (EOS). TRMM uses passive microwave to measure the brightness temperature of radiation from earth in the microwave frequencies. Surface water strongly absorbs microwave radiation compared to land, hence in passive microwave images large water bodies appear dark compared to the bright land surface. MODIS uses optical remote sensing to record radiation from visible and infrared range of the electromagnetic spectrum. Optical reflectance differences of land and water are most pronounced in the Near Infrared 0.75-1.4 μm (NIR) and Short Wave Infrared 0.75-1.4-3.0 μm (SWIR) ranges. These wavelengths are strongly absorbed by water while also being well reflected by land surfaces and vegetation. Land and Water interfaces are readily delineated using these wavelengths.

There are complementary attributes to the two remote sensing techniques applied here. The TRMM satellite has been in operation since late 1997, whilst MODIS data has only been available since 2000. So the TRMM dataset allowed flooded area to be quantified for a greater number of years compared with the MODIS data where data was only available for wetter years. Passive microwave images have low spatial resolution and the TRMM TMI

data at 37 GHz has a spatial footprint of 16 km x 10 km. In contrast, MODIS has high spatial resolution (500m x 500m), allowing greater accuracy in mapping the flooded area. The two techniques were combined to produce a relationship between modelled flood volume and annual maximum flooded area (Figure 6.4). The methodology and results for the remote sensing analyses are described in detail in Appendix 2.

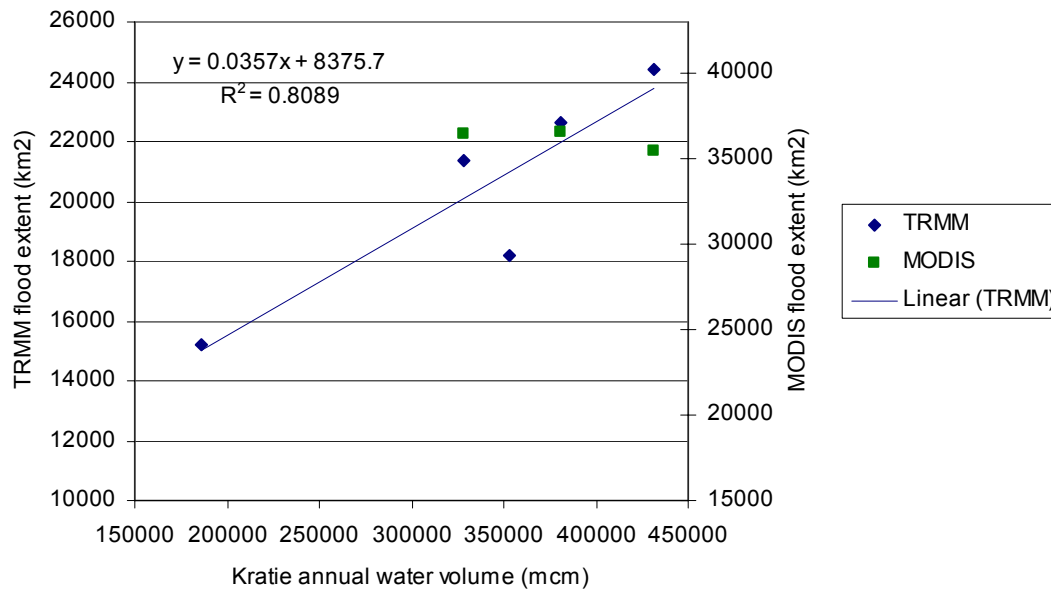


Figure 6.4. Scatterplot of TRMM (1998-2002) and MODIS (2000-2002) annual maximum flood extent for the Delta verses modelled Kratie annual water volume

The area of land flooded in the delta area each year was calculated from modelled flood volumes, using this relationship. There is uncertainty in the estimates of flooded area, but an increase in the area of flooding is likely under the median of GCM projections for 2030. Even the driest future climate projections indicate an increase in the area of flooding in the delta. The size of projected increases in flooded area shown in Figure 6.5 is intended to be indicative only. The linear relationship between flood volume and area of inundation used to estimate flooded area was derived using images with a maximum area of flooding of ~40,000 km². There is uncertainty associated with extrapolation of this relationship to greater flood volumes and areas. Furthermore, any potential impact of climate change on sea level rise and its interaction with the likely projected increase in flows at the delta have not been quantified. Nonetheless, it is likely a combination of greater peak flows and longer duration of flows into the delta and likely sea level rises will cause an increase in the severity of flood impacts in the delta.

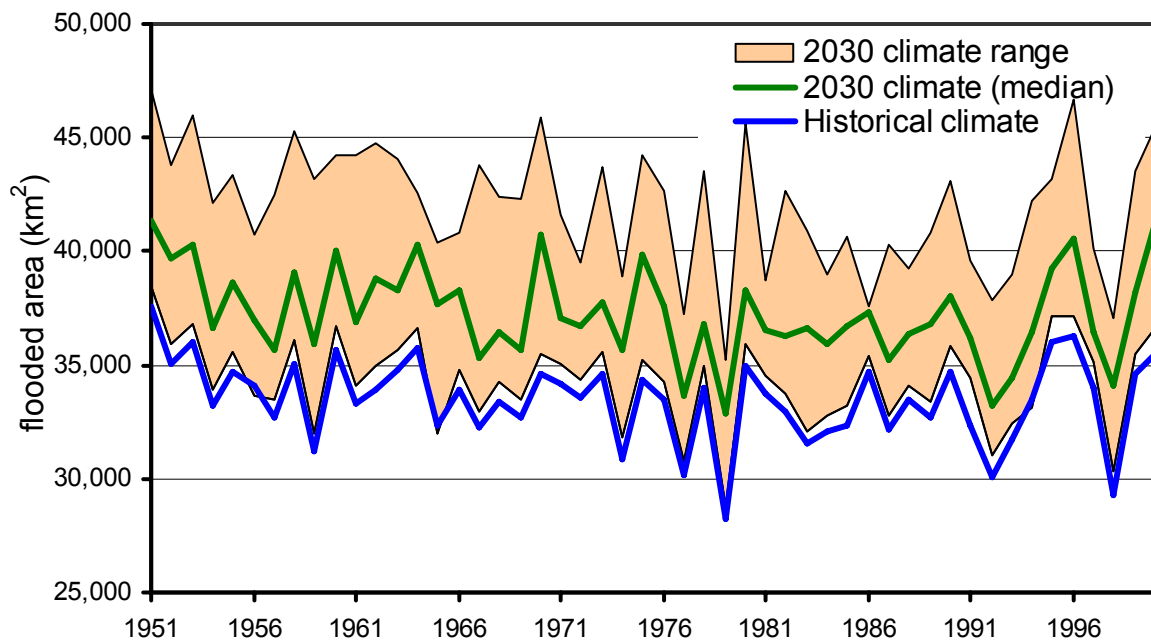


Figure 6.5. Historical (1951-2000) and future (2030) flooded area in the Mekong delta.

The actual area flooded can be mapped using both TRMM and MODIS data (Figures 6.6 and 6.7), but with greater spatial resolution using the MODIS dataset. These maps may be overlain onto other datasets to examine and quantify the impact of flooding in more detail. For example, flood maps could be used with land use maps to evaluate the area of agricultural land affected by flooding, and hence quantify the likely impacts on productivity. They could also be used with population maps to quantify the areas where the population will be most severely affected by flooding, so that remedial measures may be implemented.

Thus the increases in runoff projected for all catchments of the basin, increases discharge downstream at Kratie, resulting in greater frequency and severity of flooding in the delta region, higher minimum flows and potentially less saline intrusion in the delta (depending on sea level rise under climate change). We have quantified the likely increase in frequency of extreme flood events, and indicative areal impact of flooding in the delta region for the projected climate of 2030. Given the projected increase in runoff for all catchments of the basin, it is likely that other parts of the basin will also be adversely affected to varying degrees by an increase in flooding by 2030. The response may be readily quantified in these catchments by similar techniques to those applied in this study for Kratie. Quantification of the economic and social impacts of flooding, while important, is beyond the scope of this study.

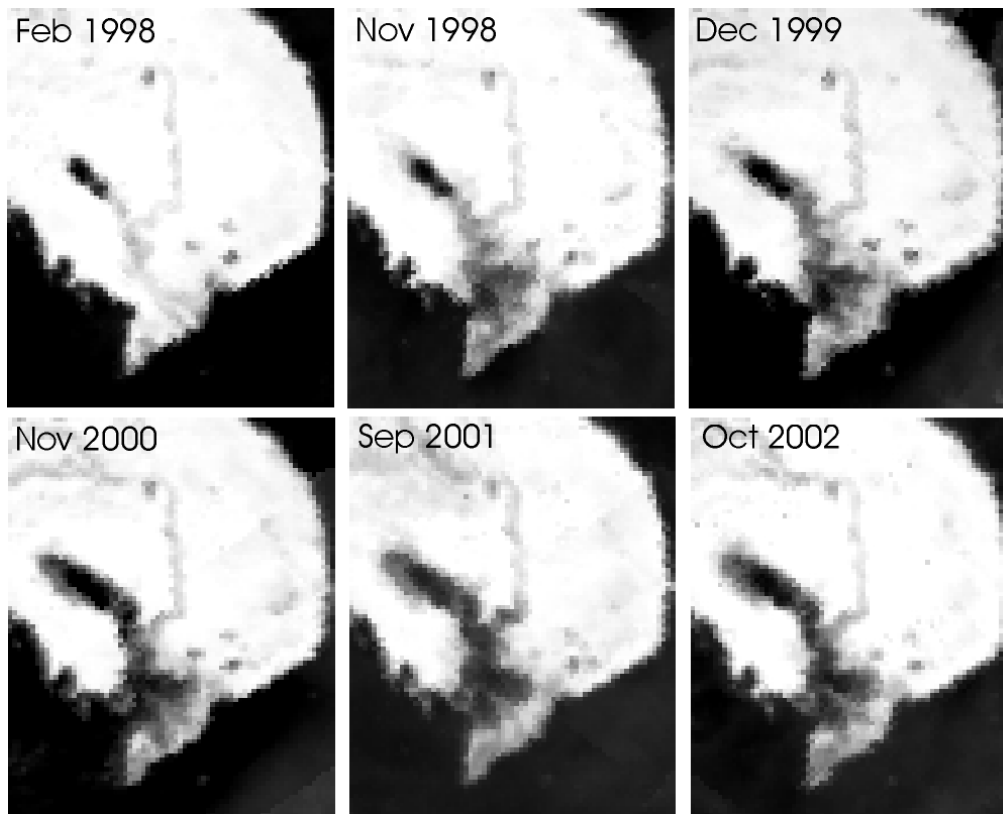


Figure 6.6. TRMM scenes of the Lower Mekong River for a dry month (Feb 1998) and the maximum flood months for 1998 – 2002. Dark areas indicate water.

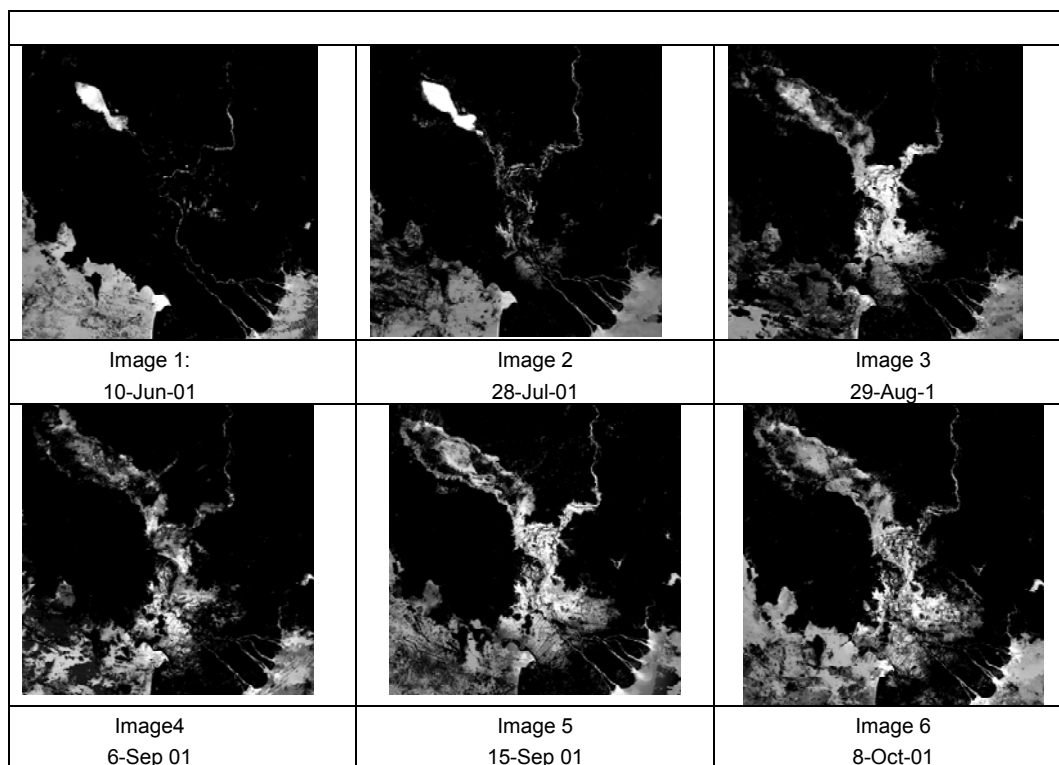


Figure 6.7. MODIS scenes of the Lower Mekong River for the flood season of 2001. Light areas indicate water.

7. RESPONSES OF THE TONLE SAP LAKE

The Tonle Sap Lake plays a key role in the livelihoods of the people of Cambodia, accounting for about 60% of Cambodia's inland fisheries production (Baran et al. 2007). The hydrology of the lake is closely linked to the productivity of capture fisheries, so any potential changes under climate change could have significant impacts on the Cambodian population. The dynamics of both the area flooded and the water levels in the lake are important for the productivity of capture fisheries, so relationships between modelled lake storage volumes and flooded area (Figure 7.1) and water level (Figure 7.2) were used to estimate lake area and water levels under historic and projected climate conditions. The remote sensing techniques and methodology used to derive the relationship between Tonle Sap modelled storage volumes and lake area are described fully in Appendix 2.

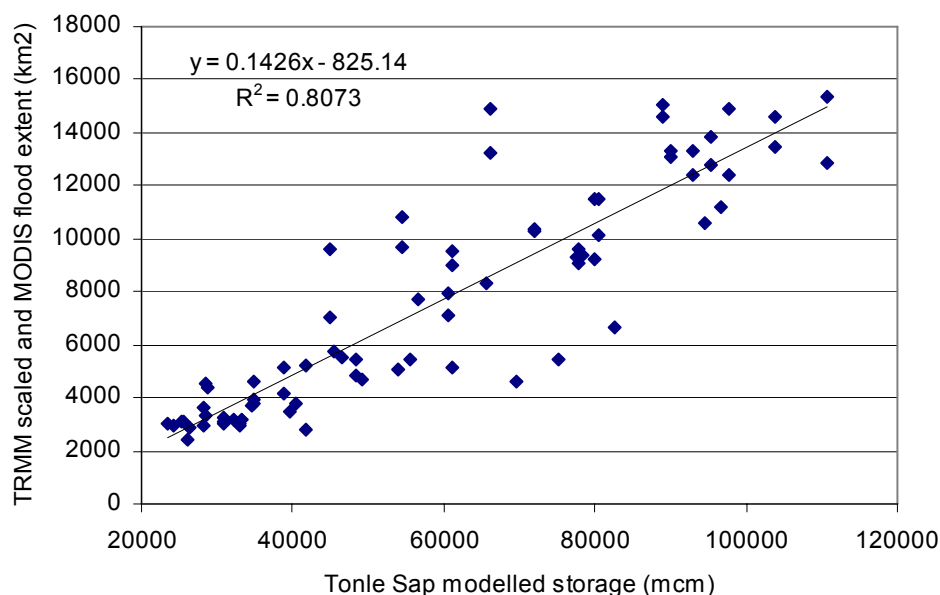


Figure 7.1. Scatterplot of the combined MODIS (2000-2002) and scaled TRMM (1998-2002) monthly flood extent for the Tonle Sap Lake versus modelled monthly water volume.

Under the most likely projections for 2030, storages in the lake will increase causing both the maximum and minimum area of the lake to increase each year (Figure 7.3). The size of projected increases in maximum area shown in Figure 7.3 is intended to be indicative only. The linear relationship between Tonle Sap storage and area used to estimate the area of the lake was derived using images with a maximum area of flooding of ~15,000 km² (Figure 7.2). There is uncertainty associated with extrapolation of this relationship to greater storages and areas. The maximum area of the lake during the wet season is projected to increase by an average of 3600 km². During the dry season, the edge of the lake is projected to expand by an average of 165 km² (Figure 7.3).

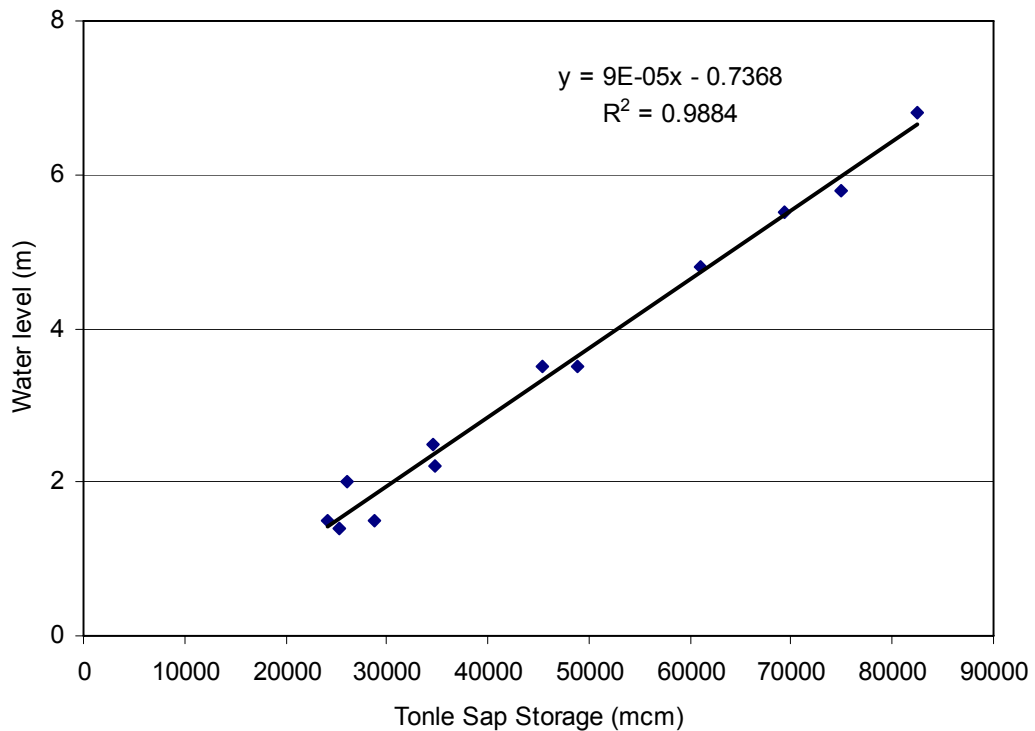


Figure 7.2. Relationship between modelled water volume in the Tonle Sap lake, and water levels in the lake derived from Baran *et al.* 2007.

Under the most likely projections for 2030 the maximum and minimum levels of the Tonle Sap Lake will also increase (Figure 7.4). Minimum levels are projected to increase by an average of 0.1 m, and maximum levels by an average of ~2.3 m each year.

The net impact of the projected increase in both maximum and minimum area is likely to be complex, with potential for both positive and negative effects. Greater flood volumes have been associated with an increase in capture fisheries from the lake, but there may be negative impacts associated with damage to agricultural areas, housing and infrastructure. Because of the likely increase in minimum area of the lake, some of the flooded forest within this area will become permanently submerged and is likely to be destroyed. The forest acts as a buffer protecting the floodplain against erosion under stormy conditions. It also provides habitat which is important as a fish breeding, feeding and shelter area (Baran *et al.* 2007). Increased runoff from the Tonle Sap catchment and upstream catchments of the Mekong is likely to increase input of sediments, influencing nutrient cycling in the lake and the fertility of cropping enterprises on the floodplain. The survival rate of fish eggs may be affected through the interaction of egg buoyancy and sediment load. Flows to and from the Mekong River will increase, and changes in flow may influence the drift of eggs, larvae and juveniles. The timing of the onset of flood is also likely to be impacted, with water levels rising earlier in the year, and the duration of the flood each year likely to increase (Figure 7.5). Clearly, the impacts of climate change on the complex ecology of the floodplain are diverse and inter-related, and require further investigation to elucidate them and determine the flow on effects on the population, livelihoods and the economy of the region.

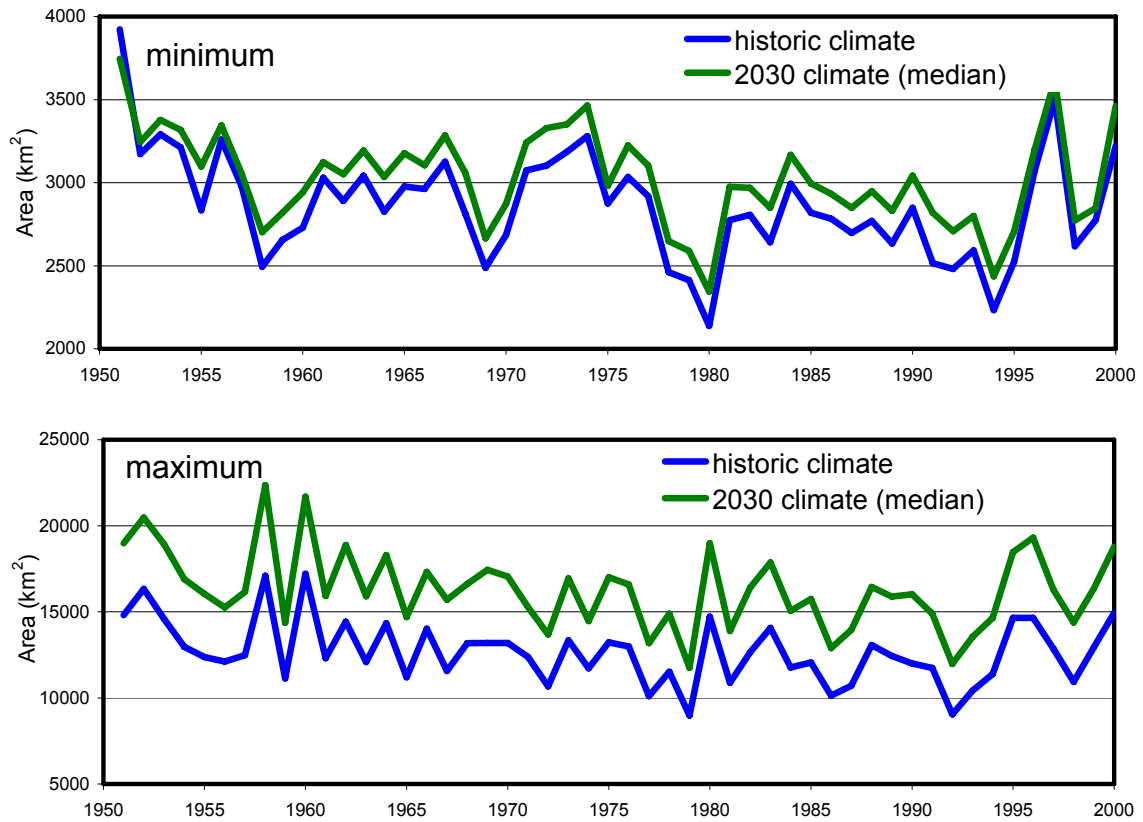


Figure 7.3. Historical (1951-2000) and future (2030) maximum and minimum area of Tonle Sap Lake

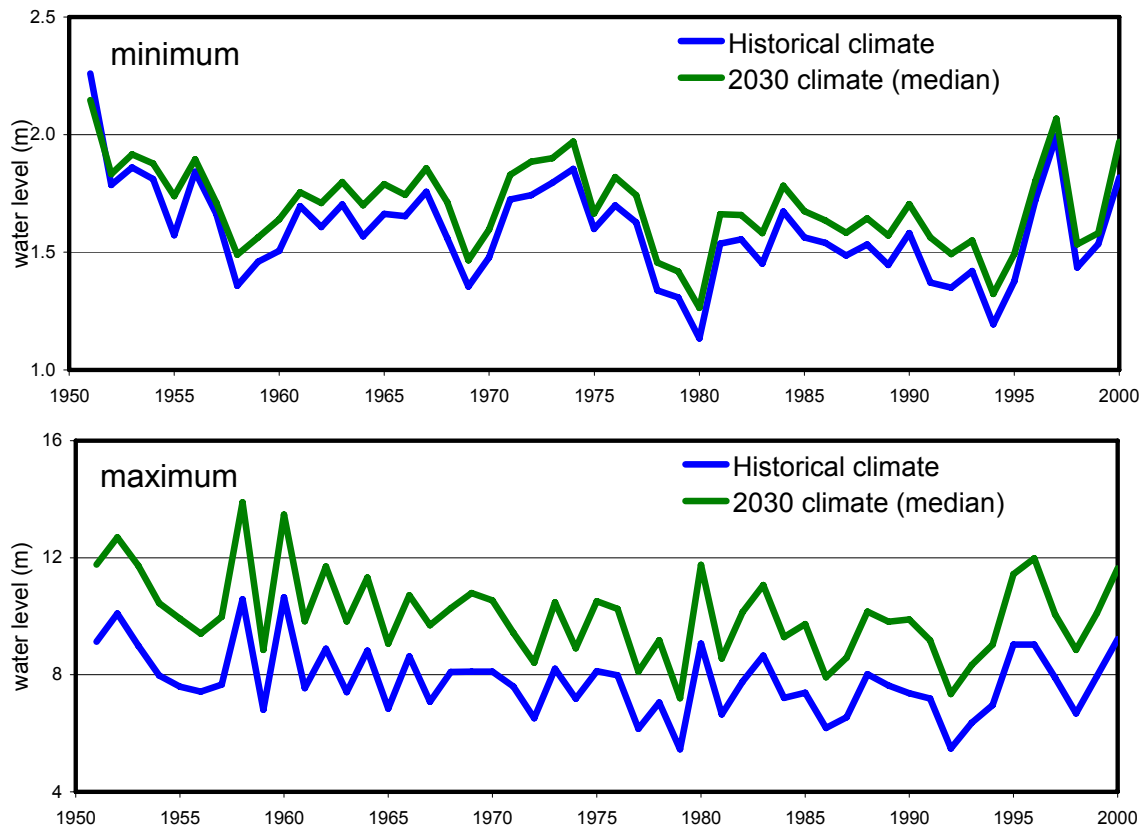


Figure 7.4. Historical (1951-2000) and future (2030) maximum and minimum annual water level of Tonle Sap Lake.

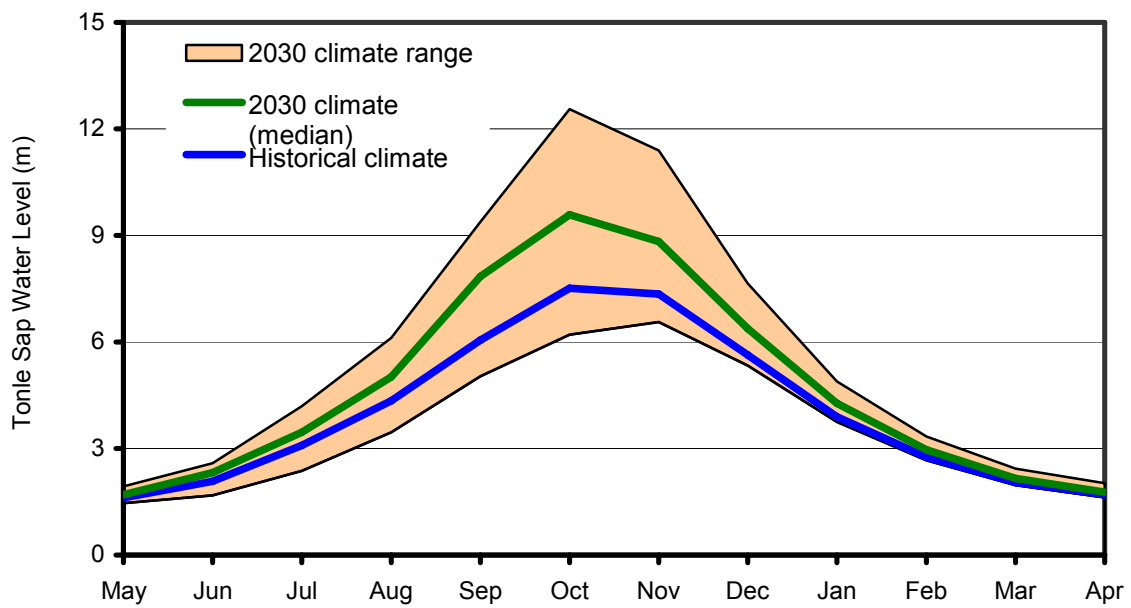
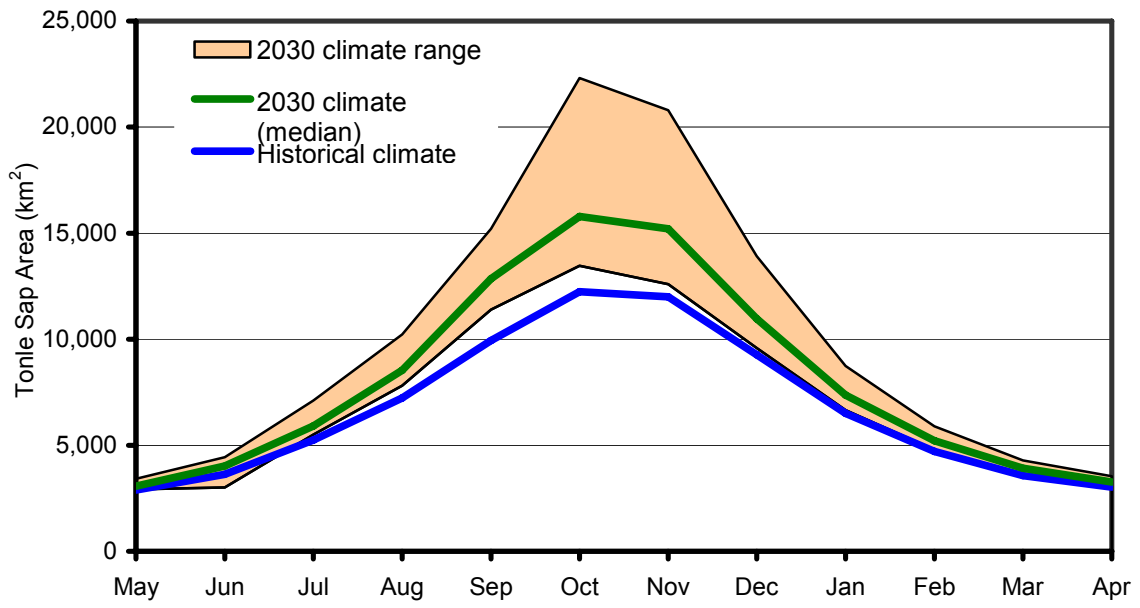


Figure 7.5. Historical (1951-2000) and future (2030) seasonal fluctuation in area and water level of Tonle Sap Lake.

8. IMPACT OF CLIMATE CHANGE ON AGRICULTURAL PRODUCTIVITY

8.1. Introduction

Nearly 85% of the Mekong's population is employed in agriculture, fisheries and forestry (MRC, 2003). Improving agricultural productivity is critical to raising the incomes of poor rural communities which ultimately helps alleviate poverty. Agricultural productivity strongly influences food security. Growth in productivity can increase and stabilize food supplies, as well as increase the ability to purchase food (Block, 1995). However, improving productivity is facing serious challenges in the future due to population growth and anticipated climate change. Total food demand will increase at a rate greater than that of population alone, due to rising incomes and changing diet preferences with urbanisation.

Variability in the water cycle driven by climate change is considered likely to significantly impact food production in the near future (Toritani et al. 2007). According to the Intergovernmental Panel on Climate Change (IPCC, 2001) such change will have both beneficial and adverse effects on both environmental and socio-economic systems, but the larger the change and the rate of change in climate, the more adverse effects predominate.

Thus, agriculture faces greatly increased demands for food on the one hand, and several threats to production due to climate change on the other. Against this background, it is important to examine the potential impact of climate change on agricultural productivity of the basin. This will help prepare adaptation strategy and its costs can be reduced by anticipation, analysis and planning.

Here we study the potential impact of climate change on the agricultural productivity of the Basin. Natural ecosystems and agricultural production systems are significantly affected by climate, such as air temperature, radiation, rainfall, wind direction and speed, to name a few (Nawata et al., 2005). Among these, the influence of rainfall is very large in both natural and ago-ecosystems. Generally, rainfall in the tropics is known to be unstable in both amount and distribution (Jackson, 1977). Regional variation is also large, thus the influence of rainfall characteristics on vegetation is rather complicated in tropical monsoon area. Agricultural production is naturally unsteady under such unstable and erratic rainfall conditions, unless irrigation systems are applied (Nawata et al., 2005).

Rice yields are highly sensitive to the transplanting date, with earlier transplanting dates resulting in a substantially higher yield than later planting dates. Hasegawa et al. (2008) showed that simulated grain yield for the crop transplanted in June was more than two times the yield for crops transplanted in August in northeast Thailand. Adequate rainfall during the land preparation and nursery period is thus very important for early transplantation of rice. Areas with a large amount of rainfall, transplanting occurred early, resulting in a long growth duration that ensured high yields; in contrast, areas with limited rainfall had later transplanting and shorter growth duration (Hasegawa et al., 2008).

Adequate water during the total growing period is needed for vigorous growth and high yield. Because plants have to recover from transplanting and for formation of the roots, adequate water supply just following transplanting is important. For high yields, a certain level of water depth is required in the paddy field at different growth stages (Doorenbos and Kassam, 1979). The most sensitive periods to water deficit are flowering and the second half of the vegetative period. When moisture content of the soil decreases to 70 to 80% of the saturation value, rice yields begin to decline. At a soil water content of 50% of saturation,

yield decrease is 50 to 70 percent. At a soil water content of 30%, no yield can be expected and plants die when soil water content is below 20% (Doorenbos and Kassam, 1979).

Studies on the impact of climate change on agricultural productivity of the Mekong are very limited. Kono et al. (2001) developed a GIS-based crop modelling method for evaluating the productivity of rain fed agriculture at the regional level, and applied the model to lowland paddy in Northeast Thailand. They estimated and mapped the potential yields and attainable yields under water limitations. Hoanh et al. (2003) assessed the impacts of climate change and climate variability on food production, food security and the environment (ecological and social), and developed adaptation strategies to alleviate the negative impacts on food and environment for the Mekong River Basin. SEA START RC (2006) studied the impact of climate change on hydrological condition and rain-fed agriculture in Southeast Asia with a focus on the lower Mekong River basin. They also assessed the vulnerability and adaptation of rain-fed farming to climate change impacts. Toritani et al. (2007) evaluated the variability in the water cycle and its impact on food production on a regional scale by constructing and developing a hydrological process and crop yield estimation model. The model has been applied to the North-eastern region of Thailand and the Mekong Delta of Vietnam. Sawano et al. (2008) modelled the dependence of the crop calendar on rainfall patterns based on a survey of the region's farmers as part of an effort to provide a stronger basis for regional yield estimates. Coupling this model with a simple crop model, Hasegawa et al. (2008) estimated the regional yields of rain fed lowland rice in Northeast Thailand.

The models developed by Kono et al., (2001), Sawano et al. (2008), Hasegawa et al., (2008), and Toritani et al. (2007) are potential tools to use to assess the impact of climate change on agricultural productivity. However, none of these studies used future climate projections to assess these impacts. Furthermore, these models have also only been applied to part of the Basin. Thus the impact assessment of SEA START RC (2006) and the studies of Hoanh et al. (2003) are based on field scale models applied to few locations in the Basin.

In this study, we use 11 different climate simulation models to generate projections for future (2030) climatic conditions. We used these data as input to a water-balance model and FAO yield response model to assess the regional impact of climate change on agricultural productivity.

8.2. Method

We used a soil water balance simulation model and FAO crop water production function given by Doorenbos and Kassam (1979) to estimate the impact of climate change at regional scale on the productivity of major crops grown in the basin.

8.2.1. Soil-Water Balance Simulation Model

The soil-water balance simulation model is based on the FAO Irrigation and Drainage Paper 56 (Allen *et al.* 1998), and similar to that of the CROPWAT model developed by FAO. The model simulates soil water for upland crops and ponded water depth and soil water for rice at a 10-day time step. The inputs to the model are monthly rainfall and potential evaporation, crop coefficients, rooting depth, crop planting time and growing period, length of growth stages, soil properties such as field capacity, wilting point, saturated moisture content, depletion factor, maximum and minimum ponded water depth and percolation rate for rice. The model can simulate both irrigated and rain fed crops. The outputs of the model are actual crop evapotranspiration (ET_a), potential crop evapotranspiration under well-watered conditions, irrigation requirement (for irrigated crops), and effective rainfall during the cropping period. The model has been used to estimate ET_a and irrigation water requirements for a range of crops grown in the Murray-Darling Basin (Mainuddin *et al.*, 2007 and Qureshi

et al., 2007). The model has also been used in the Lower Mekong River Basin to estimate the water productivity of the crops grown in the Basin (Mainuddin et al. 2008).

We used historical (1950-2002) and future (2030) climate data generated for 52 years by 11 GCMs, as described in Chapter 3 above. We undertook the soil-water balance simulation for projected climate outputs for each of the 11 GCMs separately, as well as for historical climate data. We modelled both rain fed and well-watered or irrigated conditions. Outputs from the model such as actual and maximum crop evapotranspiration, growing season rainfall and irrigation requirements are used for further analysis to estimate the impact on productivity using crop-water production function.

8.2.2. Crop-Water Production Function

We estimated crop yield using the crop-water production function given by Doorenbos and Kassam (1979) as;

$$1 - \frac{Y_a}{Y_m} = Ky \left[1 - \frac{ET_a}{ET_m} \right] \quad (8.1)$$

Or

$$\frac{Y_a}{Y_m} = 1 - Ky \left[1 - \frac{ET_a}{ET_m} \right] \quad (8.2)$$

Where:

- Y_a = actual harvested yield
- Y_m = maximum harvested yield
- Ky = yield response factor
- ET_a = actual evapotranspiration
- ET_m = maximum evapotranspiration

Y_a/Y_m is the relative yield.

8.2.3. Yield impact on rain fed crops

For rain fed crops, actual evapotranspiration (ET_a) is often less than the potential maximum evapotranspiration (ET_m) due to periodic stress experienced by the crop as a result of insufficient rainfall or dry periods. The relative yield for the historical condition is

$$\left(\frac{Y_a}{Y_m} \right)_{\text{Historical}} = 1 - Ky \left[1 - \left(\frac{ET_a}{ET_m} \right)_{\text{Historical}} \right] \quad (8.3)$$

For climate change condition,

$$\left(\frac{Y_a}{Y_m} \right)_{\text{Projected}} = 1 - Ky \left[1 - \left(\frac{ET_a}{ET_m} \right)_{\text{Projected}} \right] \quad (8.4)$$

In Equation (4), we have used maximum, minimum and median values of projected ET_a from rain fed simulation for 2030 conditions. Median value of ET_m for well watered condition is considered as the projected ET_m for 2030. We then compare the relative yield (Y_a/Y_m) of

projected maximum, minimum and median climate change conditions with the historical relative yield to show the impact of climate change on crop productivity.

8.2.4. Yield impact on irrigated crops

For the irrigated crops, mostly grown in the dry season, ET_a is generally equal to ET_m as additional evapotranspiration demand is met by irrigation supply. However, irrigation requirements (IR) in the future could be more or less due to anticipated change in rainfall and potential evapotranspiration. If the irrigation requirements are less than the historical requirements then the productivity of the crop will not be affected and the diversion of water from the river for irrigation will be less compared to the historical diversion. As a result, flow in the river in the dry season would increase. If more water is required for irrigation due to climate change, more diversion of water from the irrigation sources such as the river would be necessary. If the irrigation is maintained at the historical level then crop would suffer water stress and the productivity will be affected.

In this study, we estimated the productivity impact of irrigated crops assuming that the existing level of irrigation will be maintained and no additional water would be available for irrigation. In this case,

$$\text{Projected } ET_a = \text{Projected } ET_m - (IR_{\text{Projected}} - IR_{\text{Historical}}) \quad (8.5)$$

We used maximum, minimum and median values of projected ET_a to determine the impact of climate change on the productivity of irrigated crops using Equation (8.4).

8.2.5. Data Sources

Province-wise data of planted and harvested area, yield and production of different crops for Laos and Cambodia were obtained from the Regional Data Exchange System on food and agricultural statistics in Asia and Pacific countries maintained by the FAO Regional Office for the Asia Pacific Region (<http://www.faorap-apcas.org/>). Data for Thailand were collected from the Statistical Year Books published by the Office of Agricultural Economics of the Ministry of Agriculture and Cooperative of the Royal Thai Government (<http://www.oae.go.th/English/index.htm>). Data for Vietnam were from the General Statistical Office of Vietnam (http://www.gso.gov.vn/default_en.aspx?tabid=469&idmid=3).

Rice is the predominant crop in the basin. Three types of rice, lowland rice, dry season rice, and upland rice are grown in Laos and Cambodia. Lowland rice is the main rain fed rice; dry season rice is fully irrigated rice. Upland rice is also mostly rain fed grown in the upland areas of the country. Three types of rice are also grown in Vietnam; they are called summer-autumn rice, winter-spring rice and spring-summer rice (Nesbitt, 2005). Summer-autumn rice is the main lowland rain fed rice, winter-spring rice is dry season irrigated rice and spring-summer rice is the upland rice grown in the upland areas (mostly in the Central Highlands) and flood-prone lowland rice grown in flood-prone lowlands (mostly grown in the Delta). Spring-summer rice is also mostly rain fed. Rain fed rice (which is termed as major rice in the statistical database) and dry season irrigated rice (which is termed as 2nd rice in the statistical database) are grown in Thailand.

Apart from rice, upland crops (crops other than rice are generally termed together as upland crops) are also grown in the basin. Sugarcane, maize, soybean and cassava are the major upland crops. For this study, we have considered rice (all seasons), sugarcane, maize and soybean to determine the impact of climate change on yield. Cassava was not considered due to the unavailability of the yield response factor. Table 8.1 shows the crops considered with their growing season and length of growing periods.

Table 8.1. List of crops considered with their growing season and growing period

Country	Crop	Growing season	Growing period (days)
Laos	Main rain fed rice	Jun-Oct	130
	Irrigated rice	Nov – Mar	130
	Upland rice	May – Sep	130
	Maize	May – Sep	125
	Soybean	Sep – Jan	135
	Sugarcane	May – Feb	280
Thailand	Main rain fed rice	Jun-Oct	130
	Irrigated rice	Nov – Mar	130
	Maize	May – Sep	125
	Soybean	Sep – Jan	135
	Sugarcane	May – Feb	280
	Cambodia	Main rain fed rice	Jul – Nov
Irrigated rice		Nov – Mar	130
Upland rice		May – Sep	130
Maize		May – Sep	125
Soybean		Sep – Jan	135
Sugarcane		May – Feb	280
Vietnam		Main rain fed rice	Jul – Nov
	Irrigated rice	Nov – Mar	120
	Upland/flood-prone rice	Apr – Aug	120
	Maize	Nov – Mar	125
	Soybean	Nov – Mar	135
	Sugarcane	May – Feb	280

Agriculture in the lower Mekong Basin is dominated by rain fed agriculture (Makara *et al.*, 2001, Kono *et al.*, 2001, Nesbitt *et al.*, 2004, Chea *et al.*, 2004). The area of land dedicated to growing other crops is much smaller than that dedicated to rice and fluctuates in area from year to year. Almost all the crops other than the dry season rice in Laos, second rice in northeast Thailand and dry season rice in Cambodia are rain fed (Nesbitt, 2005). Some upland crops may also be grown in the dry season with full or supplementary irrigation, but we consider them to be very small compared to the area of rain fed crops. Moreover, no seasonal data on area and production of the upland crops are available. We therefore assumed that all the upland crops grown in Laos, northeast Thailand and Cambodia were rain fed. Upland crops are grown in the Mekong Delta in the dry season (November-April) except sugarcane, which are grown around the year (Nesbitt, 2005). Therefore, we can consider that these crops are partially or fully irrigated. However, it is possible that some of these crops are also grown in rain fed condition particularly in the Central Highlands.

In the model, crop coefficients, rooting depth and depletion factor were taken from Allen *et al.* 1998. Crop planting time and growing periods (Table 8.1) were mostly based on the cropping pattern used by the Mekong River Commission (Nesbitt, 2005). We also used cropping information (planting and harvesting time, percentage of area under different rice crops) available from Phaloeun *et al.* (2004), Chea *et al.* (2001), Sihathep *et al.* 2001, Makara *et al.* (2001) and Allen *et al.* (1998). Yield response factor, K_y , are taken from the FAO Irrigation and Drainage Paper 46 (Smith, 1992). Soil properties vary from field to field across the Basin (Homma *et al.*, 2001). No soil properties (as distinct from soil type) data were available. Therefore, we assumed a range of soil types such as coarse sandy loam, clay, clay loam, silt loam, very fine sandy loam and loamy very fine sand for modelling, and used average values in the analysis.

The crop water use and the impact of climate change on crop productivity that we have estimated is thus a generalised regional assessment. We believe that it is reasonable, given

that the crop coefficient approach is based on empirical crop factors – that is, on regressions of a very large number of observations of water use by many crops in many locations. Alternative approaches of using complex model would mostly require much more data, especially soil hydraulic property data, and these are not available. Complex model with slightly inaccurate data may propagate error and can render complex results meaningless (Cook *et al.*, 2006). Our aim is to find indicators to point out the main issues, and we believe this approach is adequate.

The model was run considering the sub-basin as the spatial unit. The production and crop data are available at the administrative province level. Figure 8.1 shows the overlay of the administrative provinces boundary with the sub-basin boundary. Majority of the sub-basins covers the provinces from two riparian countries.

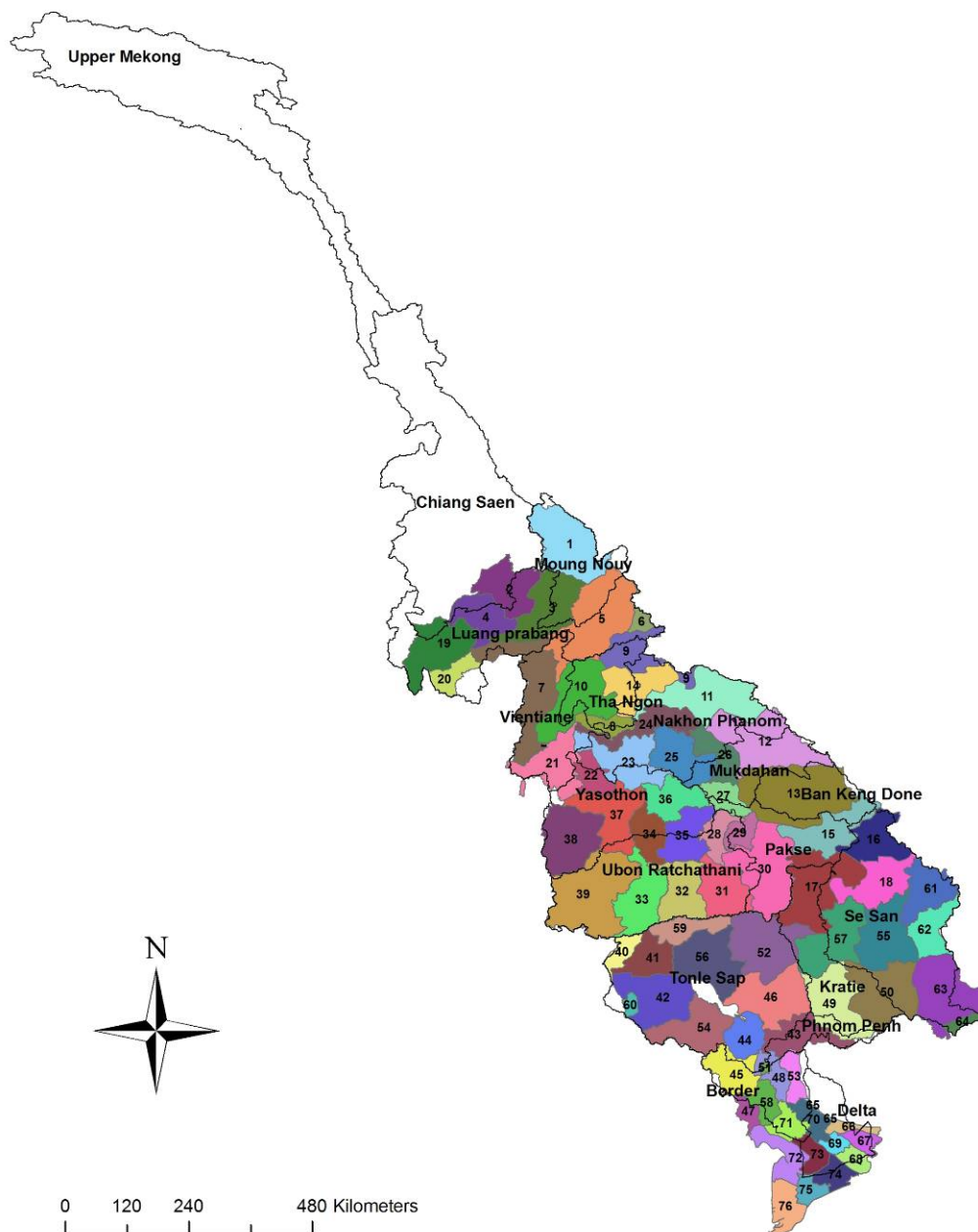


Figure 8.1. Overlay of provincial administrative boundary with the sub-basin boundary. Coloured and numbered polygons are the provinces (1-18 are in Laos, 19-40 are in Thailand, 41-60 are in Cambodia and 61-76 are in Vietnam). Black lines are the sub-basin boundary.

Se San sub-basin covers the provincial area of Laos, Cambodia and Vietnam. Of the 18 sub-basins no data on cropping were available for the upper two (Upper Mekong and Chiang Saen) sub-basins; so they are excluded from the analysis.

For the historical condition the model was run for 52 years (1950-2002) and the average of these excluding first two years is considered here as the historical or baseline scenario. For climate change scenarios, we also used the model with the generated climate change data of 52 years separately for each model. The average of these 52 years simulation result excluding first two years was considered as representative for the 2030 climate condition for that model. After arranging the data of the 11 models in descending order we then considered second from the top as the maximum and second from the bottom as the minimum, the difference of which was considered as 2030 climate range. The median value was considered as the most representative

8.3. Impact of climate change on growing season rainfall

Figures 8.2 and 8.3 show rainfall during the growing season for all rice crops (Figure 8.2) and for the upland crops sugarcane, maize and soybean (Figure 8.3) for the sub-basins. Although there is uncertainty in the projections, 2030 growing season rainfall is likely to be greater than historical for all crops except for irrigated rice in every sub-basin. Even under the drier range of projections from different GCMs, growing season rainfall is projected to be greater than historical for rain fed rice, upland rice, sugarcane and maize in all but the upper 4 (Moung Nouy, Luang Prabang, Vientiane and Tha Ngon) sub-basins. The increase in growing season rainfall is generally most significant in the middle low rainfall region of the lower Basin (Nakhon Phanom, Mukdahan, Yasothon, Ubon Ratchathani and Pakse), the area mostly covering Northeast Thailand.

For irrigated rice, which is grown during the dry season, projected (2030) growing season rainfall is likely to be lower than historical for all sub-basins except Moung Nouy (Figure 8.2). The highest reductions in projected rainfall would be in Se San, Ban Keng Done and Border catchments. There is uncertainty in projected growing season rainfall for irrigated rice, but outputs from the majority of GCMs indicate that rainfall will be reduced, and projections at the high end of the 2030 climate range are similar to historical rainfall data.

Growing season evapotranspiration (ET_a) is likely to increase in all crops and across the basin under the future (2030) climate (data not shown). The size of this increase differs for different crops, and for different parts of the basin, and for some crops in some regions increases are negligible. Increases in evapotranspiration result primarily from increased potential evaporation resulting from increasing temperatures across the basin under the projected future climate. For all crops except irrigated rice, the likely increase in growing season rainfall may also contribute to increased growing season evapotranspiration through increased soil water availability.

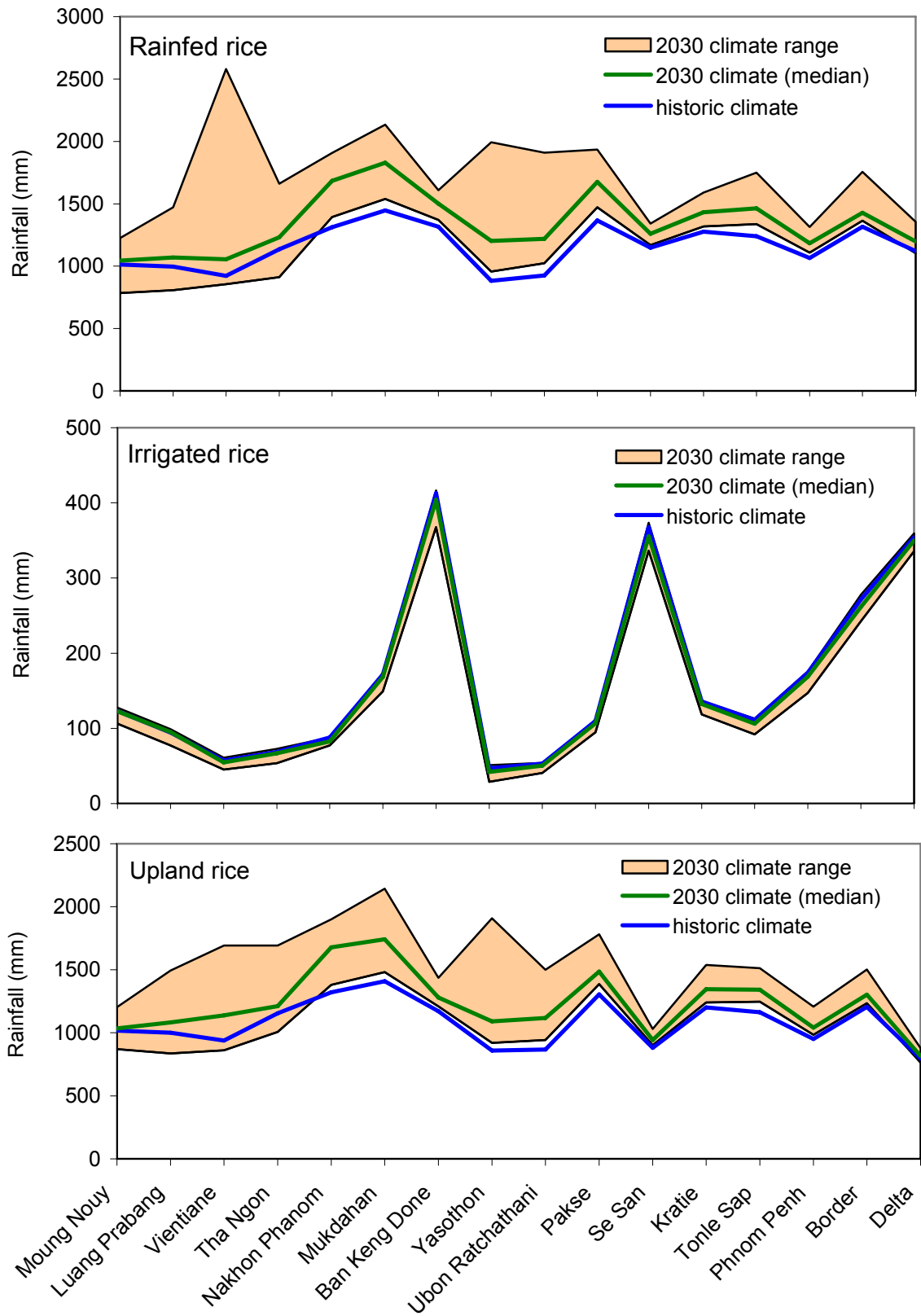


Figure 8.2. Projected and historical rainfall during the growing season of rice crops

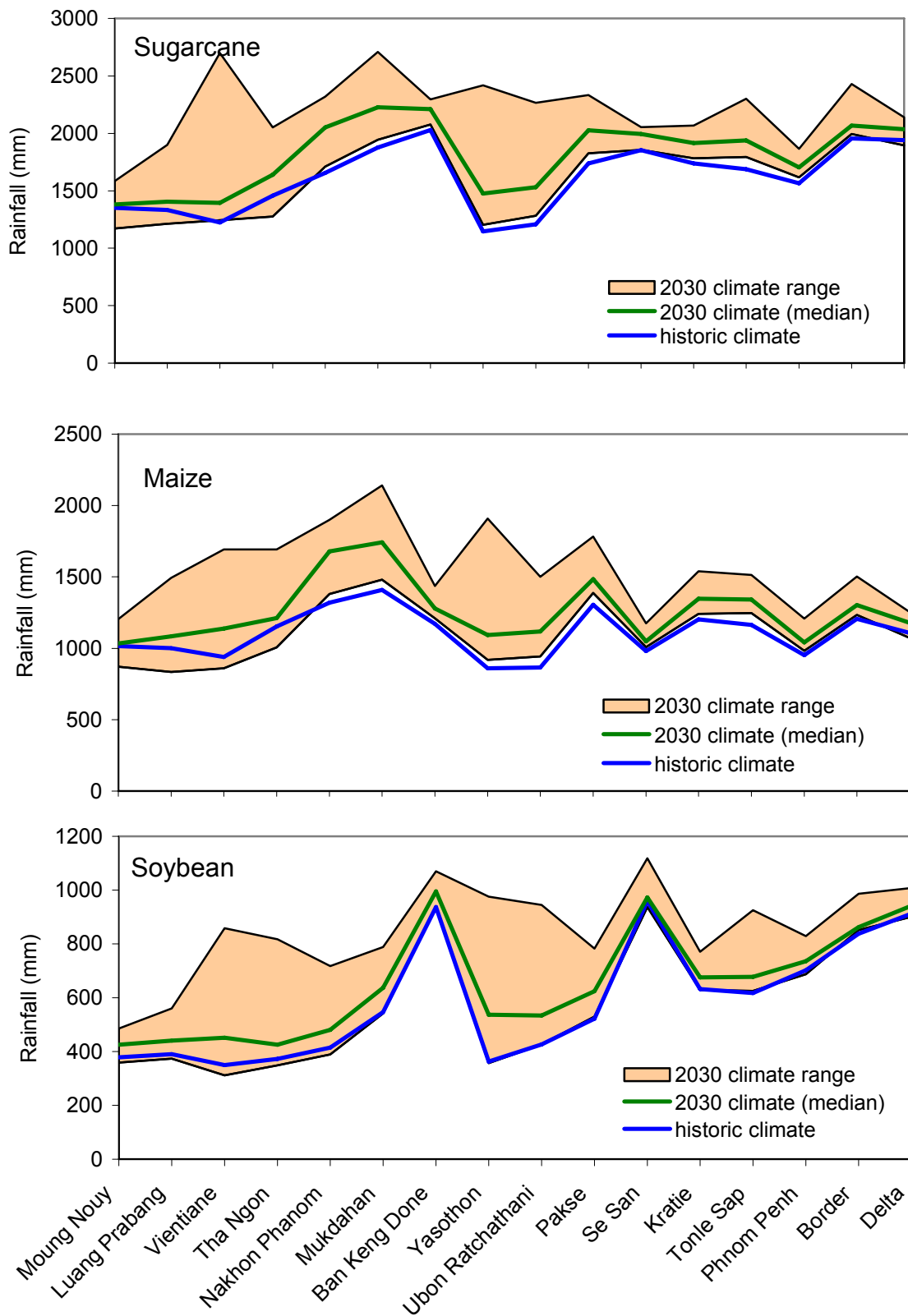


Figure 8.3. Projected and historical rainfall during the growing season of sugarcane, maize and soybean crops

8.4. Impact of climate change on crop productivity

The impact of climate change on productivity is shown for important crops of the basin below expressed as relative yield (Y_a/Y_m) for each sub-basin. Relative yield is the ratio of actual yield to potential yield, calculated for both historic climate and future (2030) climate projections. We may expect a trend of increasing productivity across the basin for all crops except irrigated rice, since growing season rainfall (Figures 8.2 and 8.3) and evapotranspiration (data not shown) are likely to increase for all crops except irrigated rice under projections of future (2030) climate. However, the response in relative yield to climate change is variable for different crops in different parts of the basin, as shown in Figures 8.4 to 8.9 below. For some crops in some parts of the basin, the relative yield is 1 under both historic and most likely 2030 climate projections. This implies that yield is likely to be unaffected by climate change, since crop water requirements for evapotranspiration are met under both historic and likely future climate conditions. For some crops in some parts of the basin, relative yield is projected to decrease under likely future (2030) climate, and in others relative yield is likely to increase. Thus increasing growing season rainfall and evapotranspiration under the likely future climate do not necessarily translate to increased yield, since potential evaporation is also likely to increase.

8.4.1. Rain fed rice

Figure 8.4 shows the impact of climate change on the relative yield of rain fed rice. The result suggests that yield would slightly decrease (up to 1.5%) in the upper 4 sub-basins (Moung Nouy, Luang Prabang, Vientiane and Tha Ngon) comprising the areas of upper Laos and the provinces of Northern Thailand. The highest increase (3.3%) would be in the sub-basins Yasothon and Ubon Ratchathani, the sub-basins mostly covering Northeast Thailand. There is no change in productivity in the other sub-basins. The uncertainty, the difference between maximum and minimum relative yield, is higher in the upper basin (Moung Nouy, Luang Prabang, Vientiane and Tha Ngon) and comparatively lower in Yasothon and Ubon Ratchathani.

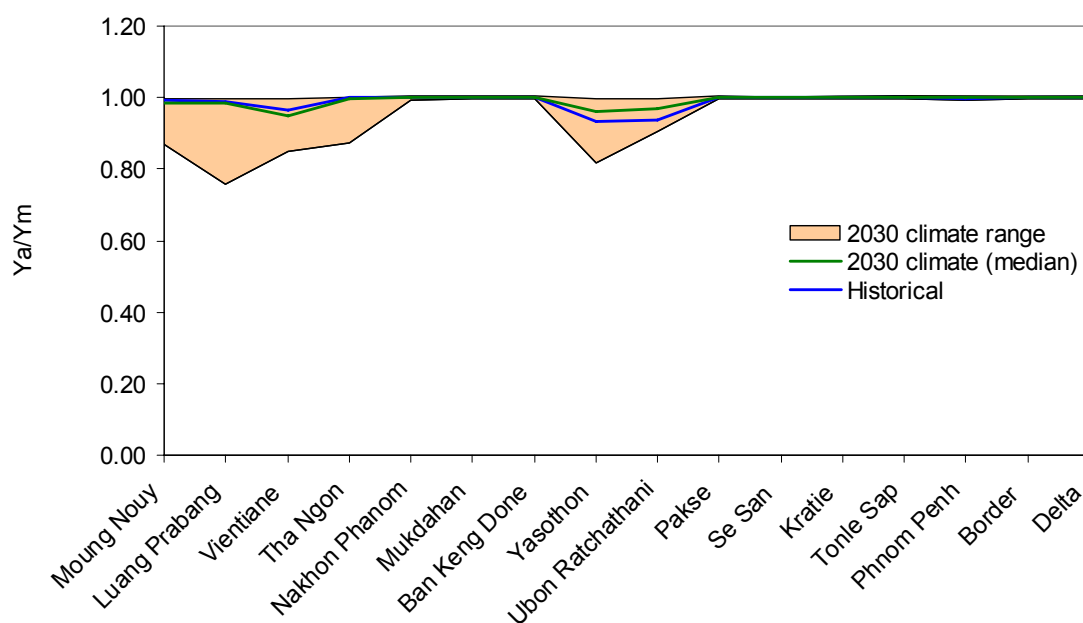


Figure 8.4. Projected and historical relative yield of rain fed lowland rice

8.4.2. Upland/flood-prone Rice

Upland rice is also grown in rain fed conditions in the upland areas such as the northern areas of Laos, upland areas of Cambodia and Central Highland areas of Vietnam. It is traditionally been grown under slash-and-burn systems with long fallows, which restore soil fertility and reduce insect and weed pressure (Saito et al., 2006). Upland rice is not grown in Thailand and the area in Cambodia is only 2% of the total cultivated area (Makara et al., 2001). In Vietnam, upland rice is considered with the flood-prone rice grown in the Delta region because they share the same growing period. We refer to them jointly as spring-summer rice. However, the area and production is highly dominated by the flood-prone rice grown in the Delta region. In 2004, the area of flood-prone rice was 96% of the total area under spring-summer rice having 97% of the total production. Flood-prone rice is grown earlier than the main rain fed rice so that harvesting can take place before the peak flows in the river.

The result suggests that yield would slightly decrease or remain the same in the upper 4 sub-basins (Moung Nouy, Luang Prabang, Vientiane and Tha Ngon) comprising the areas of upper Laos and the provinces of Northern Thailand (Figure 8.5). For the remaining catchments, the projected relative yield for the 2030 median condition is lower than the historical relative yield. The highest decrease is in the sub-basins Vientiane and Tha Ngon (1.9%). In the Delta, relative yield decreases by 1.5%. The difference between the maximum and minimum relative yield is highest in Luang Prabang (15.9 %, -12.8 to +3.1) and the lowest is in the Delta (5.5%, -5.5 to 0%).

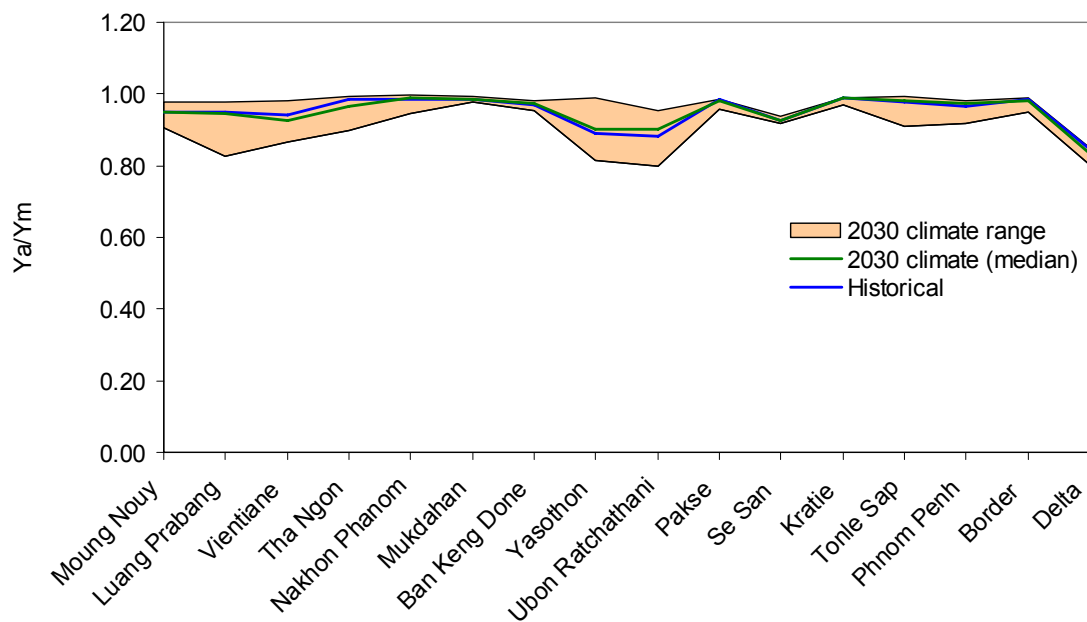


Figure 8.5. Projected and historical relative yield of upland/flood-prone rice

8.4.3. Sugarcane

Sugarcane is grown all over the basin. However industrial scale sugarcane is grown in Thailand and Vietnam. In Laos and Cambodia, the cultivation of sugarcane is more for consumption as juice. Sugarcane is grown mostly in rain fed condition, though supplementary irrigation may be applied to some fields.

The increase in relative yield for the 2030 median condition is almost negligible (Figure 8.6). The highest increase in relative yield for 2030 median condition is 1% in Yasothon sub-basin.

Chinavanno (2004b) stated that yield of sugarcane would increase in Northeast Thailand due to climate change but did not specify the amount.

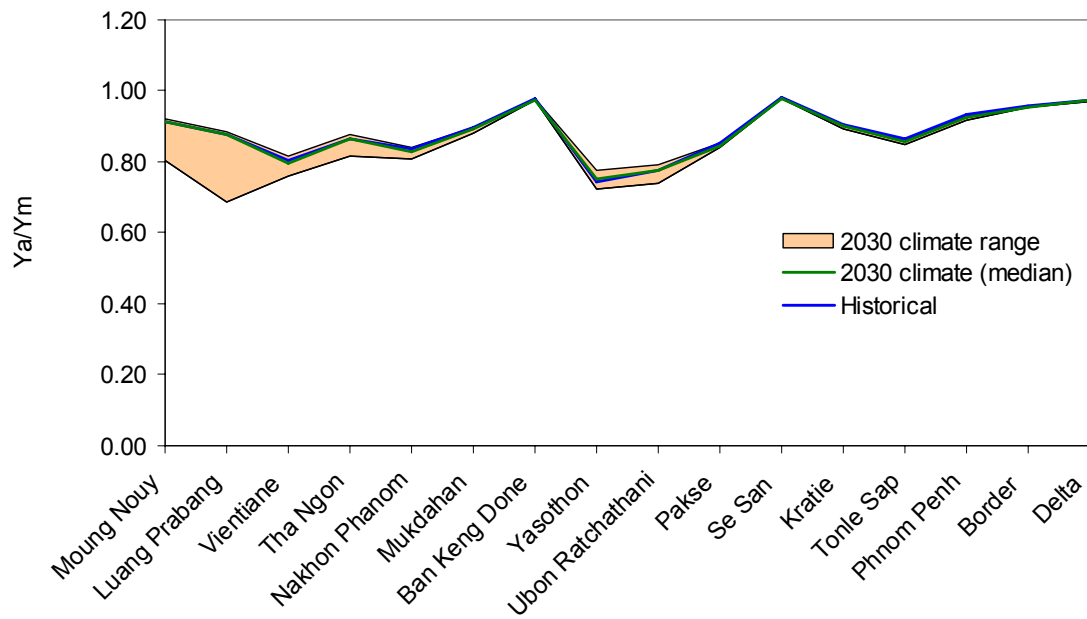


Figure 8.6. Projected and historical relative yield of sugarcane

8.4.4. Maize

Maize is the most important crop in the lower Mekong Basin among the upland crops in terms of harvested area. Maize cultivation has been doubled in Laos and Cambodia during the period of 1993-2003 and increased four fold in Vietnam during the period of 1995-2004. In Thailand, cultivated area has slightly decreased over the same period. There is no impact of the change in climate on relative yield. Chinavanno (2004b), based on analysis done using the data of Khon Kaen province (No. 37 in Figure 8.1) of Northeast Thailand, showed that different scenarios of CO₂ conditions affected the flowering and maturity days of maize and that yield would increase. The relative yield of irrigated maize grown in dry season in the Delta also almost remains unchanged (decreases about 2% for the 2030 median climate condition).

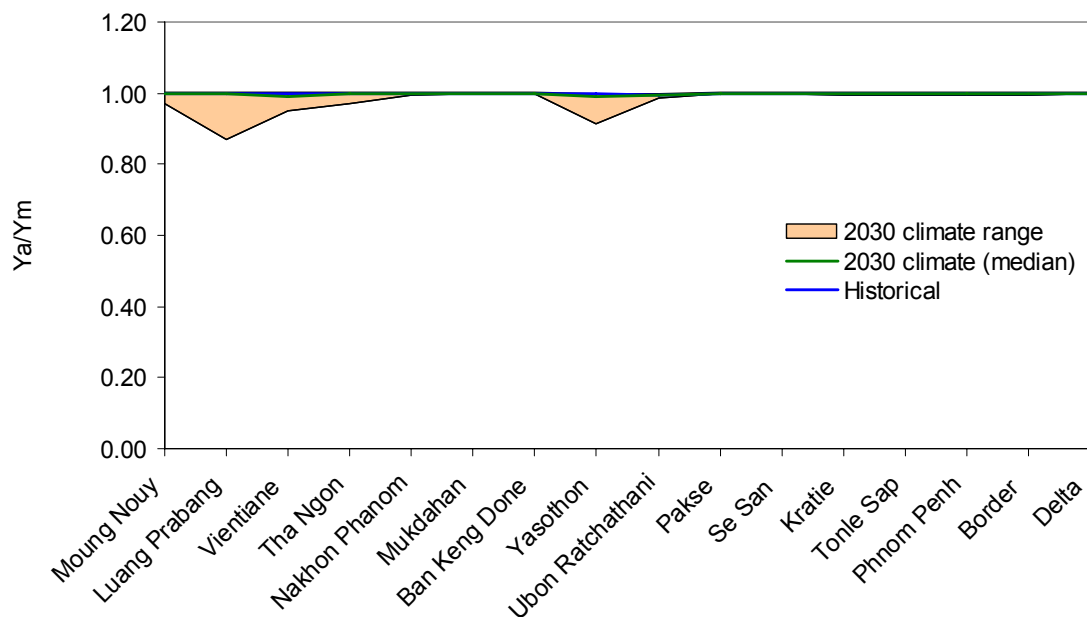


Figure 8.7. Projected and historical relative yield of maize

8.4.5. Soybean

The impact of climate change on the productivity of soybean is similar to that of the maize (Figure 8.8). The relative yield is almost unaffected. Relative yield for 2030 median climate condition is slightly higher compared to the historical (1.0 to 1.6%) relative yield in Vientiane, Yasothon and Ubon Ratchathani sub-basins. For the remaining sub-basins, the relative yield is either the same as historical or slightly lower (up to 0.7%) than the historical relative yield. The relative yield of irrigated soybean grown in dry season in the Delta also almost remains unchanged (decreases about 2% for the 2030 median climate condition).

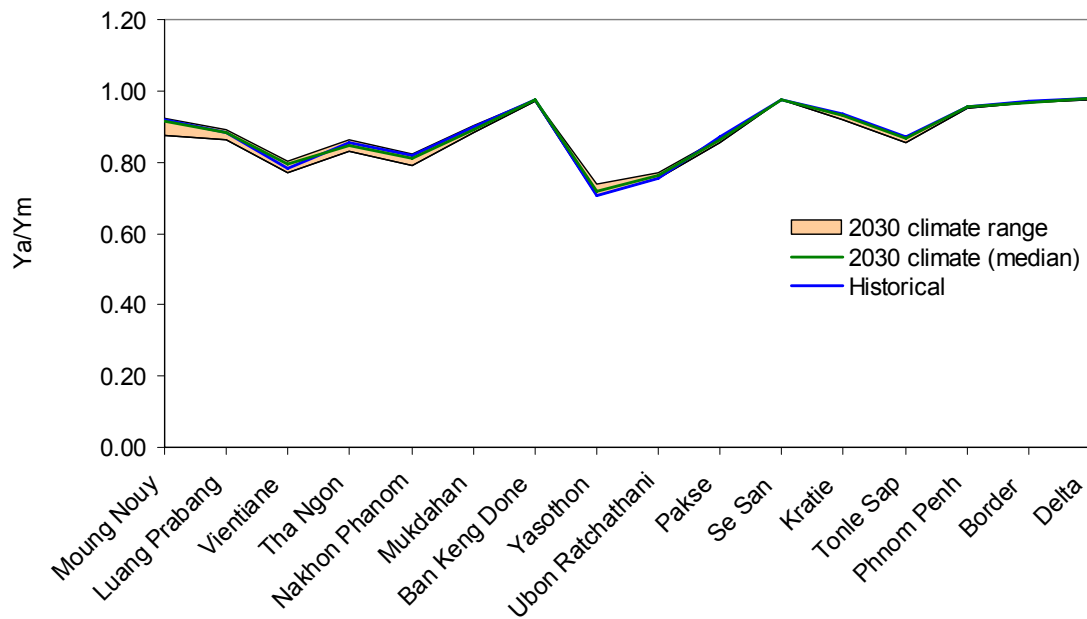


Figure 8.8. Projected and historical relative yield of soybean

8.4.6. Irrigated rice

Under future climate projections, potential evaporation is likely to increase across the basin, and growing season rainfall for irrigated rice likely to decrease in all sub-basins except Moung Nouy. This suggests increasing irrigation requirements for irrigated rice under the likely future climate. If irrigation applications are increased to meet the increased requirement, yields will remain similar to those under the historic climate (i.e. relative yield equal to 1). In assessing yield responses of irrigated rice to climate change we assumed that irrigation applications are maintained at the historical level. This implies that the crop would suffer water stress under the likely future climate, and yield would be affected. Figure 8.9 shows the impact of water stress on the crop yield. For median climate condition the yield would decrease by about 2%. The maximum reduction in yield could be as high as 6%.

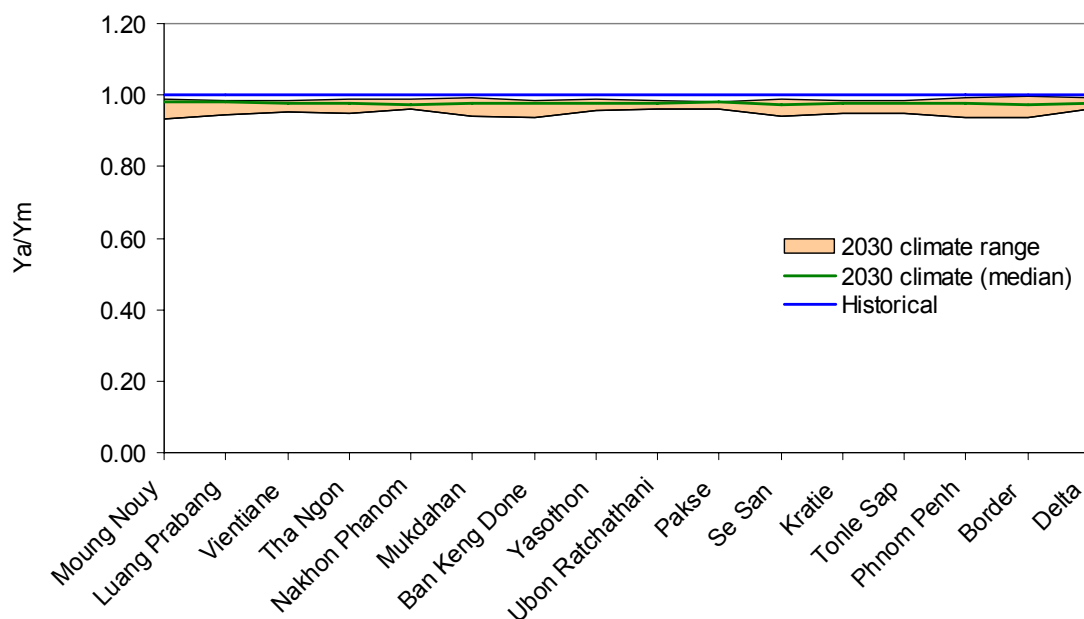


Figure 8.9. Projected and historical relative yield of irrigated rice

8.4.7. Irrigation requirements

Figure 8.10 shows the irrigation requirements of irrigated rice. Irrigation requirements for the projected maximum condition would be 3 to 8% higher than the current historical requirements. For the median condition, the increase is 1.6 to 3.4%.

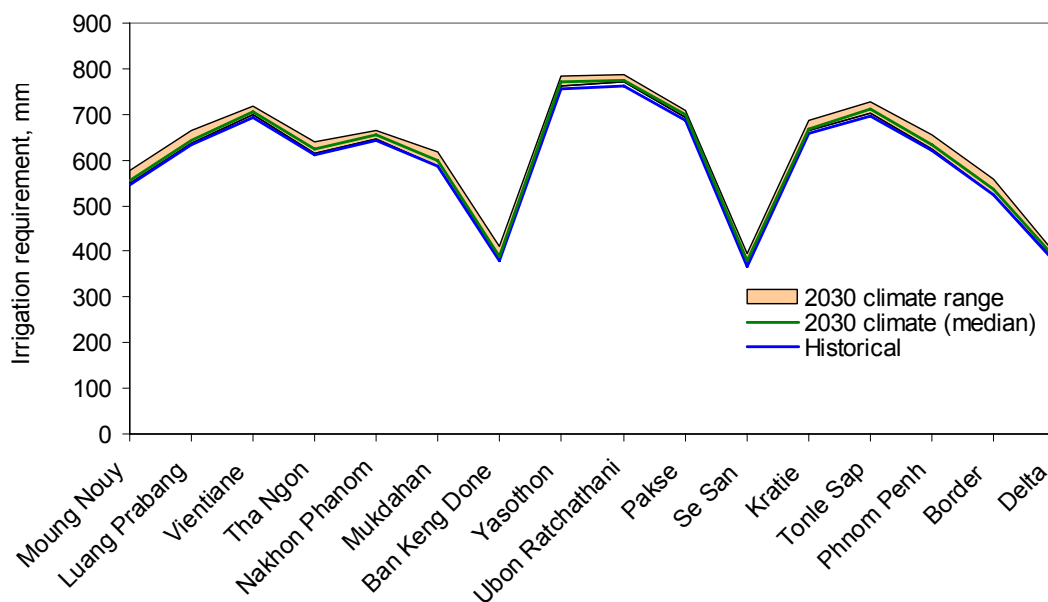


Figure 8.10. Projected and historical irrigation requirements of irrigated rice

If additional irrigation requirements are met by increasing diversion of water from the river, the increase in diversion for the whole lower Basin would range from 110 to 612 MCM. For the 2030 median climate condition the diversion would be 283 MCM. The highest diversion would be for the Delta. Figure 8.11 shows the change in water diversion due to increase irrigation requirements for the sub-basins.

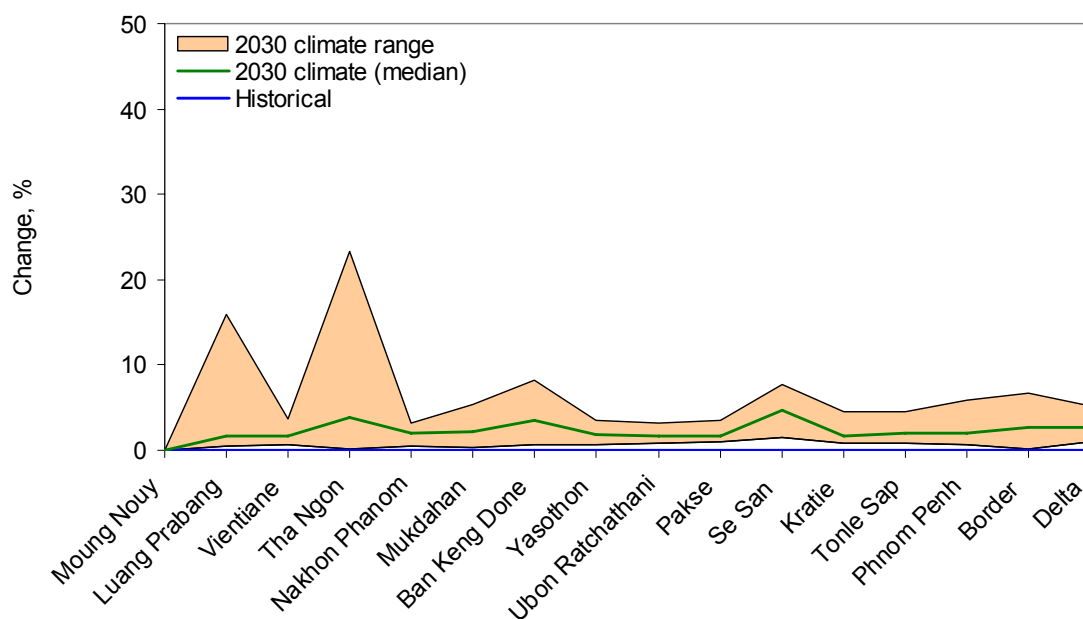


Figure 8.11. Change in total water diversion for irrigation due to climate change

Diversion of more irrigation water due to increased requirements may have several impacts as follows.

- Existing irrigation system delivery capacity may not be enough to deliver the increased requirements, hence, may need to increase the capacity at additional costs.
- Increased diversion for irrigation will reduce the dry season flow in the river which may significantly affect the river ecology and overall environment. There could be an impact on salt water intrusion in the Mekong Delta of Vietnam.
- The cost of production would increase due to the cost of additional irrigation.

8.4.8. Total productivity estimates

We undertook analyses to estimate the potential impacts of climate change on the overall productivity of the catchments and basin using assumptions that were consistent with the water resource availability analyses presented in this report. The advantage of linking productivity estimates to the water analyses is that it enables the productivity response of irrigated cropping to be assessed under conditions where water applications to irrigated crops are moderated according to availability in different sub-basins.

For the productivity analyses, we assumed the area of rain fed and dryland crops, crop factors, crop evapotranspiration and potential evaporation in each catchment were the same as for the water analyses. Since rice is the major crop across the basin, we estimated productivity assuming that all areas of rain fed and irrigated cropping were under rice cropping. We used Equation 8.2 to estimate productivity from seasonal evapotranspiration and potential evaporation estimated in the water account. As for other analyses, we used historic climate data and climate data projections for the 11 selected GCMs to estimate historic and future (2030) productivity.

Our estimate of historical total basin productivity is 42.9 million tonnes. Although there is uncertainty in the estimate, basin-wide productivity under the projected 2030 climate is likely to increase to 44.5 million tonnes, an increase of 3.6%. Even under the drier projections for future climate, productivity is projected to increase, with projected productivity ranging from 43.2 to 45.6 million tonnes. Although the basin wide productivity is projected to increase, the response in productivity differs for different catchments of the basin (Figure 8.12).

Productivity under the projected 2030 climate is likely to decrease in the Moung Nouy, Luang Prabang, Tha Ngon and Border catchments. Productivity is likely to be unaffected by climate change in Mukdahhan, Phnom Penh and Delta catchments. In the remaining catchments productivity is likely to increase, with the greatest increases in Ubon Ratchathani and Tha Ngon.

Our estimates of total productivity are based on rice production, yet we know that the area we have used in estimating productivity also includes areas of upland crops. Assuming the area planted to rice is 82% of the total cropped area (data from 2003 in Table 13.1); we estimated historic basin-wide rice production to be ~35 million tonnes. This is comparable to an estimated production of 31.2 million tonnes for 2000 (Hoanh *et al.* 2003) based on data of Maclean *et al.* (2002).

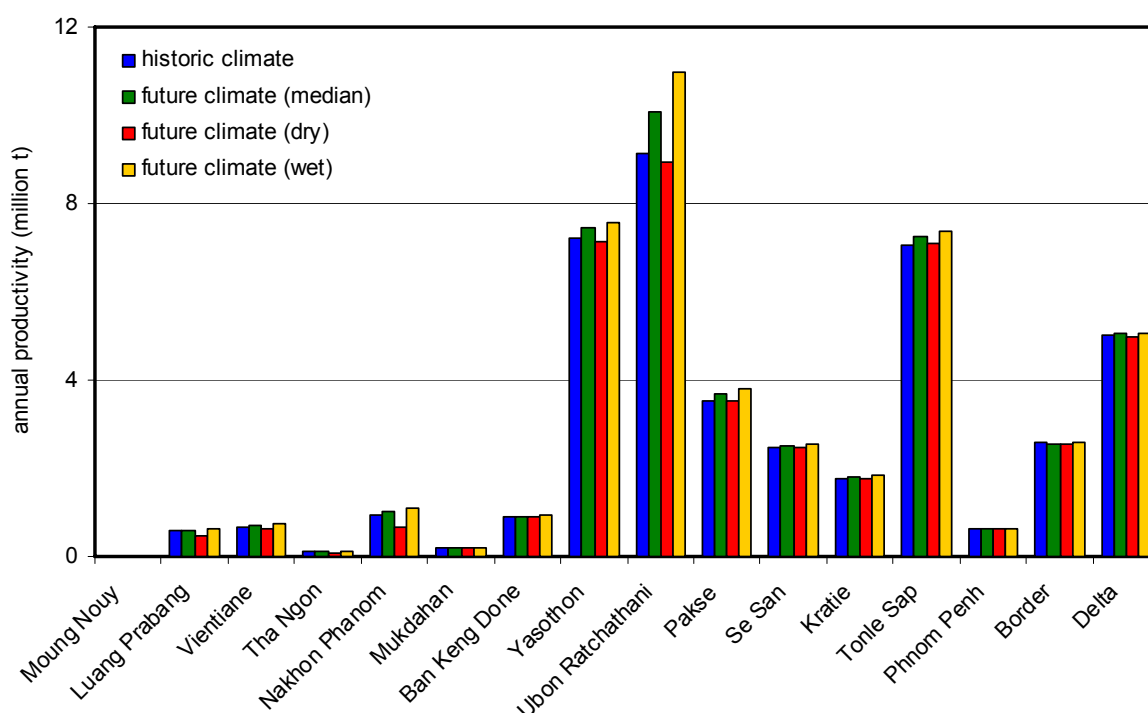


Figure 8.12. Historical (1951-2000) and future (2030) productivity

We evaluated the impact of climate and population change on food availability through expressing productivity on a per capita basis for historical and 2030 conditions. For historic conditions, basin-wide productivity per capita was 737 kg/year. Although there is uncertainty in the estimate, basin-wide productivity per capita under the projected 2030 climate is likely to decrease to 399 kg/year (ranging from 388 to 409 kg/year for projections for different GCMs). Productivity per capita is likely to decrease in all catchments of the basin (Figure 8.13), with the largest decreases in the Ban Keng Done and Kratie catchments. Even under the wettest projections for future climate, productivity per capita is likely to decrease in all catchments except Ubon Ratchathani. The projected likely decreases in productivity/capita are predominantly influenced by increases in population for each of the catchments between 2000 and 2030 (Figure 8.14).

If we assume a food requirement per capita of 300 kg/year of paddy or equivalent (Hoanh, 2003) to estimate food demand, basin wide productivity is adequate under both historic and projected future (2030) conditions. Based on this requirement, demand would be ~17 and ~33 million tonnes respectively for 2000 and 2030 projected population. However, under historic conditions, excess production is estimated to be ~25 million tonnes, but this will be reduced to ~11 million tonnes under the likely projections for 2030.

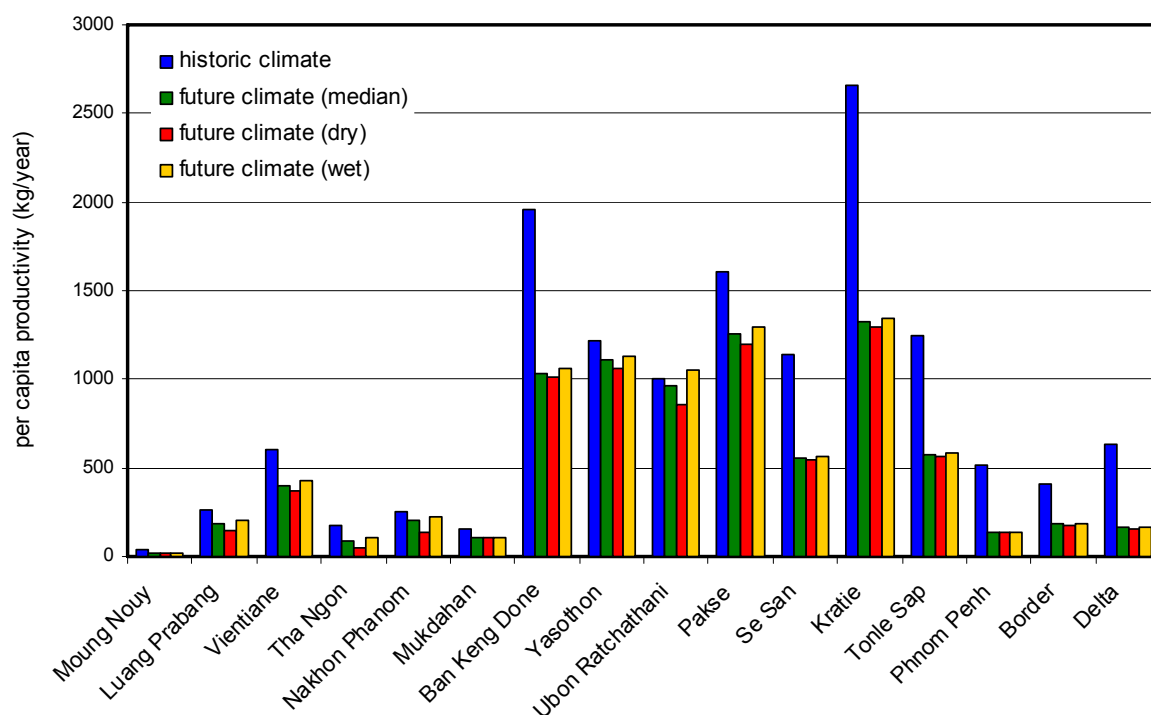


Figure 8.13. Historical (1951-2000) and future (2030) productivity per capita.

Furthermore, under the likely impacts of climate change there will be an increase in the number of catchments with a deficit in production (Figure 8.14). Under 2000 conditions, productivity is inadequate to meet demand in 5 of the northern catchments of the Lower Mekong Basin (Moung Noy, Luang Prabang, Tha Ngon, Nakhon Phanom and Mukdahan). Under likely projected (2030) climate and population conditions, the deficit in production will become greater for these catchments. Furthermore, production is likely to become inadequate to meet demand for the Phnom Penh, Border and Delta catchments in the south of the basin, where population increases are projected to be greatest (Figure 2.9). Production in excess of food demand will be reduced for all the remaining catchments of the basin except Ubon Ratchathani, where production in excess of demand is projected to increase.

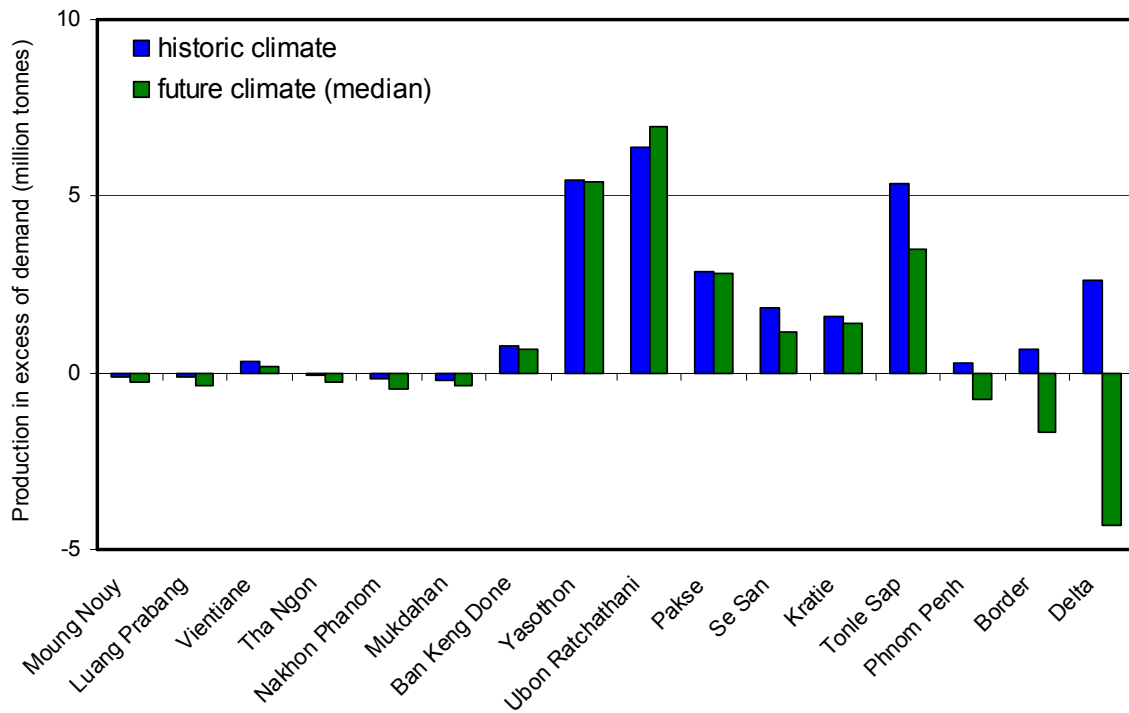


Figure 8.14. Historical (1951-2000) and future (2030) production in excess of demand. Negative values indicate production is insufficient to meet demand.

8.4.9. Discussion of productivity responses

The analyses of productivity presented above are intended to be indicative only of basin and catchment responses to climate change for the following reasons:

- It is possible that increases in future productivity may occur, through reasons unrelated to climate change e.g. varietal improvement and changes in crop management. There has been a historical trend of increasing yields across the basin. It is likely yield increases will result from the use of high yielding varieties of rice replacing low yielding local varieties, increased application of fertilizer, better management practices, and increased application of herbicides and pesticides (Schiller et al., 2001; Sipaseuth, et al., 2001; Pandey, 2001; Rickman et al, 2001; Kono et al, 2001; Fukai and Kam, 2004). Nitrogen fertilizer use in Northeast Thailand has been increased by about 600% from 1976 to 2000 (Hasegawa et al., 2008). According to Hasegawa et al. (2008), nitrogen input is the most important factor responsible for the upward trend in regional yield in Northeast Thailand. High yielding varieties of rice have also not been widely adopted in Laos, Thailand and Cambodia (Hasegawa et al, 2008; Boualaphanh et al., 2001; Sengxua and Linquist, 2001; Buu and Lang, 2004; Kono et al, 2001; Makara et al, 2004).
- Yield impacts of climate change may not be fully captured by simulations using monthly climate data. It is possible that uneven distribution of rainfall within the month may cause periods of water stress to occur which could reduce yield. Nawata et al. (2005) showed that the number of rainy days in the rainy season has a large regional variation in Northeast Thailand, but it was not correlated to annual rainfall. In the regions of the basin with lowest annual rainfall, the south-western parts, some areas had a lot of rainy days, whilst some humid regions, such as southern part of Nakhon Phanom province, had a small number of rainy days in the rainy season. For agricultural production, the number of rainy days is more important than mean rainfall amount per rainy day or annual rainfall. Well-distributed rain may reduce the

occurrence of drought (Nawata et al., 2005). Dry spells, which are one of the biggest factors reducing agricultural productivity and stability in Northeast Thailand and Laos (Fukai, 1993), may occur with lower frequency in areas with abundant rainy days in the rainy season (Nawata et al., 2005). The duration of rainy season also has large regional variation and is not strongly correlated to annual rainfall (Nawata et al., 2005).

- There will be likely negative impacts of increased flooding on crop yields, which haven't been considered in these analyses. Runoff is projected to increase in all catchments under the most likely projections for future climate, resulting in higher flow in the river during the wet season, the growing period of rain fed crops. Although rice is an aquatic plant and grows well under submerged conditions, deep and prolonged submersion of paddy rice adversely affects plant growth. High yielding varieties are more susceptible to flood damage than most traditional varieties. The most susceptible stages for whole plant submergence are head development and flowering (Doorenbos and Kassam, 1979). The likely impact of climate change on the severity of flooding (Figure 6.3) and the area inundated (Figure 6.5) in the Mekong Delta have been quantified in this study, but it is likely that productivity in other parts of the basin will be affected. It could be that the impact of climate change on the yield of rain fed crops would not be from water shortages, but rather would be from flooding and excessive water in the field. Wassmann et al. (2004) showed that rice production will be affected through excessive flooding in the tidally inundated areas and longer flooding periods in the central part of the Vietnamese Mekong Delta as a result of the sea level rise due to climate change. These adverse impacts could affect all three cropping seasons, main rain fed crop, winter-spring crop and summer-autumn crop unless preventative measures are taken. SEA START RC (2006) based on farmer interview in Thailand and Lao PDR stated that extreme climate events may cause loss of rice productivity by average 30-50% from flood in moderate flood year.
- This study considers the impact of changing potential evaporation and rainfall on productivity, through their influence on water availability, but does not include direct impacts of temperature changes. Increases in temperature may directly affect the growth and yield of rice and other crops in several other ways. For example, the phenology of crops may be influenced through increased temperatures, and their developmental phases shortened. Chinavanno (2004b) showed that different scenarios of climatic condition affected the flowering and maturity days of maize and some features of sugarcane phenology. The response of rice to temperature differs with variety (Doorenbos and Kassam, 1979). However, in general, temperatures between 22 and 30° are required for good growth at all stages but during flowering and yield formation small differences between day and night temperatures are required for good yield. Optimum daytime air and water temperatures for the growth of rice are in the range of 28 to 35°C (Doorenbos and Kassam, 1979). The impact of any changes in atmospheric carbon dioxide on crop yield has also not been considered in this study.
- These analyses do not take into account any adverse effects of waterlogging on crop yield. It is possible that the incidence and severity of waterlogging could increase in the wet season due to higher rainfall under the likely future climate. The soil of the upland crops should preferably be well-aerated and well-drained, since upland crops (sugarcane, maize, and soybean) are susceptible to water logging (Doorenbos and Kassam, 1979). Water logging during flowering of maize can reduce grain yields by 50% or more (Doorenbos and Kassam, 1979).
- The impact of changing saline intrusion in the Mekong Delta under climate change, and possible impacts on crop productivity have not been considered. The results of this study suggests that minimum flows at Kratie will increase under the likely impacts of climate change (Figure 6.2), potentially reducing the area of saline intrusion in the

delta area. This may increase agricultural productivity through increasing the area under crops, and reducing the salinity of groundwater used for irrigation. However, any impact of sea level rise and saline intrusion under climate change has not been quantified in this study.

- This study does not consider any adaptive responses to climate change that may influence the future productivity of cropping systems.
- The estimate of total productivity of crops in each catchment under historic and likely future climate relies on areas of rain fed and irrigated cropping determined by remote sensing techniques. Validation of these areas will increase confidence in productivity estimates.
- Our estimates of productivity per capita and food demand are derived using estimates of historical (2000) and future (2030) population. Our estimate of 2000 population for the basin corresponds well with estimates from other studies. However, there is great variability amongst published estimates of future population of the basin, and in this study we derived two contrasting estimates by using population growth rates derived from different sources. We chose the higher of the two estimates to calculate productivity per capita and food demand for 2030. These values therefore represent a lower productivity per capita and greater food demand than would have been derived under the more conservative estimate of 2030 population.

Despite the limitations to these analyses of the likely impacts of climate change on crop productivity, the study provides indicative results of the likely responses in productivity to changing water availability under future climate.

Other studies have investigated the potential impact of climate change on productivity of agricultural crops. Chinavanno (2004b) studied the potential impact of climate change using data from field experiments in Chiang Rai, Sakhon Nakhon and Sa Keaw (province no. 19 25 and 40, respectively in Figure 8.1) provinces of Thailand. The study used the MRB-Rice Shell, which links the CERES-Rice model with spatial databases. The study found no significant difference between the observed and simulated yield of rice in dry, medium and wet climate change scenarios. Results of the present study are also similar to that of Chinavanno (2004b). SEA START RC (2006) using a crop growth simulation model showed that yield of rice in the study sites (Ubon Ratchathani province, No. 30 in Figure 8.1) in Thailand will increase by 3-6%; but may be reduced by almost 10% in Lao PDR (Savannakhet province, No. 13 in Figure 8.1). They found that rice production in the Mekong River delta in Viet Nam may be severely impacted by climate change, especially summer-autumn crop production, where yield may be reduced by over 40%. In the results of the regional study presented here, yield is likely to increase in Thailand's Ubon Ratchathani and Yasothon by about 3.3%, but will be unaffected in the Mekong delta and in sub-basin Ban Keng Done (where the study site of Laos is located for SEA START RC study). The reason for this could be that we did not consider the impact of excessive water in the rice field.

9. INDICATIVE CLIMATE CHANGE RESPONSES FOR ALTERNATIVE IPCC SCENARIOS

To give perspective on the results presented for responses to changing climate for the A1B scenario projections, we applied the pattern scaling technique to give indicative projections of changes in basin mean temperature and mean annual precipitation for the 5 remaining IPCC scenarios. We used the local temperature change per degree of global warming and percent rainfall change per degree of global warming derived for each GCM for each catchment. We multiplied these values by the global warming projected for 2030, 2050 and 2070 for the A1F1, A2, B2, A1T, and B1 scenarios (from Figure SMP-3 of the IPCC (2007) report) to give the pattern scaling factors for each scenario. We scaled the historical monthly precipitation and temperature series of 1951-2002 to obtain projected temperatures and precipitation for each GCM and for each IPCC scenario. The projected precipitation and temperature responses are intended to be indicative only. Ruosteenoja *et al.* 2003 analysed the validity of applying this pattern scaling technique to estimate climate responses for IPCC scenarios, using local changes in temperature and precipitation per degree of global warming derived for different a scenario. They concluded that the technique was valid, with better correlations obtained for temperature projections than for projected precipitation. They also concluded that correlations were better when the scenario for which climate projections were sought was subject to similar forcings to the scenario for which the local temperature and precipitation responses per degree of global warming had been derived.

Projections for all scenarios indicate a progressive increase in the mean temperature and mean annual precipitation for the Mekong Basin for 2030, 2050 and 2070 (Figure 9.1). Lines for each scenario in Figure 9.1 are the best estimate of temperature and precipitation responses taken as the median of projected responses from 11 climate models. The mean of the 6 scenario projections indicates increases in temperatures relative to the historic of 1.0, 1.5 and 2.2°C for 2030, 2050 and 2070 respectively. The mean increase in annual rainfall is 0.251, 0.434 and 0.66 m for 2030, 2050 and 2070. The range in projections for different models is 0.6 °C for temperature and 0.86 m for rainfall in 2030. These ranges increase progressively for both temperature and rainfall in 2050 and 2070 as the projections for different scenarios diverge. Thus uncertainty around projections of future temperature and precipitation for the basin, represented by the variation in scenario projections, increases progressively with time.

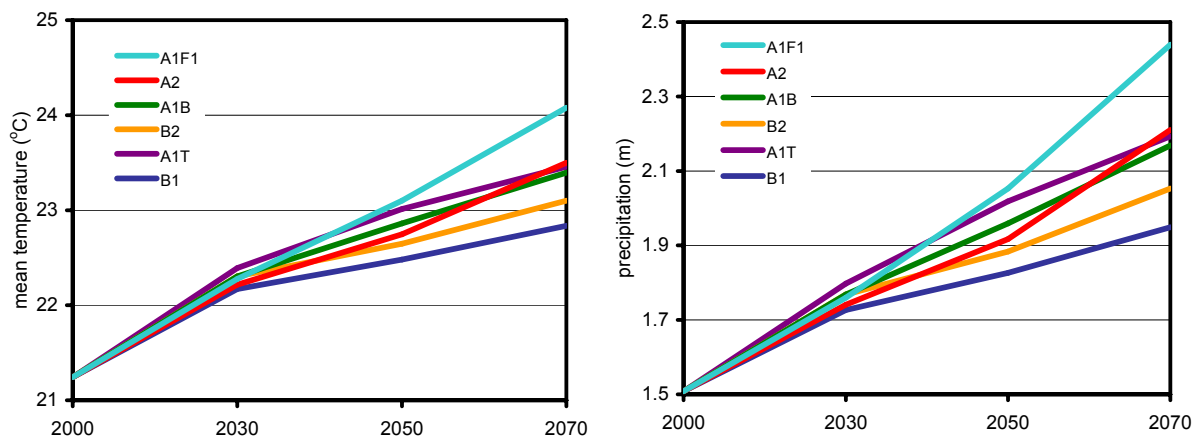


Figure 9.1. Projected mean temperature and mean annual precipitation for the Mekong Basin for different IPCC scenarios at 2030, 2050 and 2070.

The A1B scenario projections for rainfall and temperature lie towards the middle of the range of projected rainfall and temperature at 2030, 2050 and 2070. Thus in considering the results for the A1B scenario presented in this report, it is important to bear in mind that if the world progresses down a different development pathway from that described by the A1B scenario, changes in temperature and precipitation could be either bigger or smaller than those described in this report. It is also important to bear in mind that the reported results are for 2030, and that further increases in both temperature and precipitation are possible beyond this timeframe.

10. RECOMMENDATIONS

- One of the key likely impacts of climate change identified in this study is an increase in runoff across the basin, and associated increased flood risk. The frequency of extreme flood events downstream of Kratie is likely to increase from an annual probability of 5% to 76%. We have also applied remote sensing techniques to provide indicative estimates of the increase in area affected by flooding. Further research is needed:
 - a) To assess the potential impact of increased runoff on the flood response for other catchments of the basin, to identify regions potentially at risk from increasing frequency of significant or extreme events.
 - b) Further more detailed remote sensing analyses would allow mapping of the areas most likely to be impacted by flooding, and the land use in those areas (urban, agricultural, infrastructure etc). This would enable a broader and more complete analysis of the impacts on the basin, so that a targeted response can be developed.
 - c) The potential impact of sea level rise is included in the flood analyses
- Production from fisheries is a key source of food for the population of the Mekong Basin, with the Tonle Sap Lake providing a critical source of food for Cambodia. The changing flows and water levels that result from increased runoff will undoubtedly modify the complex ecology of rivers, waterbodies and floodplains which influence the productivity of fisheries. The likely response in productivity for key areas of the basin needs to be assessed, so that appropriate measures for mitigation can be sought.
- This study has produced indicative results on the likely responses in agricultural productivity to climate change, and concluded that food scarcity is likely to increase in parts of the basin as a result of population growth. More detailed research using a calibrated rice model is required to assess the impact of factors not considered in this analysis. The area of cultivated land likely to be adversely affected by flooding, and the resulting impact on productivity also need to be assessed. This is required to characterise the likely distribution and severity of food scarcity across the basin so that appropriate responses may be developed.
- The study may be expanded to examine the water resources availability in the basin for the remaining IPCC scenarios (A1F1, A2, B2, A1T, and B1 scenarios).
- The potential impacts of climate change should be assessed for each of the scenarios included in the Basin Development Plan.
- The impacts of climate change on groundwater are complex and difficult to assess with current information. However, it is possible that increased water demand, especially in the dry season, may lead to increased groundwater use. Some groundwater in southern Cambodia is arsenic contaminated, so potential increased use could be a serious problem.
- This study investigated the impacts of likely future climate on water resource availability in the Mekong basin. Similar analyses may be undertaken for other basins or regions of interest to AusAID, including a comparative assessment of the regions most likely to be adversely affected by impacts of climate change.

11. APPENDIX 1

11.1. Global climate change model selection

Global Climate Models are the best tools available for making climate change projections. Patterns of climate change for the Mekong Basin are readily obtainable from GCMs' simulations. However, there are significant differences between GCMs with regard to climate changes simulated at the regional scale, particularly for precipitation. Thus to represent this uncertainty results from a range of GCMs are commonly used in the construction of regional projections. To select a suitable set of GCMs from 24 GCMs used in the AR4 report of the Intergovernmental Panel on Climate Change (IPCC), we used statistical methods to objectively quantify the relative ability of each model in simulating climate over the Mekong Basin.

The similarity in the spatial and temporal climate patterns was quantified by the pattern correlation coefficient and root mean square (RMS) difference between observed and simulated datasets (Taylor, 2001). The pattern correlation coefficient quantifies the similarity in the spatial and temporal pattern of observed and simulated values, with a correlation coefficient of 1 indicating a perfect match between the datasets. The RMS quantifies the difference in magnitude between observed and simulated values, with a RMS of 0 indicating a perfect match between observed and simulated values. In calculating these parameters, values for each catchment were weighted according to the catchment area, since there was large variation in the area of Mekong catchments. Pattern correlation and RMS error were initially calculated for monthly catchment mean datasets for both temperature and precipitation. However, monthly datasets gave low pattern correlations for precipitation data and low RMS for precipitation and temperature for all GCM simulations in some months (Figures 11.3 and 11.4). Monthly precipitation data were summed and temperature data averaged to give seasonal values for May to October to represent the wet season of the south west monsoon, and from November to April to represent the dry season. Pattern correlation and RMS error were calculated from seasonal precipitation and temperature datasets. We used 11 GCMs in the construction of scenarios of change in precipitation, selected on the basis of relative model ability to simulate seasonal temperature and precipitation. Pattern correlation coefficients for both monthly and seasonal precipitation were expressed as mm per day by dividing by the number of days in the month and the season, respectively. To objectively compare the models, thresholds levels for pattern correlations and RMS error were adopted, similar to those used by Suppiah et al (2006) in their simple demerit point system approach. Model simulations whose pattern correlation or RMS error did not meet these thresholds were rejected. A threshold for rejecting model simulations with a RMS error > 2.0 was adopted for both seasonal temperature and precipitation. Different thresholds were applied for pattern correlations for seasonal temperature and rainfall, since correlations were generally lower for seasonal rainfall than for temperature. A threshold for rejecting simulations with pattern correlations < 0.8 was adopted for temperature in both seasons. Model simulations with pattern correlations < 0.8 for seasonal rainfall from May to October, and < 0.6 for seasonal rainfall for November to April, were rejected.

11.1.1. Assessment of climate change model performance

Figures 11.1 to 11.4 show pattern correlation coefficients and root mean square errors for observed versus simulated monthly temperature and precipitation for the Mekong catchments for the years 1960-1999. In these figures, the model points which lie closest to the top left-hand corner of each figure (i.e. with the highest correlation and lowest RMS error) are the best performing models for the parameter under comparison. All of the 24 GCM

simulations represented the temporal and spatial pattern of monthly temperature of the Mekong catchments well, with pattern correlations of 0.92 or greater (Figures 1.1 and 1.2). However the magnitude of temperature was less well represented, with RMS errors greater than 2.0 for the majority of models in some months (Figures 1.1 and 1.2).

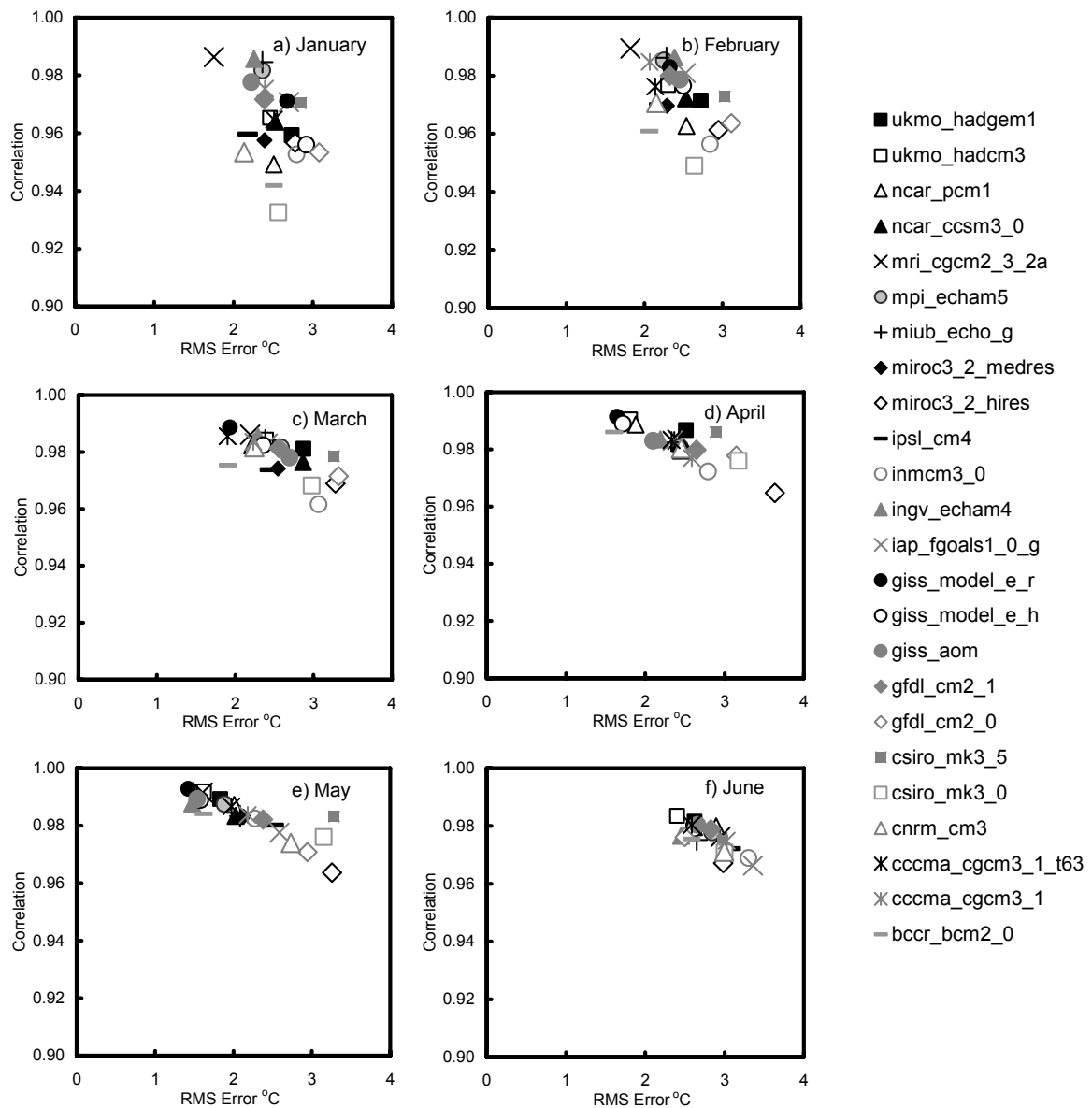


Figure 11.1. Pattern correlation and RMS error for observed versus simulated monthly temperature for January to June

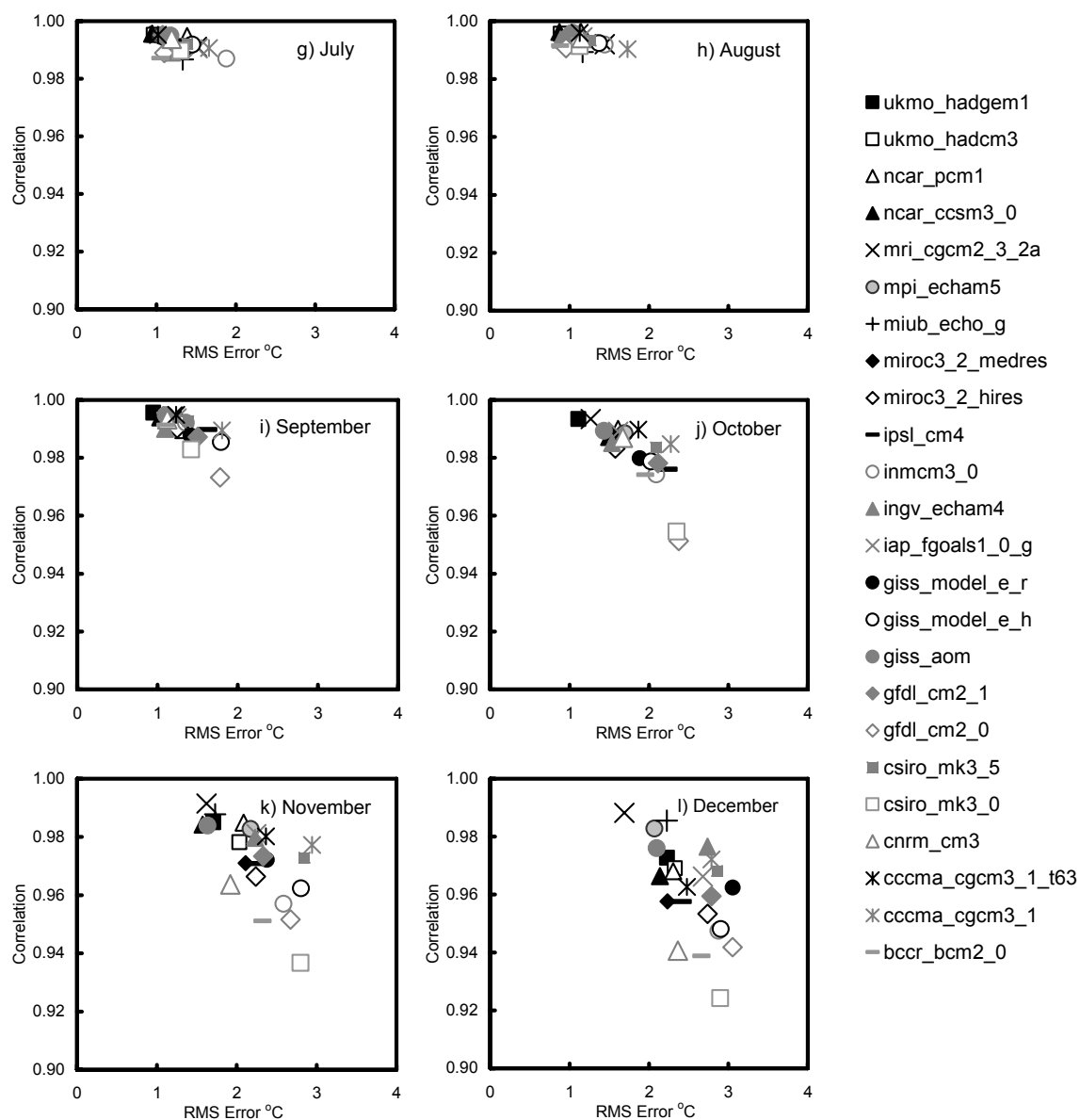


Figure 11.2. Pattern correlation and RMS error for observed versus simulated monthly temperature for July to December

Similarly rainfall magnitudes were poorly represented by the majority of models in some months with RMS error > 2.0 for most models (Figures 1.3 and 1.4). The temporal and spatial pattern of monthly precipitation was also less well represented generally by the GCM simulations, as pattern correlations were low for the majority of models. Correlations were less than 0.6 for all models in the drier months of January, February, March and December, and less than 0.8 for the majority of models in each month.

Models were selected on their capacity to represent seasonal temperature and precipitation for wet (May to October) and dry (November to April) seasons (Figure 11.5 and 11.6). Both the pattern and magnitude of temperature was well represented by all models for May to October, and by most models for November to April (Figure 11.5). The spatial and temporal pattern of precipitation from November to April was poorly represented, with pattern correlations less than 0.8 for all models. The spatial and temporal pattern of seasonal precipitation was better represented in the wet compared with the dry season with higher correlations for all models in the wet season. Conversely, the magnitude of dry season precipitation was better represented than wet season amounts for all models. A total of 11 models met the thresholds for pattern correlations and RMS error for both seasons. These

models (ncar_ccsm3_0; miub_echo_g; micro3_2_medres; micro3_2_hires; inv_echam4; giss_aom; csiro_mk3_0, cnrm_cm3, cccma_cgcm3_1_t63; cccma_cgcm3_1 and bccr_bcm2_0) were used to make climate changed projections described in this report.

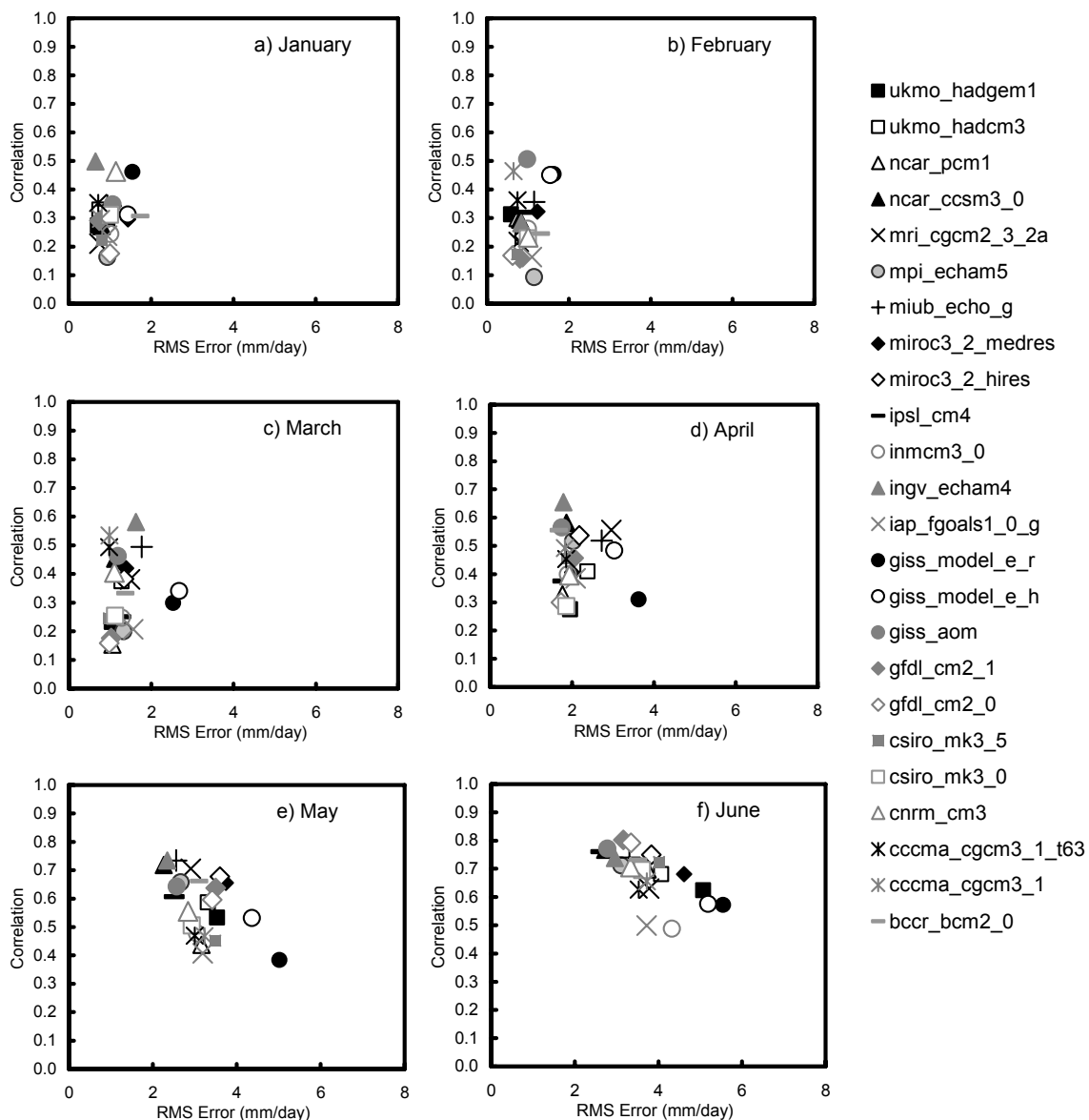


Figure 11.3. Pattern correlation and RMS error for observed versus simulated monthly precipitation for January to June.

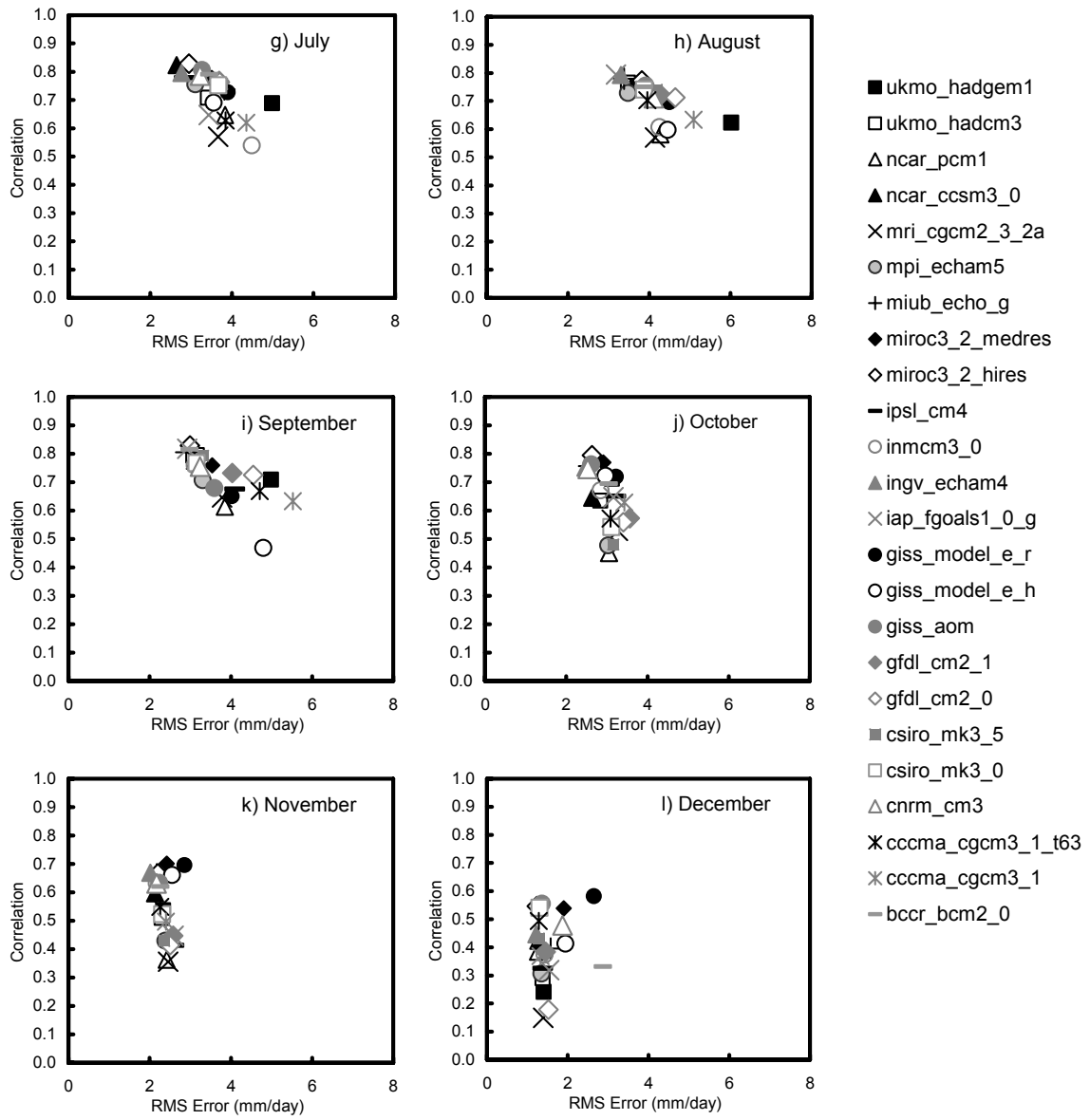


Figure 11.4. Pattern correlation and RMS error for observed versus simulated monthly precipitation for July to December.

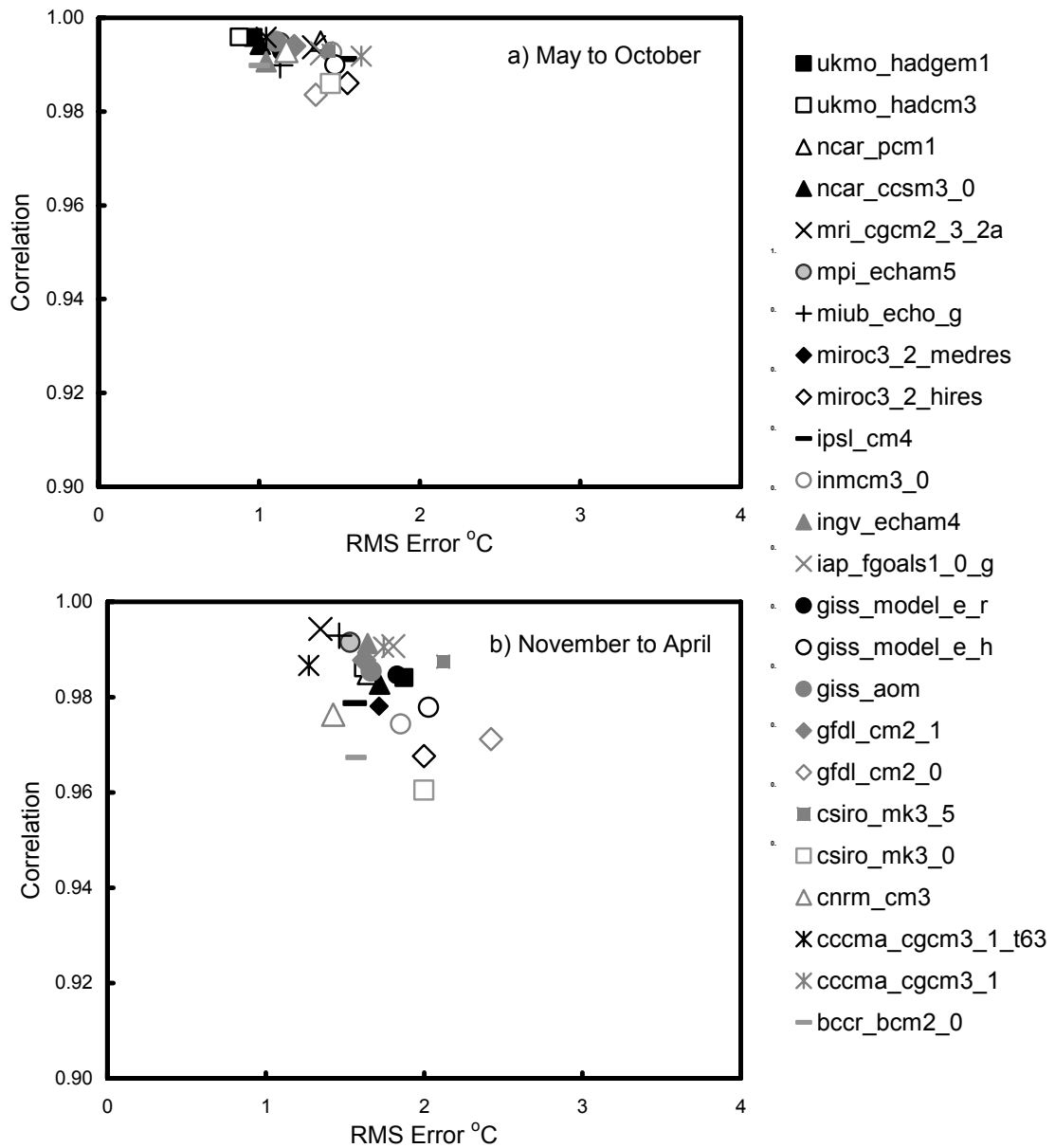


Figure 11.5. Pattern correlation and RMS error for observed versus simulated seasonal temperature for wet (May to October) and dry (November to April) seasons.

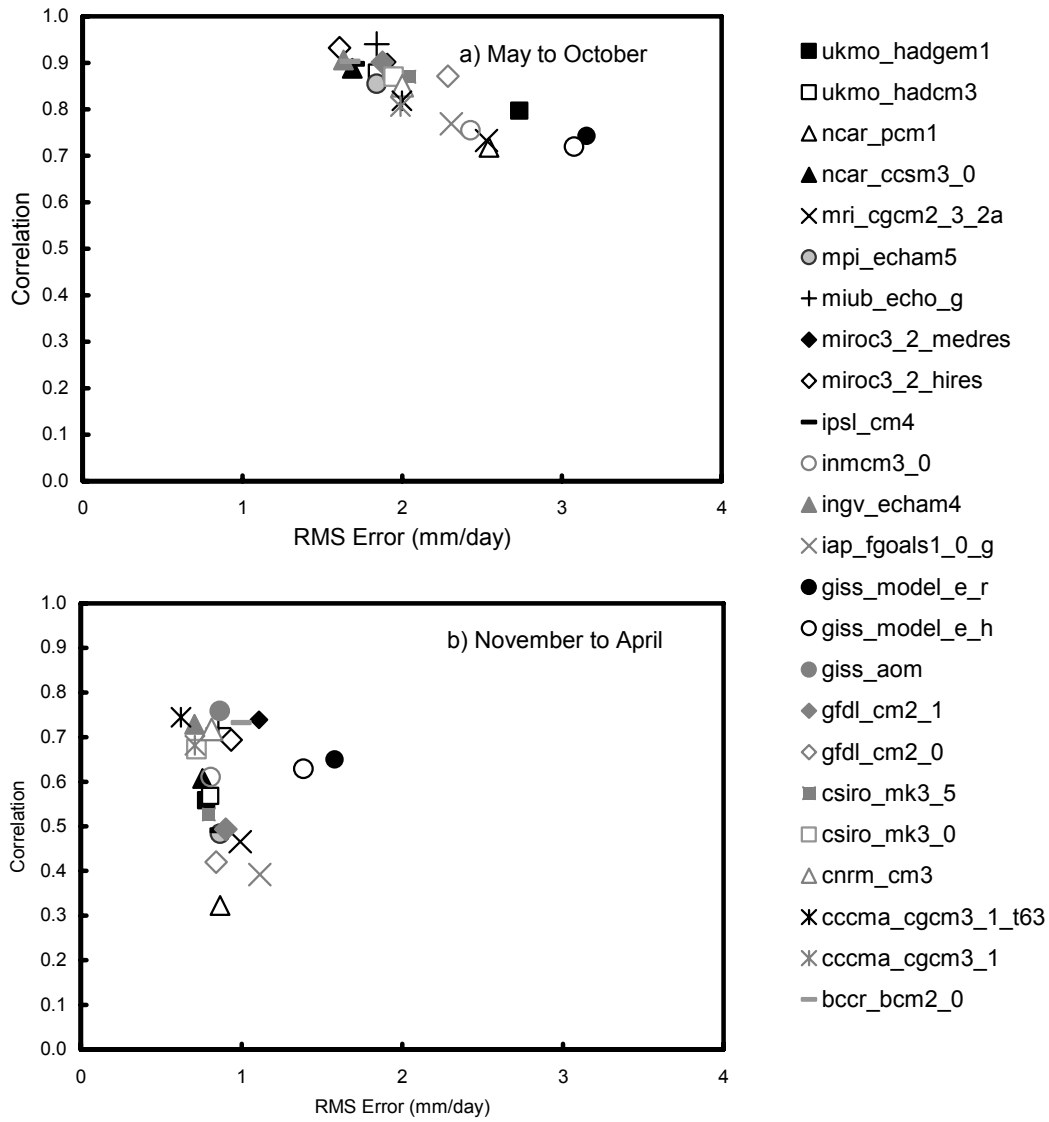


Figure 11.6. Pattern correlation and RMS error for observed versus simulated seasonal precipitation for wet (May to October) and dry (November to April) seasons.

12. APPENDIX 2

MAPPING WATER EXTENT AND CHANGE FOR THE MEKONG DELTA AND THE TONLE SAP USING OPTICAL AND PASSIVE MICROWAVE REMOTE SENSING

12.1. Introduction to observing surface water using remote sensing

Mapping the land and ocean surface using remote sensing technologies has long been recognized as a useful tool. The application of remote sensing enables relatively detailed spatial information to be collected over large areas, including those which are inaccessible by land. Furthermore, remotely sensed imagery can be acquired over the same regions at frequent intervals, allowing for relatively accurate temporal analysis. This section of the report uses optical and passive microwave remote sensing to map the flood extent for the Lower Mekong River for the time periods that the data are available. Both the optical and passive microwave datasets are sensitive to surface water enabling them to map flooding events through time. The remote sensing instruments and methods used to map floods in the Lower Mekong are described in detail in the following sections, followed by a combined method for mapping flood extent.

12.2. Mapping Floods using Optical

12.2.1. Mapping Floods using Optical Remote Sensing

The aim of this study is to investigate the potential for the MODIS (Moderate Resolution Imaging Spectroradiometer) optical remote sensing instrument to produce historical flood maps of the Tonle Sap and Mekong Delta.

The term Optical remote sensing refers to the use of instruments to record radiation from visible and infrared range of the electromagnetic spectrum. Optical reflectance differences of land and water are most pronounced in the Near Infrared 0.75-1.4 μm (NIR) and Short Wave Infrared 0.75-1.4-3.0 μm (SWIR) ranges. These wavelengths are strongly absorbed by water while also being well reflected by land surfaces and vegetation. Land and water interfaces are readily delineated using these wavelengths. Optical remote sensing does suffer some drawbacks for flood mapping. Optical wavelengths are scattered and absorbed by cloud and water vapour and gaining cloud free imagery over flooded areas has proven problematic. The use of sensor and satellite combinations that offer wide coverage and short revisit times has allowed the development of specialised composite image products that allow the investigation of relatively recent and past flooding events.

12.2.2. MODIS background.

MODIS is the latest instrument in use as part NASA's Earth Observation System (EOS). Two instruments orbit the Earth on two near-polar orbiting satellites, Terra and Aqua. Both instruments observe the entire Earth's surface every 1 to 2 days with adjacent passes offering large amounts of overlap at higher latitudes. As a result the EOS is able to generate composite images of a target area that combine multiple passes over a time window of 8 days 16 days or longer depending on the specific image product. The composite images have the advantage in being able to use the best pixel(s) available for any given location over the compositing period. For this project two products were assessed for their suitability for flood mapping in the Mekong. These were;

1. The product referred to as 'MOD43B4 Nadir BRDF-Adjusted Reflectance (NBAR). This is a product originating from the MODIS/Terra platform. It provides a Nadir BRDF-Adjusted Reflectance of 7 bands for a 16-Day period over the Globe at 1kilometre. This is usually referred to just as MOD43B4.

2. The product referred to as 'MODIS/Terra Surface Reflectance 8-Day L3 Global 500m SIN Grid V005'. As the long name suggests this is an 8 day composite produced at 500m pixel resolution for 7 bands as a Global Grid

12.2.3. Method.

The flood mapping method was one used to classify open water in large scale water accounting studies in Australia.(Kirby et al 2008) and (Guershman et al 2008). The method they describe is reproduced here.

The Open Water index was developed for quantifying temporal and spatial patterns of open water surfaces in Australia.

The open water index is based on the combination of the Enhanced Vegetation Index (EVI) (Huete et al. 2002) and the Global Vegetation Moisture Index (GVMI) (Ceccato et al. 2002a; Ceccato et al. 2002b):

$$EVI = G \cdot \frac{\rho_{NIR} - \rho_{red}}{\rho_{NIR} + C_1 \cdot \rho_{red} - C_2 \cdot \rho_{blue} + L} \quad (12.1)$$

$$GVMI = \frac{(\rho_{NIR} + 0.1) - (\rho_{SWIR2} + 0.02)}{(\rho_{NIR} + 0.1) + (\rho_{SWIR2} + 0.02)} \quad (12.2)$$

where ρ_{red} , ρ_{nir} , ρ_{blue} and ρ_{swir2} are the reflectances in red, near-infrared, blue and shortwave infrared 2 respectively and correspond to MODIS bands 1, 2, 3 and 6. In the EVI formula, G , C_1 , C_2 and L are parameters that account for aerosol scattering and absorption and their values are 2.5, 6, 7.5 and 1 respectively (Huete et al. 2002).

The EVI and GVMI were shown to be useful for distinguishing between vegetated and open water areas. Figure 12.1 shows the distribution of different land cover types in the space defined by the two indices.

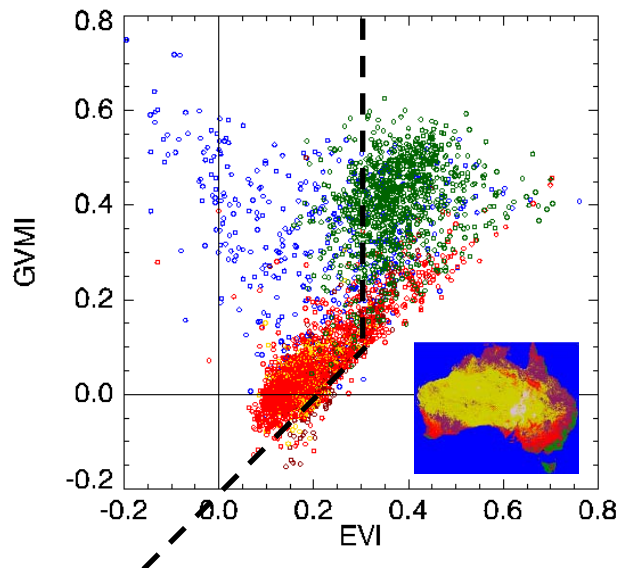


Figure 12.1. Scatterplot of the Global Vegetation Moisture Index (GVMI) and the Enhanced Vegetation Index (EVI) in Australia. Point colour indicates vegetation type (inset map) as: blue=water, green=forests, red=grasslands and croplands, yellow=shrublands and brow=woodlands. The dotted line indicates the criteria for separating the open water from the vegetation domain.

An Open Water Index (OWI) was calculated as:

$$\begin{aligned} OWI &= 0 && \text{when } EVI \geq 0.2 \text{ and} \\ OWI &= GVMI - EVI && \text{when } EVI < 0.2 \end{aligned}$$

Then an “Open Water Likelihood” index was calculated as:

$$OWL = \frac{1}{1 + \exp(-50 \cdot (OWI - 0.1))}$$

The expression above gives a sigmoidal function which is exemplified in Figure 12.2.

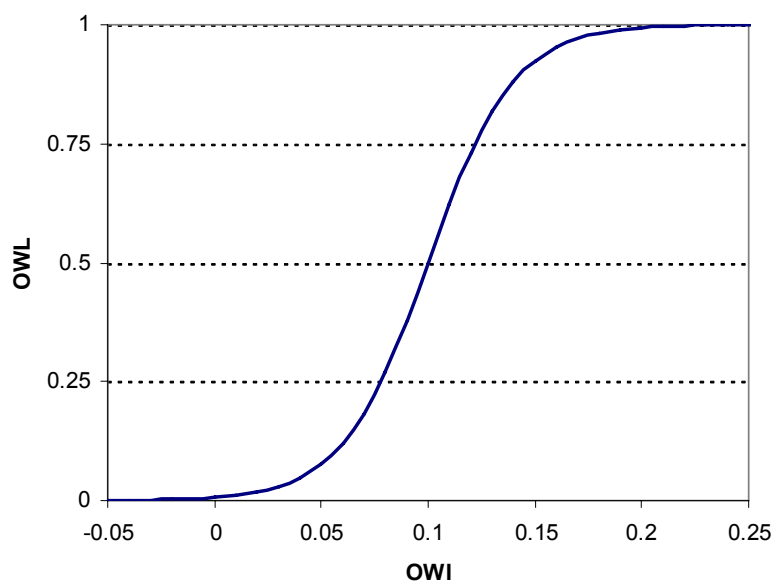


Figure 12.2. Relationship between the open water likelihood and the open water index through the sigmoidal function.

The OWL can be interpreted as the likelihood that a given pixel contains water or, additionally, as the proportion of the pixel occupied by open water. It is important to note that the two indices presented here have not been validated with field measurements.

Use of MOD43B4 Nadir BRDF-Adjusted Reflectance (NBAR) Product.

The initial attempt to calculate the Open Water Index was made using the MOD43B4 image product. MOD43B4 has been used successfully to calculate OWI in a number of prior Australian studies (Kirby et al, 2008) and (Guerschman et al, 2008). This imagery is a product with consistent corrected nadir reflectance that accounts for difference due to changes in illumination, views angles and geometric effects with an image swath and over multiday image series.

The times series of 16 day images from Feb 2000 to December 2002 were downloaded from The Land Processes Distributed Active Archive Center (LP DAAC) (<http://edcdaac.usgs.gov/main.asp>). The data were supplied as Integerised Sinusoidal Grid tiles. These were mosaiced, reprojected to Geographic coordinates and subsetted for the Lower Mekong using the MODIS Reprojection Tool (MRT). In initial trials attempting to calculate the OWI on the 16 day image series for the year 2000 it quickly became apparent that MOD43B4 was unsuitable for the study due to extensive cloud cover for much of the wet season (June-November)

The product employs a semi empirical RossThick–LiSparse model to generate the MODIS BRDF/albedo. This model requires at least 7 good observations of a pixel location over the 16 day period to correct observed reflectance to ‘vertical’ or nadir reflectance. In other words an image pixel must be observed by MODIS through clear skies nearly 50% of the 16 day period. This severely limits the full BRDF calculation and other measures reliant on archetypal BRDF albedo estimates are employed to fill the gaps. (Schaaf et al 2002) Even these methods are reliant on some good quality flagged reflectance data. The prevalence of cloud and high water vapour regularly preclude even their use.

Further investigation the use of the MOD43B4 product for OWI calculation was abandoned.

Use of MOD09A1 Surface Reflectance Product.

The MOD09A1 Surface Reflectance imagery is a simpler MODIS composite product. Each MOD09A1 pixel contains the best possible surface reflectance observation during an 8-day period as selected on the basis of high observation coverage, low view angle, the absence of clouds or cloud shadow, and aerosol loading.

(<http://edcdaac.usgs.gov/modis/mod09a1v5.asp>). The prime focus of this product is to provide widest coverage possible which does impact on image quality.

The times series of 8 day images from Feb 2000 to December 2002 were downloaded from The Land Processes Distributed Active Archive Center (LP DAAC)

(<http://edcdaac.usgs.gov/main.asp>). The data was prepared for the study as for the previous MOD43B4 time series. Both the OWI and OWL were then calculated for each 8 day image.

The OWI images were then visually assessed for cloud contamination. Very contaminated images were removed from the series. Cloud contamination of the imagery was still considered a source of possible error and the study time frame precluded any validation comparison with other flood area estimates. Further, in order to reduce cloud effects to a minimum a very conservative approach was taken in categorising pixels as flooded. Rather than applying the Open Water Likelihood” (OWL), an OWI threshold of 0.2 was adopted. This threshold provides ~100% certainty that the pixel is flooded (Guerschman et al, 2008). The resulting classification and flood area estimates are expected to be underestimates. Once the threshold was set, regions of interest were then defined for the Tonle Sap and the Mekong Delta and flooded area statistics for each image were analysed.

12.2.4. Results.

The years analysed (2000 – 2002) are all classified as being having flood events significantly above average or extreme (MRC, 2007). The images in Figure 12.3. below demonstrates the change observed as the Wet Season commences. Tonle Sap can be seen in the north western corner, the coast Gulf of Thailand is in the south west and the Mekong Delta flows in to the South China Sea in the south west. Image 1 shows the initial dry season extent of the Tonle Sap.

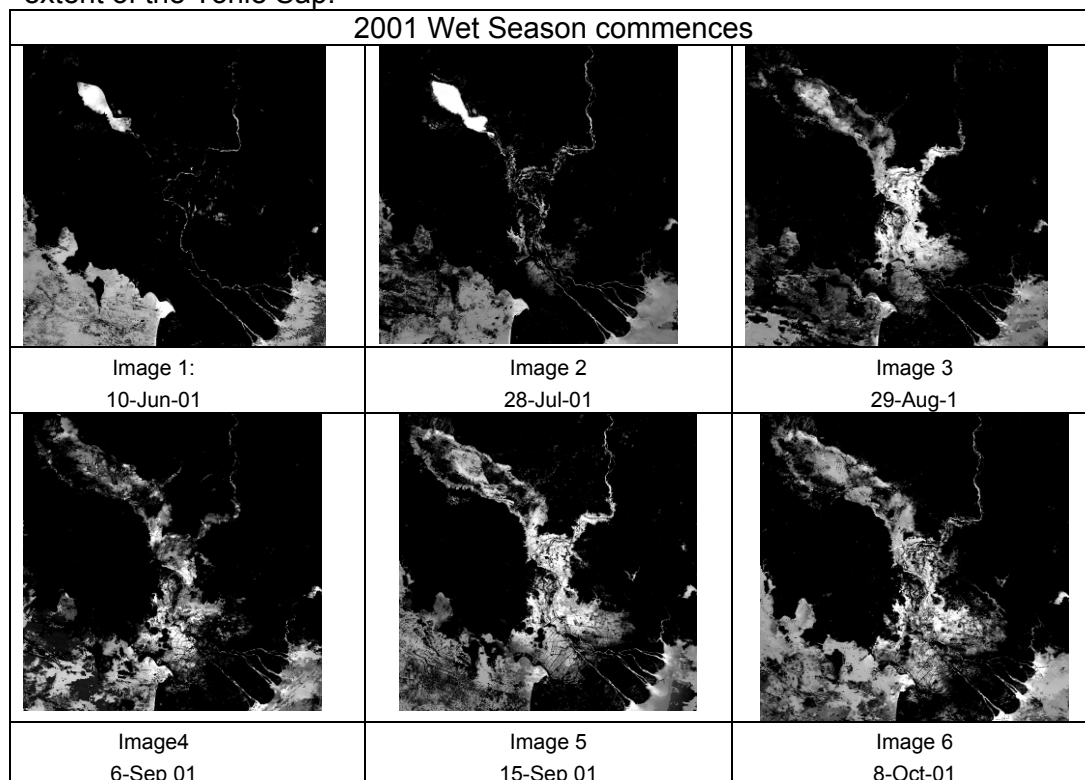


Figure 12.3. Changes in inundated area shown by a time series of Modis images in 2001.

The series shows increasing inundation and the river rises and the flood fills the lake and the Mekong Delta. Fully flooded pixels in these images appear as grey to white. It is also apparent that the OWI threshold (Open Water Index) of 0.2 tends to exclude significant areas of 'mixed pixels'. These may contain a significant proportion of flooding but the reflectances are also influenced by vegetation, soil on shorelines, or water discolouration. Further work on validation is required to improve and refine this classification.

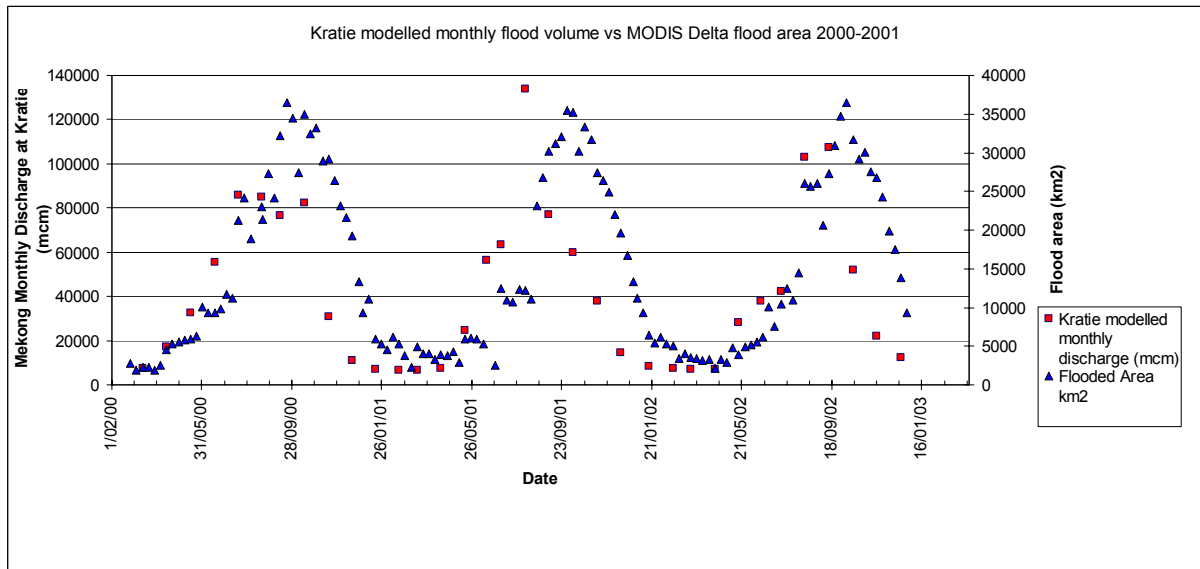


Figure 12.4. Modelled flood volumes at Kratie and Modis flood areas for 2000 to 2002.

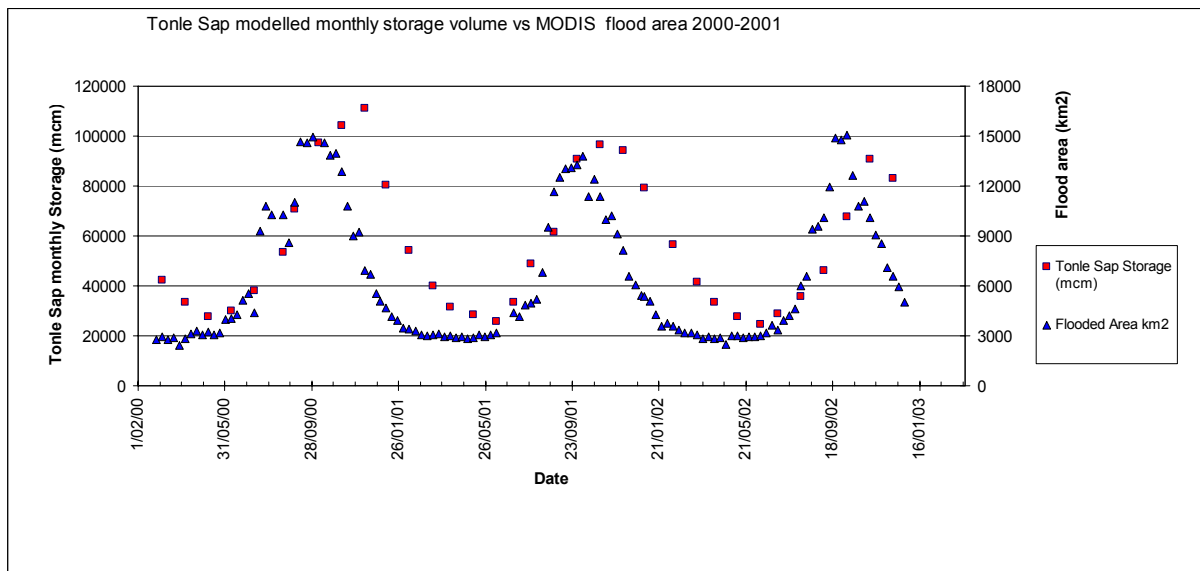


Figure 12.5. Modelled Tonle Sap Lake monthly storage and Lake Area 2000 to 2002.

The three years from the MODIS archive (2000 – 2002) that coincide with the river model period (1951- 2002) were all considered extreme flood years. The flood estimates for the Mekong Delta and Tonle Sap are shown in Figure 12.4 and Figure 12.5. The plots were prepared to compare the calculated flooded area with modelled river discharge and lake storage. The plots demonstrate a number of useful features about OWI produced from the MOD09A1 imagery.

1. The measured flooded area in the dry seasons return to virtually the same level for the three years observed in both areas. This supports the contention that the calculating the OWI is providing a consistent classification over time with this MODIS product. This also improves our confidence in the use of the MODIS imagery to assess the proportion of water with the larger TRMM pixels.
2. Each rising arm of the flooded area plot illustrates the impact of increased cloud at the beginning of the rainy season. Imagery for these periods are more highly contaminated; there are more unusable images and those that are used produced a larger scatter of values than those analysed for the descending portions of the plot.
3. Despite the high cloud contamination at the beginning of the wet season, the frequency of observation from the MODIS sensor allowed enough clear imagery to be collected to capture the maximum flood extent both in Tonle Sap and the Mekong Delta.
4. The flood area curves for the Delta vs. Kratie behave as expected (Figure 12.4.). Flood volumes at Kratie rise prior to observation of increasing flooding in the Delta. The flood peak occurs in the Delta about one month after the Kratie flood volumes peak. The flooded area declines until Kratie returns to base flow.
5. The behaviour of the Tonle Sap appears more complicated. (Figure 12.5.). The flooded area increases and recedes according to the seasons but appears to be out of phase with the modelled storage. It seems to indicate that the lake has reached the limit of its spread. If this is so the storage increase might equate to an increase in lake depth. Investigation of this proposition is beyond the scope of this study. Another possibility is that that phase shift between flooded area and lake storage is an artefact of modelling. This seems more likely as flooded area estimates are calculated from direct observations.
6. Validation of specific flooded areas of the maps was beyond the scope of this study however the maximum areas for each year do appear to tally with maximum areas modelled of reported by other researchers

12.2.5. Discussion

The aim of this study was to investigate the potential for the MODIS optical remote sensing instrument to produce historical flood maps of the Tonle Sap and Mekong Delta. The work has demonstrated that plausible maps can be created using the Open Water Index method from the MOD09A1 product (8 day composite of surface reflectance using available best pixel). Visual comparison of RADARSAT derived Inundation maps displayed on the MRC website look promising. Though the images below appear similar important information about the left hand map (such as the projection, pixel size and date of acquisition) are not known precluding more rigorous comparison.

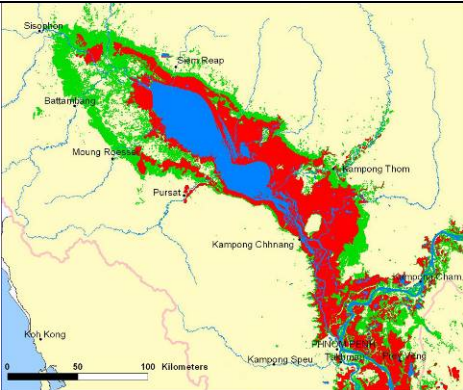
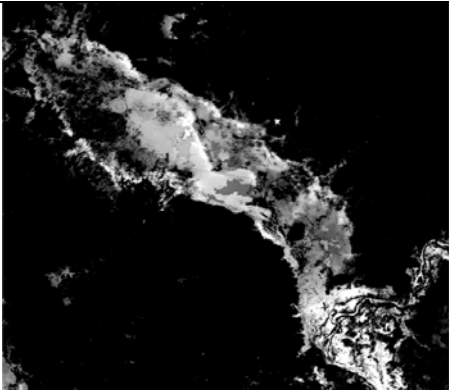
	
<p>Mekong River Commission RADARSAT™ derived maps of Tonle Sap. (blue=permanent water; red= max flood extent 1999; green=flood extent Oct 2000) from MRC website http://www.mrcmekong.org/MfS/html/flood_radarsat.html</p>	<p>MODIS derived OWI map for 15th Oct 2000. grey & white pixels classed at open water</p>

Figure 12.6. Comparison of RADARSAT derived map and Modis image for the Tonle Sap Lake

Further validation of the OWI method is required against independent data such as the MRC inundation maps produced for the periods studied. At the time of writing these maps had not been acquired.

The relationships between flood volumes (river discharge and lake storage) and the satellite based flooded area estimates are discussed in Section 12.4

12.3. Mapping Floods using Passive Microwave

12.3.1. TRMM background

Passive microwave instruments measure the brightness temperature of radiation from earth in the microwave frequencies. Surface water strongly absorbs microwave radiation compared to land, hence in passive microwave images large water bodies appear dark compared to the bright land surface. In this study, the Tropical Rainfall Measuring Mission's (TRMM) Microwave Imager (TMI) instrument was used to map surface water in the Tonle Sap and Delta region of the Mekong River Basin. Whilst the TRMM satellite is specifically designed to map global rainfall, it also produces land products. The TRMM satellite has been in operation since late 1997, and has been acquiring data ever since. It orbits around the earth approximately every 90 minutes making it possible to have near global data coverage every one to two days.

12.3.2. Method

Level 1B11 Brightness Temperature swath data (i.e. not yet geometrically corrected) for 1998 to 2002 were downloaded from NASA's TRMM website http://daac.gsfc.nasa.gov/data/datapool/TRMM_DP/01_Data_Products/01_Orbital/ for the Mekong region and geometrically projected into latitude/longitude on a WGS'84 datum with a pixel size of 10 km x 10 km. Due to time restrictions, only data for the wet season, July to December, were downloaded for 1999 and 2002. All processing of the TRMM data was done using an image processing package called ENVI/IDL which allows for the use of specialized remote sensing applications in ENVI, along with the ability to write your own applications in the programming language IDL (<http://www.ittvis.com/>). In this case the microwave brightness temperature at 37 GHz is used to map surface water for the Mekong river since it provides the best balance between spatial resolution (i.e. the level of detail visible in the image) and atmospheric interference effects (due to clouds and rain) (Brakenridge et al. 2007). The TRMM TMI produces both horizontal and vertical polarized images, but the former is used for this study since it has been shown to be more sensitive to moisture (Brakenridge et al. 2007). For the current project, only data acquired during the daytime were used, to help improve the contrast between the cool water and warm land. A rainfall mask was also applied to the imagery to remove these effects from the data. This was done using a simple mask from the TMI's data, where the 85 GHz vertical band is subtracted from the 22 GHz band (Ferraro et al. 1998). Any pixel with a mask digital number greater than 600 was masked as rain and removed from further processing. The remaining data were then composited, or stitched, together to form one image for each month. Where there was overlap, such that there was more than one image within the month for the same position on the ground, the lowest brightness temperature value was used. This is because water has a low brightness temperature, so it helped ensure all flood events would be captured in the imagery where possible.

One of the challenges of passive microwave images is their low spatial resolution. The TRMM TMI data at 37 GHz has a spatial footprint of 16 km x 10 km, meaning details of less than 10 km in size are not going to be visible. Fortunately the strong absorption of water in the microwave frequency means it has a large influence on the overall brightness temperature of a pixel, even if its proportion within a pixel is relatively low. Hence, parts of the Mekong River north of Kratie are visible in the TRMM TMI 37 GHz imagery even though the width of the Mekong River is generally less than 2 km. This challenge of mixed pixels

(i.e. where a pixel contains part water/ part land in this case) in the TRMM data benefits from the higher spatial resolution of the MODIS data to interpret and develop a set of rules for mapping the mixed pixels.

In this project, a cloud-free scene was selected from the MODIS MOD43B dataset to determine a set of rules for mixed water/non-water pixels in the TRMM data. The MOD43B data are 16-day composited (i.e. where, for all MODIS scenes over the 16-day period, the average brightness value of cloud-free data is calculated for every location on the ground) and normalized for brightness variations due to the different observation and sun angles (called the Bidirectional Reflectance Distribution Function). This 16-day image (starting on Julian day 337, or 2nd December 2000) was chosen here since it represented the longest time period with minimum cloud effects for matching against the equivalent TRMM composite scene. Here an average TRMM composite image was used for the same 16-day period to match the MOD43B compositing method. The Optical Water Index (OWI – see Optical section for explanation) was calculated for the MODIS scene providing a water mask, before it was resampled, or averaged to make its pixel size (1 km x 1 km) match the TRMM 10 km x 10 km pixel size. This resampling process essentially gave the proportion of water (based on MODIS) within each corresponding TRMM pixel.

An area around Tonle Sap Lake and Kratie was used to generate a set of rules for the mixed water/non-water pixels, since it included pixels that were 100% water in the TRMM data, as well as dry pixels. The MODIS water proportion was plotted against the TRMM Digital Number (Figure 12.7). (Digital Number can be converted to brightness temperature in TRMM data by dividing by 100 before adding 100).

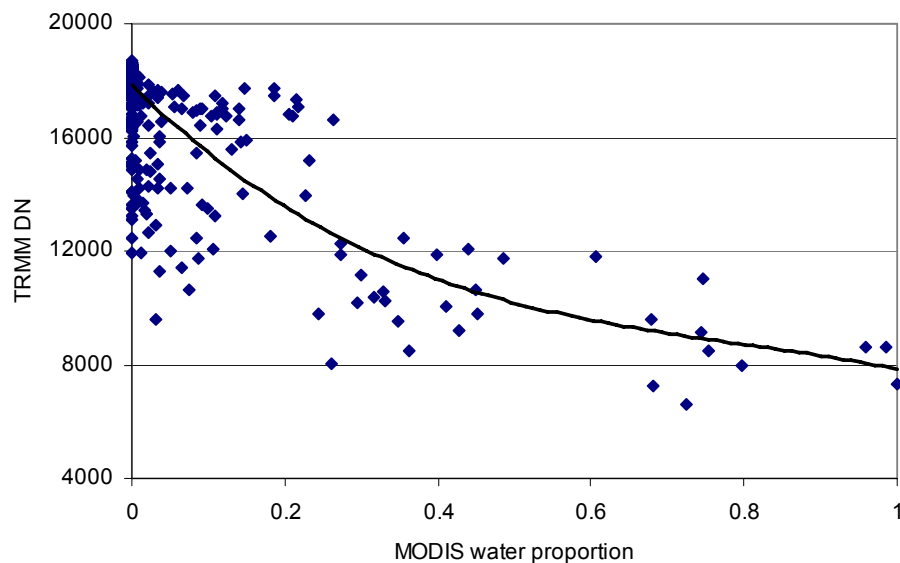


Figure 12.7. Scatterplot of TRMM Digital Number versus proportion of water (from MODIS) for the Tonle Sap and Kratie area for the 16-day period starting 2nd December 2000.

A third order polynomial was fitted against the curve and used to divide the TRMM Digital Number into proportion of water. Essentially the TRMM Digital Numbers were divided into ranges spanning 2000, and the average curve value within a digital number range determined the proportion of water (Table 12.1). Hence the extent of water within an area on a TRMM image was calculated by separating all the pixels into a digital number range in Table 12.1, and adding up water extent based on the first column.

Table 12.1. TRMM Digital Number ranges used to represent proportion of water within each pixel.

% Water	TRMM DN range
100%	< 8000
80%	8000-10000
40%	10000-12000
20%	12000-14000
<10%	14000-16000
0%	> 16000

This method was used for both the Tonle Sap Lake area and the Delta (which includes all areas of the river south of Kratie), and compared to the modelled storage volume for the Tonle Sap, and modelled flood volumes for Kratie (described in Chapter 6).

12.3.3. Results

The flood area for the Delta region was mapped in the TRMM monthly data for 1998 to 2002, and the maximum flood area for each year was recorded and compared to the modelled annual flood volume as measured at Kratie. These results are shown in Figure 12.8 (The observed peak flow data only existed for 1998 and 1999, hence it was not used for annual analysis). As can be seen, the annual flood volume shows a close relationship to TRMM mapped flood extent with a linear correlation R^2 of 0.8. The year 1998 was considered to be a relatively dry year, while 2000, 2001 and 2002 were relatively wet, enabling the TRMM data to capture these different events.

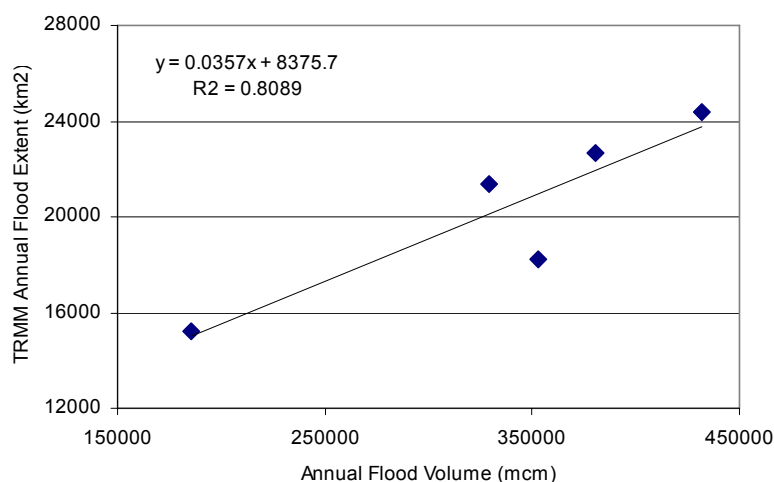


Figure 12.8. Scatterplot of modelled annual flood volumes for Kratie verses TRMM mapped flood extent for the Delta for 1998 to 2002

The TRMM data had its maximum flood extent occurring in later months compared to the modelled flow measurements. The modelled peak flows at Kratie for 1998 to 2002 occurred in August, September, July, August and September respectively, while for the TRMM data it was November, December, November, September and October. Figure 12.9 shows the TRMM scenes containing the maximum flood events for each year, as well as an image from the dry season (in this case February 1998) to show the observable changes.

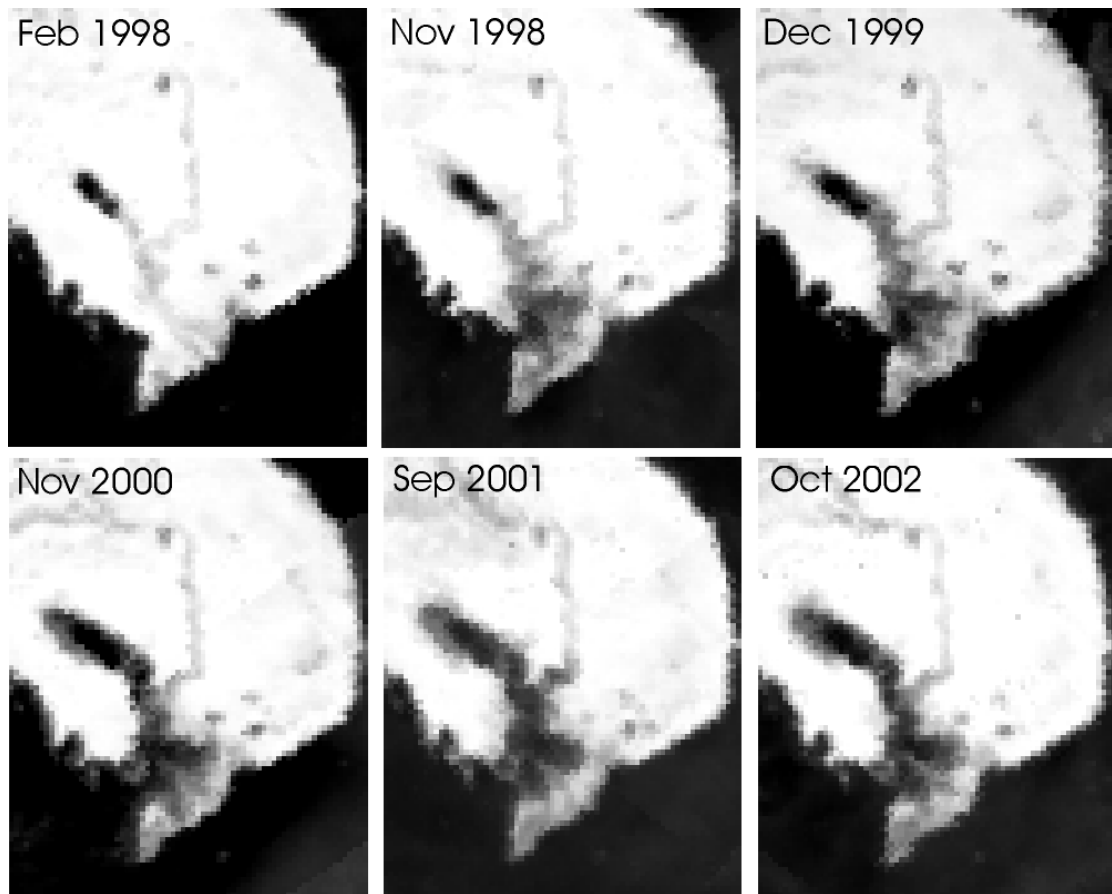


Figure 12.9. TRMM scenes of the Lower Mekong River for a dry month (Feb 1998) and the maximum flood months for 1998 – 2002. Dark areas indicate water.

As Figure 12.9 shows, Tonle Sap is visible even in the dry seasons, however the delta very much changes with the seasons. The large floods of 2000, 2001 and 2002 clearly show up as being large and dark in the Delta region. The maximum flood observed from both the modelled flood volume and TRMM flood extent for the existing data was during the wet season of 2001. Figure 12.10 shows the percentage of water within the TRMM pixels as determined from Table 12.1. for this flood event in the Tonle Sap region and the Delta including downstream from Kratie. As can be seen, much of the area appears to have some surface water within it.

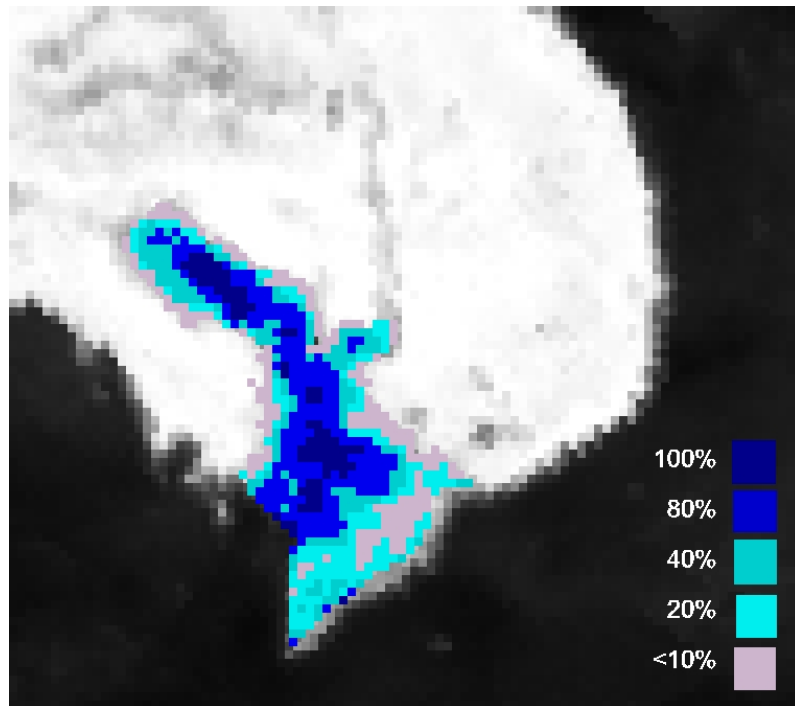


Figure 12.10. Percentage of water within TRMM pixels showing flood extent for the 2001 wet season for Tonle Sap and the Mekong Delta.

The Tonle Sap region was also analysed using the same method for calculating flood extent in the TRMM data. In this case the monthly data was examined against modelled monthly storage calculations (Figure 12.11). The results show a good linear correlation, with an R^2 of 0.82. It must be noted that the modelled monthly Tonle Sap storage is averaged for the month, whereas the TRMM flood extent is essentially the maximum flood for the month. This may explain any outlier points occurring above the average line of points in Figure 12.11.

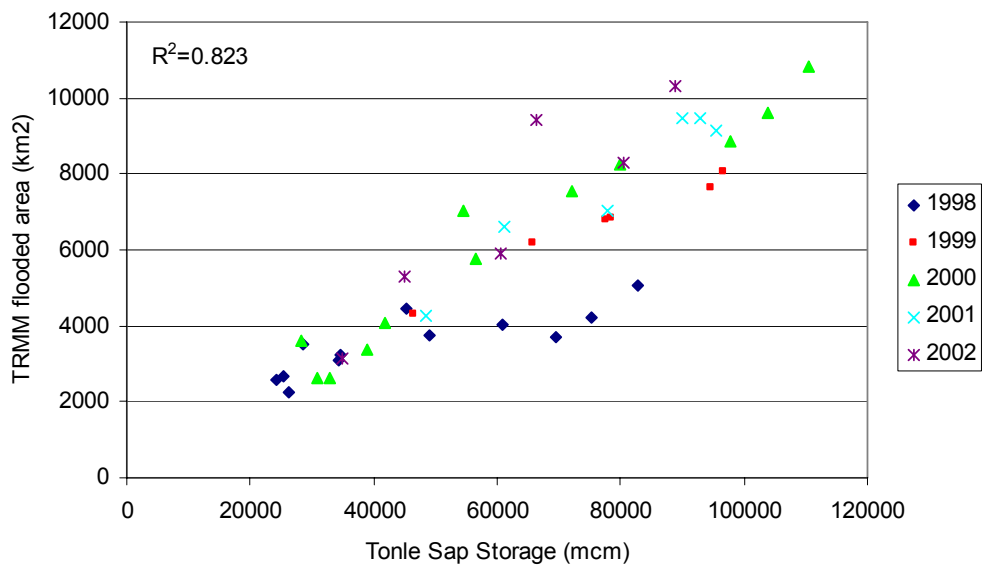


Figure 12.11. Scatterplot of monthly storage volume for Tonle Sap versus TRMM flood extent for 1998-2002.

12.3.4. Discussion

The results here show that there is potential for mapping flood extent for the lower Mekong River using TRMM passive microwave data. There are very good correlations between modelled flood volume and flood extent as mapped from the TRMM monthly data. This region has such large flood events that they are able to be viewed with imagery of 10 km x 10 km pixel size. It must be noted that there were only five years available for analysis in this study, so ideally more years need to be investigated to further examine the relationships between modelled/observed water flows and flood extent as determined by the TRMM passive microwave data.

12.4. Potential of combining Optical and Passive Microwave remote sensing for mapping water extent and change for the Lower Mekong River

Both the MODIS and TRMM have advantages in their ability to map surface water for the Lower Mekong River. The MODIS pixel size of 500 m x 500 m shows lots of detail that is not possible to see in the TRMM 10 km x 10 km pixels. However, the TRMM data was operating from late 1997 enabling it to capture the dry year of 1998 as well as the wetter years of 2000, 2001 and 2002.

The MODIS and TRMM data points were combined to compare results, and determine the best relationships to use with the modelled water volumes. Figure 12.12 shows the TRMM (1998-2002) and MODIS (2000-2002) monthly flood extent for the Tonle Sap Lake, plotted against the modelled Tonle Sap water volumes.

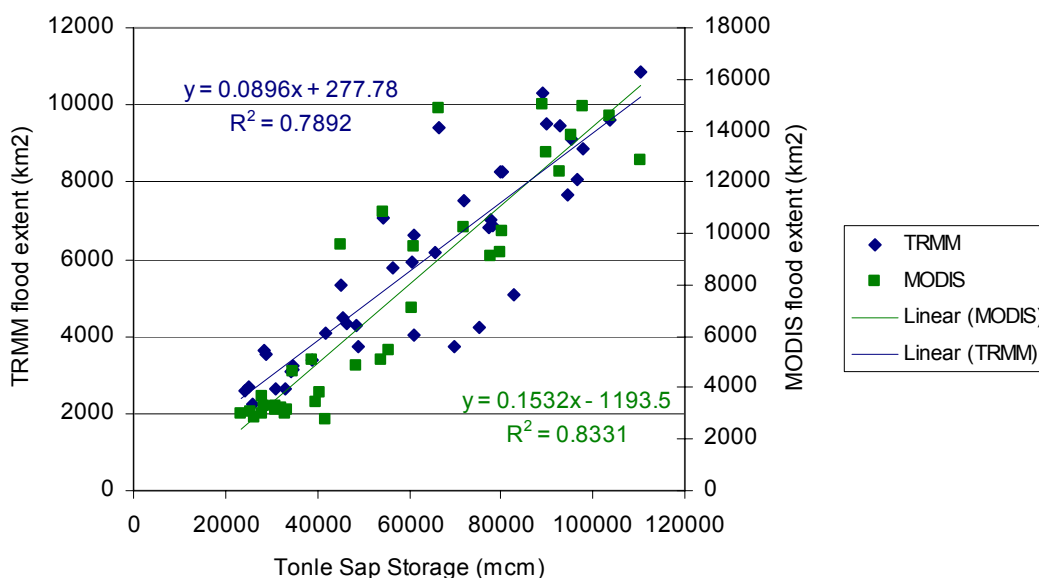


Figure 12.12. Scatterplot of TRMM (1998-2002) and MODIS (2000-2002) mapped flood extent verses modelled monthly storage water volume for Tonle Sap Lake.

Figure 12.12 shows similar linear relationships between the TRMM extent and modelled storage as well as the MODIS extent and modelled storage. The TRMM has a similar correlation to the MODIS with an R^2 of 0.79 compared to the MODIS R^2 of 0.83. There is a large difference in flood extent with the TRMM having a maximum around 10000 km² while the MODIS is around 15000 km².

For the Mekong Delta region, there were only three years of data from the MODIS for comparison with the TRMM data (Figure 12.13). While 2001 was the wettest year modelled, as well as mapped with the TRMM data, the MODIS data for 2001 did not have the largest flood area compared to 2000 and 2001. This may be due to increased cloud cover occurring

during wetter periods, and hence limiting the number of MODIS scenes available for mapping flood extent.

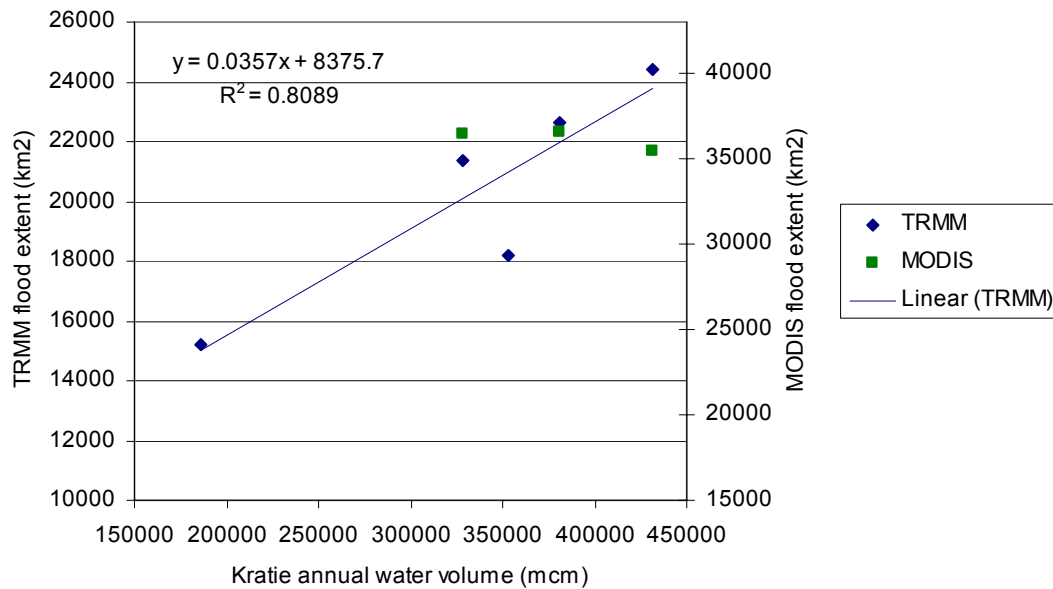


Figure 12.13. Scatterplot of TRMM (1998-2002) and MODIS (2000-2002) annual maximum flood extent for the Delta versus modelled Kratie annual water volume.

Independent research has mapped the Tonle Sap flood extent up to 15000 km². Given this information, it appears that the TRMM is most likely underestimating flood extent due to mixed water/non-water pixels, while the MODIS is giving a more realistic estimate. This is expected since the MODIS data has a higher spatial resolution, and hence can map more detail. Hence, to utilize the 1998 TRMM dry year and the good correlations between the TRMM and modelled flood data, as well as the more accurate MODIS flood areas, a combined approach is adopted for estimating flood area. For Tonle Sap, the monthly data for the TRMM and MODIS for 2000 to 2002 were regressed against each other (Figure 12.14).

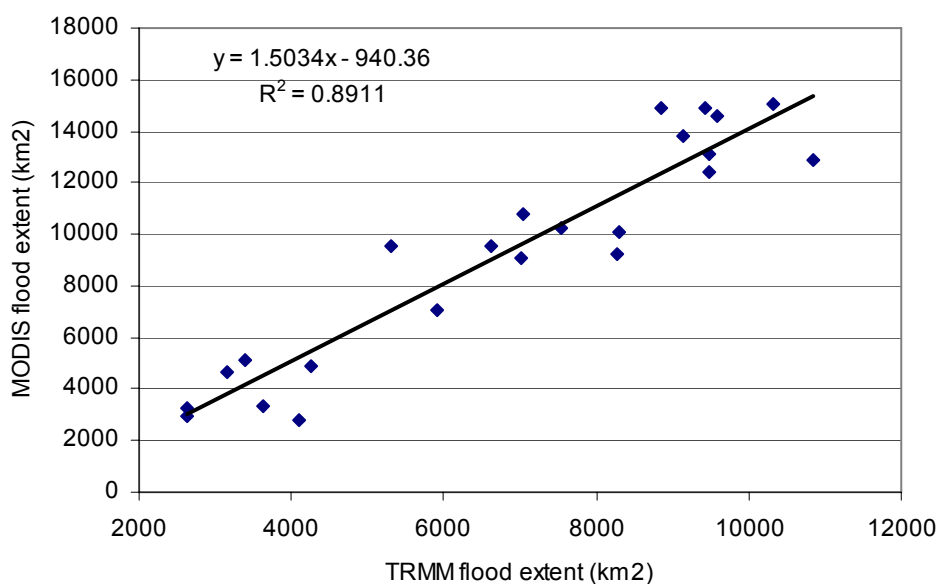


Figure 12.14. Scatterplot of Tonle Sap Lake monthly maximum flood extent for TRMM versus MODIS for 2000-2002.

This regression had an R^2 of 0.89, with the linear relationship shown on the graph. This relationship was used to scale the TRMM data up to MODIS so both datasets could be used to generate a relationship between modelled monthly flow data and flood extent as measured by remote sensing imagery. This produced an R^2 of 0.807, and a linear relationship shown in equation 12.3.

$$y = 0.1426 * x - 825.14 \dots\dots\dots\text{Equation 12.3}$$

where x is the modelled storage (in mcm) and y is the mapped flood extent from the combined TRMM / MODIS dataset (in km^2).

There were fewer points available to apply a similar approach for mapping the annual flood extent for the Mekong Delta using remote sensing data (Figure 12.13). Instead an offset was calculated such that the difference between the three common TRMM / MODIS points (2000, 2001 and 2002) equalled zero. This offset (13342 km^2) was then added to the TRMM data to scale it up to MODIS flood extent (Figure 12.15). When the scaled TRMM and MODIS data were combined and regressed against the modelled annual flood volume measurements the correlation had an R^2 of 0.662 and a linear relationship as shown in equation 12.4.

$$y = 0.0318 * x + 23428 \dots\dots\dots\text{Equation 12.4}$$

where x is the modelled annual flood volume for Kratie (in mcm) and y is the mapped flood extent from the combined TRMM / MODIS dataset (in km^2). While this relationship is not as good as the one for Tonle Sap Lake it provides the best estimate available from the remote sensing data based on the limited years available, and it utilizes the advantages gained from adopting both the TRMM and MODIS data.

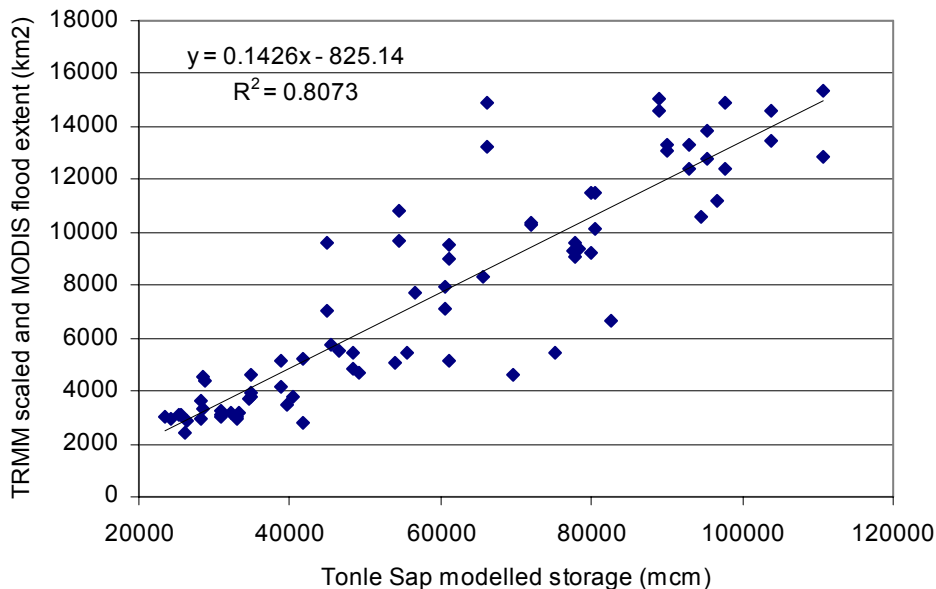


Figure 12.15. Scatterplot of the combined MODIS (2000-2002) and scaled TRMM (1998-2002) monthly flood extent for the Tonle Sap Lake verses modelled monthly water volume.

Interpretation of Figure 12.15 shows that the maximum flood extent mapped using remote sensing is up to 37700 km^2 . To enable this relationship to be only used for interpolation, rather than extrapolation, this equates to an annual flood volume of 443916 (mcm) at Kratie, as was modelled here.

12.4.1. Summary

Both the optical and passive microwave remote sensing data show a relationship with modelled water volume when they are used to map flood water extent. The TRMM passive microwave data has the advantage of being unaffected by cloud cover (while not raining), as well as having data for 1998 which was a relatively dry year in recent times. However its large pixel size (10 km x 10 km) does make it difficult to address the mixed water/non-water pixels. The higher resolution MODIS data was used here to develop a set of rules for interpreting these mixed pixels. The MODIS optical imagery was greatly affected by cloud cover, particularly in the beginning of the wet season, but when combined into 8-day composites it enabled a significant amount of data to be retrieved for the Lower Mekong River. Its pixel size (500 m x 500 m) is much smaller than the TRMM data, hence the water extent could be mapped in more detail. Unfortunately there were no MODIS data for 1998 so this relatively dry year could not be included in the analysis here. The final method adopted for mapping flood water extent in the Tonle Sap Lake and the Mekong Delta, was to combine the TRMM and MODIS data to overcome each instruments disadvantages and utilize their complementary qualities.

13. APPENDIX 3

CURRENT AND RECENT TRENDS IN AGRICULTURAL PRODUCTIVITY

Apart from rice, upland crops (crops other than rice are generally termed together as upland crops) are also grown in the basin. Sugarcane, maize, soybean and cassava are the major upland crops (Table 13.1). For this study, we have considered rice (all seasons), sugarcane, maize and soybean to determine the impact of climate change on yield. Cassava was not considered due to the unavailability of the yield response factor.

Table 13.1. Harvested area of different crops grown in the basin as percentage of the total harvested area, 1995-2003

Crop	1995	1996	1997	1998	1999	2000	2001	2002	2003
Main rainfed rice	63.9	63.8	63.3	63.9	64.6	64.1	64.0	64.7	64.6
Irrigated rice	8.3	7.6	8.0	7.6	7.4	7.2	6.8	6.4	6.3
Upland/flood-prone rice	9.3	10.0	10.4	11.0	11.4	11.9	11.9	11.7	11.1
Maize	4.7	5.0	5.2	5.4	4.7	4.8	4.8	5.0	5.0
Cassava	6.7	6.5	6.1	5.1	5.2	5.4	4.9	4.5	4.7
Soybean	0.8	0.7	0.7	0.8	0.8	0.8	0.7	0.8	1.0
Sugarcane	3.2	3.3	3.3	3.3	3.3	3.0	3.6	3.7	4.0
Other upland crops	3.1	3.1	3.0	2.8	2.7	2.7	3.2	3.3	3.4
Total rice	81.5	81.4	81.7	82.6	83.3	83.2	82.7	82.7	82.0
Total upland crops	18.5	18.6	18.3	17.4	16.7	16.8	17.3	17.3	18.0

The provincial and regional differences in average productivity or yield of rice and its trend during 1993-2004 are shown in Figures 13.1 and 13.2. Yield of rice varies from 1.0 to over 5.0 t/ha, with the highest yield in the Delta region of Vietnam, moderate yields in some part of Laos and the Vietnam Highlands and the lowest yields in Cambodia and Northeast Thailand. The regions of highest productivity are those of highest rainfall or irrigation water use. The lower productivity of Northeast Thailand presumably results from the lower rainfall, longer annual dry period, poorer soil nutrition, cultivation of local varieties and low fertilizer applications, etc. Drought is a major production constraint for rain fed lowland rice, being particularly severe in Northeast Thailand. It also affects large areas of rice cultivation in Laos and Cambodia (Fukai 2001). In these countries, late season drought is common, amounting to yield losses as high as 35% in Thailand (Jongdee *et al.* 1997). In all regions, productivity increased from 1993 to 2004, with the increase being more prominent in Laos and Vietnam. For Cambodia and Thailand, the yield has been almost stagnant since 2000 with slight variations from year to year.

The total production of rice is dominated by the production of rain fed rice. However, the yield of rice grown in different seasons is different. Figures 13.3, 13.4 and 13.5 show the regional average yield of main rain fed rice, irrigated rice and upland/flood-prone rice. For Cambodia, separate production data of different types of rice were not available, therefore, not shown in the figures. Upland rice is not grown in Thailand. As can be seen from the Figures 13.2 and 13.3, the yield and trend of rain fed rice is quite similar to that of the overall rice production. The yield of irrigated rice is surprisingly higher in Laos than that of Thailand and Vietnam. However, the yield of upland rice is much lower in Laos, even lower than the main rain fed rice. Among the three rice crops grown in Vietnam, the yield of upland/flood-prone rice is the highest.

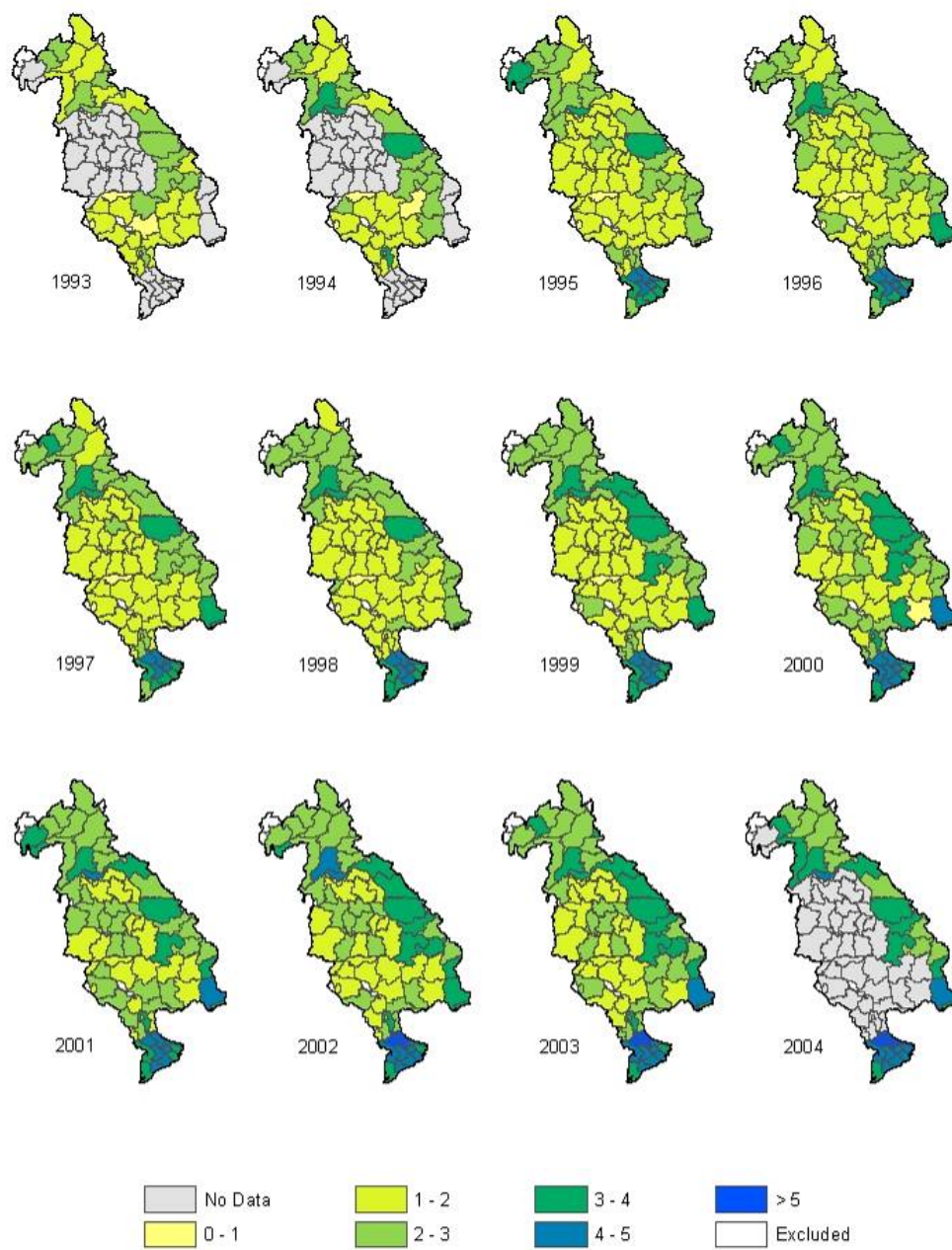


Figure 13.1. Spatial and temporal variability of average yield (tonne/ha) of rice in the lower Mekong Basin

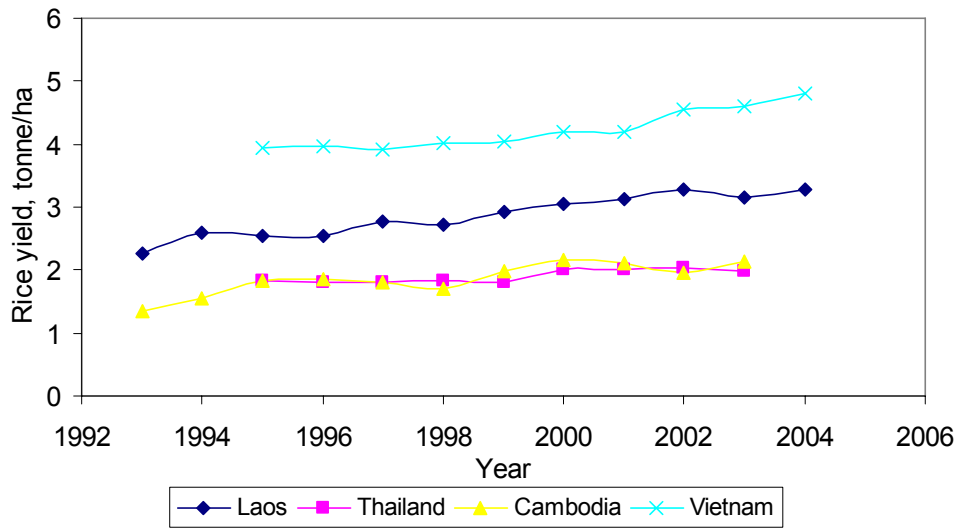


Figure 13.2. Regional average yield of rice

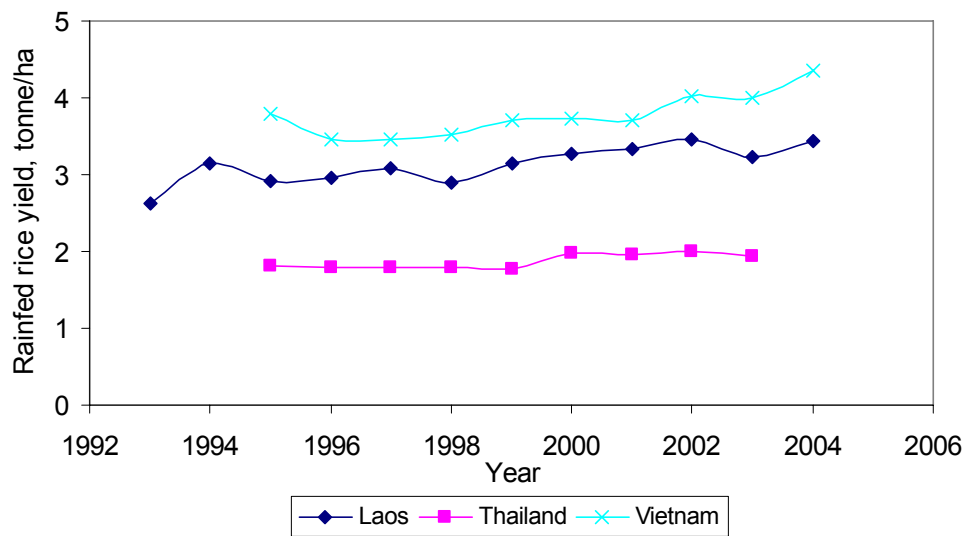


Figure 13.3. Regional average yield of main rain fed rice

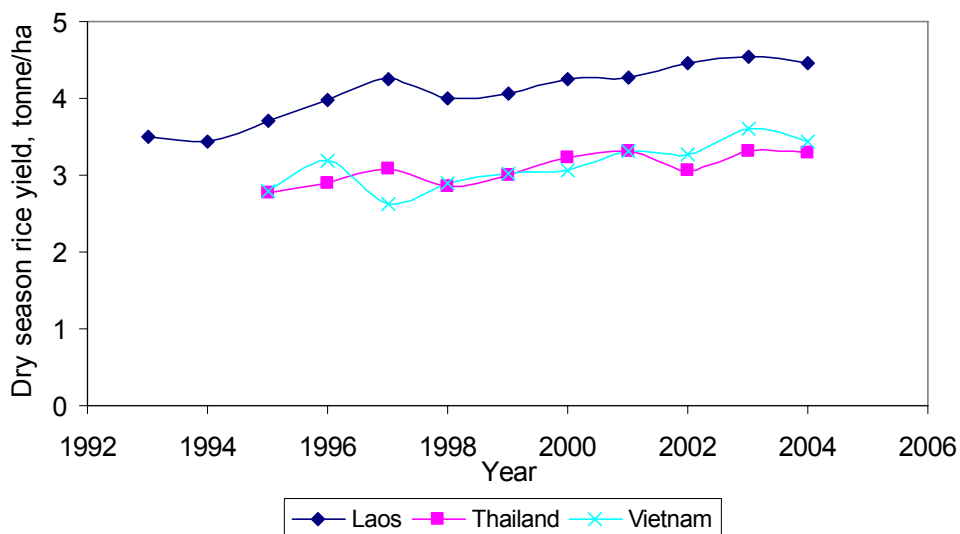


Figure 13.4. Regional average yield of irrigated rice

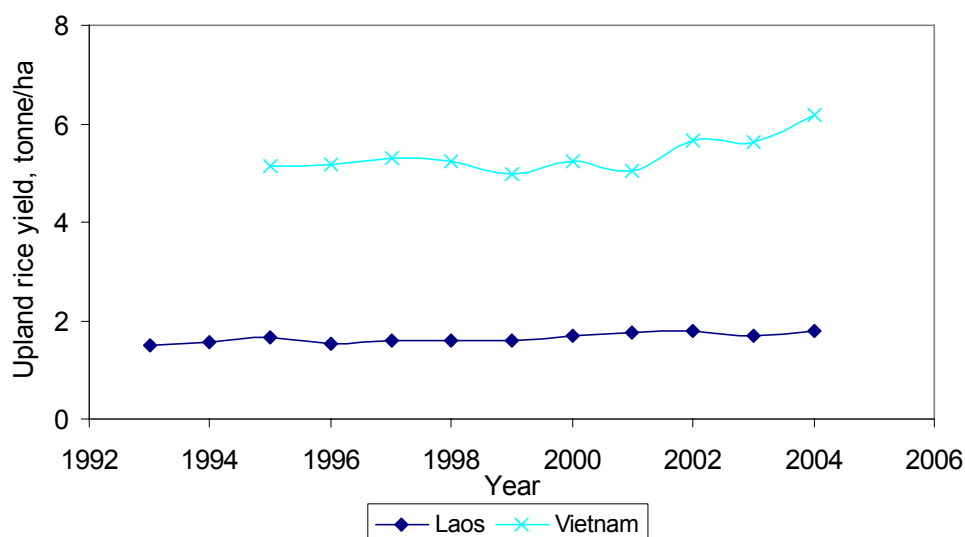


Figure 13.5. Regional average yield of upland/flood-prone rice

The spatial variation of the yield of rain fed rice among the provinces within a country was not high (Table 13.2). The variation is highest in Cambodia and Thailand and the lowest in the Mekong Delta. There is a slightly decreasing trend of CV over the years, indicating less variation of yield among the provinces. However, the variation of the rainfall during the growing season of rain fed rice is generally higher (Table 13.3). There is no correlation between the total CV of total rainfall during the growing season and CV of yield indicating that the variation in yield is not due to the variation of total rainfall. Despite the widely different water availability, observed provincial yields were generally unaffected by the difference in rainfall during the growing season. The increase in yield over the years was mostly because of cultivating high yielding varieties and high fertilizer use (Hasegawa et al., 2008).

Table 13.2. Inter-provincial coefficient of variation (CV) of the yield of main rain fed rice

Country	1993	1994	1995	1996	1997	1998	1999	2000	2001	2002	2003	2004
Laos	0.15	0.10	0.17	0.14	0.11	0.19	0.05	0.02	0.10	0.09	0.08	0.14
Thailand			0.24	0.20	0.19	0.19	0.21	0.18	0.20	0.18	0.15	
Cambodia	0.41	0.48	0.39	0.42	0.41	0.40	0.42	0.29	0.27	0.29	0.24	
Vietnam			0.15	0.13	0.16	0.16	0.16	0.14	0.13	0.15	0.11	0.12

Table 13.3. Inter-provincial coefficient of variation (CV) of the rainfall during the growing season of main rain fed rice

Country	1993	1994	1995	1996	1997	1998	1999	2000	2001	2002	2003	2004
Laos	0.21	0.19	0.19	0.26	0.24	0.22	0.24	0.18	0.14	0.35	0.27	0.28
Thailand			0.19	0.28	0.14	0.16	0.13	0.22	0.13	0.17	0.21	
Cambodia	0.19	0.11	0.19	0.17	0.16	0.23	0.16	0.16	0.25	0.25	0.23	
Vietnam			0.21	0.24	0.20	0.03	0.11	0.04	0.07	0.11	0.08	0.09

Main rain fed rice production accounts for 2/3 (67%) of the total basin (lower basin) production (Table 13.4). Upland/flood-prone rice and irrigated rice production is about 26% and 7% of the total production. Of the 4 riparian countries in the lower Mekong Basin, Vietnam produces more than half of the total rice production of the basin (Table 13.4), followed by Thailand (more than 30%). Laos and Cambodia combined produce only about 19% of the total rice production. More than 95% of the production of total rice in Vietnam is from the Mekong Delta. The remaining 5% is from the Central Highlands.

Table 13.4. Distribution (%) of total rice production in the lower Mekong Basin by region and type of rice

Region	1995	1996	1997	1998	1999	2000	2001	2002	2003
Laos	5.2	5.1	5.8	5.7	6.5	6.6	6.9	7.0	6.6
Thailand	34.3	32.4	33.7	31.5	30.1	30.9	32.4	29.8	30.5
Cambodia	11.8	11.4	11.0	9.2	11.6	11.1	11.4	10.5	12.0
Vietnam	48.7	51.1	49.5	53.6	51.9	51.5	49.3	52.8	50.9
Type of rice for the whole Lower Mekong Basin									
Main rainfed rice	67.9	66.2	65.9	65.0	66.8	65.7	66.6	65.8	66.7
Irrigated rice	10.7	10.5	9.2	9.1	9.1	8.6	8.2	7.5	7.5
Upland/flood-prone rice	21.5	23.3	24.9	26.0	24.2	25.7	25.1	26.7	25.8

In contrast to rice, the yield of sugarcane is high in Thailand (Figure 13.6), presumably reflecting the use of greater inputs for a crop grown commercially (as opposed to for subsistence). This suggests that, in Thailand at least, better crop management with greater inputs can lead to higher yields. The yield is also higher in Vietnam, almost similar to that of Thailand. Much less was grown elsewhere, and we presume that the larger, more commercially grown crops of those two regions led to better management and higher yields. Yield of maize and soybean are also higher in Thailand and Vietnam and lower in Laos and Cambodia (Figures 13.7 and 13.8).

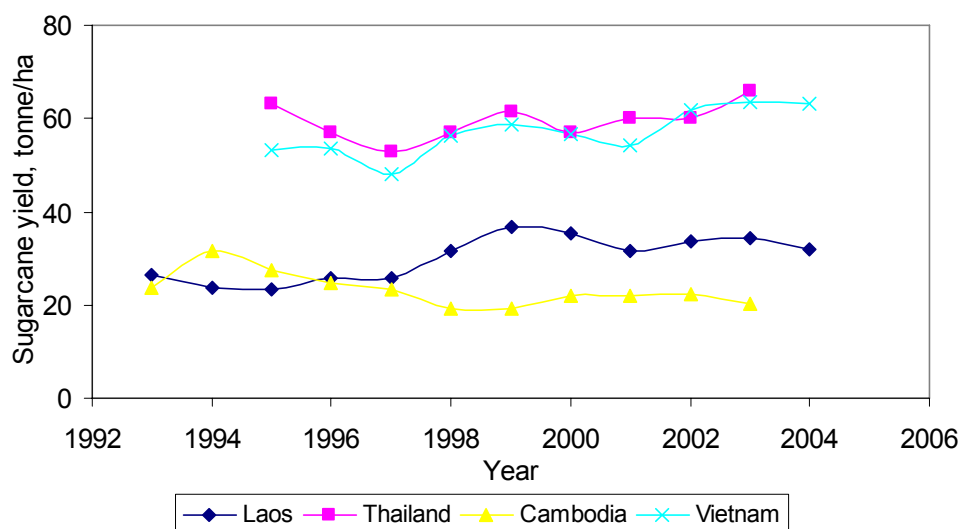


Figure 13.6. Regional average yield of sugarcane

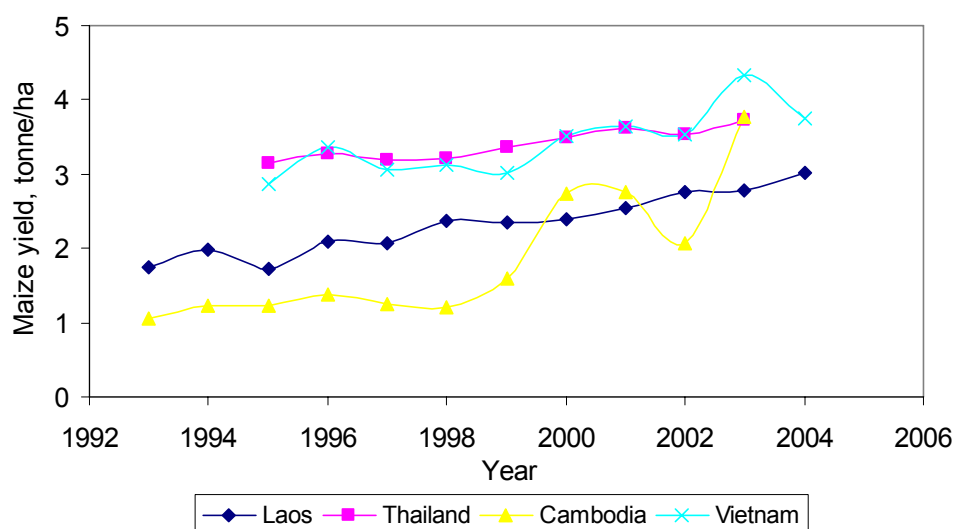


Figure 13.7. Regional average yield of maize

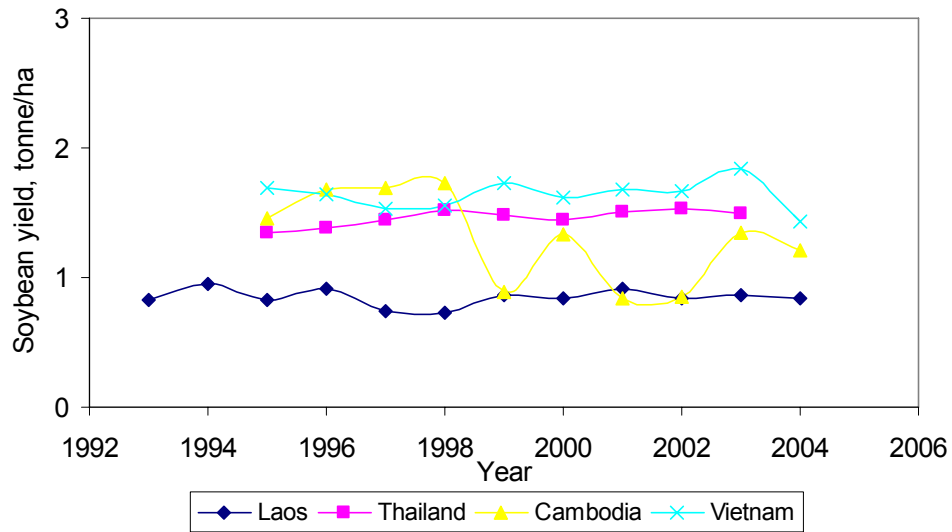


Figure 13.8. Regional average yield of soybean

14. REFERENCES

- Allen, R. G., Pereira, L. S., Raes, D., and Smith, M., 1998. Crop Evapotranspiration: Guidelines for Computing Crop Water Requirements. FAO Irrigation and Drainage Paper 56, FAO, Rome.
- AusAID, 2007. The Greater Mekong Subregion. Australia's Strategy to Promote Integration and Co-operation 2007-2011. Australian Agency for International development (AusAID). 30pp.
- Baran, E., P. Starr, and Y. Kura 2007. Influence of Built structures on Tonle Sap fisheries. Cambodia National Mekong Committee and the WorldFish Center, Phnom Penh, Cambodia.
- Berg, M., Stengel, C., Trang, P.T.K., Viet, P.H., Sampson, M., Leng, M., Samreth, S., and Fredericks, D., 2007. Magnitude of arsenic pollution in the Mekong and Red River Deltas – Cambodia and Vietnam. *Science of the Total Environment*, vol. 372: 413-425.
- Block, S. A., 1995. The recovery of agricultural productivity in sub-Saharan Africa. *Food Policy*, Vol. 20, No. 5: pp. 385-405.
- Boualaphanh, C., Inthaphanya, P. and Ratsabandit, S. 2001. Rice improvement methods for Laos. In: Fukai, S. and Basnayake, J. (ed.) *Increased Lowland Rice Production in the Mekong Region*. ACIAR Proceedings 101, Canberra.
- Brakenridge, G.R., Nghiem, S.V., Anderson, E., Mic, R., 2007. Orbitla microwave measurement of river discharge and ice status. *Water Resources Research*, 43, W04405, doi:10.1029/2006WR005238.
- Buu, B. C. and Lang, N. T. 2004. Improving rice productivity under water constraints in the Mekong Delta, Vietnam. In: Seng V., Craswell, E., Fukai, S. and Fisher, K. (eds.), *Water in Agriculture: Proceedings of a CARDI International Conference 'Research on Water in Agricultural Production in Asia for the 21st Century'*, Phnom Penh, Cambodia, 25-28 November 2003. Australian Centre for International Agricultural Research, Canberra.
- Burnett, W.C. and Bokuniewicz, 2002. Are groundwater inputs into the coastal zone important? In: *Low-lying coastal areas hydrology and integrated coastal zone management*. Proceedings International Symposium Bremerhaven, Germany, 9-12 September, 2002, Deutsches IHP/OHP National Komitee, Koblenz.
- Buschmann, J., Berg, M., Stengel, C. and Sampson, M., 2007. Arsenic and Manganese contamination of drinking water resources in Cambodia: coincidence of risk areas with low relief topography. *Environmental Science and Technology* Volume 41 No. 7.
- Ceccato, P., Flasse, S., & Gregoire, J.-M., 2002a. Designing a spectral index to estimate vegetation water content from remote sensing data: Part 2. Validation and applications. *Remote Sensing of Environment*, 82, 198-207
- Ceccato, P., Gobron, N., Flasse, S., Pinty, B., & Tarantola, S., 2002b. Designing a spectral index to estimate vegetation water content from remote sensing data: Part 1: Theoretical approach. *Remote Sensing of Environment*, 82, 188-197
- Chea, S. Cramb, R. A. and Fukai, S., 2004. The Economics of Rice Double-Cropping with Supplementary Irrigation in the Rain fed Lowlands of Cambodia: A Survey in Two Provinces. In: *Water in Agriculture*, Seng, V., Craswell, E., Fukai, S., and Fisher, K. (eds), Australian centre of International Agricultural Research, Canberra.
- Chea, S. Cramb, R. A., Nesbitt, H., Fukai, S., Chan, P. and Cox, P. 2001. Crop intensification of rice-based farming systems in Cambodia. In: Fukai, S. and Basnayake, J. (ed.) *Increased Lowland Rice Production in the Mekong Region*. ACIAR Proceedings 101, Canberra.
- Chinvanno, S. 2004a. Information for sustainable development in light of climate change in Mekong River Basin. Southeast Asia START Regional Center, Bangkok, Thailand. Retrieved December, 2006 from:
http://203.159.5.16/digital_gms/Proceedings/A77_SUPPAKORN_CHINAVANNO.pdf

- Chinavanno, S. 2004b. Building capacity of Mekong River countries to assess impacts from climate change- case study approach on assessment of community vulnerability and adaptation to impact of climate change on water resources and food production. Final Report of APN CAPaBLE Project. Southeast Asia START Regional Centre.
- CIAP, 1999. Cambodia-IRRI-Australia project annual research report. Cambodia 178pp.
- Cook, S., Gichuki, F. and Turrall, H., 2006. Agricultural Water Productivity: Issues, Concepts and Approaches, Basin Focal Project Working Paper No. 1, available on http://www.waterandfood.org/fileadmin/CPWF_Documents/Documents/Basin_Focal_Projects/BFP_restricted/Paper_1_Final_14JY06.pdf
- Ding, Y., Y.E. Baisheng, S, Liu, 2007. Short Glacier Inventory of China. Chapter 4. Progress in studies of snow and ice.
- Doorenbos, J. and Kassam, A. H. 1979. Yield response to water. FAO Irrigation and Drainage Paper 33, FAO, Rome.
- Dyurgerov, M.B. and M.F. Meier, 2005. Glaciers and the changing earth system: a 2004 snapshot. Institute of Arctic and Alpine Research, University of Colorado, Occasional Paper No. 58. 117pp.
- Falkenmark M., and G. Lindh, 1976. Water for a starving world. Westview press, Boulder Colorado, 204pp.
- Feldman, P.R. and Rosenboom J.W., 2001. Cambodia drinking water quality assessment; World Health Organisation of the UN (WHO) in cooperation with Cambodian Ministry of Rural Development and the Ministry of Industry, Mines and Energy. Phnom Penh.
- Ferraro, R.R., Smith, E.A., Berg, W., Huffman, G.J., 1998. A screening methodology for passive microwave precipitation retrieval algorithms. Journal of the Atmospheric Sciences, 9, 1583-1600.
- Fukai, S. 2001. Increasing Productivity of Lowland Rice in the Mekong Region. In. Fukai, S. and Basnayake, J. (ed.) Increased Lowland Rice Production in the Mekong Region. ACIAR Proceedings 101, Canberra.
- Fukai, S. and Kam, S. P. 2004. Improved crop production under water constraints. In. Seng V., Craswell, E., Fukai, S. and Fisher, K. (eds.), Water in Agriculture: Proceedings of a CARDI International Conference 'Research on Water in Agricultural Production in Asia for the 21st Century', Phnom Penh, Cambodia, 25-28 November 2003. Australian Centre for International Agricultural Research, Canberra.
- Fukui, H. 1993. Food and population in a Northeast Thai village. University of Hawaii Press, Honolulu. 421pp.
- Ghassemi, F, and Brennan, D., 2000. An evaluation of the sustainability of farming systems in the brackish water region of the Mekong Delta. Resource profile subproject: summary report. Australian Centre for International Agricultural Research. May 2000.
- GIWA (Global International Waters Assessment), 2006. Mekong River, GIWA regional assessment 55. Published by the University of Kalmar on behalf of United Nations Environment Programme.
- Fujii, H., Garsdal, H., Ward, P., Ishii, M., Morishita, K., and Boivin, T., 2003. Hydrological Roles of the Cambodian Floodplain of the Mekong River. International Journal of River Basin Management, 1(3): 1-14.
- Guerschman, J.P., Van Dijk A.I.J.M., McVicar, T.R. Van Niel, T.G., Lingtao L, Yi Liu, Peña-Arancibia, J., 2008. Actual evapotranspiration and water balance estimates from satellite observations over the Murray-Darling Basin. Canberra, CSIRO science report
- Hargreaves, G.H and Z.A. Samani, 1982. Estimating Potential Evapotranspiration. Technical note. Journal of Irrigation and Drainage 108. 225-30.

- Hasegawa, T., Sawano, S., Goto, S., Konghakote, P., Polthanee, A., Ishigooka, Y., Kuwagata, T., Toritani, H., and Furuya, J. 2008. A model driven by crop water use and nitrogen supply for simulating changes in the regional yield of rain fed lowland rice in Northeast Thailand. *Paddy Water Environment* 6: 73-82.
- Haskoning, 2000. Groundwater study. Mekong Delta. Modelling report. Haskoning BV consulting engineers and Arcadis Euroconsult, June 2000, 101pp
- Hirsch, P. and Cheong, G., 1996. Natural Resource Management in the Mekong River Basin: Perspectives for Australian Development Cooperation. Final overview report to AusAID.
- Hoanh, C.T., Guttman, H., Droogers, P. and Aerts, J., 2003. Water, climate, food and environment in the Mekong Basin in southeast Asia. Final report. International Water Management Institute (IWMI), Mekong River Commission Secretariat (MRCS), Institute of Environmental Studies (IVM)
- Hock R., 2003. Temperature index melt modelling in mountain areas. *Journal of Hydrology* 282: 104-115.
- Homma K, Horie T, Ohnishi M, Shiraiwa T, Supapoj N, Matsumoto N, Kabaki N., 2001. Quantifying the toposequential distribution of environmental resources and its relationship with rice productivity. In: Fukai S, Basnayake J (eds) Increased lowland rice production in the Mekong Region. Proceedings of an International Workshop, Vientiane, Laos, pp 281–291.
- Huete, A., Didan, K., Miura, T., Rodriguez, E.P., Gao, X., & Ferreira, L.G., 2002. Overview of the radiometric and biophysical performance of the MODIS vegetation indices. *Remote Sensing of Environment*, 83, 195-213
- Ichikawa, T., Mekpruksawong, P., Trinetra, Y., Aramaki, S., Qong, M. and Chuenchooklin, S., 2007. Salinity problem of the groundwater use for irrigation in the Lower Nam Kam Basin, Thailand. Fourth INWEPF Steering Meeting and Symposium, July 2007, Bangkok, Thailand.
- Imaizumi, M., Sukchan, S., Wichaidit, P., Srisuk, K. and Kaneko, F. (no date). Hydrological and Geochemical behaviour of saline groundwater in Phra Yun, Northeast Thailand. JIRCAS working paper No. 30.
- IPPC, 2001. Climate change 2001: Synthesis report. An assessment of the Intergovernmental Panel on Climate Change.
- IPCC, 2007. Climate Change 2007: Synthesis report. An assessment of the Intergovernmental Panel on Climate Change. Cambridge University Press.
- IPCC, 2007. Climate Change, 2007. The physical science basis. Contributions of working group 1 to the fourth assessment report of the Intergovernmental Panel on Climate Change. Cambridge University Press.
- IWMI (International Water Management Institute), 2006. Water governance in the Mekong region – the need for more informed policy-making. Water Policy Briefing Issue 22 November 2006.
- Jackson, I. J. 1977. Climate, water and agriculture in the tropics. Longman, London and New York. 248pp.
- Johnston, R., Rowcroft, P., Hortle, K.G., and McAllister, C., 2003. Integrating environmental values into resource allocation - the MRC's approach in the LMB. Paper presented at Workshop on Integrating Environmental Impacts into Water Allocation Models of the Mekong River Basin, University of Economics, Ho Chi Minh City, 15 December 2003. Available at: http://www.iucn.org/places/vietnam/our_work/ecosystems/assets/07%20Water%20Values%20in%20the%20Mekong.pdf
- Jongdee, S., Mitchell, J. H. and Fukai, S., 1997. Modelling Approach for Estimation of Rice Yield reduction due to Drought in Thailand. In. Fukai, S., Cooper, M. and Salisbury, J. (eds.) Breeding Strategies for Rain fed Lowland Rice in Drought-Prone Environments, Proceedings

of an International Workshop held at Ubon Ratchathani, Thailand, 5-8 November, 1996. Canberra, ACIAR Proceedings No. 77, 65-73.

Kazama, S., Hagiwara, T., Ranjan, P. and Sawamoto, M., 2007. Evaluation of groundwater resources in wide inundation areas of the Mekong River Basin. *Journal of Hydrology* vol 340 (3-4): 233-243.

Kiem, A.S., M.V. Geogievsky, H.P. Hapuarachchi, H. Ishidaira and K. Takeuchi, 2005. Relationship between ENSO and snow covered area in the Mekong and Yellow River Basins. In *Regional Hydrological Impacts of Climate Change – Hydroclimatic Variability*.

Kiem, A.S., H. Ishidaira, H.P. Hapuarachchi, M.C. Zho, Y. Hirabayashi and K. Takeuchi, 2008. Future hydroclimatology of the Mekong River basin simulated using the high-resolution Japan Meteorological Agency (JMA) AGCM. *Hydrological Processes* 22: 1382 - 1394.

Franks, S.W., Wagener, T., Bogh, E., Gupta, H.V., Bastidas, L., Nobre, C., Galvao, C. (des). *International Association of Hydrological Sciences (IAHS) publ. 296: Wallingford, UK. 255-264.*

Kirby, M., M. Mainuddin and J. Eastham, 2008a. Challenge Program basin water use accounts: 2. Model concepts and description. Report for the Challenge Program on Water and Food.

Kirby, M., M. Mainuddin, M. Thomas and J. Eastham, 2008b. Challenge Program basin water use accounts: 7. Mekong Basin water use account. Report for the Challenge Program on Water and Food.

Kirby, M., Van-Dijk, A. I. J. M., Mainuddin, M., Peña-Arancibia, J., Guerschman, J. P., Liu, Y., Marvanek, S., McJannet, D. L., Paydar, Z., McVicar, T. R., Van-Niel, T. G. & LI, L. T., 2008. *River Water Balance Accounts Across the MDB, 1990-2005.*

Kono, Y., Tomita, S., Nagata, Y., Iwama, K., Nawata, E., Junthotai, K., Katawatin, R., Kyuma, K., Miyagawa, S., Niren, T., Noichana, C., Sakuratani, T., Sributta, A. and Watanabe, K. 2001. A GIS-based crop-modelling approach to evaluating the productivity of rain fed lowland paddy in North-east Thailand. In Fukai, S. and Basnayake, J. (ed.) *Increased Lowland Rice Production in the Mekong Region. ACIAR Proceedings 101, Canberra.*

Kristensen, J., 2001. Food Security and Development in the Lower Mekong River Basin: A Challenge for the Mekong River Commission. Presented at Asia and Pacific Forum on Poverty: Reforming Policies and Institutions for Poverty Reduction, to be held at the Asian Development Bank, Manila, 5-9 February 2001.

Legates, D.R., 1987. A climatology of global precipitation. *Publ. Climatol.* 40 (1), 85pp.

Linquist, B. and Sengxua, P., 2001. Nitrogen management for the rain fed lowland rice systems of Laos. In Fukai, S. and Basnayake, J. (ed.) *Increased Lowland Rice Production in the Mekong Region. ACIAR Proceedings 101, Canberra.*

Maclean, J.L., Dawe, D.C., Hardy, B. and G.B. Hettel, 2002. *Rice Almanac 3rd Edition.* IRRI, Manila, Philippines, 256 pp.

Mainuddin, M., Kirby, M. and Chen, Y., 2008. Spatial and Temporal Pattern of Land and Water Productivity in the Lower Mekong River Basin. Basin Approach. Basin Focal project Working Paper No. 5, CGIAR Challenge Program on Water and Food.
http://www.waterandfood.org/fileadmin/CPWF_Documents/Documents/Basin_Focal_Projects/BFP_Publications/Spatial_Temporal_Pattern_Land_Water_Productivity_Mekong_BFPWP5_pgs1-21.pdf

- Mainuddin, M., Kirby, M. and Qureshi, E., 2007. Integrated Hydrologic-Economic Modelling for Analyzing Environmental Water Allocation Strategies of the Murray-Darling River Basin. *Agricultural Water Management*, 93. 123-135.
- Makara, O., Fukai, S., Fisher, K. S., Basnayake, J., Cooper, M. and Nesbitt, H., 2004. Drought response index for identifying drought resistant genotypes for rain fed lowland rice in Cambodia. In: Seng V., Craswell, E., Fukai, S. and Fisher, K. (eds.), *Water in Agriculture: Proceedings of a CARDI International Conference 'Research on Water in Agricultural Production in Asia for the 21st Century'*, Phnom Penh, Cambodia, 25-28 November 2003. Australian Centre for International Agricultural Research, Canberra.
- Makara, O., Sarom, M., and Nesbitt, H. J., 2001. Rice Production Systems in Cambodia. In: Fukai, S. and Basnayake, J. (ed.) *Increased lowland rice production in the Mekong Region*. ACIAR Proceedings 101, Canberra.
- Miyagawa S, Kuroda T., 1988a. Variability of yield and yield components of rice in rain-fed paddy fields of Northeast Thailand. *Jpn J Crop Sci* 57(3):527–534.
- Morishita, K.; Garsdal, H.; Masumoto, T. Hydrological monitoring system for the Cambodian Floodplains. 2004. Proc. of the 2nd Asia Pacific Association of Hydrology and Water Resources Conference, 1: 191-199.
- MRC, 1997. Mekong River Basin diagnostic study – Final report. Report number MKG/R. 97010. Mekong River Commission, Bangkok, Thailand.
- MRC, 2003. State of the Basin Report 2003. Mekong River Commission, Phnom Penh, Cambodia.
- MRC, 2005. Overview of the hydrology of the Mekong basin. Mekong River Commission, Vientiane.
- MRC, 2005. Water used for agriculture in the Lower Mekong Basin. MRC discussion paper, August 2005. 61pp.
- MRC, 2007. Annual Mekong Flood Report 2006, Mekong River Commission, Vientiane. 76pp.
- MRC and UNEP, 1997. Mekong River Basin diagnostic study. Final report. Mekong River Commission (MRC), Bangkok, Thailand and United Nations Environment Programme (UNEP).
- Milne-Home, W.A., Iast, R., Souk, B., Lertsirivorakul, R., Oondara, B. (no date). Groundwater flow, salinity processes and irrigation development in the Champone District, Lao PDR.
- Nawata, E., Nagata, Y., Sasaki, A., Iwama, K. and Sakuratani, T. 2005. Mapping of climate data in Northeast Thailand: Rainfall. *Tropics*, 14(2): 191-201.
- NEDECO, 1993. Master plan for the Mekong Delta in Viet Nam. A perspective for sustainable development of land and water resources. A report to Government of Vietnam State Planning Committee, World Bank, Mekong Secretariat, UNDP. Netherlands Engineering Consultants, Arheim, The Netherlands.
- Nesbitt, H., Johnston, R. and Solieng, M., 2004. Mekong River Water: Will River Flows meet Future Agricultural Needs in the Lower Mekong Basin? In: *Water in Agriculture*, Seng, V., Craswell, E., Fukai, S., and Fisher, K. (eds), Australian Centre of International Agricultural Research Proceedings No. 116, Canberra.
- Nesbitt, H.J., 2005. Water Used for Agriculture in the Lower Mekong Basin. MRC Technical Paper No, 11, Mekong River Commission, Vientiane, Lao PDR XXpp ISSN: 1683-1489.
- Pandey, S. 2001. Economics of lowland rice production in Laos: opportunities and challenges. In: Fukai, S. and Basnayake, J. (ed.) *Increased lowland rice production in the Mekong Region*. ACIAR Proceedings 101, Canberra.

- Pattanee, S., Phuriphanphinyo, N. and Cheevaprasert, S., 2002. Thailand's strategic planning and management of water resources and Mekong Basin perspectives. Presentation to MRC, Phnom Penh Cambodia.
- Pech, S. and Sunada, K., 2008. Population Growth and Natural-Resources Pressures in the Mekong River Basin. *AMBIO: A Journal of the Human Environment*: Vol. 37, No. 3 pp. 219–224
- Peng, P. and Pin, N., 2000. Groundwater contamination in Cambodia. Country paper.
- Phaloeun, C., Basnayake, J., Ngoy, C. K., Fukai, S. and Sarom, M., 2004. The Effect of Water Availability on Rice-based Double Cropping in Rain fed Lowlands in Cambodia. In: Seng, V., Craswell, E., Fukai, S., and Fisher, K. (eds), *Water in Agriculture, Proceedings of a CARDI International Conference: Research on Water in Agricultural Production in Asia for the 21st Century*, Phnom Penh, Cambodia, 25-28 November 2003. 72-85.
- Podger, G.M., Beecham, R.E., Blackmore, D., Stein, R. and Perry, C., 2004. Modelled Observations on Development Scenarios in the Lower Mekong Basin, *Mekong Water Resources Assistance Strategy*, World Bank, Nov. 2004, Vientiane.
- Polya, D.A., Gault, A.G., Bourne, N.J., Lythoge, P.R. and Cooke, D.A., 2003. Coupled HPLC-ICP-MS analysis indicates highly hazardous concentrations of dissolved arsenic species are present in the Cambodian wellwaters. *R. Soc. Chem. Spec. Publ.* 2008: 127-140.
- Polya, D.A., Gault, A.G., Diebe, N., Feldman, P., Rosenboom, J.W., Gilligan, E., Fredericks, D., Milton, A.H., Sampson, M., Rowland, H.A., Lythoge, P.R., Jones, J.C., Middleton, C. and Cooke, D.A., 2005. Arsenic hazard in shallow Cambodian groundwaters. *Mineral Mag.* 69:809-823.
- Privette, J. and D. Roy, 2002. First operational BRDF, albedo and nadir reflectance products from MODIS, *Remote Sensing of Environment*, 83,135–148,
- Qureshi, M. E., Connor, J. Kirby, M., and Mainuddin, M., 2007. Economic assessment of acquiring water for environmental flows in the Murray Basin. *Australian Journal of Agricultural and Resource Economics*, 51: 283-303.
- Roy, D.P., Lewis, P., Schaaf, C.B., Devadiga, S., and L. Boschetti, 2006. The Global Impact of Clouds on the Production of MODIS Bidirectional Reflectance Model-Based Composites for Terrestrial Monitoring., *Vol.3, no.4*, 452-6
- Rickman, J. F., Pyseth, M., Bunna, S. and Sinath, P., 2001. Direct seeding of rice in Cambodia. In: Fukai, S. and Basnayake, J. (ed.) *Increased lowland rice production in the Mekong Region*. ACIAR Proceedings 101, Canberra.
- Ringler, C., 2001. Optimal Water Allocation in the Mekong River Basin. ZEF-Discussion Papers on Development Policy No. 38, Centre for Development Research, Bonn: pp 50.
- Ruosteenoja, K, T.R.Carter, K. Jylha and H. Tuomenvirta, 2003. Future climate in the world regions: an intercomparison of model-based projections for the new IPCC emissions scenarios. Finnish Environment Institute, PO Box 140, Fin-00251 Helsinki.
- Saito, K., Linqvist, B., Keobualapha, B., Phanthaboon, K., Shiraiwa, T. and Horie, T., 2006. Cropping intensity and rainfall effects on upland rice yields in northern Laos. *Plant and Soil*, 284. 175-185.
- Sawano, S., Hasegawa, T., Goto, S., Konghakote, P., Polthanee, A., Ishigooka, Y., Kuwagata, T. and Toritani, H. 2008. Modelling the dependence of the crop calendar for rain fed rice on precipitation in Northeast Thailand. *Paddy Water Environment* 6: 83-90.
- Schiller, J. M., Linqvist, B., Douangsila, K., Inthapanya, P., Boupaha, B. D., Inthavong, S. and Sengxua, P., 2001. Constraints to rice production system in Laos. In: Fukai, S. and Basnayake, J. (ed.) *Increased lowland rice production in the Mekong Region*. ACIAR Proceedings 101, Canberra.

- SEI (Stockholm Environment Institute), 1997. Comprehensive Assessment of the Freshwater Resources of the World. UN, UNDP, UNEP, FAO, UNESCO, WMO, UNIDO, World Bank, SEI. WMO, Geneva. 33pp.
- Seng, V., Touch, V., Ban, B., Shimizu, K., Tomoyuki, T. and Takao, M., 2006. Identification of irrigation by pumping groundwater in Cambodia. Soil and Water Sciences Division, Cambodian Agricultural Research and Development Institute, Cambodia.
- Sihathep, V., Sipaseuth, C., Phothisane, C., Thammavong, A., Sengkeo, Phamixay, S., Senthonghae, M., Chanphengsay, M., Linqvist, B., and Fukai, S., 2001. Response to Dry-Season Irrigated Rice to Sowing Time at Four Sites in Laos. In. Fukai, S. and Basnayake, J. (ed.) Increased lowland rice production in the Mekong Region. ACIAR Proceedings 101, Canberra.
- Sinath C., 2001. Investment in land and water in Cambodia. Irrigated Agriculture Department, Ministry of water Resources and Meteorology, Phnom Penh, Cambodia.
- Sipaseuth, P., Inthapanya, P., Siyavong, V., Sihathep, M., Chanphengsay, M., Schiller, J. M., Linqvist, B. and Fukai, S., 2001. Agronomic practices for improving yields of rain fed lowland rice in Laos. In. Fukai, S. and Basnayake, J. (ed.) Increased lowland rice production in the Mekong Region. ACIAR Proceedings 101, Canberra.
- Sivapalan, M., Blöschl, G., Zhang, L., and Vertessy, R., 2003. Downward approach to hydrological prediction. *Hydrological Processes*, 17, 2101-2111.
- Smith, M. 1992. CROPWAT: A computer program for irrigation planning and management. FAO Irrigation and Drainage Paper 46, FAO, Rome.
- Snidvongs, A., Choowaew, S. and Chinvano, S., 2003. Background paper: Impact of climate change on water and wetland resources in Mekong River Basin: directions for preparedness and action. Regional Centre Report No 12. Southeast Asia START, Bangkok, Thailand. Retrieved December, 2006 from:
http://www.iucn.org/themes/climate/wl/documents/regional_waterstudies/southeast-asia-final.pdf
- Snidvongs, A., and Teng, S-K, 2006. Global International Waters Assessment, Mekong River, GIWA Regional assessment 55. Retrieved December, 2006 from:
<http://www.giwa.net/publications/r55.phtml>
- Southeast Asia START Regional Centre (SEA START RC). 2006. Final Technical Report: Southeast Asia Regional Vulnerability to Changing Water Resources and Extreme Hydrological Events due to Climate Change. SEA START RC Technical Report No. 15, Bangkok, Thailand. 142pp.
- SRES, 2000. Special report on Emission Scenarios: Summary for Policymakers. Contribution of Working Group I to the Fourth Assessment report of the Intergovernmental Panel on Climate Change, 17pp.
- SRMP, 1999. Methods of irrigation and fertilizing of coffee. Technical note No. 8. Support to water resources management project report.
- Stanger, G., Truong, V.T., Ngoc, L.T.M., and Thanh, T.T., 2005. Arsenic in groundwaters of the Lower Mekong. *Environ, Geochem. Health*. 27:241-357.
- Suppiah, R., B. Preston, P.H. Whetton, K.L. McInnes, R.N. Jones, I Macadam, J Bathols and D. Kirono, 2006. An updated report on: Assessment of climate change, impacts and risk management strategies relevant to South Australia. CSIRO, Australia
- Taylor, K.E., 2001. Summarising multiple aspects of model performance in a single diagram. *J. Geophys. Res.* 106; 7183-7192.
- The Government of Vietnam, 2003. Vietnam's Initial national Communication to the UNFCCC, Hanoi, Vietnam. 135pp.

- Toritani, H., Hasegawa, T., Kuwagata, T., Ohno, Hiroyuki, Ishigooka, Y., Goto, S., Sakamoto, T., Sawano, S., Hayano, M., Polthanee, A. and Konghakote, P. 2007. Evaluation of the relationship between the variability in the water cycle and the demand for water for food production in the Northeastern region of Thailand. Proceedings of the International Workshop on Assessment of Changes in Water Cycles on Food Production and Alternative Scenarios – Implications for Policy Making. November 22, 2007, Epochal Tsukuba, Japan.
- Trang, P.T.K., Berg, M., Viet, P.H., Van Mui, N. and Van der Meer, J.R., 2005. Bacterial bioassay for rapid and accurate analysis of arsenic in highly variable groundwater samples. *Environ Sci. Technol.* 39:7625-7630.
- Wassmann, R., Hien, N. X., Hoanh, C. T., and Toung, T. P. 2004. Sea level rise affecting the Vietnamese Mekong Delta: Water elevation in the flood season and implications for rice production. *Climate Change*, Vol. 66, No. 1-2: 89-107.
- WEPA (no date). State of water environmental issues: Myanmar. Policies : <http://www.wepa-db.net/policies/state/vietnam/seaareas.htm>
- WEPA (no date-A). State of water environmental issues: Viet Nam. Policies : <http://www.wepa-db.net/policies/state/vietnam/seaareas.htm>.
- Whetton, P.H., P.J. Raynor, A.B. Pitcock and M.R. Haylock, 1994. An assessment of possible climate change in the Australian region based on an intercomparison of general circulation modelling results. *J. Climate* 7; 441-463.
- Whetton, P.H., K.L. McInnes, R.N. Jones, K.J. Hennessy R. Suppiah, C.M. Page, J. Bathols and P. Durack, 2005. Climate change projections for Australia for impact assessment and policy applications: A review. CSIRO Technical Paper. 001, Aspendale, Victoria, CSIRO Marine and Atmospheric research, 34 pp.
- White, I., 2002. Water management in the Mekong delta: changes, conflicts and opportunities. UNESCO's International Hydrological Programme. Technical documents in hydrology, No 61, UNESCO, Paris, 2002.
- Williamson, D.R., Peck, A.J. and Turner, J.V., 1989. Groundwater hydrology and salinity in a valley in Northeast Thailand. In *Groundwater Contamination: proceedings of the Symposium held during the Third IAHS Scientific Assembly, Baltimore, MD.* IAHS publication No. 185: 147-154. `///`*



Contact Us

Phone: 1300 363 400

+61 3 9545 2176

Email: enquiries@csiro.au

Web: www.csiro.au

Your CSIRO

Australia is founding its future on science and innovation. Its national science agency, CSIRO, is a powerhouse of ideas, technologies and skills for building prosperity, growth, health and sustainability. It serves governments, industries, business and communities across the nation.